

World Journal of *Gastroenterology*

World J Gastroenterol 2018 December 21; 24(47): 5297-5414



**REVIEW**

- 5297 Hepatitis C: From inflammatory pathogenesis to anti-inflammatory/hepatoprotective therapy
Li H, Huang MH, Jiang JD, Peng ZG

MINIREVIEWS

- 5312 Split liver transplantation: Current developments
Hackl C, Schmidt KM, Süsal C, Döhler B, Zidek M, Schlitt HJ
- 5322 Novel oral-targeted therapies for mucosal healing in ulcerative colitis
Antonelli E, Villanacci V, Bassotti G
- 5331 Percutaneous ablation for perivascular hepatocellular carcinoma: Refining the current status based on emerging evidence and future perspectives
Kang TW, Lim HK, Cha DI

ORIGINAL ARTICLE**Basic Study**

- 5338 *Piwi like RNA-mediated gene silencing 1* gene as a possible major player in gastric cancer
Araújo T, Khayat A, Quintana L, Calcagno D, Mourão R, Modesto A, Paiva J, Lima A, Moreira F, Oliveira E, Souza M, Othman M, Liehr T, Abdelhay E, Gomes R, Santos S, Assumpção P
- 5351 Relationship between *Fusobacterium nucleatum*, inflammatory mediators and microRNAs in colorectal carcinogenesis
Proença MA, Biselli JM, Succi M, Severino FE, Berardinelli GN, Caetano A, Reis RM, Hughes DJ, Silva AE
- 5366 Bypassing major venous occlusion and duodenal lesions in rats, and therapy with the stable gastric pentadecapeptide BPC 157, L-NAME and L-arginine
Amic F, Drmic D, Bilic Z, Krezic I, Zizek H, Peklic M, Klicek R, Pajtak A, Amic E, Vidovic T, Rakic M, Milkovic Perisa M, Horvat Pavlov K, Kokot A, Tvrdeic A, Boban Blagaic A, Zovak M, Seiwert S, Sikiric P
- 5379 Novel screening test for celiac disease using peptide functionalised gold nanoparticles
Kaur A, Shimoni O, Wallach M

Case Control Study

- 5391 Analyzing predictors of graft survival in patients undergoing liver transplantation with donors aged 70 years and over
Caso-Maestro O, Jiménez-Romero C, Justo-Alonso I, Calvo-Pulido J, Lora-Pablos D, Marcacuzco-Quinto A, Cambra-Molero F, García-Sesma A, Pérez-Flecha M, Muñoz-Arce C, Loinaz-Seguro C, Manrique-Municio A

**Retrospective Cohort Study**

- 5403** Five years of fecal microbiota transplantation - an update of the Israeli experience

Greenberg SA, Youngster I, Cohen NA, Livovsky DM, Strahilevitz J, Israeli E, Melzer E, Paz K, Fliss-Isakov N, Maharshak N

ABOUT COVER

Editorial board member of *World Journal of Gastroenterology*, Haruhiko Sugimura, MD, PhD, Professor, Department of Tumor Pathology, Hamamatsu University School of Medicine, Hamamatsu 431-3192, Japan

AIMS AND SCOPE

World Journal of Gastroenterology (*World J Gastroenterol*, *WJG*, print ISSN 1007-9327, online ISSN 2219-2840, DOI: 10.3748) is a peer-reviewed open access journal. *WJG* was established on October 1, 1995. It is published weekly on the 7th, 14th, 21st, and 28th each month. The *WJG* Editorial Board consists of 642 experts in gastroenterology and hepatology from 59 countries.

The primary task of *WJG* is to rapidly publish high-quality original articles, reviews, and commentaries in the fields of gastroenterology, hepatology, gastrointestinal endoscopy, gastrointestinal surgery, hepatobiliary surgery, gastrointestinal oncology, gastrointestinal radiation oncology, gastrointestinal imaging, gastrointestinal interventional therapy, gastrointestinal infectious diseases, gastrointestinal pharmacology, gastrointestinal pathophysiology, gastrointestinal pathology, evidence-based medicine in gastroenterology, pancreatology, gastrointestinal laboratory medicine, gastrointestinal molecular biology, gastrointestinal immunology, gastrointestinal microbiology, gastrointestinal genetics, gastrointestinal translational medicine, gastrointestinal diagnostics, and gastrointestinal therapeutics. *WJG* is dedicated to become an influential and prestigious journal in gastroenterology and hepatology, to promote the development of above disciplines, and to improve the diagnostic and therapeutic skill and expertise of clinicians.

INDEXING/ABSTRACTING

World Journal of Gastroenterology (*WJG*) is now indexed in Current Contents[®]/Clinical Medicine, Science Citation Index Expanded (also known as SciSearch[®]), Journal Citation Reports[®], Index Medicus, MEDLINE, PubMed, PubMed Central and Directory of Open Access Journals. The 2018 edition of Journal Citation Reports[®] cites the 2017 impact factor for *WJG* as 3.300 (5-year impact factor: 3.387), ranking *WJG* as 35th among 80 journals in gastroenterology and hepatology (quartile in category Q2).

EDITORS FOR THIS ISSUE

Responsible Assistant Editor: *Xiang Li*
Responsible Electronic Editor: *Yan Huang*
Proofing Editor-in-Chief: *Lian-Sheng Ma*

Responsible Science Editor: *Xue-Jiao Wang*
Proofing Editorial Office Director: *Ze-Mao Gong*

NAME OF JOURNAL
World Journal of Gastroenterology

ISSN
ISSN 1007-9327 (print)
ISSN 2219-2840 (online)

LAUNCH DATE
October 1, 1995

FREQUENCY
Weekly

EDITORS-IN-CHIEF
Andrzej S Tarnawski, MD, PhD, DSc (Med),
Professor of Medicine, Chief Gastroenterology, VA
Long Beach Health Care System, University of California, Irvine, CA, 5901 E. Seventh Str., Long Beach, CA 90822, United States

EDITORIAL BOARD MEMBERS
All editorial board members resources online at <https://www.wjgnet.com/1007-9327/editorialboard.htm>

EDITORIAL OFFICE
Ze-Mao Gong, Director
World Journal of Gastroenterology
Baishideng Publishing Group Inc
7901 Stoneridge Drive, Suite 501,
Pleasanton, CA 94588, USA
Telephone: +1-925-2238242
Fax: +1-925-2238243
E-mail: editorialoffice@wjgnet.com
Help Desk: <https://www.fjpublishing.com/helpdesk>
<https://www.wjgnet.com>

PUBLISHER
Baishideng Publishing Group Inc
7901 Stoneridge Drive, Suite 501,
Pleasanton, CA 94588, USA
Telephone: +1-925-2238242
Fax: +1-925-2238243
E-mail: bpgoffice@wjgnet.com
Help Desk: <https://www.fjpublishing.com/helpdesk>
<https://www.wjgnet.com>

PUBLICATION DATE
December 21, 2018

COPYRIGHT
© 2018 Baishideng Publishing Group Inc. Articles published by this Open-Access journal are distributed under the terms of the Creative Commons Attribution Non-commercial License, which permits use, distribution, and reproduction in any medium, provided the original work is properly cited, the use is non commercial and is otherwise in compliance with the license.

SPECIAL STATEMENT
All articles published in journals owned by the Baishideng Publishing Group (BPG) represent the views and opinions of their authors, and not the views, opinions or policies of the BPG, except where otherwise explicitly indicated.

INSTRUCTIONS TO AUTHORS
Full instructions are available online at <https://www.wjgnet.com/bpg/gerinfo/204>

ONLINE SUBMISSION
<https://www.fjpublishing.com>

Hepatitis C: From inflammatory pathogenesis to anti-inflammatory/hepatoprotective therapy

Hu Li, Meng-Hao Huang, Jian-Dong Jiang, Zong-Gen Peng

Hu Li, Jian-Dong Jiang, Zong-Gen Peng, Institute of Medicinal Biotechnology, Chinese Academy of Medical Sciences and Peking Union Medical College, Beijing 100050, China

Meng-Hao Huang, Division of Gastroenterology and Hepatology, Department of Medicine, Indiana University School of Medicine, Indianapolis, IN 46202, United States

Jian-Dong Jiang, Institute of Materia Medica, Chinese Academy of Medical Sciences and Peking Union Medical College, Beijing 100050, China

ORCID number: Hu Li (0000-0002-7609-9399); Meng-Hao Huang (0000-0002-2389-8680); Jian-Dong Jiang (0000-0002-1138-2943); Zong-Gen Peng (0000-0001-7662-6892).

Author contributions: All the authors contributed to the search and analysis of the literature and to the writing of the paper.

Supported by CAMS Innovation Fund for Medical Sciences, No. 2017-I2M-3-012; National Natural Science Foundation of China, No. 81773788 and 81621064; and National Mega-Project for “R&D for Innovative Drugs”, Ministry of Science and Technology, China, No. 2018ZX09711001-003-010.

Conflict-of-interest statement: No potential conflicts of interest.

Open-Access: This article is an open-access article which was selected by an in-house editor and fully peer-reviewed by external reviewers. It is distributed in accordance with the Creative Commons Attribution Non Commercial (CC BY-NC 4.0) license, which permits others to distribute, remix, adapt, build upon this work non-commercially, and license their derivative works on different terms, provided the original work is properly cited and the use is non-commercial. See: <http://creativecommons.org/licenses/by-nc/4.0/>

Manuscript source: Unsolicited manuscript

Corresponding author to: Zong-Gen Peng, PhD, Professor, Institute of Medicinal Biotechnology, Chinese Academy of Medical Sciences and Peking Union Medical College, No. 1, Tiantan Xili, Beijing 100050, China. pengzonggen@imb.pumc.edu.cn
Telephone: +86-10-63166129

Fax: +86-10-63017302

Received: October 19, 2018

Peer-review started: October 19, 2018

First decision: November 22, 2018

Revised: November 27, 2018

Accepted: November 30, 2018

Article in press: November 30, 2018

Published online: December 21, 2018

Abstract

Hepatitis C virus (HCV) infection commonly causes progressive liver diseases that deteriorate from chronic inflammation to fibrosis, cirrhosis and even to hepatocellular carcinoma. A long-term, persistent and uncontrolled inflammatory response is a hallmark of these diseases and further leads to hepatic injury and more severe disease progression. The levels of inflammatory cytokines and chemokines change with the states of infection and treatment, and therefore, they may serve as candidate biomarkers for disease progression and therapeutic effects. The mechanisms of HCV-induced inflammation involve classic pathogen pattern recognition, inflammasome activation, intrahepatic inflammatory cascade response, and oxidative and endoplasmic reticulum stress. Direct-acting antivirals (DAAs) are the first-choice therapy for effectively eliminating HCV, but DAAs alone are not sufficient to block the uncontrolled inflammation and severe liver injury in HCV-infected individuals. Some patients who achieve a sustained virologic response after DAA therapy are still at a long-term risk for progression to liver cirrhosis and hepatocellular carcinoma. Therefore, coupling with anti-inflammatory/hepatoprotective agents with anti-HCV effects is a promising therapeutic regimen for these patients during or after treatment with DAAs. In this review, we discuss the relationship between inflammatory mediators and HCV infection, summarize the mechanisms

of HCV-induced inflammation, and describe the potential roles of anti-inflammatory/hepatoprotective drugs with anti-HCV activity in the treatment of advanced HCV infection.

Key words: Hepatitis C virus infection; Liver disease; Inflammatory pathogenesis; Anti-inflammatory and hepatoprotective therapy

© **The Author(s) 2018.** Published by Baishideng Publishing Group Inc. All rights reserved.

Core tip: Inflammatory responses triggered by hepatitis C virus (HCV) infection lead to severe progressive liver diseases. Some inflammatory cytokines and chemokines may serve as biomarkers for the disease progression and therapeutic effect in chronic hepatitis C (CHC) patients. The inflammatory pathogenesis in HCV-infected patients is complicated, including classic pathogen pattern recognition, inflammasome activation, intrahepatic inflammatory cascade response, and oxidative and endoplasmic reticulum stress. Direct-acting antivirals (DAAs) are not sufficient to block the uncontrolled inflammation and disease progression in severe CHC patients. Therefore, coupling with anti-inflammatory/hepatoprotective agents with anti-HCV effects is a promising therapeutic regimen for advanced HCV-infected patients during or after treatment with DAAs.

Li H, Huang MH, Jiang JD, Peng ZG. Hepatitis C: From inflammatory pathogenesis to anti-inflammatory/hepatoprotective therapy. *World J Gastroenterol* 2018; 24(47): 5297-5311
URL: <https://www.wjgnet.com/1007-9327/full/v24/i47/5297.htm>
DOI: <https://dx.doi.org/10.3748/wjg.v24.i47.5297>

INTRODUCTION

Hepatitis C virus (HCV) belongs to the genus *Hepacivirus* in the family *Flaviviridae* and is a positive single-stranded RNA virus that is approximately 9.6 kb. The HCV genome encodes three structural (Core, E1 and E2) and seven non-structural (NS) proteins (NS1 or P7, NS2, NS3, NS4A, NS4B, NS5A and NS5B)^[1]. As a kind of hepatic tropism virus, HCV mainly replicates in the hepatocyte cytoplasm and frequently causes acute or chronic hepatitis C (CHC), which has an estimated prevalence of 71 million people and is responsible for approximately 399000 deaths annually^[1,2]. CHC patients generally experience liver diseases ranging from liver fibrosis and cirrhosis to hepatocellular carcinoma (HCC) and suffer from metabolic disorders such as lipid abnormalities, steatosis, insulin resistance, and iron load dysregulation^[3]. These abnormalities are aggravated by long-term hepatic inflammatory responses. Upon HCV infection, the immune responses in the liver are initiated by parenchymal cells (hepatocytes), non-parenchymal liver cells [Kupffer cells (KCs) and hepatic stellate cells

(HSCs)] and immune cells (macrophages, mast cells, dendritic cells and natural killer cells) recruited to the liver, resulting in the spontaneous elimination of acute HCV infection^[4]. However, in 70%-80% of cases, the immune responses fail to eliminate the virus during the acute phase, leading to chronic infection^[4]. Persistent HCV replication in hepatocytes leads to uncontrolled inflammation and chemokine production. The excessive cytokines, as inflammatory agents, further cause inflammation in the liver, which eventually exacerbates tissue damage and liver disease progression^[5].

Direct antiviral treatment is undoubtedly the first choice for the treatment of HCV infection. Currently, several direct-acting antivirals (DAAs) have been approved for clinical use, including NS3/4A, NS5A and NS5B inhibitors and fixed-dose combined agents^[6]. The combinational use of these DAAs has become the standard treatment regimen for the treatment of HCV infection, which greatly improves sustained virologic response (SVR) rates to over 90%, shortens the treatment duration and reduces adverse effects, when compared with the traditional interferon (IFN) plus ribavirin treatment^[6]. However, HCV is just the initiator for pathophysiological processes, while persistent inflammatory cytokine storms (known as hypercytokinaemia) and HCV-induced hepatocyte damage exacerbate the progression of severe liver diseases^[7-10]. DAAs primarily control viral replication but are not sufficient to restore HCV-induced liver dyshomeostasis and advanced liver diseases. Clinically, there are different conclusions about the contribution of current DAA therapy to reducing cirrhosis and HCC, and a subset of patients are still subjected to the risk of cirrhosis, HCC and liver failure even after achieving an SVR^[6,7,11]. Given these limitations of DAA therapy, anti-inflammatory and hepatoprotective drugs with anti-HCV effects become a good choice for those individuals. These drugs have advantages in suppressing inflammation/oxidative stress, reducing hepatocyte injury and alanine aminotransferase (ALT)/aspartate aminotransferase (AST) levels and preventing the development of liver fibrosis^[12]. Therefore, although anti-inflammatory/hepatoprotective drugs would not replace DAAs, they can be used as a supplement to DAA therapy for preventing HCV relapse and liver disease progression during or after DAA therapy.

HCV INFECTION AND INFLAMMATORY MARKERS

Most inflammatory cytokine and chemokine levels are positively correlated with the HCV load and decline after antiviral therapy. Although the role of inflammatory mediators in HCV infection after treatment with DAAs has not received much attention, previous research still reported that one or more of these inflammatory mediators might serve as inflammatory biomarkers

Table 1 Potential inflammatory biomarkers of hepatitis C

Biomarker	Clinical relevance	Ref.
TNF- α	Promoting development of insulin resistance and diabetes during HCV infection; Hepatic TNF- α was associated with increased inflammatory activity, hepatic fibrosis, liver injury and HCC	[15-19]
IL-6	Evaluating the progression of CHC to cirrhosis; Plasma IL-6 positively correlated with illness duration and viral load in HBV/HCV co-infected patients	[13,20]
IL-8	Associated with interferon therapy non-response and high histologic activities in CHC patients	[29,30]
IL-18	Plasma IL-18 concentration was positively correlated with ALT and AST levels in HBV/HCV co-infected patients; A marker for evaluating the effect of IFN on the immune state	[20,21]
CXCL-9	Potential marker for evaluating the progression of CHC to cirrhosis	[13,14]
CXCL-10	CXCL-10 level in hepatocytes correlated with histological severity and hepatic lobule inflammation; A marker of viral response and therapeutic outcome	[5,13,14,23,24]

TNF- α : Tumor necrosis factor- α ; IL-6/-8/-18: Interleukin-6/-8/-18; HCV: Hepatitis C virus; HCC: Hepatocellular carcinoma; CHC: Chronic hepatitis C; ALT: Alanine aminotransferase; AST: Aspartate aminotransferase; IFN: Interferon; HBV: Hepatitis B virus.

in CHC patients (Table 1). For instance, Costantini *et al.*^[13,14] revealed that several serum mediators, including interleukin (IL)-6 and IL-8, C-X-C motif ligand (CXCL)-9, CXCL-10, CXCL-12 and macrophage migration inhibitory factor (MIF), might be used as potential markers for evaluating the progression of chronic hepatitis to cirrhosis. Hepatic tumor necrosis factor (TNF)- α was associated with increased inflammatory activity, hepatic fibrosis and liver injury in CHC^[15-17]. Meanwhile, TNF- α has been identified as the key molecule promoting the development of insulin resistance and diabetes during HCV infection, and patients with severe liver disease and HCC have a higher TNF- α /IL-10 ratio^[18,19]. In patients co-infected with HCV and hepatitis B virus (HBV), plasma IL-6 concentrations were positively correlated with illness duration and viral load, whereas the IL-18 concentration was positively correlated with ALT and AST levels and might evaluate the effect of IFN on the immune state^[20,21]. The above results suggest that the level of inflammatory factors in hepatitis C patients might be used as a reference for disease progression during HCV infection and antiviral therapy.

Chemokines play a more extensive role in the pathogenesis of CHC-related liver diseases and are even considered markers and therapeutic targets in CHC^[22]. Among the various chemokines, human IFN-induced protein (CXCL-10) is the most widely studied. In CHC patients, the levels of peripheral blood and liver CXCL-10, along with C-C motif ligand (CCL)-5, IFN-inducible T cell α chemo attractant (I-TAC) and macrophage inflammatory protein (MIP)-1 α /1 β , were increased markedly^[5,23], whereas the level of CXCL-10 in hepatocytes was correlated with histological severity and hepatic lobule inflammation^[14,24,25]. CXCL-10 also serves as a marker of viral response and therapeutic outcome since a high pretreatment level of CXCL-10 indicated the inhibition of CXCR chemokine receptor (CXCR) 3-expressing T cell response, which leads to therapeutic non-responses^[5,23]. This phenomenon is also confirmed in the following cases where the virus was controlled during treatment with an increased number of CD8⁺ cells expressing high CXCR3 levels^[26]. In addition, monocyte chemotactic protein-1

(MCP-1), soluble adhesion molecule (sAM), CCL-20 and CXCL-9 were reported to predict the outcome of antiviral therapy in CHC patients^[27,28]. Chemokine IL-8 was also induced by HCV, and patients who were biochemical non-responders to IFN therapy had higher pretreatment levels of IL-8 or high histologic activities^[29,30]. Therefore, chemokine levels are important reference values for monitoring the natural course and progression of HCV-related liver diseases and even identifying different treatment response rates before treatment^[5].

However, these studies investigating the utility of inflammatory cytokines and chemokines for the prediction of treatment responses were based only on a small number of patients infected with limited HCV subtypes, most were based on IFN or IFN plus ribavirin therapy regimens, and the results did not preclude an epiphenomenon associated with the effects of IFN^[23,27]. Therefore, the use of inflammatory cytokines and chemokines as indicators of the pathological progression of HCV infection and treatment efficacy has yet to be supported by more data from larger multivariate studies of patients, especially those treated with DAAs.

MECHANISMS OF HCV-INDUCED INFLAMMATION

Because of T-cell-mediated autologous hepatocytotoxicity, the spontaneous clearance of HCV infection is not only difficult to achieve but also increases the risk of progression to chronic hepatitis and liver injury^[31]. In addition to this T-cell-mediated cytotoxic response, HCV infection alone also triggers inflammatory responses through a variety of strategies to aggravate the progression of liver diseases (Figure 1).

Inflammation responses triggered by interactions between host and HCV

Unlike receptor-mediated HCV entry processes, the occurrence of inflammation in HCV infection relies on the recognition, binding and interaction of HCV RNA and protein components with pathogen pattern recognition receptors (PRRs) or other host cellular structures, which

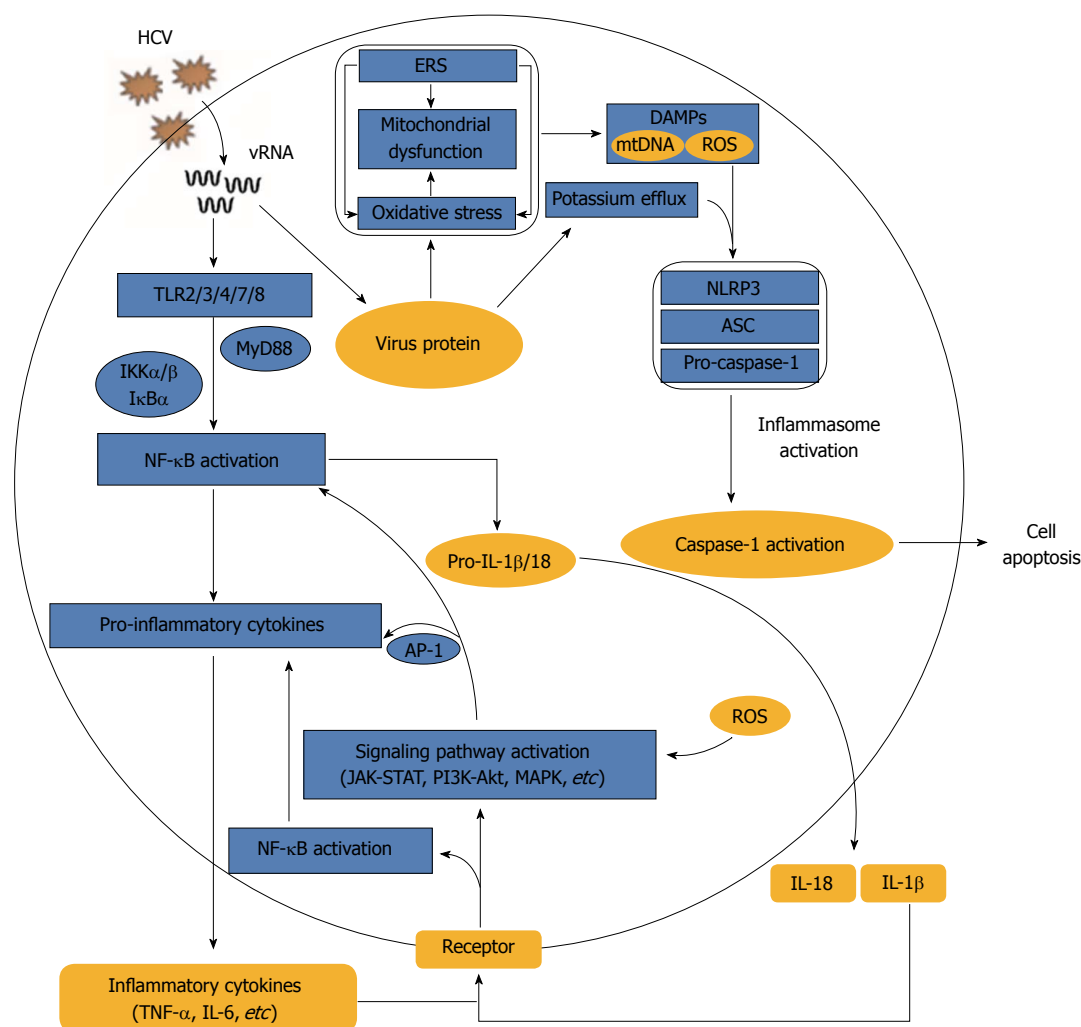


Figure 1 Mechanisms of hepatitis C virus-induced inflammation. Hepatitis C virus (HCV) RNA triggers Toll-like receptor mediated nuclear factor (NF)- κ B activation and inflammatory cytokine release, while HCV proteins mainly lead to oxidative and endoplasmic reticulum stress and potassium efflux, causing the Nod-like receptor pyrin domain containing inflammasome activation. The released inflammatory factors bind to their corresponding receptors and then directly induce NF- κ B activation or indirectly lead to signalling pathway mediated downstream inflammatory response. HCV: Hepatitis C virus; ERS: Endoplasmic reticulum stress; AP-1: Activating protein-1; ASC: Apoptosis-associated speck-like protein containing CARD; DAMP: Damage associated molecular patterns; mtDNA: Mitochondrial DNA; MyD88: Myeloid differentiation factor 88; NLRP3: Nod-like receptor pyrin domain containing 3; ROS: Reactive oxygen species; vRNA: Viral RNA; TLR: Toll-like receptor; TNF- α : Tumor necrosis factor- α ; IL: Interleukin.

in turn activate downstream immune- and inflammation-associated signal transduction pathways.

Cell surface or internal PRRs, such as Toll-like receptors (TLRs) 1-10, can discern pathogens and activate canonical signalling pathways during immune and inflammatory responses. Virus-derived pathogen-associated molecular patterns (PAMPs), HCV RNA and viral proteins could induce pro-inflammatory cytokine and chemokine production *via* several PRRs. For example, TLR3 recognized the HCV double-stranded RNA produced during HCV replication and activated TLR3 signalling, resulting in high releases of IL-8, CCL-5, MIP-1 and CXCL-10^[32,33]. Macrophages uptake HCV RNA through clathrin-mediated endocytosis, which is independent of receptor and productive infection, and therefore trigger myeloid differentiation primary response (MyD) 88-mediated TLR7 signalling to induce pro-IL-1 β mRNA expression^[34,35]. In addition, a conformation-

dependent interaction between the TLR2 and HCV core or NS3 proteins triggers the TLR2-specific inflammatory pathway^[36]. NS5A specifically activated the promoter of the TLR4 gene in both hepatocytes and B cells, thereby activating the signal transduction cascades from MyD88 to IFN regulatory factor (IRF)-3 and stimulating nuclear factor (NF)- κ B-mediated IFN- β and IL-6 secretion^[37].

In addition to the host PRRs, HCV proteins can also interact with other cellular structures and activate inflammatory pathways. The binding of HCV E2 to CD81 induced CCL-5 secretion possibly through activating mitogen-activated protein kinase (MAPK)^[38]. The transient expression of HCV NS5B in mouse liver and human hepatocytes catalysed the production of small RNA species, which activated innate immune signalling *via* TANK-binding kinase (TBK) 1, IRF-3 and NF- κ B, and eventually induced the production of IFNs and inflammatory cytokines^[39]. HCV core protein, which

is mostly implicated in liver disorders, activated signal transducer and activator of transcription (STAT) 3 in human hepatocytes, leading to subsequent immune activation, inflammation and tumorigenesis^[40]. In short, the over-replication of HCV in host cells is accompanied by a broad and complex interaction of host and HCV components, eventually unbalancing signal transduction pathways, causing uncontrolled excessive inflammatory responses and further exacerbating disease progression.

Inflammasome activation upon HCV infection

An inflammasome is a large, multi-protein cytosolic complex that perceives intracellular danger signals, such as microbial pathogens, inflammatory diseases, cancers and metabolic and autoimmune disorders *via* Nod-like receptors (NLRs) and ultimately stimulates the production of the inflammatory cytokines IL-1 β and IL-18^[41,42]. Four NLR families, NLRP1, NLRP3, NLRC4 and AIM2, have been characterized to date. Among them, NLRP3, as the most extensively studied, responded to the host- and environment-derived molecules and pathogen-associated activators^[41]. Increased levels of plasma IL-1 β and IL-18 in hepatitis C patients indicated an activation of the inflammasome during HCV infection^[43].

Activation of the inflammasome and secretion of mature IL-1 β and IL-18 during HCV infection require the integration of two signals. The first is known as signal 1, which occurs when the virus is detected by a PRR or cytokine receptor, resulting in the activation of NF- κ B and consequent upregulation of pro-IL-1 β and pro-IL-18 mRNAs. Signal 2 is that NLRP3 senses HCV, recruits the adaptor protein ASC (apoptosis-associated speck-like protein containing CARD) and induces the recruitment and autocatalytic activation of caspase-1. The activated caspase-1 processes cytosolic cytokines IL-1 β and IL-18 precursors into mature secretory proteins^[34]. Although HCV infection was reported to activate the inflammasome^[35], the conclusions and proposed mechanisms differ across studies. Michael *et al*^[34] demonstrated that HCV infection induced inflammasome activation and IL-18 and IL-1 β secretion in monocytes and macrophages through the recognition of viral single-stranded RNA by TLR7 but failed to stimulate the inflammasome and cytokine production by lymphocytes, dendritic cells or hepatocytes. Other studies reported that no inflammasome activation was detected in HCV-infected Huh-7 cells^[44,45], whereas Burdette *et al*^[46] reported HCV-induced secretion of IL-1 β in Huh7.5 cells *via* induction of inflammasome complex assembly involving NALP3, ASC and caspase-1. In addition, although a previous report suggested that reactive oxygen species (ROS) are not inflammasome effectors in HCV-infected hepatocytes^[45], Chen *et al*^[44] demonstrated that HCV-RNA transfected monocytes and THP-1 derived macrophages could activate the NLRP3 inflammasome in a ROS-dependent manner, and the process was independent on retinoic acid-inducible gene 1 (RIG-1). Alternative mechanisms for inducing

inflammasomes were also reported in HCV infection. For instance, after macrophage phagocytosis of HCV, HCV induced potassium efflux and activated the NLRP3 inflammasome for the processing and secretion of IL-1 β ^[35]. The HCV P7 protein is a kind of pH-sensitive proton channel, and the decrease of extracellular pH could enhance P7 activity and then stimulate signal 2 to induce the maturation and secretion of IL-1 β from RAW264.7 macrophages^[47], whereas a report showed that high expression of P7 protein in Huh7.5 cells failed to induce IL-1 β production^[46].

Altogether, inflammasome activation triggered by HCV infection might depend on HCV RNA and the secondary effects during HCV replication, such as ROS generation, potassium efflux and P7 activity. However, the phenomenon of inflammasome activation and detailed mechanisms in response to HCV infection might vary across different cell types, and these data suggest that monocytes and macrophages are the main effector cells activated by the inflammasome after HCV infection.

Inflammatory cascade response in the hepatic microenvironment

Although hepatocytes are the major cell population in the liver and the targets of cells for HCV entry and replication, non-parenchymal cells in the liver, such as KCs and HSCs, also play key roles in HCV-induced liver diseases. KCs, which are hepatic macrophages and account for approximately 15% of the total cells in the liver^[48], exhibit limited internalization of HCV *via* phagocytosis, leading to the production of pro-inflammatory cytokines and chemokines^[35]. HSCs are activated after HCV infection and are associated with liver fibrogenesis, including collagen deposition and abnormal extracellular matrix remodelling^[49]. Crosstalk among these three kinds of liver cells plus the recruited immune cells during HCV infection in the hepatic microenvironment mediates inflammatory cascade signalling and exacerbates disease progression (Figure 2). The icons in the figure are shared by Reactome^[50].

The interaction between HCV-infected hepatocytes and HSCs enhances the inflammatory response to HCV infection^[31]. For example, in the HCV-infected hepatocyte and HSC co-culture system, IL-1 α secreted by HSCs enhanced CCAAT-enhancer-binding protein β -targeted downstream gene expression, leading to enhanced expression of IL-6, IL-8 and MIP-1 α /1 β ^[31]. Additionally, in the co-culture system of HCV replicon cells and HSCs, HCV replicon cells released transforming growth factor (TGF)- β 1 into conditioned medium and thereby induced fibrogenesis in HSCs, which was characterized by increased production of procollagen α 1 (I) and procollagen α 1 (III) and decreased expression of fibrinolytic matrix metalloproteinase (MMP)^[51]. Exosomes, which are endosomal-derived vesicles, also mediate communication between hepatocytes and HSCs. Although exosomes secreted from HCV-infected

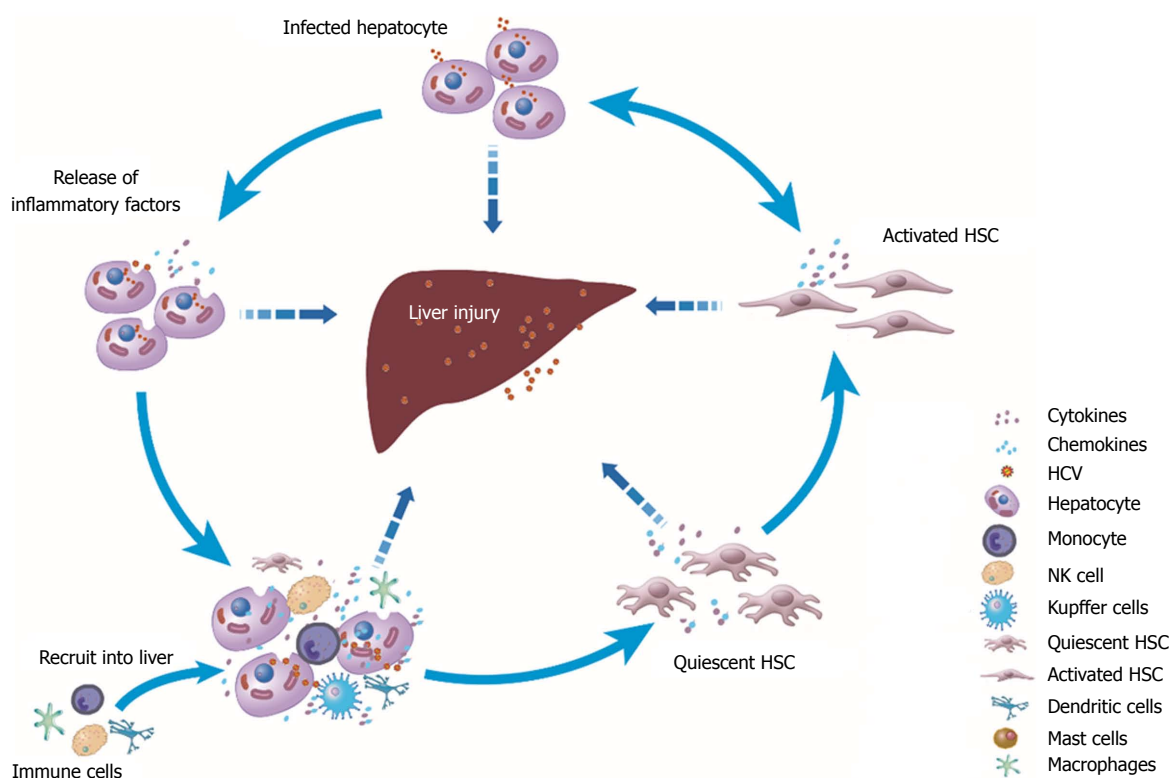


Figure 2 Inflammatory cascade responses in the hepatic microenvironment. Crosstalk among parenchymal cells (hepatocytes), non-parenchymal liver cells (Kupffer cells and hepatic stellate cells) and recruited immune cells (macrophages, mast cells, dendritic cells and natural killer cells) plus hepatitis C virus replication in the hepatic microenvironment mediates inflammatory cascade signalling and exacerbates liver injury and disease progression. HSC: Hepatic stellate cells; NK: Natural killer; HCV: Hepatitis C virus.

hepatocytes (HCV-exo) could transport small amounts of HCV RNA into HSCs, the quantity of HCV RNA carried into HSCs is gradually decreased because HSCs do not support HCV infection and replication^[52,53]. However, one study found that the miR-19a carried by HCV-exo could target suppressor of cytokine signalling 3 (SOCS3) in HSCs, leading to STAT3-mediated TGF- β signalling activation, profibrotic marker high expression and enhanced inflammatory responses^[52].

After HCV infection, the inflammatory cascades between HCV-stimulated macrophages and HSCs are also activated in the hepatic microenvironment. To mimic the effect of HCV in the blood circulation on hepatic non-parenchymal cells, Negash *et al.*^[35] exposed human THP-1 cell-derived macrophages and KCs to HCV *in vitro* and showed that they activated caspase-1 expression and enhanced IL-1 β /IL-18 secretion. Similarly, conditioned medium derived from HCV-exposed human THP-1 macrophages and KCs increased the expression of inflammatory (NLRP3, TNF- α , IL-1 β , IL-6 and CCL-5) and profibrogenic (TGF- β 1, collagen 4A1, MMP2 and α -smooth muscle actin) markers in primary human and immortalized HSCs (LX2 cells)^[54]. Further study identified that the chemokine CCL-5 in this conditioned medium induced inflammasome activation and fibrotic marker expression in HSCs, whereas TNF- α but not IL-1 β could only induce inflammasome markers^[54]. These studies emphasize that inflammatory cascade reactions could

occur between macrophages and HSCs through highly expressed inflammatory mediators during HCV infection.

Moreover, chemokines secreted by HCV-infected hepatocytes and HCV-internalized KCs recruit immune cells to the site of infection, leading to aggravation of the inflammatory response and even liver damage in CHC^[47,55]. Other molecules, such as ROS and lipid peroxidation products produced by activated KCs or injured hepatocytes, could also induce the activation of quiescent HSCs^[49]. The interactions between the HSCs and the immune cells recruited into the liver and the HCV-infected or exposed hepatocytes/macrophages mediate inflammation-related cellular signalling, together establishing a microenvironment of the liver in an excessively inflammatory state and continuing to exacerbate disease progression.

Exacerbation of the inflammatory response by oxidative and endoplasmic reticulum stress

Oxidative stress is characterized by excessive ROS accumulation *in vivo*. ROS includes radicals, such as superoxide anion (O₂^{-•}), hydroxyl radical (OH[•]) and hydrogen peroxide (H₂O₂). Superoxide anions are mainly derived from the mitochondrial electron transport chain and catalysed into H₂O₂ and OH[•] by superoxide dismutase^[56]. Hepatocytes have abundant mitochondria, which are the main source of ROS. Oxidative stress is more severe in HCV infection than in

HBV infection^[57]. Upon HCV infection, oxidative stress is thought to occur because of the expression of viral proteins, changes in the activity of oxidative enzymes, depletions of antioxidants and the ensuing chronic inflammation^[58]. HCV core protein interacts with the mitochondrial protein chaperone prohibitin, leading to impairment of mitochondrial respiratory chain function accompanied by ROS overproduction^[59]. The intracellular expression of E1, E2, NS3 and NS5A also potently enhances ROS levels by increasing intracellular calcium influx and decreasing mitochondrial transmembrane potential^[58]. In addition to mitochondria-derived ROS, cellular nicotinamide adenine dinucleotide phosphate (NADPH) oxidase also acts as an important source of ROS, generating superoxide anions by catalysing the oxidation of NADPH^[60]. Among the seven Nox enzymes (Nox1-5, Dual oxidase Duox1 and Duox2), Nox1 and Nox4 induced in hepatocytes by infecting with HCV phenotype 2a and 1b or expressing HCV proteins contribute to ROS production^[60,61]. In brief, ROS accumulation caused by HCV infection in the liver further leads to activation of the signalling factors phosphoinositide 3-kinase (PI3K), Janus kinase, MAPK pathways or transcription factor NF- κ B, activator protein-1 (AP-1), STAT3, HIF-1 α , PPAR- γ and Nrf2, and those pathways induce downstream inflammatory and immune responses^[62-65].

HCV protein expression is also accompanied by strong endoplasmic reticulum stress (ERS). HCV structural and NS proteins are continuously processed in ER-derived membrane structures^[66,67], perturbing normal ER functions and inducing ER stress^[67,68]. The unfolded protein response (UPR) is that cells respond to ERS by activating an adaptive cellular programme and alleviate ER stress by inducing protein folding and degradation in the ER and decreasing overall protein synthesis^[66]. The UPR is mediated by three ER transmembrane proteins: cleavage of activating transcription factor 6 (ATF-6), inositol-requiring enzyme 1 (IRE1) and PERK-like endoplasmic reticulum kinase (PERK) and their downstream factors X-box binding protein 1 (XBP-1) and eukaryotic initiation factor 2 α (EIF2 α)^[66]. The UPR is initially activated in HCV-infected Huh7.5.1 cells and HCV-transgenic mice, resulting in the phosphorylation of IRE1, EIF2 α and ATF-6, and splicing of XBP-1^[69]. However, HCV RNA or protein *per se* also exerts the resistance for UPR, such as XBP-1 activity downregulation in HCV-expressing cells and PERK activity inhibition by HCV E2, leading to a reduction in ER-associated protein degradation and UPR-associated translational attenuation, respectively^[66]. Virtually, there is an interaction between ERS and inflammation, and ERS might be both a trigger and a consequence of chronic inflammation^[70]. NS5A expression in the ER triggers ERS and ultimately leads to the activation of STAT3 and NF- κ B, and this pathway is sensitive to mitochondrial calcium uptake inhibitors, calcium chelators and antioxidants, therefore providing evidence for the role of ERS and oxidative stress in the

activation of the inflammatory response during HCV infection^[71]. Under severe ERS, the UPR activates the JNK/AKT pathway and phosphorylates NF- κ B protein I κ B kinase (IKK), leading to cleavage of I κ B α and activation of NF- κ B^[70]. UPR-independent Ca²⁺ release and excessive ROS and ER chaperone GRP78 that leak into the cytosol were also proposed to activate NF- κ B to induce inflammation^[70]. In turn, inflammatory factors also exacerbate ERS and oxidative stress. For example, TNF- α induced intracellular excessive generation of ROS, which in turn induced ERS, whereas IL-1 β and TNF- α also increased ERS in a nitric oxide dependent manner^[72,73].

The ERS and oxidative stress networks interact with each other and therefore play a key role in local and systemic inflammatory responses. HCV infection triggers ERS and disrupts mitochondrial signalling and cytosolic redox homeostasis, thereby inducing oxidative stress and inflammation. ERS and oxidative stress might individually or concurrently stimulate or exacerbate inflammatory responses, and *vice versa*.

ANTI-INFLAMMATORY/ HEPATOPROTECTIVE THERAPY IN HCV INFECTION

DAA has been used clinically for several years, and some limitations were reported, including drug-resistance, low efficacy in cirrhotic patients, drug interactions, liver toxicities, HBV reactivation and skin reactions^[6,74-77]. Anti-inflammatory/hepatoprotective agents have fewer side effects for the treatment of HCV-induced liver injury, fibrosis, cirrhosis or even HCC, as demonstrated by their long-term use in liver health cares in many Asian countries^[77-80]. Most of these agents are natural or naturally derived compounds, and many have anti-HCV effects. After DAA treatment, some patients are still subject to persistent disease progression and HCV relapse^[81]. Therefore, anti-inflammatory/hepatoprotective agents with anti-HCV activity might be a better treatment choice for preventing CHC progression to severe liver diseases when used in combination with or subsequent to DAA therapy. According to the chemical category and practical application in the clinic, we mainly focus on certain representative plant or plant derivative active constituents considered to be the most promising for anti-inflammatory/hepatoprotective therapy in HCV infection, including the flavonoid compound silibinin, terpenoid compound andrographolide, polyphenols compound curcumin, alkaloids oxymatrine and herb-derived antioxidant bicyclol (Figure 3)^[77,78,80].

Silibinin

Flavonoids or bioflavonoids are found in numerous plants, and over 4500 flavonoids or their subgroups have been identified to date, of which silymarin and silibinin are representative compounds^[77,80]. Silymarin is extracted from the seeds of the milk thistle *Silybum*

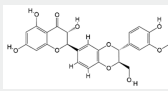
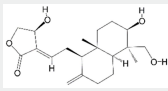
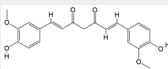
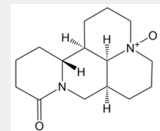
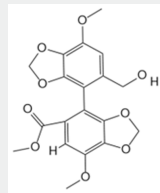
Promising anti-inflammatory/hepatoprotective agents for chronic hepatitis C						
Compound	Chemical category	Formula	Chemical structure	Mechanism of anti-HCV	Major anti-inflammatory/hepatoprotective activity	Ref.
Silibinin	Flavonoids	C ₂₅ H ₂₂ O ₁₀		Block viral entry, fusion, RNA and protein synthesis, NS5B polymerase activity and transmission.	Anti-oxidation, anti-inflammation, anti-proliferation and immunomodulation; Limit <i>de novo</i> fibrogenesis-related inflammation and prevent carcinogenesis in hepatocellular carcinoma.	[81-83,85]
Andrographolide	Terpenoid	C ₂₀ H ₃₀ O ₅		Inhibit HCV protein synthesis, RNA replication and infection; Activate the antiviral IFN response and suppress HCV NS3/4A protease activity.	Scavenge free radicals, decrease lipid peroxidation, regulate immune responses and prevent infection and cancer; Depletion of glutathione, induction of cytochrome P450, normalization of the levels of hepatitis markers.	[78,93,96-98,101]
Curcumin	Polyphenol	C ₂₁ H ₂₀ O ₆		Inhibit HCV replication by inducing HO-1- and AKT-related signaling pathways; Block viral entry into human hepatocytes.	Suppress severe cytokine storm, alleviate liver injury or fibrosis, inhibit HSC activation, suppress activation of leptin signaling, enhance AMP-activated protein kinase activity.	[79,105-112]
Oxymatrine	Alkaloids	C ₁₅ H ₂₄ N ₂ O ₂		Inhibit HCV replication by destabilizing heat stress cognate 70 mRNA and downregulating the expression of Hsc70.	Reduce serum transaminase or alkaline phosphatase level, modulate TLR4-dependent inflammatory pathways, attenuate liver injury and improve experimental hepatic fibrosis, exert anti-cancer effects; Treatment of chemotherapy-induced hepatotoxicity.	[118-120,122-126]
Bicyclol	Herb-derived synthetic compounds	C ₁₉ H ₁₈ O ₉		Decrease HCV load in the clinic without reported mechanism.	Exert hepatoprotective and anti-inflammatory effects in chemical-, immunological-, fatty-, drug-induced and surgery-caused liver injury animal models; Prevent hepatic fibrosis induced by CCl ₄ , dimethylnitrosamine, bovine serum albumin and bile duct ligation.	[127,134,136-139]

Figure 3 Promising anti-inflammatory/hepatoprotective agents for chronic hepatitis C. HCV: Hepatitis C virus; IFN: Interferon; NS: Non-structural; HO-1: Heme oxygenase-1; TLR: Toll-like receptor.

marianum and comprises at least seven flavonolignans (silybin A, silybin B, isosilybin A, isosilybin B, silychristin, isosilychristin and silydianin) and one flavonoid (taxifolin)^[81,82]. Silibinin (formerly named silybin) is the major bioactive compound of silymarin and is widely used for the treatment of insulin resistance, alcoholic/non-alcoholic liver disease and viral hepatitis because of its antioxidative, anti-inflammatory, anti-proliferative and immunomodulatory properties^[81-84]. *In vitro* and *in vivo* studies showed that silymarin/silibinin could stimulate the expression of lysophosphatidylcholine acyltransferase, reduce the level of liver cirrhotic platelet-activating factor or block the activation of major signalling pathways, such as NF- κ B and TGF- β signalling, thus limiting *de novo* fibrogenesis-related inflammation and preventing carcinogenesis in HCC^[82,85]. Moreover, silymarin and silibinin were found to inhibit HCV infection in cell cultures by blocking viral entry, fusion, RNA and protein synthesis, NS5B polymerase activity and transmission^[84]. Although

oral administration of silymarin had little effect on liver enzyme activity and viral load in HCV-infected patients due to its rapid metabolism and low bioavailability^[86-88], intravenous injection of water-soluble, succinate-conjugated silibinin formulations showed significant antiviral effects in CHC patients who failed to treatment with the standard pegylated IFN/ribavirin therapy^[89,90].

Other flavonoids, such as epigallocatechin-3-gallate, naringenin, quercetin, luteolin and apigenin, also have potential anti-HCV activities, hepatoprotective and anti-inflammatory activities^[77,91,92]. Therefore, these agents are expected to be developed for the treatment of hepatitis C patients with advanced liver diseases.

Andrographolide

Among the various secondary metabolites produced by plants, terpenoids are phytochemicals with potential therapeutic applications for the treatment of liver cancer, of which labdane diterpenoid compound andrographolide

(C₂₀H₃₀O₅) is isolated from the stem and leaf of *Andrographis paniculata* and was initially used to treat upper respiratory tract infections with good safety but was later reported to have anti-inflammatory/hepatoprotective effects^[78,79]. Its mechanisms of action are mainly *via* scavenging free radicals, decreasing lipid peroxidation, regulating immune responses and preventing infection and cancer^[78,93]. *In vitro* and *in vivo*, the anti-inflammatory activities of andrographolide were attributed to the attenuation of the protein kinase C, extracellular signal-regulated kinase (ERK)1/2 or PI3K/AKT pathways, leading to the inhibition of NF-κB signalling pathway activation^[93-95]. The anti-hepatotoxic activities of andrographolide were correlated with depletion of glutathione, induction of cytochrome P450 or normalization of the levels of hepatitis markers such as alkaline phosphatase and glutamic pyruvate transaminase^[96-98]. The synthetic analogues of andrographolide exhibit analgesic, antipyretic and anti-inflammatory effects without notable toxicity in animal models^[99,100]. Moreover, andrographolide was reported to inhibit HCV protein synthesis, RNA replication and infection^[101]. Detailed mechanisms showed that andrographolide activates p38 MAPK phosphorylation and stimulates Nrf2-mediated heme oxygenase (HO)-1 expression, thereby increasing the amounts of its metabolite biliverdin, which was found to activate the antiviral IFN response and suppress HCV NS3/4A protease activity^[101,102]. These findings support a clinical trial of andrographolide and its derivatives for the treatment of severe CHC.

Curcuminoids

Curcumin, a hydrophobic polyphenol derived from the rhizome of the herb turmeric (*Curcuma longa*), has been widely used as a spice and colorant in foods^[103]. To date, extensive clinical studies have proven its pharmacological properties of anti-inflammatory, antioxidant, antiviral, anticancer, hypoglycaemic, wound-healing and antimicrobial activities and showed that curcumin is safe and well tolerated^[104]. In view of these observations, curcumin is predominantly used to treat inflammatory diseases *via* multiple mechanisms involving inflammatory transcription factors, cytokines, redox status or protein kinases^[105]. Curcumin suppresses the severe cytokine storm caused by infection with severe viruses, such as HIV, HSV, HBV and HCV, and might be potentially useful to treat inflammation induced by Ebola virus infection^[106]. For its hepatoprotective property, curcumin alleviates liver injury or fibrosis by targeting platelet-derived growth factor-β receptor, TGF-β, TLRs, MMPs and peroxisome proliferator-activated receptors and decreasing inflammatory cytokines^[78]. *In vitro* studies showed that curcumin inhibits HSC activation *via* preventing leptin from increasing intracellular glucose levels^[107], suppressing advanced glycation end-product-dependent activation of leptin signalling^[108] or enhancing AMP-activated protein kinase (AMPK) activity^[109] and therefore reduces liver fibrosis. In addition, evidence suggests that

curcumin has anticarcinogenic and chemopreventive effects through arresting the cell cycle and/or inducing apoptosis in a p53 dependent manner^[103], as well as by activating caspase cascades^[105]. Curcumin also inhibits HCV replication by inducing HO-1- and AKT-related signalling pathways^[110,111] or by blocking viral entry into human hepatocytes^[112]. Therefore, based on the available pharmacological data obtained from *in vitro* and *in vivo* studies, as well as clinical trials, there is an opportunity to translate curcumin into clinics for therapy of CHC with hepatic cirrhosis and HCC in the near future.

Oxymatrine

Oxymatrine and its active metabolite matrine are the major alkaloid aqueous extracts from the root of *Sophora flavescens*, *Sophora tonkinensis* and *Sophora alopecuroides*^[113]. Clinically, oxymatrine has been used to treat chronic hepatitis B and leukopenia caused by tumour radiotherapy and chemotherapy in China^[113,114]. In recent years, many laboratory and clinical trials have also shown the antiviral activity of oxymatrine against HCV in cell cultures and human studies^[115-117]. Oxymatrine or its derivatives destabilize heat stress cognate 70 (Hsc70) mRNA and thereby downregulate the expression of Hsc70^[118-120]. As Hsc70 is packaged into HCV particles and becomes a structural component of the virus in the assembly process, oxymatrine or its derivatives could inhibit HCV replication^[118,121]. Oxymatrine could also inhibit inflammatory activity as defined by reducing serum transaminase or alkaline phosphatase levels, modulating TLR4-dependent inflammatory pathways, attenuating liver injury and improving experimental hepatic fibrosis by downregulating fibrosis-related gene expression, decreasing collagen deposits, inducing apoptosis of HSCs or inhibiting lipid peroxidation^[122-126]. Furthermore, accumulating research suggests that oxymatrine has anticancer effects, which might have therapeutic effects on HCC caused by HCV infection, but could also be used in the treatment of chemotherapy-induced hepatotoxicity^[127,128]. Therefore, oxymatrine is expected to be used in CHC patients with liver inflammation or injury and could improve chemotherapy-induced hepatotoxicity or increase the survival rate of HCC patients.

Bicyclol

To date, although the effects of ROS and the host redox system on HCV replication remain unclear^[56,63] and different antioxidants show controversial anti-HCV effects^[63,129-131], clinical evidence suggests that antioxidant therapy might alleviate necroinflammation and fibrosis progression^[131,132]. Classical antioxidants, such as glutathione (GSH)^[63], N-acetyl cysteine (NAC)^[133] and vitamin E^[130], have been reported to treat hepatitis C with efficacy. In addition, bicyclol (4,4'-dimethoxy-5,6,5',6'-bis(methylenedioxy)-2-hydroxymethyl-2'-methoxycarbonyl biphenyl), a synthetic compound derived from schizandrin C extracted from the Chinese

medicinal herb *Fructus schisandrae*, has potent antioxidative and certain anti-HCV effects in the clinic with safety^[134,135]. Clinically, bicyclol tablets are used in many countries to treat various non-viral hepatitis and chronic hepatitis B and C accompanied by mild and moderate serum aminotransferase abnormality. Preclinical pharmacological experiments also showed that bicyclol exerts hepatoprotective and anti-inflammatory effects in chemical-, immunological-, fatty-, drug-induced and surgery-caused liver injury animal models^[135]. Bicyclol also prevents hepatic fibrosis induced by CCl₄, dimethylnitrosamine, bovine serum albumin and bile duct ligation^[136-139]. Although the detailed mechanism varies in different models, the overall effect of bicyclol is derived from stabilizing mitochondrial and hepatocyte membranes, scavenging free radicals, reducing lipid peroxides, enhancing antioxidant gene expression or activity or inhibiting liver cell apoptosis, and thus achieves anti-inflammatory, antioxidant and liver cell-protective activities^[135,140]. These effects of bicyclol and its antiviral activities make bicyclol a promising drug for treating CHC patients with liver injury or co-infection with HBV.

CONCLUSION

Inflammation is a common feature of most liver diseases, and inflammatory cytokines and chemokines produced after HCV infection accelerate hepatocyte damage and liver disease progression. HCV infection triggers inflammation through various mechanisms including pathogen pattern recognition, inflammasome activation and intrahepatic inflammatory cascades, while oxidative and ER stress coexist with and exacerbate inflammation and liver injury (Figures 1 and 2). HCV infection is a predisposing factor in the pathological process, but the long-term inflammatory responses and oxidative stress induced by the virus might further destroy the liver microenvironment and cause irreversible liver tissue damage^[7,11]. Direct antiviral therapy might not be sufficient to stop the progression of liver disease in the context of inflammation, oxidative stress, liver tissue damage and metabolic dysregulation. Although anti-inflammatory/hepatoprotective drugs might not provide a fast-acting remedy for the treatment of HCV infection as DAAs do, they can serve as an adjunct to DAAs by exerting comprehensive effects. These effects include the following: (1) decreasing uncontrolled inflammatory cytokine and chemokine levels; (2) directly protecting against oxidative stress or enhancing antioxidant gene expression; (3) restoring mitochondrial function, regulating liver enzyme levels and protecting against liver cell damage; (4) inhibiting HCV replication; and (5) improving the efficacy of IFN antiviral therapy *in vivo*^[80,129,141]. Given the status of excessive inflammation and liver microenvironment dyshomeostasis in chronic HCV-infected patients, care for hepatitis C should extend beyond merely achieving an SVR to encompass an anti-inflammatory/hepatoprotective strategy concurrently with

or after DAA therapy. Meanwhile, their anti-HCV effects could prevent HCV relapse after the DAA treatment.

REFERENCES

- 1 **Rebbani K**, Tsukiyama-Kohara K. HCV-Induced Oxidative Stress: Battlefield-Winning Strategy. *Oxid Med Cell Longev* 2016; **2016**: 7425628 [PMID: 27293514 DOI: 10.1155/2016/7425628]
- 2 **Perlin CM**, Ferreira VL, Borba HHL, Wiens A, Ivantes CAP, Lenzi L, Pontarolo R. Quality of life in Brazilian patients with treated or untreated chronic hepatitis C. *Rev Inst Med Trop Sao Paulo* 2017; **59**: e81 [PMID: 29267589 DOI: 10.1590/S1678-9946201759081]
- 3 **Wong RJ**, Gish RG. Metabolic Manifestations and Complications Associated With Chronic Hepatitis C Virus Infection. *Gastroenterol Hepatol* (NY) 2016; **12**: 293-299 [PMID: 27499712]
- 4 **Heim MH**, Thimme R. Innate and adaptive immune responses in HCV infections. *J Hepatol* 2014; **61**: S14-S25 [PMID: 25443342 DOI: 10.1016/j.jhep.2014.06.035]
- 5 **Zeremski M**, Petrovic LM, Talal AH. The role of chemokines as inflammatory mediators in chronic hepatitis C virus infection. *J Viral Hepat* 2007; **14**: 675-687 [PMID: 17875002 DOI: 10.1111/j.1365-2893.2006.00838.x]
- 6 **Geddawy A**, Ibrahim YF, Elbahie NM, Ibrahim MA. Direct Acting Anti-hepatitis C Virus Drugs: Clinical Pharmacology and Future Direction. *J Transl Int Med* 2017; **5**: 8-17 [PMID: 28680834 DOI: 10.1515/jtim-2017-0007]
- 7 **Conti F**, Buonfiglioli F, Scuteri A, Crespi C, Bolondi L, Caraceni P, Foschi FG, Lenzi M, Mazzella G, Verucchi G, Andreone P, Brillanti S. Early occurrence and recurrence of hepatocellular carcinoma in HCV-related cirrhosis treated with direct-acting antivirals. *J Hepatol* 2016; **65**: 727-733 [PMID: 27349488 DOI: 10.1016/j.jhep.2016.06.015]
- 8 **Huang JF**, Yu ML, Dai CY, Chuang WL. Glucose abnormalities in hepatitis C virus infection. *Kaohsiung J Med Sci* 2013; **29**: 61-68 [PMID: 23347806 DOI: 10.1016/j.kjms.2012.11.001]
- 9 **D'Elia RV**, Harrison K, Oyston PC, Lukaszewski RA, Clark GC. Targeting the "cytokine storm" for therapeutic benefit. *Clin Vaccine Immunol* 2013; **20**: 319-327 [PMID: 23283640 DOI: 10.1128/CVI.00636-12]
- 10 **Huang CF**, Hsieh MY, Yang JF, Chen WC, Yeh ML, Huang CI, Dai CY, Yu ML, Lin ZY, Chen SC, Chuang WL, Huang JF. Serum hs-CRP was correlated with treatment response to pegylated interferon and ribavirin combination therapy in chronic hepatitis C patients. *Hepatol Int* 2010; **4**: 621-627 [PMID: 21063486 DOI: 10.1007/s12072-010-9200-8]
- 11 **Morgan TR**, Ghany MG, Kim HY, Snow KK, Shiffman ML, De Santo JL, Lee WM, Di Bisceglie AM, Bonkovsky HL, Dienstag JL, Morishima C, Lindsay KL, Lok AS; HALT-C Trial Group. Outcome of sustained virological responders with histologically advanced chronic hepatitis C. *Hepatology* 2010; **52**: 833-844 [PMID: 20564351 DOI: 10.1002/hep.23744]
- 12 **Hsu CC**, Lien JC, Chang CW, Chang CH, Kuo SC, Huang TF. Yuwen02f1 suppresses LPS-induced endotoxemia and adjuvant-induced arthritis primarily through blockade of ROS formation, NFkB and MAPK activation. *Biochem Pharmacol* 2013; **85**: 385-395 [PMID: 23142712 DOI: 10.1016/j.bcp.2012.11.002]
- 13 **Costantini S**, Capone F, Guerriero E, Maio P, Colonna G, Castello G. Serum cytokine levels as putative prognostic markers in the progression of chronic HCV hepatitis to cirrhosis. *Eur Cytokine Netw* 2010; **21**: 251-256 [PMID: 21081303 DOI: 10.1684/ecn.2010.0214]
- 14 **Zeremski M**, Dimova R, Brown Q, Jacobson IM, Markatou M, Talal AH. Peripheral CXCR3-associated chemokines as biomarkers of fibrosis in chronic hepatitis C virus infection. *J Infect Dis* 2009; **200**: 1774-1780 [PMID: 19848607 DOI: 10.1086/646614]
- 15 **Zampino R**, Marrone A, Restivo L, Guerrera B, Sellitto A, Rinaldi L, Romano C, Adinolfi LE. Chronic HCV infection and inflammation: Clinical impact on hepatic and extra-hepatic

- manifestations. *World J Hepatol* 2013; **5**: 528-540 [PMID: 24179612 DOI: 10.4254/wjh.v5.i10.528]
- 16 Neuman MG, Schmilovitz-Weiss H, Hilzenrat N, Bourliere M, Marcellin P, Trepo C, Mazulli T, Moussa G, Patel A, Baig AA, Cohen L. Markers of inflammation and fibrosis in alcoholic hepatitis and viral hepatitis C. *Int J Hepatol* 2012; **2012**: 231210 [PMID: 22530132 DOI: 10.1155/2012/231210]
 - 17 Jonsson JR, Barrie HD, O'Rourke P, Clouston AD, Powell EE. Obesity and steatosis influence serum and hepatic inflammatory markers in chronic hepatitis C. *Hepatology* 2008; **48**: 80-87 [PMID: 18571785 DOI: 10.1002/hep.22311]
 - 18 Aroucha DC, do Carmo RF, Moura P, Silva JL, Vasconcelos LR, Cavalcanti MS, Muniz MT, Aroucha ML, Siqueira ER, Cahú GG, Pereira LM, Coêlho MR. High tumor necrosis factor- α /interleukin-10 ratio is associated with hepatocellular carcinoma in patients with chronic hepatitis C. *Cytokine* 2013; **62**: 421-425 [PMID: 23602201 DOI: 10.1016/j.cyt.2013.03.024]
 - 19 Knobler H, Schattner A. TNF- α , chronic hepatitis C and diabetes: a novel triad. *QJM* 2005; **98**: 1-6 [PMID: 15625348 DOI: 10.1093/qjmed/hci001]
 - 20 Falasca K, Ucciferri C, Dalessandro M, Zingariello P, Mancino P, Petrarca C, Pizzigallo E, Conti P, Vecchiet J. Cytokine patterns correlate with liver damage in patients with chronic hepatitis B and C. *Ann Clin Lab Sci* 2006; **36**: 144-150 [PMID: 16682509]
 - 21 Jia H, Du J, Zhu S, Ma Y, Cai H. Clinical observation of serum IL-18, IL-10 and sIL-2R levels in patients with chronic hepatitis C pre- and post antiviral treatment. *Chin Med J (Engl)* 2003; **116**: 605-608 [PMID: 12875732]
 - 22 Fallahi P, Ferrari SM, Giuggioli D, Sebastiani M, Colaci M, Ferri C, Antonelli A. Chemokines in the Pathogenesis and as Therapeutical Markers and Targets of HCV Chronic Infection and HCV Extrahepatic Manifestations. *Curr Drug Targets* 2017; **18**: 786-793 [PMID: 26240054 DOI: 10.2174/1389450116666150804105937]
 - 23 Larrubia JR, Benito-Martínez S, Calvino M, Sanz-de-Villalobos E, Parra-Cid T. Role of chemokines and their receptors in viral persistence and liver damage during chronic hepatitis C virus infection. *World J Gastroenterol* 2008; **14**: 7149-7159 [PMID: 19084927 DOI: 10.3748/wjg.14.7149]
 - 24 You CR, Park SH, Jeong SW, Woo HY, Bae SH, Choi JY, Sung YC, Yoon SK. Serum IP-10 Levels Correlate with the Severity of Liver Histopathology in Patients Infected with Genotype-1 HCV. *Gut Liver* 2011; **5**: 506-512 [PMID: 22195251 DOI: 10.5009/gnl.2011.5.4.506]
 - 25 Harvey CE, Post JJ, Palladinetti P, Freeman AJ, Ffrench RA, Kumar RK, Marinos G, Lloyd AR. Expression of the chemokine IP-10 (CXCL10) by hepatocytes in chronic hepatitis C virus infection correlates with histological severity and lobular inflammation. *J Leukoc Biol* 2003; **74**: 360-369 [PMID: 12949239 DOI: 10.1189/jlb.0303093]
 - 26 Larrubia JR, Calvino M, Benito S, Sanz-de-Villalobos E, Perna C, Pérez-Hornedo J, González-Mateos F, García-Garzón S, Bienvenido A, Parra T. The role of CCR5/CXCR3 expressing CD8⁺ cells in liver damage and viral control during persistent hepatitis C virus infection. *J Hepatol* 2007; **47**: 632-641 [PMID: 17560677 DOI: 10.1016/j.jhep.2007.04.009]
 - 27 Butera D, Marukian S, Iwamaye AE, Hembrador E, Chambers TJ, Di Bisceglie AM, Charles ED, Talal AH, Jacobson IM, Rice CM, Dustin LB. Plasma chemokine levels correlate with the outcome of antiviral therapy in patients with hepatitis C. *Blood* 2005; **106**: 1175-1182 [PMID: 15860662 DOI: 10.1182/blood-2005-01-0126]
 - 28 Yamauchi K, Akbar SM, Horike N, Michitaka K, Onji M. Increased serum levels of macrophage inflammatory protein-3 α in chronic viral hepatitis: prognostic importance of macrophage inflammatory protein-3 α during interferon therapy in chronic hepatitis C. *J Viral Hepat* 2002; **9**: 213-220 [PMID: 12010510 DOI: 10.1046/j.1365-2893.2002.00354.x]
 - 29 Kaplanski G, Farnarier C, Payan MJ, Bongrand P, Durand JM. Increased levels of soluble adhesion molecules in the serum of patients with hepatitis C. Correlation with cytokine concentrations and liver inflammation and fibrosis. *Dig Dis Sci* 1997; **42**: 2277-2284 [PMID: 9398806 DOI: 10.1023/A:1018818801824]
 - 30 Fukuda R, Ishimura N, Ishihara S, Chowdhury A, Moriyama N, Nogami C, Miyake T, Niigaki M, Tokuda A, Satoh S, Sakai S, Akagi S, Watanabe M, Fukumoto S. Intrahepatic expression of pro-inflammatory cytokine mRNAs and interferon efficacy in chronic hepatitis C. *Liver* 1996; **16**: 390-399 [PMID: 9021719 DOI: 10.1111/j.1600-0676.1996.tb00768.x]
 - 31 Nishitsuji H, Funami K, Shimizu Y, Ujino S, Sugiyama K, Seya T, Takaku H, Shimotohno K. Hepatitis C virus infection induces inflammatory cytokines and chemokines mediated by the cross talk between hepatocytes and stellate cells. *J Virol* 2013; **87**: 8169-8178 [PMID: 23678168 DOI: 10.1128/JVI.00974-13]
 - 32 Li K, Li NL, Wei D, Pfeffer SR, Fan M, Pfeffer LM. Activation of chemokine and inflammatory cytokine response in hepatitis C virus-infected hepatocytes depends on Toll-like receptor 3 sensing of hepatitis C virus double-stranded RNA intermediates. *Hepatology* 2012; **55**: 666-675 [PMID: 22030901 DOI: 10.1002/hep.24763]
 - 33 Wagoner J, Austin M, Green J, Imaizumi T, Casola A, Brasier A, Khabar KS, Wakita T, Gale M Jr, Polyak SJ. Regulation of CXCL-8 (interleukin-8) induction by double-stranded RNA signaling pathways during hepatitis C virus infection. *J Virol* 2007; **81**: 309-318 [PMID: 17035306 DOI: 10.1128/JVI.01411-06]
 - 34 Chattergoon MA, Latanich R, Quinn J, Winter ME, Buckheit RW 3rd, Blankson JN, Pardoll D, Cox AL. HIV and HCV activate the inflammasome in monocytes and macrophages via endosomal Toll-like receptors without induction of type 1 interferon. *PLoS Pathog* 2014; **10**: e1004082 [PMID: 24788318 DOI: 10.1371/journal.ppat.1004082]
 - 35 Negash AA, Ramos HJ, Crochet N, Lau DT, Doehle B, Papic N, Delker DA, Jo J, Bertoletti A, Hagedorn CH, Gale M Jr. IL-1 β production through the NLRP3 inflammasome by hepatic macrophages links hepatitis C virus infection with liver inflammation and disease. *PLoS Pathog* 2013; **9**: e1003330 [PMID: 23633957 DOI: 10.1371/journal.ppat.1003330]
 - 36 Dolganiuc A, Oak S, Kodys K, Golenbock DT, Finberg RW, Kurt-Jones E, Szabo G. Hepatitis C core and nonstructural 3 proteins trigger toll-like receptor 2-mediated pathways and inflammatory activation. *Gastroenterology* 2004; **127**: 1513-1524 [PMID: 15521019 DOI: 10.1053/j.gastro.2004.08.067]
 - 37 Machida K, Cheng KT, Sung VM, Levine AM, Fount S, Lai MM. Hepatitis C virus induces toll-like receptor 4 expression, leading to enhanced production of beta interferon and interleukin-6. *J Virol* 2006; **80**: 866-874 [PMID: 16378988 DOI: 10.1128/JVI.80.2.866-874.2006]
 - 38 Nattermann J, Nischalke HD, Feldmann G, Ahlenstiel G, Sauerbruch T, Spengler U. Binding of HCV E2 to CD81 induces RANTES secretion and internalization of CC chemokine receptor 5. *J Liver Hepat* 2004; **11**: 519-526 [PMID: 15500552 DOI: 10.1111/j.1365-2893.2004.00545.x]
 - 39 Yu GY, He G, Li CY, Tang M, Grivennikov S, Tsai WT, Wu MS, Hsu CW, Tsai Y, Wang LH, Karin M. Hepatic expression of HCV RNA-dependent RNA polymerase triggers innate immune signaling and cytokine production. *Mol Cell* 2012; **48**: 313-321 [PMID: 22959272 DOI: 10.1016/j.molcel.2012.07.032]
 - 40 Basu A, Meyer K, Lai KK, Saito K, Di Bisceglie AM, Grosso LE, Ray RB, Ray R. Microarray analyses and molecular profiling of Stat3 signaling pathway induced by hepatitis C virus core protein in human hepatocytes. *Virology* 2006; **349**: 347-358 [PMID: 16545852 DOI: 10.1016/j.virol.2006.02.023]
 - 41 Davis BK, Wen H, Ting JP. The inflammasome NLRs in immunity, inflammation, and associated diseases. *Annu Rev Immunol* 2011; **29**: 707-735 [PMID: 21219188 DOI: 10.1146/annurev-immunol-031210-101405]
 - 42 Martinon F, Burns K, Tschopp J. The inflammasome: a molecular platform triggering activation of inflammatory caspases and processing of proIL-beta. *Mol Cell* 2002; **10**: 417-426 [PMID: 12191486 DOI: 10.1016/S1097-2765(02)00599-3]
 - 43 Capone F, Guerriero E, Colonna G, Maio P, Mangia A, Castello G, Costantini S. Cytokine profile evaluation in patients with hepatitis C virus infection. *World J Gastroenterol* 2014; **20**:

- 9261-9269 [PMID: 25071319 DOI: 10.3748/wjg.v20.i28.9261]
- 44 **Chen W**, Xu Y, Li H, Tao W, Xiang Y, Huang B, Niu J, Zhong J, Meng G. HCV genomic RNA activates the NLRP3 inflammasome in human myeloid cells. *PLoS One* 2014; **9**: e84953 [PMID: 24400125 DOI: 10.1371/journal.pone.0084953]
 - 45 **Shrivastava S**, Mukherjee A, Ray R, Ray RB. Hepatitis C virus induces interleukin-1 β (IL-1 β)/IL-18 in circulatory and resident liver macrophages. *J Virol* 2013; **87**: 12284-12290 [PMID: 24006444 DOI: 10.1128/JVI.01962-13]
 - 46 **Burdette D**, Haskett A, Presser L, McRae S, Iqbal J, Waris G. Hepatitis C virus activates interleukin-1 β via caspase-1-inflammasome complex. *J Gen Virol* 2012; **93**: 235-246 [PMID: 21994322 DOI: 10.1099/vir.0.034033-0]
 - 47 **Farag NS**, Breiting U, El-Azizi M, Breiting HG. The p7 viroporin of the hepatitis C virus contributes to liver inflammation by stimulating production of Interleukin-1 β . *Biochim Biophys Acta Mol Basis Dis* 2017; **1863**: 712-720 [PMID: 27979709 DOI: 10.1016/j.bbdis.2016.12.006]
 - 48 **Vollmar B**, Menger MD. The hepatic microcirculation: mechanistic contributions and therapeutic targets in liver injury and repair. *Physiol Rev* 2009; **89**: 1269-1339 [PMID: 19789382 DOI: 10.1152/physrev.00027.2008]
 - 49 **Atzori L**, Poli G, Perra A. Hepatic stellate cell: a star cell in the liver. *Int J Biochem Cell Biol* 2009; **41**: 1639-1642 [PMID: 19433304 DOI: 10.1016/j.biocel.2009.03.001]
 - 50 **Sidiropoulos K**, Viteri G, Sevilla C, Jupe S, Webber M, Orlic-Milacic M, Jassal B, May B, Shamovsky V, Duenas C, Rothfels K, Matthews L, Song H, Stein L, Haw R, D'Eustachio P, Ping P, Hermjakob H, Fabregat A. Reactome enhanced pathway visualization. *Bioinformatics* 2017; **33**: 3461-3467 [PMID: 29077811 DOI: 10.1093/bioinformatics/btx441]
 - 51 **Schulze-Krebs A**, Preimel D, Popov Y, Bartenschlager R, Lohmann V, Pinzani M, Schuppan D. Hepatitis C virus-replicating hepatocytes induce fibrogenic activation of hepatic stellate cells. *Gastroenterology* 2005; **129**: 246-258 [PMID: 16012951 DOI: 10.1053/j.gastro.2005.03.089]
 - 52 **Devhare PB**, Sasaki R, Shrivastava S, Di Bisceglie AM, Ray R, Ray RB. Exosome-Mediated Intercellular Communication between Hepatitis C Virus-Infected Hepatocytes and Hepatic Stellate Cells. *J Virol* 2017; **91** [PMID: 28077652 DOI: 10.1128/JVI.02225-16]
 - 53 **Florimond A**, Chouteau P, Bruscella P, Le Seyec J, Mèroux E, Ahnou N, Mallat A, Lotersztajn S, Pawlotsky JM. Human hepatic stellate cells are not permissive for hepatitis C virus entry and replication. *Gut* 2015; **64**: 957-965 [PMID: 25063678 DOI: 10.1136/gutjnl-2013-305634]
 - 54 **Sasaki R**, Devhare PB, Steele R, Ray R, Ray RB. Hepatitis C virus-induced CCL5 secretion from macrophages activates hepatic stellate cells. *Hepatology* 2017; **66**: 746-757 [PMID: 28318046 DOI: 10.1002/hep.29170]
 - 55 **Takahashi K**, Asabe S, Wieland S, Garaigorta U, Gastaminza P, Isogawa M, Chisari FV. Plasmacytoid dendritic cells sense hepatitis C virus-infected cells, produce interferon, and inhibit infection. *Proc Natl Acad Sci USA* 2010; **107**: 7431-7436 [PMID: 20231459 DOI: 10.1073/pnas.1002301107]
 - 56 **Brault C**, Levy PL, Bartosch B. Hepatitis C virus-induced mitochondrial dysfunctions. *Viruses* 2013; **5**: 954-980 [PMID: 23518579 DOI: 10.3390/v5030954]
 - 57 **Fujita N**, Sugimoto R, Ma N, Tanaka H, Iwasa M, Kobayashi Y, Kawanishi S, Watanabe S, Kaito M, Takei Y. Comparison of hepatic oxidative DNA damage in patients with chronic hepatitis B and C. *J Viral Hepat* 2008; **15**: 498-507 [PMID: 18331251 DOI: 10.1111/j.1365-2893.2008.00972.x]
 - 58 **Ivanov AV**, Bartosch B, Smirnova OA, Isagulians MG, Kochetkov SN. HCV and oxidative stress in the liver. *Viruses* 2013; **5**: 439-469 [PMID: 23358390 DOI: 10.3390/v5020439]
 - 59 **Tsutsumi T**, Matsuda M, Aizaki H, Moriya K, Miyoshi H, Fujie H, Shintani Y, Yotsuyanagi H, Miyamura T, Suzuki T, Koike K. Proteomics analysis of mitochondrial proteins reveals overexpression of a mitochondrial protein chaperon, prohibitin, in cells expressing hepatitis C virus core protein. *Hepatology* 2009; **50**: 378-386 [PMID: 19591124 DOI: 10.1002/hep.22998]
 - 60 **de Mochel NS**, Seronello S, Wang SH, Ito C, Zheng JX, Liang TJ, Lambeth JD, Choi J. Hepatocyte NAD(P)H oxidases as an endogenous source of reactive oxygen species during hepatitis C virus infection. *Hepatology* 2010; **52**: 47-59 [PMID: 20578128 DOI: 10.1002/hep.23671]
 - 61 **Boudreau HE**, Emerson SU, Korzeniowska A, Jendrysik MA, Leto TL. Hepatitis C virus (HCV) proteins induce NADPH oxidase 4 expression in a transforming growth factor beta-dependent manner: a new contributor to HCV-induced oxidative stress. *J Virol* 2009; **83**: 12934-12946 [PMID: 19812163 DOI: 10.1128/JVI.01059-09]
 - 62 **Reuter S**, Gupta SC, Chaturvedi MM, Aggarwal BB. Oxidative stress, inflammation, and cancer: how are they linked? *Free Radic Biol Med* 2010; **49**: 1603-1616 [PMID: 20840865 DOI: 10.1016/j.freeradbiomed.2010.09.006]
 - 63 **Kuroki M**, Ariumi Y, Ikeda M, Dansako H, Wakita T, Kato N. Arsenic trioxide inhibits hepatitis C virus RNA replication through modulation of the glutathione redox system and oxidative stress. *J Virol* 2009; **83**: 2338-2348 [PMID: 19109388 DOI: 10.1128/JVI.01840-08]
 - 64 **Presser LD**, McRae S, Waris G. Activation of TGF- β 1 promoter by hepatitis C virus-induced AP-1 and Sp1: role of TGF- β 1 in hepatic stellate cell activation and invasion. *PLoS One* 2013; **8**: e56367 [PMID: 23437118 DOI: 10.1371/journal.pone.0056367]
 - 65 **Machida K**, Cheng KT, Lai CK, Jeng KS, Sung VM, Lai MM. Hepatitis C virus triggers mitochondrial permeability transition with production of reactive oxygen species, leading to DNA damage and STAT3 activation. *J Virol* 2006; **80**: 7199-7207 [PMID: 16809325 DOI: 10.1128/JVI.00321-06]
 - 66 **Tardif KD**, Waris G, Siddiqui A. Hepatitis C virus, ER stress, and oxidative stress. *Trends Microbiol* 2005; **13**: 159-163 [PMID: 15817385 DOI: 10.1016/j.tim.2005.02.004]
 - 67 **von dem Bussche A**, Machida R, Li K, Loevinsohn G, Khander A, Wang J, Wakita T, Wands JR, Li J. Hepatitis C virus NS2 protein triggers endoplasmic reticulum stress and suppresses its own viral replication. *J Hepatol* 2010; **53**: 797-804 [PMID: 20801537 DOI: 10.1016/j.jhep.2010.05.022]
 - 68 **Liberman E**, Fong YL, Selby MJ, Choo QL, Cousens L, Houghton M, Yen TS. Activation of the grp78 and grp94 promoters by hepatitis C virus E2 envelope protein. *J Virol* 1999; **73**: 3718-3722 [PMID: 10196264]
 - 69 **Merquiol E**, Uzi D, Mueller T, Goldenberg D, Nahmias Y, Xavier RJ, Tirosh B, Shibolet O. HCV causes chronic endoplasmic reticulum stress leading to adaptation and interference with the unfolded protein response. *PLoS One* 2011; **6**: e24660 [PMID: 21949742 DOI: 10.1371/journal.pone.0024660]
 - 70 **Hasnain SZ**, Lourie R, Das I, Chen AC, McGuckin MA. The interplay between endoplasmic reticulum stress and inflammation. *Immunol Cell Biol* 2012; **90**: 260-270 [PMID: 22249202 DOI: 10.1038/icb.2011.112]
 - 71 **Waris G**, Tardif KD, Siddiqui A. Endoplasmic reticulum (ER) stress: hepatitis C virus induces an ER-nucleus signal transduction pathway and activates NF-kappaB and STAT-3. *Biochem Pharmacol* 2002; **64**: 1425-1430 [PMID: 12417255 DOI: 10.1016/S0006-2952(02)01300-X]
 - 72 **Kacheva S**, Lenzen S, Gurgul-Convey E. Differential effects of proinflammatory cytokines on cell death and ER stress in insulin-secreting INS1E cells and the involvement of nitric oxide. *Cytokine* 2011; **55**: 195-201 [PMID: 21531147 DOI: 10.1016/j.cyt.2011.04.002]
 - 73 **Xue X**, Piao JH, Nakajima A, Sakon-Komazawa S, Kojima Y, Mori K, Yagita H, Okumura K, Harding H, Nakano H. Tumor necrosis factor alpha (TNFalpha) induces the unfolded protein response (UPR) in a reactive oxygen species (ROS)-dependent fashion, and the UPR counteracts ROS accumulation by TNFalpha. *J Biol Chem* 2005; **280**: 33917-33925 [PMID: 16107336 DOI: 10.1074/jbc.M505818200]
 - 74 **Federico A**, Aitella E, Sgambato D, Savoia A, De Bartolomeis F, Dallio M, Ruocco E, Pezone L, Abbondanza C, Loguercio C,

- Astarita C. Telaprevir may induce adverse cutaneous reactions by a T cell immune-mediated mechanism. *Ann Hepatol* 2015; **14**: 420-424 [PMID: 25864225]
- 75 **Kim S**, Han KH, Ahn SH. Hepatitis C Virus and Antiviral Drug Resistance. *Gut Liver* 2016; **10**: 890-895 [PMID: 27784846 DOI: 10.5009/gnl15573]
 - 76 **Dyson JK**, Hutchinson J, Harrison L, Rotimi O, Tiniakos D, Foster GR, Aldersley MA, McPherson S. Liver toxicity associated with sofosbuvir, an NS5A inhibitor and ribavirin use. *J Hepatol* 2016; **64**: 234-238 [PMID: 26325535 DOI: 10.1016/j.jhep.2015.07.041]
 - 77 **Wang C**, Ji D, Chen J, Shao Q, Li B, Liu J, Wu V, Wong A, Wang Y, Zhang X, Lu L, Wong C, Tsang S, Zhang Z, Sun J, Hou J, Chen G, Lau G. Hepatitis due to Reactivation of Hepatitis B Virus in Endemic Areas Among Patients With Hepatitis C Treated With Direct-acting Antiviral Agents. *Clin Gastroenterol Hepatol* 2017; **15**: 132-136 [PMID: 27392759 DOI: 10.1016/j.cgh.2016.06.023]
 - 78 **Lam P**, Cheung F, Tan HY, Wang N, Yuen MF, Feng Y. Hepatoprotective Effects of Chinese Medicinal Herbs: A Focus on Anti-Inflammatory and Anti-Oxidative Activities. *Int J Mol Sci* 2016; **17**: 465 [PMID: 27043533 DOI: 10.3390/ijms17040465]
 - 79 **Chua LS**. Review on liver inflammation and antiinflammatory activity of *Andrographis paniculata* for hepatoprotection. *Phytother Res* 2014; **28**: 1589-1598 [PMID: 25043965 DOI: 10.1002/ptr.5193]
 - 80 **Domitrović R**, Potočnjak I. A comprehensive overview of hepatoprotective natural compounds: mechanism of action and clinical perspectives. *Arch Toxicol* 2016; **90**: 39-79 [PMID: 26377694 DOI: 10.1007/s00204-015-1580-z]
 - 81 **Kriss M**, Burchill M. HCV and nonhepatic malignancy: Is pre-emptive direct-acting antiviral therapy indicated prior to treatment? *Hepatology* 2018; **67**: 4-6 [PMID: 28768054 DOI: 10.1002/hep.29414]
 - 82 **Federico A**, Dallio M, Loguercio C. Silymarin/Silybin and Chronic Liver Disease: A Marriage of Many Years. *Molecules* 2017; **22** [PMID: 28125040 DOI: 10.3390/molecules22020191]
 - 83 **Neha**, Jaggi AS, Singh N. Silymarin and Its Role in Chronic Diseases. *Adv Exp Med Biol* 2016; **929**: 25-44 [PMID: 27771919 DOI: 10.1007/978-3-319-41342-6_2]
 - 84 **Polyak SJ**, Ferenci P, Pawlotsky JM. Hepatoprotective and antiviral functions of silymarin components in hepatitis C virus infection. *Hepatology* 2013; **57**: 1262-1271 [PMID: 23213025 DOI: 10.1002/hep.26179]
 - 85 **Stanca E**, Serviddio G, Bellanti F, Vendemiale G, Siculella L, Giudetti AM. Down-regulation of LPCAT expression increases platelet-activating factor level in cirrhotic rat liver: potential antiinflammatory effect of silybin. *Biochim Biophys Acta* 2013; **1832**: 2019-2026 [PMID: 23851051 DOI: 10.1016/j.bbadis.2013.07.005]
 - 86 **Gordon A**, Hobbs DA, Bowden DS, Bailey MJ, Mitchell J, Francis AJ, Roberts SK. Effects of Silybum marianum on serum hepatitis C virus RNA, alanine aminotransferase levels and well-being in patients with chronic hepatitis C. *J Gastroenterol Hepatol* 2006; **21**: 275-280 [PMID: 16460486 DOI: 10.1111/j.1440-1746.2006.04138.x]
 - 87 **Hawke RL**, Schrieber SJ, Soule TA, Wen Z, Smith PC, Reddy KR, Wahed AS, Belle SH, Afdhal NH, Navarro VJ, Berman J, Liu QY, Doo E, Fried MW, SyNCH Trial Group. Silymarin ascending multiple oral dosing phase I study in noncirrhotic patients with chronic hepatitis C. *J Clin Pharmacol* 2010; **50**: 434-449 [PMID: 19841158 DOI: 10.1177/0091270009347475]
 - 88 **Wen Z**, Dumas TE, Schrieber SJ, Hawke RL, Fried MW, Smith PC. Pharmacokinetics and metabolic profile of free, conjugated, and total silymarin flavonolignans in human plasma after oral administration of milk thistle extract. *Drug Metab Dispos* 2008; **36**: 65-72 [PMID: 17913795 DOI: 10.1124/dmd.107.017566]
 - 89 **Ferenci P**, Scherzer TM, Kerschner H, Rutter K, Beinhardt S, Hofer H, Schöniger-Hekele M, Holzmann H, Steindl-Munda P. Silibinin is a potent antiviral agent in patients with chronic hepatitis C not responding to pegylated interferon/ribavirin therapy. *Gastroenterology* 2008; **135**: 1561-1567 [PMID: 18771667 DOI: 10.1053/j.gastro.2008.07.072]
 - 90 **Rutter K**, Scherzer TM, Beinhardt S, Kerschner H, Stättermayer AF, Hofer H, Popow-Kraupp T, Steindl-Munda P, Ferenci P. Intravenous silibinin as 'rescue treatment' for on-treatment non-responders to pegylated interferon/ribavirin combination therapy. *Antivir Ther* 2011; **16**: 1327-1333 [PMID: 22155914 DOI: 10.3851/IMP1942]
 - 91 **Tipoe GL**, Leung TM, Liong EC, Lau TY, Fung ML, Nanji AA. Epigallocatechin-3-gallate (EGCG) reduces liver inflammation, oxidative stress and fibrosis in carbon tetrachloride (CCl₄)-induced liver injury in mice. *Toxicology* 2010; **273**: 45-52 [PMID: 20438794 DOI: 10.1016/j.tox.2010.04.014]
 - 92 **Lee MH**, Yoon S, Moon JO. The flavonoid naringenin inhibits dimethylnitrosamine-induced liver damage in rats. *Biol Pharm Bull* 2004; **27**: 72-76 [PMID: 14709902 DOI: 10.1248/bpb.27.72]
 - 93 **Chao WW**, Lin BF. Isolation and identification of bioactive compounds in *Andrographis paniculata* (Chuanxinlian). *Chin Med* 2010; **5**: 17 [PMID: 20465823 DOI: 10.1186/1749-8546-5-17]
 - 94 **Tsai HR**, Yang LM, Tsai WJ, Chiou WF. Andrographolide acts through inhibition of ERK1/2 and Akt phosphorylation to suppress chemotactic migration. *Eur J Pharmacol* 2004; **498**: 45-52 [PMID: 15363974 DOI: 10.1016/j.ejphar.2004.07.077]
 - 95 **Lim JC**, Chan TK, Ng DS, Sagineedu SR, Stanslas J, Wong WS. Andrographolide and its analogues: versatile bioactive molecules for combating inflammation and cancer. *Clin Exp Pharmacol Physiol* 2012; **39**: 300-310 [PMID: 22017767 DOI: 10.1111/j.1440-1681.2011.05633.x]
 - 96 **Chatuphonprasert W**, Jarukamjorn K, Kondo S, Nemoto N. Synergistic increases of metabolism and oxidation-reduction genes on their expression after combined treatment with a CYP1A inducer and andrographolide. *Chem Biol Interact* 2009; **182**: 233-238 [PMID: 19737545 DOI: 10.1016/j.cbi.2009.09.001]
 - 97 **Jaruchotikamol A**, Jarukamjorn K, Sirisangtrakul W, Sakuma T, Kawasaki Y, Nemoto N. Strong synergistic induction of CYP1A1 expression by andrographolide plus typical CYP1A inducers in mouse hepatocytes. *Toxicol Appl Pharmacol* 2007; **224**: 156-162 [PMID: 17825862 DOI: 10.1016/j.taap.2007.07.008]
 - 98 **Kapil A**, Koul IB, Banerjee SK, Gupta BD. Antihepatotoxic effects of major diterpenoid constituents of *Andrographis paniculata*. *Biochem Pharmacol* 1993; **46**: 182-185 [PMID: 8347130 DOI: 10.1016/0006-2952(93)90364-3]
 - 99 **Suebsasana S**, Pongnaratorn P, Sattayasai J, Arkaravichien T, Tiamkao S, Aromdee C. Analgesic, antipyretic, anti-inflammatory and toxic effects of andrographolide derivatives in experimental animals. *Arch Pharm Res* 2009; **32**: 1191-1200 [PMID: 19784573 DOI: 10.1007/s12272-009-1902-x]
 - 100 **Li J**, Huang W, Zhang H, Wang X, Zhou H. Synthesis of andrographolide derivatives and their TNF- α and IL-6 expression inhibitory activities. *Bioorg Med Chem Lett* 2007; **17**: 6891-6894 [PMID: 17962017 DOI: 10.1016/j.bmcl.2007.10.009]
 - 101 **Lee JC**, Tseng CK, Young KC, Sun HY, Wang SW, Chen WC, Lin CK, Wu YH. Andrographolide exerts anti-hepatitis C virus activity by up-regulating haeme oxygenase-1 via the p38 MAPK/Nrf2 pathway in human hepatoma cells. *Br J Pharmacol* 2014; **171**: 237-252 [PMID: 24117426 DOI: 10.1111/bph.12440]
 - 102 **Chandramohan V**, Kaphle A, Chekuri M, Gangarudraiah S, Bychapur Siddaiah G. Evaluating Andrographolide as a Potent Inhibitor of NS3-4A Protease and Its Drug-Resistant Mutants Using In Silico Approaches. *Adv Virol* 2015; **2015**: 972067 [PMID: 26587022 DOI: 10.1155/2015/972067]
 - 103 **Esatbeyoglu T**, Huebbe P, Ernst IM, Chin D, Wagner AE, Rimbach G. Curcumin--from molecule to biological function. *Angew Chem Int Ed Engl* 2012; **51**: 5308-5332 [PMID: 22566109 DOI: 10.1002/anie.201107724]
 - 104 **Mantzorou M**, Pavlidou E, Vasios G, Tsagalioti E, Giaginis C. Effects of curcumin consumption on human chronic diseases: A narrative review of the most recent clinical data. *Phytother Res* 2018; **32**: 957-975 [PMID: 29468820 DOI: 10.1002/ptr.6037]
 - 105 **Shehzad A**, Rehman G, Lee YS. Curcumin in inflammatory diseases. *Biofactors* 2013; **39**: 69-77 [PMID: 23281076 DOI: 10.1002/biof.1066]
 - 106 **Sordillo PP**, Helson L. Curcumin suppression of cytokine release

- and cytokine storm. A potential therapy for patients with Ebola and other severe viral infections. *In Vivo* 2015; **29**: 1-4 [PMID: 25600522]
- 107 **Tang Y**, Zheng S, Chen A. Curcumin eliminates leptin's effects on hepatic stellate cell activation via interrupting leptin signaling. *Endocrinology* 2009; **150**: 3011-3020 [PMID: 19299451 DOI: 10.1210/en.2008-1601]
 - 108 **Samuhasaneeto S**, Thong-Ngam D, Kulaputana O, Suyasanant D, Klaikeaw N. Curcumin decreased oxidative stress, inhibited NF-kappaB activation, and improved liver pathology in ethanol-induced liver injury in rats. *J Biomed Biotechnol* 2009; **2009**: 981963 [PMID: 19606259 DOI: 10.1155/2009/981963]
 - 109 **Fu Y**, Zheng S, Lin J, Ryerse J, Chen A. Curcumin protects the rat liver from CCl4-caused injury and fibrogenesis by attenuating oxidative stress and suppressing inflammation. *Mol Pharmacol* 2008; **73**: 399-409 [PMID: 18006644 DOI: 10.1124/mol.107.039818]
 - 110 **Chen MH**, Lee MY, Chuang JJ, Li YZ, Ning ST, Chen JC, Liu YW. Curcumin inhibits HCV replication by induction of heme oxygenase-1 and suppression of AKT. *Int J Mol Med* 2012; **30**: 1021-1028 [PMID: 22922731 DOI: 10.3892/ijmm.2012.1096]
 - 111 **Kim K**, Kim KH, Kim HY, Cho HK, Sakamoto N, Cheong J. Curcumin inhibits hepatitis C virus replication via suppressing the Akt-SREBP-1 pathway. *FEBS Lett* 2010; **584**: 707-712 [PMID: 20026048 DOI: 10.1016/j.febslet.2009.12.019]
 - 112 **Anggakusuma**, Colpitts CC, Schang LM, Rachmawati H, Frentzen A, Pfaender S, Behrendt P, Brown RJ, Bankwitz D, Steinmann J, Ott M, Meuleman P, Rice CM, Ploss A, Pietschmann T, Steinmann E. Turmeric curcumin inhibits entry of all hepatitis C virus genotypes into human liver cells. *Gut* 2014; **63**: 1137-1149 [PMID: 23903236 DOI: 10.1136/gutjnl-2012-304299]
 - 113 **Azzam HS**, Goertz C, Fritts M, Jonas WB. Natural products and chronic hepatitis C virus. *Liver Int* 2007; **27**: 17-25 [PMID: 17241377 DOI: 10.1111/j.1478-3231.2006.01408.x]
 - 114 **Yu YY**, Wang QH, Zhu LM, Zhang QB, Xu DZ, Guo YB, Wang CQ, Guo SH, Zhou XQ, Zhang LX. A clinical research on oxymatrine for the treatment of chronic hepatitis B. *Zhonghua Gan Zang Bing Za Zhi* 2002; **10**: 280-281 [PMID: 12223140]
 - 115 **Chen N**, Liu YH, Liu XJ, Chen YR, Guo YH, Liu M. [Oxymatrine inhibits target cell infection in the HCVcc system]. *Zhonghua Gan Zang Bing Za Zhi* 2016; **24**: 40-45 [PMID: 26983388 DOI: 10.3760/cma.j.issn.1007-3418.2016.01.008]
 - 116 **Chen Y**, Li J, Zeng M, Lu L, Qu D, Mao Y, Fan Z, Hua J. [The inhibitory effect of oxymatrine on hepatitis C virus in vitro]. *Zhonghua Gan Zang Bing Za Zhi* 2001; **9** Suppl: 12-14 [PMID: 11509127]
 - 117 **Li J**, Li C, Zeng M. [Preliminary study on therapeutic effect of oxymatrine in treating patients with chronic hepatitis C]. *Zhongguo Zhong Xi Yi Jie He Za Zhi* 1998; **18**: 227-229 [PMID: 11475748]
 - 118 **Li YH**, Wu ZY, Tang S, Zhang X, Wang YX, Jiang JD, Peng ZG, Song DQ. Evolution of matrinic ethanol derivatives as anti-HCV agents from matrine skeleton. *Bioorg Med Chem Lett* 2017; **27**: 1962-1966 [PMID: 28320615 DOI: 10.1016/j.bmcl.2017.03.025]
 - 119 **Basile A**, Pascale M, Franceschelli S, Nieddu E, Mazzei MT, Fossa P, Turco MC, Mazzei M. Matrine modulates HSC70 levels and rescues ΔF508-CFTR. *J Cell Physiol* 2012; **227**: 3317-3323 [PMID: 22170045 DOI: 10.1002/jcp.24028]
 - 120 **Du NN**, Li X, Wang YP, Liu F, Liu YX, Li CX, Peng ZG, Gao LM, Jiang JD, Song DQ. Synthesis, structure-activity relationship and biological evaluation of novel N-substituted matrinic acid derivatives as host heat-stress cognate 70 (Hsc70) down-regulators. *Bioorg Med Chem Lett* 2011; **21**: 4732-4735 [PMID: 21757347 DOI: 10.1016/j.bmcl.2011.06.071]
 - 121 **Peng ZG**, Fan B, Du NN, Wang YP, Gao LM, Li YH, Li YH, Liu F, You XF, Han YX, Zhao ZY, Cen S, Li JR, Song DQ, Jiang JD. Small molecular compounds that inhibit hepatitis C virus replication through destabilizing heat shock cognate 70 messenger RNA. *Hepatology* 2010; **52**: 845-853 [PMID: 20593456 DOI: 10.1002/hep.23766]
 - 122 **Zhao HW**, Zhang ZF, Chai X, Li GQ, Cui HR, Wang HB, Meng YK, Liu HM, Wang JB, Li RS, Bai ZF, Xiao XH. Oxymatrine attenuates CCl4-induced hepatic fibrosis via modulation of TLR4-dependent inflammatory and TGF-β1 signaling pathways. *Int Immunopharmacol* 2016; **36**: 249-255 [PMID: 27179304 DOI: 10.1016/j.intimp.2016.04.040]
 - 123 **Chai NL**, Fu Q, Shi H, Cai CH, Wan J, Xu SP, Wu BY. Oxymatrine liposome attenuates hepatic fibrosis via targeting hepatic stellate cells. *World J Gastroenterol* 2012; **18**: 4199-4206 [PMID: 22919254 DOI: 10.3748/wjg.v18.i31.4199]
 - 124 **Wu XL**, Zeng WZ, Jiang MD, Qin JP, Xu H. Effect of Oxymatrine on the TGFβ-Smad signaling pathway in rats with CCl4-induced hepatic fibrosis. *World J Gastroenterol* 2008; **14**: 2100-2105 [PMID: 18395914 DOI: 10.3748/wjg.14.2100]
 - 125 **Shi GF**, Li Q. Effects of oxymatrine on experimental hepatic fibrosis and its mechanism in vivo. *World J Gastroenterol* 2005; **11**: 268-271 [PMID: 15633229 DOI: 10.3748/wjg.v11.i2.268]
 - 126 **Yang W**, Zeng M, Fan Z, Mao Y, Song Y, Jia Y, Lu L, Chen CW, Peng YS, Zhu HY. [Prophylactic and therapeutic effect of oxymatrine on D-galactosamine-induced rat liver fibrosis]. *Zhonghua Gan Zang Bing Za Zhi* 2002; **10**: 193-196 [PMID: 12113677]
 - 127 **Liu Y**, Xu Y, Ji W, Li X, Sun B, Gao Q, Su C. Anti-tumor activities of matrine and oxymatrine: literature review. *Tumour Biol* 2014; **35**: 5111-5119 [PMID: 24526416 DOI: 10.1007/s13277-014-1680-z]
 - 128 **Lao Y**. Clinical study on effect of matrine injection to protect the liver function for patients with primary hepatic carcinoma after trans-artery chemo-embolization (TAE). *Zhong Yao Cai* 2005; **28**: 637-638 [PMID: 16252735]
 - 129 **Weiskirchen R**. Hepatoprotective and Anti-fibrotic Agents: It's Time to Take the Next Step. *Front Pharmacol* 2016; **6**: 303 [PMID: 26779021 DOI: 10.3389/fphar.2015.00303]
 - 130 **Huang H**, Chen Y, Ye J. Inhibition of hepatitis C virus replication by peroxidation of arachidonate and restoration by vitamin E. *Proc Natl Acad Sci USA* 2007; **104**: 18666-18670 [PMID: 18003907 DOI: 10.1073/pnas.0708423104]
 - 131 **Melhem A**, Stern M, Shibolet O, Israeli E, Ackerman Z, Pappo O, Hemed N, Rowe M, Ohana H, Zabrecky G, Cohen R, Ilan Y. Treatment of chronic hepatitis C virus infection via antioxidants: results of a phase I clinical trial. *J Clin Gastroenterol* 2005; **39**: 737-742 [PMID: 16082287]
 - 132 **Tee HP**, Kaffes AJ. Non-small-bowel lesions encountered during double-balloon enteroscopy performed for obscure gastrointestinal bleeding. *World J Gastroenterol* 2010; **16**: 1885-1889 [PMID: 20397267 DOI: 10.3748/wjg.v16.i15.1885]
 - 133 **Beloqui O**, Prieto J, Suárez M, Gil B, Qian CH, García N, Civeira MP. N-acetyl cysteine enhances the response to interferon-alpha in chronic hepatitis C: a pilot study. *J Interferon Res* 1993; **13**: 279-282 [PMID: 8228388]
 - 134 **Yang XY**, Zhuo Q, Wu TX, Liu GJ. Bicyclol for chronic hepatitis C. *Cochrane Database Syst Rev* 2007; **CD004994** [PMID: 17253534 DOI: 10.1002/14651858.CD004994.pub2]
 - 135 **Liu GT**. Bicyclol: a novel drug for treating chronic viral hepatitis B and C. *Med Chem* 2009; **5**: 29-43 [PMID: 19149648 DOI: 10.2174/157340609787049316]
 - 136 **Zhen YZ**, Li NR, He HW, Zhao SS, Zhang GL, Hao XF, Shao RG. Protective effect of bicyclol against bile duct ligation-induced hepatic fibrosis in rats. *World J Gastroenterol* 2015; **21**: 7155-7164 [PMID: 26109801 DOI: 10.3748/wjg.v21.i23.7155]
 - 137 **Gu Y**, Zhao J, Yao XM, Li Y. Effects of bicyclol on immunological liver fibrosis in rats. *J Asian Nat Prod Res* 2010; **12**: 388-398 [PMID: 20496196 DOI: 10.1080/10286021003789047]
 - 138 **Hu QW**, Liu GT. Effects of bicyclol on dimethylnitrosamine-induced liver fibrosis in mice and its mechanism of action. *Life Sci* 2006; **79**: 606-612 [PMID: 16603200 DOI: 10.1016/j.lfs.2006.02.025]
 - 139 **Li Y**, Li Y, Liu GT. [Protective effects of bicyclol on liver fibrosis induced by carbon tetrachloride]. *Zhonghua Yi Xue Za Zhi* 2004; **84**: 2096-2101 [PMID: 15730626 DOI: 10.3760/j.issn:0376-2491.2004.24.012]
 - 140 **Lou XE**, Xu N, Yao HP, Chen Z. Bicyclol attenuates pro-

inflammatory cytokine and chemokine productions in CpG-DNA-stimulated L02 hepatocytes by inhibiting p65-NF-kappaB and p38-MAPK activation. *Pharmazie* 2010; **65**: 206-212 [PMID: 20383942 DOI: 10.1691/ph.2010.9679]

141 **Paracha UZ**, Fatima K, Alqahtani M, Chaudhary A, Abuzenadah A, Damanhour G, Qadri I. Oxidative stress and hepatitis C virus. *Virol J* 2013; **10**: 251 [PMID: 23923986 DOI: 10.1186/1743-422X-10-251]

P- Reviewer: Ciccone M, Tenca A **S- Editor:** Ma RY
L- Editor: Wang TQ **E- Editor:** Huang Y





Split liver transplantation: Current developments

Christina Hackl, Katharina M Schmidt, Caner Süsal, Bernd Döhler, Martin Zidek, Hans J Schlitt

Christina Hackl, Katharina M Schmidt, Martin Zidek, Hans J Schlitt, Department of Surgery, University Hospital Regensburg, Regensburg 93053, Germany

Caner Süsal, Bernd Döhler, Collaborative Transplant Study (CTS), Institute of Immunology, Heidelberg University, Heidelberg 69120, Germany

ORCID number: Christina Hackl (0000-0002-1346-7238); Katharina M Schmidt (0000-0001-7750-8150); Caner Süsal (0000-0003-2521-8201); Bernd Döhler (0000-0003-0051-096X); Martin Zidek (0000-0002-1931-438X); Hans J Schlitt (0000-0002-3874-0296).

Author contributions: Hackl C contributed to conception and design, acquisition of data, drafting the article, critical revision for important intellectual content, and final approval of the version to be published; Schmidt KM and Zidek M contributed to conception and design, critical revision for important intellectual content, and final approval of the version to be published; Süsal C and Döhler B contributed to acquisition of data, critical revision for important intellectual content, and final approval of the version to be published; Schlitt HJ contributed to conception and design, acquisition of data, drafting the article, critical revision for important intellectual content, and final approval of the version to be published.

Conflict-of-interest statement: The authors declare no conflicts of interest.

Open-Access: This article is an open-access article which was selected by an in-house editor and fully peer-reviewed by external reviewers. It is distributed in accordance with the Creative Commons Attribution Non Commercial (CC BY-NC 4.0) license, which permits others to distribute, remix, adapt, build upon this work non-commercially, and license their derivative works on different terms, provided the original work is properly cited and the use is non-commercial. See: <http://creativecommons.org/licenses/by-nc/4.0/>

Manuscript source: Invited manuscript

Corresponding author to: Christina Hackl, MD, Department of Surgery, University Medical Center Regensburg, Franz Josef Strauss Allee 11, Regensburg 93053, Germany. christina.hackl@ukr.de
Telephone: +49-941-94416806

Fax: +49-941-9446802

Received: July 9, 2018

Peer-review started: July 10, 2018

First decision: July 18, 2018

Revised: October 9, 2018

Accepted: October 21, 2018

Article in press: October 21, 2018

Published online: December 21, 2018

Abstract

In 1988, Rudolf Pichlmayr pioneered split liver transplantation (SLT), enabling the transplantation of one donor liver into two recipients - one pediatric and one adult patient. In the same year, Henri Bismuth and colleagues performed the first full right/full left split procedure with two adult recipients. Both splitting techniques were rapidly adopted within the transplant community. However, a SLT is technically demanding, may cause increased perioperative complications, and may potentially transform an excellent deceased donor organ into two marginal quality grafts. Thus, crucial evaluation of donor organs suitable for splitting and careful screening of potential SLT recipients is warranted. Furthermore, the logistic background of the splitting procedure as well as the organ allocation policy must be adapted to further increase the number and the safety of SLT. Under defined circumstances, in selected patients and at experienced transplant centers, SLT outcomes can be similar to those obtained in full organ LT. Thus, SLT is an important tool to reduce the donor organ shortage and waitlist mortality, especially for pediatric patients and small adults. The present review gives an overview of technical aspects, current developments, and clinical outcomes of SLT.

Key words: Liver transplantation; Organ shortage; In situ split; Extended right lobe; Left lateral lobe; Living donor

© The Author(s) 2018. Published by Baishideng Publishing

Group Inc. All rights reserved.

Core tip: As of today, split liver transplantation (SLT) is a widely adopted but yet technically demanding approach to enable liver transplantation especially in very young recipients, and to reduce organ shortage and waitlist mortality. In contrast to full organ liver transplantation, many technical evaluations concerning the donor organ, the recipient, as well as the splitting procedure and the organ allocation policy, must be considered before a SLT can safely be performed. The present review gives insight into current controversies, technical challenges, and clinical outcomes of SLT.

Hackl C, Schmidt KM, Süsal C, Döhler B, Zidek M, Schlitt HJ. Split liver transplantation: Current developments. *World J Gastroenterol* 2018; 24(47): 5312-5321
URL: <https://www.wjgnet.com/1007-9327/full/v24/i47/5312.htm>
DOI: <https://dx.doi.org/10.3748/wjg.v24.i47.5312>

INTRODUCTION

The first orthotopic liver transplant (LT), published by Thomas E Starzl, was performed in a 3-year-old patient diagnosed with biliary atresia^[1]. During the following years shortage of size-matched grafts for children became an evident dilemma. In the 1980s, Henri Bismuth introduced the method of graft size reduction to enable the use of adult donor grafts for pediatric LT^[2]. However, by thus reducing waitlist mortality for pediatric or small adult patients, this technique in parallel increased the organ shortage for adult recipients by sacrificing the remnant liver. In 1988, Rudolf Pichlmayr was the pioneer of split liver transplantation (SLT), enabling the transplantation of one donor liver into two recipients - one pediatric and one adult patient^[3]. In the same year Bismuth and colleagues performed the first full right/full left split procedure with two adult recipients^[4]. Both split techniques were rapidly adopted within the transplant community and already in 1990, Christoph Broelsch published a report on the outcome of 30 split liver transplants^[5].

While in the 1980s the waitlist mortality of pediatric recipients was 40%, SLT and living donor liver transplantation (LDLT) helped reduce it down to 10% in infants and to 5% in older children today^[6]. A novel analysis of the development of graft survival rates in LT performed in pediatric patients and reported to the Collaborative Transplant Study (CTS, <https://www.ctstransplant.org>) is shown in Figure 1. Graft survival in pediatric LT is steadily increasing and current 5-year post-transplant graft survival is nearly 80%. Furthermore, SLT and LDLT enabled LT of very small infants and newborns. Since 1995, the proportion of 0-5-year-old children among recipients of pediatric LT has remained nearly constant at 65%, with a high proportion (almost 30%) in less than 1-year-old infants (Figure 2). As shown in

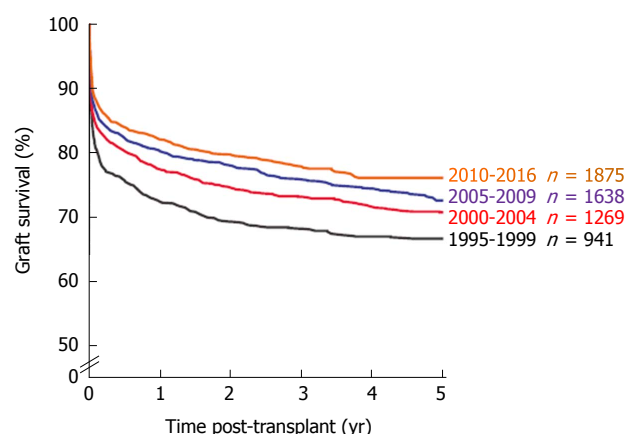


Figure 1 Graft survival of liver transplants in 0-17-year-old pediatric patients by transplant year from 1995-2016. Collaborative Transplant Study data are derived from 95 transplant centers in 22 countries (87% European transplants).

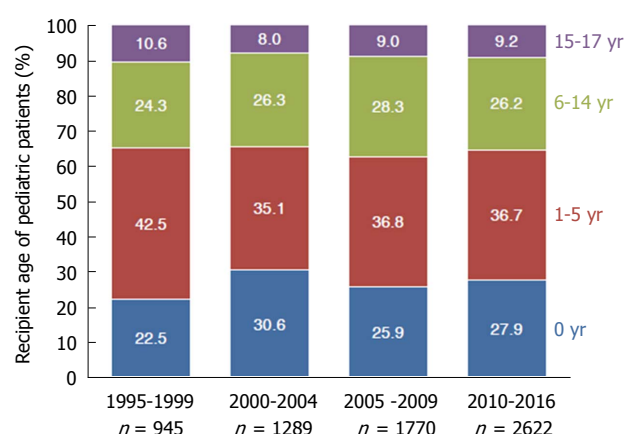


Figure 2 Different pediatric age groups and distribution of liver transplants by transplant year from 1995-2016.

Figure 3A, the ratio of LDLT has been steadily increasing in pediatric LT since 1995. Today, approximately one third of livers transplanted into pediatric recipients are derived from living donors (Figure 3A). On the other hand, the absolute number of livers transplanted into pediatric recipients from deceased donors has not decreased, and thus SLT resulted in an extension of the organ pool and reduction of donor organ scarcity for pediatric as well as adult LT recipients.

Performing a SLT is technically highly demanding in adult patients and may cause increased perioperative complications. The rate of living donors is steadily increasing in patients receiving an SLT and is currently reported to be 46% (Figure 3B). When comparing SLT recipients and full organ recipients, rates of LT using reduced size or split grafts have been steadily increasing until the period of 2000-2004 and since then has leveled off at 13%-15% (Figure 3C). In the first decades of SLT, increased complication rates caused hesitation to further spread the use of SLT. Ethical discussions were raised whether by splitting a liver, an excellent organ is converted into two marginal quality grafts^[5,7-9]; whether

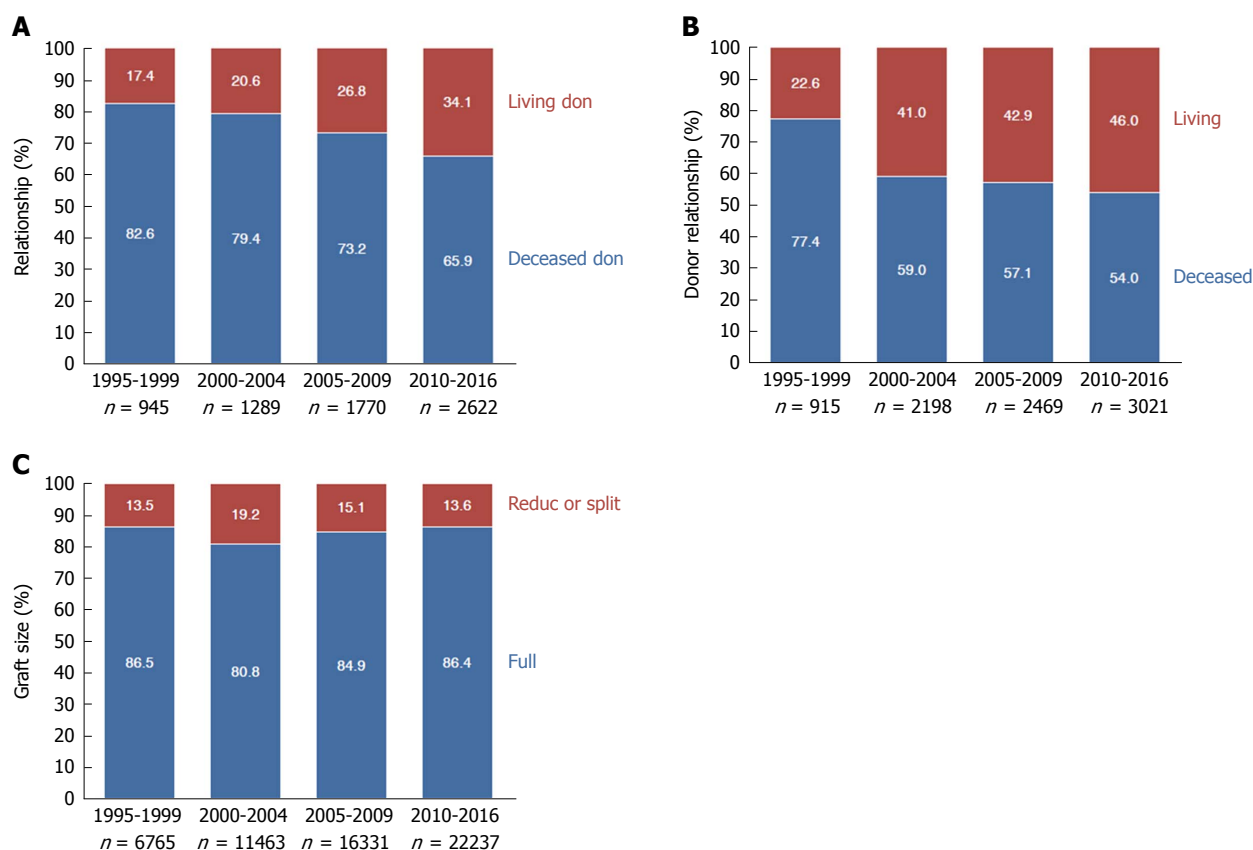


Figure 3 Pediatric (A) and split or reduced liver transplants from living or deceased donors (B) and all liver transplants categorized according to graft size (C) by transplant year from 1995-2016.

an adult recipient should be allowed to refuse a split organ remains an unresolved ethical issue. Complication rates of up to 66.7% after SLT *versus* 45.1% after full organ LT have been described^[10,11], especially due to early biliary complications (18.8% in SLT vs 7.5% in full organ LT) and portal vein thrombosis (14.6% in SLT vs 3.6% in full organ LT)^[11].

In recent years experienced transplant centers have published favorable SLT outcomes similar to those obtained in full organ LT^[12-15], supporting the argument that under defined conditions SLT should continue to be promoted. Therefore, allocation policies focusing on increasing SLT must be developed and transplant centers should be encouraged to perform SLT whenever safe and possible.

SURGICAL TECHNIQUES

Using the “classical” form of SLT, the liver is divided into a left lateral lobe (LLL) graft (segments II + III) for a pediatric or small adult recipient and an extended right lobe (eRL) graft (segments I + IV-VIII) for an adult recipient (Figure 4, yellow line)^[16]. During the splitting procedure the hepatoduodenal ligament is first dissected from the left side for adequate identification of the left hepatic artery. Then, the left portal vein is dissected, resulting in a deportalization of segment IV. The following dissection of the liver parenchyma is

performed at the right side of the falciform and round ligament, ending between the left and middle hepatic vein. Bile ducts of segments I and IV should be carefully saved while the hilar plate is sharply divided, including segment II and III bile ducts at the longitudinal section of the left portal vein. Finally, the dissected left portal vein, left artery, and left hepatic vein are divided. In the case of very small pediatric recipients, monosegment grafts consisting of segment II or segment III only can be applied.

In contrast, full size splits consisting of segments I-IV and segments V-VIII (Figure 4, black line) enable transplantation of two adult recipients, although the left lobe (without segment I) is generally only suitable for a small adult. Here, the safe biliary drainage of all segments is especially crucial. In contrast to a “classical split”, the transection plane of the liver parenchyma is significantly larger. Furthermore, due to the lack of a clear anatomic structure like the falciform ligament to indicate the resection line, *in situ* splitting (*i.e.*, splitting before cold perfusion) should, whenever possible, be preferred. Potential anatomic variants of blood vessels and bile ducts must be carefully evaluated. Especially in full splits, the principle of avoiding multiple small anastomoses, defined by Henri Bismuth^[4], is crucial. A normal left lobe consists of a single portal vein and a single hepatic duct, a venous outflow, which often has a common ostium (left + middle vein), and often multiple

Table 1 Recently published formulae to calculate the liver volume

Ref.	Formula	Patient group	Technique
Urata <i>et al</i> ^[20] , 1995	LV (mL) = 706.2 × BSA (m ²) + 2.4	96 patients (65 pediatric)	CT
Vauthey <i>et al</i> ^[21] , 2002	Based on BSA: LV = -794.41 + 1267.28 × BSA (m ²) $r^2 = 0.46$; $P < 0.0001$ Based on patient weight: LV = 191.80 + 18.51 × body weight (kg) $r^2 = 0.49$; $P < 0.0001$	292 adults	CT
Heinemann <i>et al</i> ^[17] , 1999	LV (mL) = 1072.8 × BSA (m ²) - 345.7	1332 patients	Autopsy
Kokudo <i>et al</i> ^[19] , 2015	LV = 203.3 - (3.61 × age) + [58.7 × thoracic width (cm)] - [463.7 × race (1 = Asian, 0 = Caucasian)]	180 Japanese and 160 Swiss patients	CT
Herden <i>et al</i> ^[18] , 2013	Children 0 to ≤ 1 yr: LV (mL) = 143.062973 + 4.274603051 × body length (cm) + 14.78817631 × body weight (kg) Children > 1 yr to < 16 yr: LV (mL) = 20.2472281 + 3.339056437 × body length (cm) + 13.11312561 × body weight (kg)	388 pediatrics	Autopsy

LV: Liver volume; BSA: Body surface area; CT: Computed tomography.

branches of small hepatic arteries. A “normal” right lobe consists of a single right artery, but often shows multiple venous branches, hepatic ducts, and sometimes even multiple branches of the portal vein. During the full split procedure it is recommended that the left lobe retains the celiac trunk, whereas the right lobe retains the main hepatic duct, the main portal vein, and the caval vein. For adequate venous drainage the left common ostium of the left and middle vein is anastomosed with the recipient venous cuff created from all three hepatic veins during a piggyback LT technique. For excellent venous outflow of the right lobe, reconstruction of the middle vein must be considered, and for reduction of the risk of a small-for-size syndrome, portal inflow modification of the recipient needs deliberation. Potential modifications are: (1) splenic artery ligation, (2) splenectomy, (3) creating a hemi-portocaval shunt, and (4) (temporary) preservation of preexisting portocaval collaterals. If a relevant small-for-size syndrome still occurs, early retransplantation must be considered.

A crucial aspect to avoid small-for-size (or, in small infants, large-for-size) syndromes is the meticulous evaluation of the donor liver volume. For the Caucasian population, liver volume can be calculated as 1072.8 × body surface area (m²) - 345.7^[17]. However, multiple formulae exist to calculate the liver volume of a potential donor, considering weight, body surface area, ethnicity, and thoracoabdominal circumference (see overview in Table 1^[17-21]).

In LDLT, a minimal graft-to-recipient weight ratio of 0.6%-0.8% has been suggested^[22-24]. However, since LDLT grafts are derived from very healthy donors under ideal organ procurement conditions that include a minimal cold ischemia time, the minimal graft-to-recipient weight ratio considered safe in deceased donor SLT appears to be 0.8%-1.0%^[8,22,25,26]. As a simplified estimation, the liver weight represents 2% of the body weight of a normal weight adult. A LLL split thus consists of approximately 250 mL of liver parenchyma

and an eRL of 1100 mL of liver parenchyma. However, due to the often mal- or non-perfused segments IV and I in eRL grafts, their functional liver parenchyma is often smaller. A full left split consists of approximately 400 mL liver parenchyma, thus being sufficient for adult recipients up to a body weight of 40-50 kg. A full right split with 800-1000 mL of liver parenchyma serves recipients up to 80-100 kg body weight, assuming a perfect venous drainage of the whole parenchyma of the right lobe^[27,28]. An overview of mostly used grafts in living donor and deceased donor SLT is given in Figure 5. Within the CTS population the majority of SLT performed using living donors are either LLL (38.4%) or extended right splits (41%). In contrast, in 4241 SLTs performed with deceased donor organs from 1995-2016 a significant variation in types of SLTs exists (Figure 5).

The “classical form” of SLT from deceased donors, namely left lateral or eRL SLT, is currently performed in approximately 74% of SLT, whereas full left/right lobe SLT is performed in 17% of SLT (Figure 6A). As illustrated in Figure 6B, left lateral splits are used in 33.9% of the cases for less than 1-year-old recipients and in 50.1% of the cases for 1-5-year-old recipients. A minority of left lateral SLT grafts is used for recipients older than 6 years. Left lobe SLT grafts are used in 12.3% of the cases for less than 1-year-old recipients, in 31.6% of the cases for 1-5-year-old recipients, and in 37.7% of the cases for 6-14-year-old recipients. In contrast, almost 90% of right lobe or eRL grafts are used for adult recipients (Figure 6B), and 16.8% of left lobe splits are used for (small) adult recipients.

When SLT from living donor organs were analyzed within the CTS population, 637 right lobe, 217 left lobe, and 594 LLL donations were performed from 1995-2016 (Figure 6C). In adult recipients, 95.1% of right lobes, 18.4% of left lobes, and 5.1% of LLL were used, whereas 27.6% of left lobes and more than 80% of LLL were used for 0-5-year-old infants (Figure 6C).

The decision making for deceased donor SLT

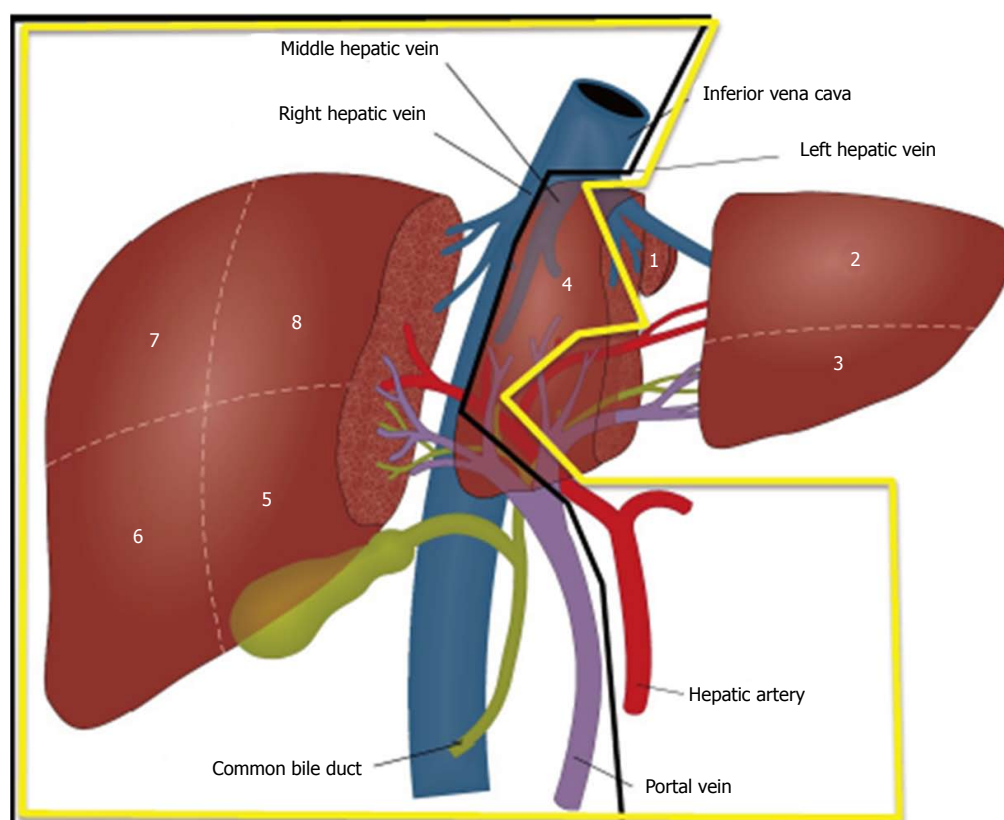


Figure 4 Scheme of a “classical” extended right lobe/left lateral lobe split (yellow line) and a full left/full right split (black line).

must factor in careful donor selection, logistic aspects concerning the split procedure, and the condition of the recipient. Concerning donor selection, Liu *et al.*^[28] recommended the following criteria for “classical” SLT: hemodynamically stable patients younger than 55 years, duration of ICU treatment less than 5 d, fatty degeneration of the liver of less than 30%, GGT < 50 U/L, GPT < 60 U/L, and serum sodium < 160 mmol/L. For full right/left SLT, donors should weigh more than 70 kg, be younger than 40 years, duration of ICU treatment less than 3 d, and fatty degeneration of the liver should be less than 10%^[28]. These criteria slightly differ between transplant programs world-wide (see Table 2). Analyzing the CTS data, the median age of deceased donor livers used for SLT is 28–30 years and has remained constant since 1995 (Figure 7A). However, the median age of the deceased donor livers slightly increases in relation to the age of the recipient (Figure 7B). This reflects ongoing discussions of the influence of donor age on long-term outcomes after LT and SLT^[29]. At the same time these data show that the maximum donor age tolerated for SLT in most transplant programs (see Table 2) is not exhausted and decision making for SLT may be stricter than needed^[29].

ETHICAL ISSUES

Because splitting a liver is a technically demanding procedure, outstanding surgical expertise is warranted. If the split procedure is performed *in situ*, up to 3 h more

operating time during organ procurement is needed and might result in quality impairment regarding other organs procured from the same donor. If the split is performed after donor hepatectomy, *i.e.*, *ex situ* in the recipient center, a respective longer cold ischemia time of the donor liver will result.

A current analysis of 37333 deceased donor LT in the United States revealed that 2352 (6.3%) of these livers met strict criteria for potential split, however only 1418 livers (3.8%) were indeed split. During the study period, less children died on the waitlist than livers were procured that could potentially have been split and used for SLT. Thus, an infant waitlist mortality of 10% and pediatric waitlist mortality of 5% in the United States could theoretically be eliminated by promoting SLT^[6]. An overview of rates of SLT and criteria to perform a SLT in different transplant programs is given in Table 2. While most programs show SLT of up to 6%, programs in the United Kingdom, Brazil, and Argentina reach 10%. The highest rate of SLT is in the Northern Italian region at a rate of 20%. According to ideal evaluation regimes of donor organs, *in situ* splitting and a modified allocation policy promoting SLT in Northern Italy, this region is a pioneer in promoting SLT with a very high outcome quality in selected patients (see Outcome section). When comparing the rates of SLT reported to the International Registry in Organ Donation and Transplantation (IRODaT) for 2016, variations of SLT rates between 0% and 20% have been published (Table 3). A weakness of this database is the voluntary reporting of SLT rates

Table 2 Criteria and rates of split liver transplantation in different transplant programs according to the transplant programs homepages

Program	Rate of SLT	Donor age	Weight/BMI	Transaminases	Other criteria
UNOS	1%-4% (but according to UNOS criteria > 10% eligible)	< 40	< 28 kg/m ²	< 3 × ULN	Single vasopressor
ET	6%	< 50	> 50 kg		
United Kingdom	10.6%	< 40	> 50 kg		< 5 d ICU
Argentina/Brazil	10%	< 47	umbilical perimeter < 92 cm	AST < 42 U/L ALT < 29 U/L	
Oceania	6%				
Scandia-transplant	?	< 51	< 26 kg/m ²	ALT/AST < 3 × normal	< 4 d ICU
Saudi-Arabia	5.6%				
South Africa	3%				
Japan	1.8%				
Italy	8% (Northern Italy: 20%)	< 60		Near-normal liver function tests	< 5 d ICU Low inotropic support

ALT: Alanine transaminase; AST: Aspartate aminotransferase; ET: Eurotransplant; ICU: Intensive care unit; SLT: Split liver transplantation.

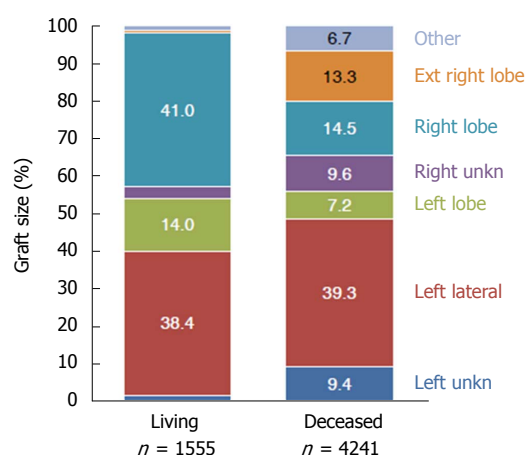


Figure 5 Split or reduced liver transplants from 1995-2016 categorized according to graft size.

to the IRODaT, resulting in underrated SLT rates and a lack of deceased donor organs due to religious and cultural reasons in Asian countries (where in contrast a huge expertise in LDLT exists). Nevertheless, based on published criteria to perform an SLT in different transplant programs and reported SLT numbers, a significant discrepancy can be stated in most transplant programs, and SLT should be further promoted.

OUTCOMES

In a recent Korean analysis, 86 eRL deceased donor split LT in adult recipients were compared to 303 deceased donor full organ LT. Of note, less than 25% of LT in South Korea are performed using deceased donors, *i.e.*, a great surgical expertise in *in situ* splitting for LDLT exists. Groups were matched for recipient age, MELD score, duration of ischemia, and graft-to-recipient weight ratio. Donors of eRL splits were significantly younger. There was no significant difference in complication rates and 5-year graft survival rates between deceased donor SLT and full organ

LT (89% vs 93%, $P > 0.05$). However, the 5-year overall survival rate and graft failure-free survival rate (both 63%) of eRL splits were significantly worse than in the full organ LT group (79%, $P = 0.05$). Factors resulting in a reduced overall survival in eRL recipients were a MELD-score greater than 30 and donor-recipient weight ratio less than 1.0. In subgroup analyses the outcome of both groups was equivalent if a donor-recipient weight ratio greater than 1.0 was observed in the eRL recipients^[30].

A recent European Liver Transplant Registry analysis of 1500 pediatric recipients of left lateral split LT between 2006 and 2014 described SLT as safe when identified risk factors were avoided. Risk factors for graft failure in multivariate analyses were urgency of SLT, recipient body weight less than 6 kg, donor age greater than 50 years, and a prolonged cold ischemia time (HR = 1.07/h). The authors concluded that recipients less than 6 kg and recipients needing urgent SLT needed cold ischemia times less than 6 h and careful graft/recipient size matching^[31]. Another recent analysis of the European Liver Transplant Registry showed the impact of the Eurotransplant (ET) allocation policy on the outcome of eRL SLT. Current SLT allocation by ET allocates a splittable organ primarily to the pediatric LT center. After splitting, eRL splits are mostly reallocated to a second transplant center. Of the 5351 LTs analyzed, 269 were eRL SLTs. Patient survival rates showed no significant differences in eRL SLT vs whole organ LT (5-year overall survival of 73.6% after whole organ as well as after eRL LT). However, cold ischemia times were significantly longer in eRL recipients (12.1 ± 3.3 h vs 8.3 ± 2.8 h, $P < 0.001$) and eRL recipients had a significantly higher risk for retransplantation (14.4% after eRL SLT; 10.2% after whole organ LT, $P = 0.02$). Furthermore, overall survival correlated with a MELD-score greater than 14 in eRL recipients, whereas this correlation was only seen for MELD-scores greater than 20 in whole organ LT recipients^[32].

A critical point of this analysis was that splitting

Table 3 Numbers of liver transplantations, living-donor liver transplantations, deceased donor liver transplantations, and split liver transplantations and the rate of split liver transplantation in deceased donor liver transplantation performed in different transplant programs in 2016 according to the International Registry in Organ Donation and Transplantation

	Total number	Living donors	Deceased donors	Split-liver	Split-liver (%)
UNOS	8082	367	7715	0	0
Eurotransplant					
Germany	821	61	760	74	9.01
Austria	154	2	152	6	3.90
Croatia	121	0	121	0	0
Netherlands	147	0	147	0	0
Belgium	302	46	256	1	0.33
Luxemburg	0	0	0	0	0
Hungary	74	0	74	0	0
Slovenia	27	0	27	0	0
Scandiatransplant	0				
Sweden	199	2	197	0	0
Norway	100	0	100	0	0
Finland	61	0	61	0	0
Iceland	0	0	0	0	0
Denmark	57	0	57	0	0
China	-	-	-	-	-
India	-	-	-	-	-
Japan	438	381	57	8	1.83
South Korea	1473	965	508	36	2.44
Australia	314	2	312	65	20.70
Brazil	2037	157	1880	0	0
Argentina	349	37	312	0	0
Mexico	178	3	175	0	0
Canada	582	73	509	0	0
South Africa	69	15	54	2	2.90
United Kingdom	953	32	921	101	10.60
France	1317	5	1312	0	0
Spain	1159	28	1131	0	0
Italy	1220	7	1213	98	8.03
Poland	345	28	317	0	0
Czech Republic	179	1	178	0	0
Balttransplant	33	0	33	0	0

was mainly performed *ex situ* in the transplant center accepting the LLL, resulting in reallocation and prolonged cold ischemia time of the eRL. In contrast, in Northern Italy where the splitting procedures are mostly performed as *in situ* splits, reported excellent outcomes of 382 eRL SLTs in a multicenter analysis^[33]. Since this publication, all deceased donor livers from donors less than 50 years of age and not allocated to high urgency patients in Italy are now evaluated for SLT. If SLT is done, allocation of the eRL is performed center-specific outside the MELD allocation system^[34]. Recently, the first long-term analysis of 119 matched-pair recipients of whole LT recipients vs eRL SLT recipients in Italy showed contradictory results; full organ recipients had significantly longer 1-year, 5-year and 10-year overall survival rates compared to SLT recipients (1 year: 93% vs 73%, 5 years: 87% vs 65%; 10 years: 83% vs 60%, $P < 0.001$)^[35]. Also graft survival rates were substantially better in full organ recipients (1 year: 90% vs 76%; 5 years: 84% vs 57%; 10 years: 81% vs 52%, $P < 0.001$). When analyzing the subgroup of patients who survived the first year after LT, 5- and 10-year patient and graft survival did not show more significant differences in this publication. The authors identified the following risk

factors for SLT recipients: (1) donor age less than 50 years, (2) graft-to-recipient weight ratio less than 1.0, (3) retransplantation and (4) recipients with UNOS status I-IIa. The authors concluded that SLT using eRL grafts, if used after careful evaluation and in selected patients, can achieve long-term outcomes similar to full organ LT, but should not be performed in patients with risk factors^[35].

THE FUTURE OF SLT

Recent clinical research has investigated the influence of normothermic machine perfusion on procured livers. A first report on feasibility and safety of normothermic recovery of an initially rejected liver graft was published by the Birmingham group in 2016^[36], and they subsequently reported on five additional similar cases^[37]. In 2018, the same group published the first splitting procedure (eRL/LLL) during normothermic machine perfusion^[38]. Although this marginal organ was not used for LT after the split procedure, further research and development of this technique may positively impact future numbers of SLT in a monitored and safe manner.

Another ongoing discussion is the need to modify organ allocation to promote SLT. The sickest first policy,

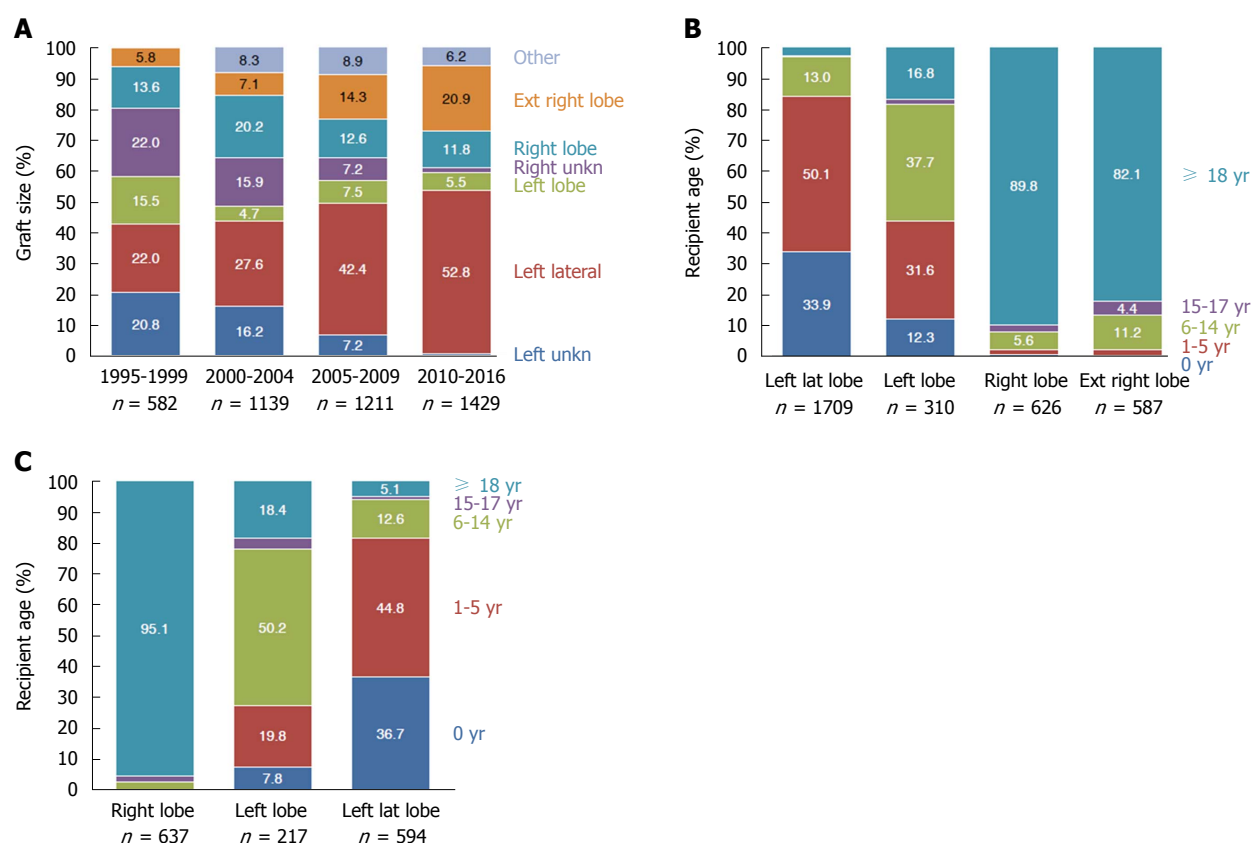


Figure 6 Split or reduced liver transplants from 1995-2016 from deceased donors categorized according to (A) graft size, (B) recipient age, and (C) from living donors categorized according to recipient age.

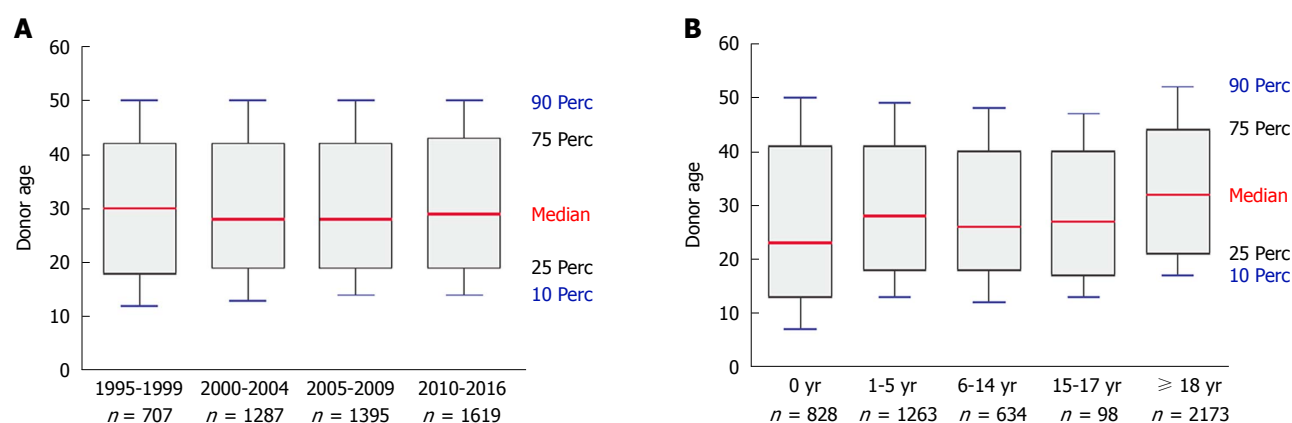


Figure 7 Distribution of donor age according to transplant year (A) and recipient age (B) in deceased donor split or reduced liver transplantations performed from 1995-2016.

represented by the Model of End Stage Liver Disease (MELD) was implemented in UNOS in 2002 and in ET at the end of 2006^[39,40]. SLT allocation according to the MELD system allocates a splittable organ primarily to the center of the recipient with highest priority (mostly the pediatric patient). After splitting is confirmed, the unused split is reallocated to a second transplant center. This allocation practice results in reduced rates of *in situ* splitting, prolonged cold ischemia times, and potentially higher complication rates with SLT. Center-based allocation is performed in countries with few transplant

centers, *e.g.*, Australia and the United Kingdom. In these programs reported SLT rates significantly exceed SLT rates in MELD-based allocation regions. As the Northern Italian experience has shown, all deceased donor livers meeting criteria to perform SLT, and not allocated to high urgency patients, should be offered for SLT. If SLT is performed, then the allocation of both splits should be performed center-specific outside the MELD allocation system to create another incentive for the transplant centers willing and able to perform an SLT. *In situ* splitting should be performed whenever possible, but realize that

such a new policy may result in further centralization of transplant surgery or even discrimination of centers not able to perform SLT. Also, a center-based allocation system is more prone to subjective decision making and should be critically monitored. Strasberg and colleagues have suggested a nation- or transplant program-wide focus of organ allocation based on the number of lives saved, rather than the MELD-based sickest first policy^[41]. Due to the increasing shortage of donor organs and still relevant waitlist mortality, such a policy would be an essential step towards improved quantities without reduction of quality in LT.

CONCLUSION

SLT, although technically demanding, is a routine and safe procedure resulting in increased numbers of LT, increased feasibility of LT in very young recipients, and in reduced waitlist mortality. Short and long-term outcomes and survival can be similar to whole organ LT if meticulous evaluations of donor organs and SLT recipients are performed, and logistics of organ allocation and splitting procedures are adapted. Because donor organ scarcity remains a primary problem in LT today, SLT is a valid solution and should be further promoted by both transplant program regulations and participating transplant centers/surgeons. Organ allocation policies should be adapted to create further incentives for LT centers willing and able to perform SLT. Safety must continue to have highest priority in LT and SLT.

ACKNOWLEDGEMENTS

The authors thank Professor Edward Geissler for language editing.

REFERENCES

- 1 Starzl TE, Marchioro TL, Vonkaulla KN, Hermann G, Brittain RS, Waddell WR. Homotransplantation of the liver in humans. *Surg Gynecol Obstet* 1963; **117**: 659-676 [PMID: 14100514]
- 2 Bismuth H, Houssin D. Reduced-sized orthotopic liver graft in hepatic transplantation in children. *Surgery* 1984; **95**: 367-370 [PMID: 6367125]
- 3 Pichlmayr R, Ringe B, Gubernatis G, Hauss J, Bunzendahl H. [Transplantation of a donor liver to 2 recipients (splitting transplantation)--a new method in the further development of segmental liver transplantation]. *Langenbecks Arch Chir* 1988; **373**: 127-130 [PMID: 3287073 DOI: 10.1007/BF01262776]
- 4 Azoulay D, Castaing D, Adam R, Savier E, Delvart V, Karam V, Ming BY, Dannaoui M, Krissat J, Bismuth H. Split-liver transplantation for two adult recipients: feasibility and long-term outcomes. *Ann Surg* 2001; **233**: 565-574 [PMID: 11303140 DOI: 10.1097/0000658-200104000-00013]
- 5 Broelsch CE, Emond JC, Whittington PF, Thistlethwaite JR, Baker AL, Lichter JL. Application of reduced-size liver transplants as split grafts, auxiliary orthotopic grafts, and living related segmental transplants. *Ann Surg* 1990; **212**: 368-375; discussion 375-377 [PMID: 2396888 DOI: 10.1097/0000658-199009000-00015]
- 6 Perito ER, Roll G, Dodge JL, Rhee S, Roberts JP. Split liver transplantation and pediatric waitlist mortality in the United States: potential for improvement. *Transplantation* 2018; Epub ahead of print [PMID: 29684000 DOI: 10.1097/TP.0000000000002249]
- 7 Vagefi PA, Parekh J, Ascher NL, Roberts JP, Freise CE. Outcomes with split liver transplantation in 106 recipients: the University of California, San Francisco, experience from 1993 to 2010. *Arch Surg* 2011; **146**: 1052-1059 [PMID: 21931003 DOI: 10.1001/archsurg.2011.218]
- 8 Hashimoto K, Quintini C, Aucejo FN, Fujiki M, Diago T, Watson MJ, Kelly DM, Winans CG, Eghtesad B, Fung JJ, Miller CM. Split liver transplantation using Hemiliver graft in the MELD era: a single center experience in the United States. *Am J Transplant* 2014; **14**: 2072-2080 [PMID: 25040819 DOI: 10.1111/ajt.12791]
- 9 Emond JC, Whittington PF, Thistlethwaite JR, Cherqui D, Alonso EA, Woodle IS, Vogelbach P, Busse-Henry SM, Zucker AR, Broelsch CE. Transplantation of two patients with one liver. Analysis of a preliminary experience with 'split-liver' grafting. *Ann Surg* 1990; **212**: 14-22 [PMID: 2363599]
- 10 Diamond IR, Fecteau A, Millis JM, Losanoff JE, Ng V, Anand R, Song C; SPLIT Research Group. Impact of graft type on outcome in pediatric liver transplantation: a report From Studies of Pediatric Liver Transplantation (SPLIT). *Ann Surg* 2007; **246**: 301-310 [PMID: 17667510 DOI: 10.1097/SLA.0b013e3180caa415]
- 11 Hackl C, Schlitt HJ, Melter M, Knoppke B, Loss M. Current developments in pediatric liver transplantation. *World J Hepatol* 2015; **7**: 1509-1520 [PMID: 26085910 DOI: 10.4254/wjh.v7.i11.1509]
- 12 Moussaoui D, Toso C, Nowacka A, McLin VA, Bednarkiewicz M, Andres A, Berney T, Majno P, Wildhaber BE. Early complications after liver transplantation in children and adults: Are split grafts equal to each other and equal to whole livers? *Pediatr Transplant* 2017; **21** [PMID: 28261944 DOI: 10.1111/ptr.12908]
- 13 Doyle MB, Maynard E, Lin Y, Vachharajani N, Shenoy S, Anderson C, Earl M, Lowell JA, Chapman WC. Outcomes with split liver transplantation are equivalent to those with whole organ transplantation. *J Am Coll Surg* 2013; **217**: 102-112; discussion 113-114 [PMID: 23639200 DOI: 10.1016/j.jamcollsurg.2013.03.003]
- 14 Cauley RP, Vakili K, Fullington N, Potanos K, Graham DA, Finkelstein JA, Kim HB. Deceased-donor split-liver transplantation in adult recipients: is the learning curve over? *J Am Coll Surg* 2013; **217**: 672-684.e1 [PMID: 23978530 DOI: 10.1016/j.jamcollsurg.2013.06.005]
- 15 Battula NR, Platto M, Anbarasan R, Perera MT, Ong E, Roll GR, Ferraz Neto BH, Mergental H, Isaac J, Muiresan P, Sharif K, Mirza DF. Intention to Split Policy: A Successful Strategy in a Combined Pediatric and Adult Liver Transplant Center. *Ann Surg* 2017; **265**: 1009-1015 [PMID: 27257738 DOI: 10.1097/SLA.0000000000001816]
- 16 Busutil RW, Goss JA. Split liver transplantation. *Ann Surg* 1999; **229**: 313-321 [PMID: 10077042 DOI: 10.1097/0000658-199903000-00003]
- 17 Heinemann A, Wischhusen F, Püschel K, Rogiers X. Standard liver volume in the Caucasian population. *Liver Transpl Surg* 1999; **5**: 366-368 [PMID: 10477836 DOI: 10.1002/lt.500050516]
- 18 Herden U, Wischhusen F, Heinemann A, Ganschow R, Grabhorn E, Vettorazzi E, Nashan B, Fischer L. A formula to calculate the standard liver volume in children and its application in pediatric liver transplantation. *Transpl Int* 2013; **26**: 1217-1224 [PMID: 24118382 DOI: 10.1111/tri.12198]
- 19 Kokudo T, Hasegawa K, Uldry E, Matsuyama Y, Kaneko J, Akamatsu N, Aoki T, Sakamoto Y, Demartines N, Sugawara Y, Kokudo N, Halkic N. A new formula for calculating standard liver volume for living donor liver transplantation without using body weight. *J Hepatol* 2015; **63**: 848-854 [PMID: 26057995 DOI: 10.1016/j.jhep.2015.05.026]
- 20 Urata K, Kawasaki S, Matsunami H, Hashikura Y, Ikegami T, Ishizone S, Momose Y, Komiyama A, Makuuchi M. Calculation of child and adult standard liver volume for liver transplantation. *Hepatology* 1995; **21**: 1317-1321 [PMID: 7737637 DOI: 10.1002/hep.1840210515]
- 21 Vauthey JN, Abdalla EK, Doherty DA, Gertsch P, Fenstermacher MJ, Loyer EM, Lerut J, Materne R, Wang X, Encarnacion A, Herron D, Mathey C, Ferrari G, Charnsangavej C, Do KA, Denys

- A. Body surface area and body weight predict total liver volume in Western adults. *Liver Transpl* 2002; **8**: 233-240 [PMID: 11910568 DOI: 10.1053/jlts.2002.31654]
- 22 **Hashimoto K**, Fujiki M, Quintini C, Aucejo FN, Uso TD, Kelly DM, Egthesad B, Fung JJ, Miller CM. Split liver transplantation in adults. *World J Gastroenterol* 2016; **22**: 7500-7506 [PMID: 27672272 DOI: 10.3748/wjg.v22.i33.7500]
 - 23 **Kaido T**, Mori A, Ogura Y, Hata K, Yoshizawa A, Iida T, Yagi S, Uemoto S. Lower limit of the graft-to-recipient weight ratio can be safely reduced to 0.6% in adult-to-adult living donor liver transplantation in combination with portal pressure control. *Transplant Proc* 2011; **43**: 2391-2393 [PMID: 21839274 DOI: 10.1016/j.transproceed.2011.05.037]
 - 24 **Selzner M**, Kashfi A, Cattral MS, Selzner N, Greig PD, Lilly L, McGilvray ID, Therapondos G, Adcock LE, Ghanekar A, Levy GA, Renner EL, Grant DR. A graft to body weight ratio less than 0.8 does not exclude adult-to-adult right-lobe living donor liver transplantation. *Liver Transpl* 2009; **15**: 1776-1782 [PMID: 19938139 DOI: 10.1002/lt.21955]
 - 25 **Lee WC**, Chan KM, Chou HS, Wu TJ, Lee CF, Soong RS, Wu TH, Lee CS. Feasibility of split liver transplantation for 2 adults in the model of end-stage liver disease era. *Ann Surg* 2013; **258**: 306-311 [PMID: 23108123 DOI: 10.1097/SLA.0b013e3182754b8e]
 - 26 **Hong JC**, Yersiz H, Busuttil RW. Where are we today in split liver transplantation? *Curr Opin Organ Transplant* 2011; **16**: 269-273 [PMID: 21467935 DOI: 10.1097/MOT.0b013e31828346572e]
 - 27 **Lee SG**. Living-donor liver transplantation in adults. *Br Med Bull* 2010; **94**: 33-48 [PMID: 20144939 DOI: 10.1093/bmb/ldq003]
 - 28 **Liu H**, Li R, Fu J, He Q, Li J. Technical Skills Required in Split Liver Transplantation. *Ann Transplant* 2016; **21**: 408-415 [PMID: 27363540 DOI: 10.12659/AOT.896351]
 - 29 **Lué A**, Solanas E, Baptista P, Lorente S, Araiz JJ, Garcia-Gil A, Serrano MT. How important is donor age in liver transplantation? *World J Gastroenterol* 2016; **22**: 4966-4976 [PMID: 27275089 DOI: 10.3748/wjg.v22.i21.4966]
 - 30 **Yoon KC**, Song S, Jwa EK, Lee S, Kim JM, Kim OK, Hong SK, Yi NJ, Lee KW, Kim MS, Hwang S, Suh KS, Lee SK. Survival Outcomes in Split Compared to Whole Liver Transplantation. *Liver Transpl* 2018; Epub ahead of print [PMID: 29747216 DOI: 10.1002/lt.25196]
 - 31 **Angelico R**, Nardi A, Adam R, Nadalin S, Polak WG, Karam V, Troisi RI, Muiesan P; European Liver and Intestine Transplant Association (ELITA). Outcomes of left split graft transplantation in Europe: report from the European Liver Transplant Registry. *Transpl Int* 2018; **31**: 739-750 [PMID: 29505674 DOI: 10.1111/tri.13147]
 - 32 **Andrassy J**, Wolf S, Lauseker M, Angele M, van Rosmalen MD, Samuel U, Rogiers X, Werner J, Guba M; Eurotransplant Liver Advisory Committee. Higher retransplantation rate following extended right split-liver transplantation: An analysis from the eurotransplant liver follow-up registry. *Liver Transpl* 2018; **24**: 26-34 [PMID: 29144580 DOI: 10.1002/lt.24980]
 - 33 **Maggi U**, De Feo TM, Andorno E, Cillo U, De Carlis L, Colledan M, Burra P, De Fazio N, Rossi G; Liver Transplantation and Intestine North Italy Transplant Study Group. Fifteen years and 382 extended right grafts from in situ split livers in a multicenter study: Are these still extended criteria liver grafts? *Liver Transpl* 2015; **21**: 500-511 [PMID: 25545700 DOI: 10.1002/lt.24070]
 - 34 **Cillo U**, Burra P, Mazzaferro V, Belli L, Pinna AD, Spada M, Nanni Costa A, Toniutto P; I-BELT (Italian Board of Experts in the Field of Liver Transplantation). A Multistep, Consensus-Based Approach to Organ Allocation in Liver Transplantation: Toward a "Blended Principle Model". *Am J Transplant* 2015; **15**: 2552-2561 [PMID: 26274338 DOI: 10.1111/ajt.13408]
 - 35 **Ross MW**, Cescon M, Angelico R, Andorno E, Rossi G, Pinna A, De Carlis L, Baccarani U, Cillo U, Colledan M, Mazzaferro V, Tisone G, Rossi M, Tuzzolino F, Pagano D, Gruttadauria S, Mazariegos G, Gridelli B, Spada M. A matched pair analysis of multicenter longterm follow-up after split-liver transplantation with extended right grafts. *Liver Transpl* 2017; **23**: 1384-1395 [PMID: 28650108 DOI: 10.1002/lt.24808]
 - 36 **Perera T**, Mergental H, Stephenson B, Roll GR, Cilliers H, Liang R, Angelico R, Hubscher S, Neil DA, Reynolds G, Isaac J, Adams DA, Afford S, Mirza DF, Muiesan P. First human liver transplantation using a marginal allograft resuscitated by normothermic machine perfusion. *Liver Transpl* 2016; **22**: 120-124 [PMID: 26566737 DOI: 10.1002/lt.24369]
 - 37 **Mergental H**, Perera MT, Laing RW, Muiesan P, Isaac JR, Smith A, Stephenson BT, Cilliers H, Neil DA, Hubscher SG, Afford SC, Mirza DF. Transplantation of Declined Liver Allografts Following Normothermic Ex-Situ Evaluation. *Am J Transplant* 2016; **16**: 3235-3245 [PMID: 27192971 DOI: 10.1111/ajt.13875]
 - 38 **Stephenson BTF**, Bonney GK, Laing RW, Bhogal RH, Marcon F, Neil DAH, Perera MTPR, Afford SC, Mergental H, Mirza DF. Proof of concept: liver splitting during normothermic machine perfusion. *J Surg Case Rep* 2018; **2018**: rjx218 [PMID: 29644030 DOI: 10.1093/jscr/rjx218]
 - 39 **Malinchoc M**, Kamath PS, Gordon FD, Peine CJ, Rank J, ter Borg PC. A model to predict poor survival in patients undergoing transjugular intrahepatic portosystemic shunts. *Hepatology* 2000; **31**: 864-871 [PMID: 10733541 DOI: 10.1053/he.2000.5852]
 - 40 **Said A**, Williams J, Holden J, Remington P, Gangnon R, Musat A, Lucey MR. Model for end stage liver disease score predicts mortality across a broad spectrum of liver disease. *J Hepatol* 2004; **40**: 897-903 [PMID: 15158328 DOI: 10.1016/j.jhep.2004.02.010]
 - 41 **Strasberg SM**, Lowell JA, Howard TK. Reducing the shortage of donor livers: what would it take to reliably split livers for transplantation into two adult recipients? *Liver Transpl Surg* 1999; **5**: 437-450 [PMID: 10477846 DOI: 10.1002/lt.500050508]

P- Reviewer: Bramhall S, Hilmi I, Tao R **S- Editor:** Gong ZM

L- Editor: Filipodia **E- Editor:** Huang Y





Novel oral-targeted therapies for mucosal healing in ulcerative colitis

Elisabetta Antonelli, Vincenzo Villanacci, Gabrio Bassotti

Elisabetta Antonelli, Gastroenterology Section, Perugia General Hospital, San Sisto (Perugia) 06156, Italy

Vincenzo Villanacci, Pathology Unit, ASST Spedali Civili, Brescia 25100, Italy

Gabrio Bassotti, Department of Medicine, Gastroenterology and Hepatology Section, University of Perugia Medical School, San Sisto (Perugia) 06132, Italy

ORCID number: Elisabetta Antonelli (0000-0002-9475-9047); Vincenzo Villanacci (0000-0002-6774-1060); Gabrio Bassotti (0000-0002-0237-1812).

Author contributions: Antonelli E and Bassotti G conceived the study and wrote the first draft of the manuscript; Villanacci V gave important intellectual contribution and critically reviewed the manuscript; all authors reviewed and approved the final version of the manuscript.

Conflict-of-interest statement: No conflict of interest exists.

Open-Access: This article is an open-access article which was selected by an in-house editor and fully peer-reviewed by external reviewers. It is distributed in accordance with the Creative Commons Attribution Non Commercial (CC BY-NC 4.0) license, which permits others to distribute, remix, adapt, build upon this work non-commercially, and license their derivative works on different terms, provided the original work is properly cited and the use is non-commercial. See: <http://creativecommons.org/licenses/by-nc/4.0/>

Manuscript source: Invited manuscript

Corresponding author to: Gabrio Bassotti, MD, PhD, Associate Professor, Department of Medicine, Gastroenterology and Hepatology Section, University of Perugia Medical School, Piazza Lucio Severi, San Sisto (Perugia) 06132, Italy. gabassot@tin.it
Telephone: +39-075-5784423
Fax: +39-075-5847570

Received: September 27, 2018

Peer-review started: September 27, 2018

First decision: October 26, 2018

Revised: November 14, 2018

Accepted: November 16, 2018

Article in press: November 16, 2018

Published online: December 21, 2018

Abstract

Ulcerative colitis (UC), a chronic, relapsing, remitting disease of the colon and rectum, is characterized by inflammatory ulceration of the mucosa. Current UC therapy relies on controlling acute episodes and preventing relapse. To predict modifications in the natural course of UC, mucosal healing (MH) has emerged as a major treatment goal. Endoscopic evaluation is considered the gold standard for assessing MH, which can be achieved by conventional drugs and biologics in many, but not all, patients. Consequently, interest is focusing on the development of new substances for UC therapy, and new oral agents are in the pipeline. This review will focus on the ability of newly developed oral drugs to induce and maintain MH in UC patients.

Key words: Mucosal healing; New oral treatments; Ozanimod; Peficitinib; Tofacitinib; Ulcerative colitis

© **The Author(s) 2018.** Published by Baishideng Publishing Group Inc. All rights reserved.

Core tip: The disease activity of ulcerative colitis (UC) is not sufficiently controlled in a subgroup of patients under the current therapeutic regimens. New oral substances are in the pipeline for treating UC. Mucosal healing (MH) has emerged as an important predictor of modifications in the natural disease course of UC. This review describes the efficacy of new oral drugs in inducing and maintaining MH in UC.

Antonelli E, Villanacci V, Bassotti G. Novel oral-targeted therapies for mucosal healing in ulcerative colitis. *World J Gastroenterol* 2018; 24(47): 5322-5330
 URL: <https://www.wjgnet.com/1007-9327/full/v24/i47/5322.htm>
 DOI: <https://dx.doi.org/10.3748/wjg.v24.i47.5322>

INTRODUCTION

Ulcerative colitis (UC) is a chronic, relapsing, remitting inflammatory disease of the colon and rectum, causing ulceration of the mucosa. Although UC usually has a mild to moderate course, approximately 20%-25% of patients suffer at least one severe acute attack, requiring hospitalisation^[1].

Current UC treatment relies on controlling acute attacks and preventing relapse^[2] by means of first-line agents like aminosalicylates, steroids, and immunosuppressants. When conventional therapy fails because of lack of efficacy or drug intolerance, biological agents may be administered to gain disease control. However, the available agents (infliximab, adalimumab, and golimumab) are often associated with primary and, more importantly, secondary loss of response^[3]. In addition to tumor necrosis factor (TNF)- α inhibitors, the $\alpha 4\beta 7$ integrin inhibitor vedolizumab has recently been playing a major role in the therapeutic arsenal^[4].

Advances in understanding the pathophysiology of UC led to strategies that were designed to alter cytokine levels^[5]. When attempting cytokine targeting, it is important to remember the role of the cells that produce and respond to those cytokines, and that efficacy may be linked to the role of cytokines in non-immune cells, all of which may limit therapeutic success or cause unpredictable adverse events^[6].

Fortunately, additional new therapeutic options have been, and are still being, actively explored and some have already entered daily clinical practice. Mucosal healing (MH) has emerged as a major treatment goal for patients with UC^[7-9]. Although endoscopy is the gold standard for assessing MH^[10], there are several endoscopic definitions of MH, most of which are not validated. In a recent consensus agreement called the Ulcerative Colitis Endoscopic Index of Severity (UCEIS), 0 was defined as endoscopic response as were a ≥ 1 grade decrease in the Mayo endoscopic score or ≥ 2 point drop in the UCEIS^[11].

Ideally, clinical recovery should be followed by mucosal repair^[12], which is assessed by evaluating the macroscopic appearance of the mucosa at endoscopy. MH is defined as resolution of visible mucosal inflammation and ulceration at endoscopy^[13], and diverse endoscopic scoring systems were developed to assess its presence or absence^[14]. Even though the Mayo Endoscopic Score^[15] is one of the most frequently used, only the UCEIS^[16] has been validated to date^[17].

MH is crucial because it predicts long-term remission,

reduces the risk of dysplasia or cancer, lowers hospitalisation and surgery rates, and improves quality of life, thus modifying the natural course of UC by slowing down, or even preventing, disease progression^[18]. Since inflammation is limited to the mucosa in UC patients, MH has become a central therapeutic goal, which may be achieved by means of several classes of drugs, including mesalamine^[19], corticosteroids^[20], immunomodulators^[21], and biologics^[22].

In this review, we discuss the efficacy of new oral drugs, which have been recently developed and successfully tested for UC therapy, in inducing and maintaining MH.

JANUS KINASE INHIBITORS

Janus kinases (JAKs), a family of intracellular proteins, consist of JAK 1, 2, and 3 and the related kinase tyrosine kinase 2 (TYK2)^[23]. Several JAK inhibitors were developed as therapy for immune-mediated diseases like rheumatoid arthritis, IBD, and psoriasis^[24]. Some compounds with JAK inhibitor activity have been tested for efficacy as potential UC treatments. They are small molecules characterized by oral administration, short serum half-life, intracellular target, and non-antigenicity^[25]. The results of JAK treatment for UC are summarized in Table 1.

Tofacitinib

Tofacitinib^[26], a non-selective JAK inhibitor, has recently been approved in Europe for adult patients with moderate to severe active UC who responded poorly, lost response, or were intolerant to either conventional therapy or a biologic agent^[27]. A few years ago, a phase II clinical trial demonstrated for the first time that tofacitinib was effective in UC^[28]. This trial was conducted on 194 patients with moderate to severe UC who had not responded to conventional therapy, anti-TNF agents or a combined approach. Tofacitinib at doses of 0.5, 3, 10 or 15 mg was administered twice daily vs placebo for 8 wk. Patients displayed an excellent clinical response, with the highest dose group having an almost 78% response rate. The endoscopic response was defined as a decrease of at least 1 from baseline in the endoscopy subscore, and endoscopic remission was defined as an endoscopic subscore of 0. At 8 wk, endoscopic remission occurred in 1/48 patients (2%) receiving placebo, compared with 3/31 (10%) receiving 0.5 mg of tofacitinib ($P = 0.14$), 6/33 (18%) receiving 3 mg of tofacitinib ($P = 0.01$), 10/33 (30%) receiving 10 mg of tofacitinib ($P < 0.001$), and 13/49 (27%) receiving 15 mg of tofacitinib ($P < 0.001$). The post hoc analysis^[29] showed that median fecal calprotectin (FCP) concentrations at week 8 were significantly lower ($P < 0.001$) in responders than in non-responders ($P < 0.001$) with respect to endoscopic remission (44 mg/kg vs 489 mg/kg) and MH (127 mg/kg vs 753 mg/kg). Moreover, an FCP cut-off value of 150 mg/kg displayed

Table 1 Summary of treatment results with Janus kinase inhibitors in ulcerative colitis patients

Study	Drug	Study population	Treatment arm	Endoscopy endpoint	Time of observation, wk	Rate of mucosal healing
Sandborn <i>et al</i> ^[28]	Tofacitinib	Moderate to severe UC patients (<i>n</i> = 194)	Doses of 0.5, 3, 10, or 15 mg/twice daily <i>vs</i> placebo for 8 wk	Secondary end points; Endoscopic remission: an endoscopic subscore of 0	At 8 wk	Placebo 2% Tofacitinib 0.5 mg = 10%, (<i>P</i> = 0.14) Tofacitinib 3 mg = 18%, (<i>P</i> = 0.01) Tofacitinib 10 mg = 30%, (<i>P</i> < 0.001), Tofacitinib 15 mg = 27%, (<i>P</i> < 0.001) Placebo 15.6%
Sandborn <i>et al</i> ^[30]	Tofacitinib	Moderate to severe UC patients (<i>n</i> = 614)	Dose of 10 mg/ twice daily <i>vs</i> placebo for 8 wk 16 patients received tofacitinib 15 mg twice daily	Key secondary endpoint was MH (Mayo endoscopic subscore of 0 or 1)	At 8 wk	Tofacitinib 10 mg = 31.3%, (<i>P</i> < 0.001)
Sandborn <i>et al</i> ^[30]	Tofacitinib	Moderate to severe UC patients (<i>n</i> = 547)	Dose of 10 mg twice daily <i>vs</i> placebo for 8 wk; 6 received tofacitinib; 15 mg twice daily	Key secondary endpoint was MH; Mayo endoscopic subscore of 0 or 1	At 8 wk	Placebo 11.6% Tofacitinib 10 mg = 28.4%, (<i>P</i> < 0.001)
Sandborn <i>et al</i> ^[30]	Tofacitinib	Moderate to severe UC patients (<i>n</i> = 593)	Dose of 5 mg twice daily, 10 mg twice daily, or placebo for 52 wk	Key secondary end points were mucosal healing; Mayo endoscopic subscore of 0 or 1	At 52 wk	Placebo 13.1% Tofacitinib 5 mg = 37.4%, (<i>P</i> < 0.001) Tofacitinib 10 mg = 45.7%, (<i>P</i> < 0.001)
Motoya <i>et al</i> ^[31]	Tofacitinib	Moderate to severe UC patients (<i>n</i> = 121 OCTAVE Induction 1 and 2) (<i>n</i> = 63, OCTAVE Sustain)	Dose of 5 mg twice daily (OCTAVE sustain only), 10 mg twice daily, or placebo	Key secondary endpoint was MH (Mayo endoscopic subscore of 0 or 1)	At 8 wk (OCTAVE Induction 1 and 2); At 52 wk (OCTAVE sustain)	Placebo 7.7% Tofacitinib 10 mg = 24.2% (OCTAVE Induction 1 and 2) Placebo 20% Tofacitinib 5 mg = 45.5% Tofacitinib 10 mg = 57.1% (OCTAVE Sustain)
Sands <i>et al</i> ^[35]	Peficitinib	Moderate-to-severe UC (<i>n</i> = 219)	Dose of 25 mg once daily (qd), 75 mg qd, 150 mg qd, 75 mg twice daily (bid) or placebo	Secondary endpoint was MH; Mayo endoscopic subscore of 0 or 1	At 8 wk	Placebo 18.6% Peficitinib 25 mg qd = 20.5% Peficitinib 75 mg qd = 29.5% Peficitinib 150 mg qd = 45.5% (<i>P</i> < 0.05) Peficitinib 75 mg bidmg = 36.4%

UC: Ulcerative colitis; OCTAVE: Oral Clinical Trials for tofacitinib in ulcerative colitis.

the highest sensitivity and specificity for clinical (0.68 and 0.79, kappa = 0.44) and endoscopic (0.79 and 0.75, kappa = 0.38) remission. The authors concluded that daily fluctuations in FCP concentrations might account for the low agreement between FCP and endoscopic remission. In addition, residual inflammation might still persist histologically despite MH and endoscopic remission. Since safety concerns (hyperlipidemia and viral infections) emerged for patients receiving the highest dose, the US Food and Drug Administration subsequently authorized only the 10 mg dose for clinical development. Consequently, the most recent OCTAVE (Oral Clinical Trials for tofacitinib in ulcerative colitis) trials on tofacitinib induction were conducted using a 10 mg dose twice daily^[30].

OCTAVE trials: Three multi-centre, randomized, double-blind, placebo-controlled trials (OCTAVE Induction 1; OCTAVE Induction 2; and OCTAVE Sustain) were conducted on moderate to severe UC^[30]. In the OCTAVE Induction 1 and 2 trials, 1139 eligible patients were randomly assigned to induction therapy with oral tofacitinib at a dose of 10 mg twice daily or placebo for 8 wk. The primary endpoint was remission at the end of the study, and the key secondary endpoint was MH (Mayo endoscopic subscore of 0 or 1) at 8 wk. Of note, endoscopic results were centrally assessed by a blinded observer, a methodological advance that has been adopted in recent UC studies. In the OCTAVE Induction 1 trial, 18.5% of patients receiving tofacitinib achieved the primary end point, *i.e.*, remission at 8 wk compared with

8.2% of the placebo group ($P = 0.007$). In the OCTAVE Induction 2 trial, remission rates were 16.6% vs 3.6% ($P < 0.001$). Both trials displayed similar results for the key secondary endpoint. MH was achieved in 31.3% (OCTAVE 1) and 28.4% (OCTAVE 2) patients receiving tofacitinib vs 15.6% and 11.6% in the placebo groups, respectively ($P < 0.001$ for both comparisons). Although these success rates may appear unimpressive, it should be emphasized that both study populations were highly treatment-refractory. All patients had, in fact, failed to respond to conventional therapies for UC, including TNF-blockers, and approximately half were receiving corticosteroids at baseline. Nevertheless, in subgroup analyses, a consistent treatment effect of tofacitinib was observed in anti-TNF naïve and anti-TNF exposed patients.

In the OCTAVE Sustain trial, 593 patients who had completed the OCTAVE Induction 1 or 2 trial and had responded clinically to induction therapy were assigned to tofacitinib maintenance therapy (5 or 10 mg twice daily) or placebo for 52 wk. MH, a key secondary endpoint, occurred in significantly more patients than placebo in both groups. Specifically, MH was observed in 74/198 patients (37.4%) in the 5 mg group and in 90/197 (45.7%) in the 10 mg group, vs 26/198 (13.1%) in the placebo cohort ($P < 0.001$ for both comparisons). At week 24, MH was observed in 43.9% of the 5 mg group and in 46.2% of the 10 mg group vs 17.2% of the placebo group. Also at week 24, MH was maintained in 52.4% of participants with MH at baseline who received the 5 mg tofacitinib dose and in 66.3% who received 10 mg tofacitinib, compared with 21.8% in the placebo group ($P < 0.001$). Endoscopic remission, defined as an endoscopic subscore of 0, was another end-point. After 24 and 52 wk, it was observed in 16.2% and 14.6% of the 5 mg tofacitinib group and in 12.2% and 16.8% of the 10 mg tofacitinib group, respectively, vs 4% of placebo patients. Sustained endoscopic remission, defined as responses at both week 24 and 52, was 6.1% and 5.1% in the 5 mg and the 10 mg tofacitinib groups, respectively.

In post-hoc analyses of East Asian patients with active UC who were enrolled in global phase 3 induction and maintenance studies^[31], twice daily doses of 10 mg oral tofacitinib induced MH with greater efficacy than placebo. At week 8, 10 mg tofacitinib was associated with a 24.2% response rate vs 7.7% with placebo. Similarly, MH was achieved at week 52 in 45.5% of patients receiving 5 mg tofacitinib, and in 57.1% of those given 10 mg twice daily of tofacitinib vs 20.0% receiving placebo.

An ongoing, open-label, long-term extension study (OCTAVE Open)^[32] included non-responders from OCTAVE Induction 1 and 2, and patients who had completed or experienced treatment failure in OCTAVE Sustain. This trial was conducted in a subpopulation of 58 patients who achieved clinical response following 8 wk induction therapy with 10 mg twice daily tofacitinib.

The patients entered OCTAVE Sustain receiving 5 mg twice daily tofacitinib, but experienced treatment failure between week 8 and 52. In the OCTAVE Open, these patients were escalated to 10 mg tofacitinib twice daily, which induced MH in 41.4% and 60.4% patients at months 2 and 12, respectively, compared with baseline (5.2%)^[33].

Peficitinib

Peficitinib, a JAK1, JAK2, and JAK3 oral inhibitor, has an *in vitro* potency that is approximately 6- to 7-fold greater for JAK3 than for JAK1 and JAK2^[34]. In a phase 2b randomized, double-blind, placebo-controlled, dose-ranging trial, its efficacy and safety were evaluated in 219 patients with moderate-to-severe UC^[35]. Patients were equally randomized to receive oral placebo or 25, 75 or 150 mg peficitinib once daily, or 75 mg peficitinib twice daily. At week 8, patients were assessed for clinical response, and MH was one of the secondary endpoints. The Mayo endoscopic subscores were assigned by the local reader (blinded to treatment assignment) and the central reader (blinded to treatment assignment and clinical examination). Few patients achieved normal or inactive mucosal disease (endoscopy subscore of 0). At week 8, MH was observed in 20.5% (25 mg daily), 29.5% (75 mg daily), 45.5% (150 mg daily), 36.4% (75 mg twice daily) vs 18.6% of patients (placebo). While no dose-response of peficitinib was demonstrated in patients with moderate-to-severe UC, evidence of efficacy in achieving MH was suggested at doses ≥ 75 mg daily vs placebo.

Upadacitinib

Upadacitinib, a JAK 1 inhibitor, is being developed to treat rheumatoid arthritis and other inflammatory diseases. At present, it is being investigated as an oral treatment of UC^[36,37], but no results are yet available.

MODULATION OF SPHINGOSINE-1-PHOSPHATE RECEPTOR

The sphingosine-1-phosphate (S1P) receptor family consists of widely expressed receptors (S1P1 through S1P5) that are implicated in regulating multiple immunological and cardiovascular functions such as cell proliferation and migration, immune cell tracking, angiogenesis and the epithelial barrier^[38]. Targeting S1P receptors for inflammatory conditions was successful in clinical trials and is presently being investigated as a potential therapy for UC patients^[39]. The results of S1P receptor modulation to treat UC patients are summarized in Table 2.

Ozanimod

Ozanimod (RPC1063, Celgene) is a new oral selective S1P1 and S1P5 receptor modulator that is under investigation for the treatment of UC^[40]. The

Table 2 Summary of treatment results with sphingosine-1-phosphate receptor modulators, AJM300, and phospholipids in ulcerative colitis patients

Study	Drug	Study population	Treatment arm	Endoscopy endpoint	Time of observation, wk	Rate of mucosal healing
Sandborn <i>et al</i> ^[41]	Ozanimod	Moderate to severe UC patients (<i>n</i> = 197)	Dose of 0.5 mg or 1 mg or placebo, once daily	Mucosal healing (endoscopy subscore ≤ 1)	At 8 wk; at 32 wk	Placebo 12% Ozanimod 0.5 mg = 28%, (<i>P</i> = 0.03) Ozanimod 1 mg = 34%, (<i>P</i> = 0.002) At week 8 Placebo 12% Ozanimod 0.5 mg = 32%, (<i>P</i> = 0.006) Ozanimod 1 mg = 33%, (<i>P</i> = 0.005) At week 32 Placebo 29.4% AJM300 960 mg = 58.8% (<i>P</i> = 0.0014)
Yoshimura <i>et al</i> ^[46]	AJM300	Moderate to severe UC patients (<i>n</i> = 102)	Dose of 960 mg or placebo, 3 times daily	Mucosal healing, (endoscopic subscore of 0 or 1)	At 8 wk	None of 29 placebo patients DEAI (> 50%) in 11 of 29 evaluated of PC patients <i>P</i> = 0.00016
Stremmel <i>et al</i> ^[50]	Phosphatidylcholine-rich phospholipids	Chronic active, ulcerative colitis, with a clinical activity index (CAI) of > 4 (<i>n</i> = 60)	Dose of PC rich phospholipids (1.5 g / dose) or placebo, four times daily	Mucosal healing, was not formally assessed 48 patients were examined using the standard endoscopic activity index (EAI); Secondary end point analysis DEAI (> 50%)	At three mo	
Karner <i>et al</i> ^[51]	LT-02	Ulcerative colitis patients with an inadequate response to mesalazine, a disease activity score (Simple Clinical Colitis Activity Index (SCCAI)) of ≥ 5, and bloody diarrhea (<i>n</i> = 156)	Dose of LT-2 (0.8, 1.6 or 3.2 g) or placebo	Mucosal healing (endoscopic Mayo Score ≤ 1)	At 12 wk	Placebo 40.0% LT-2 0.8 g = 57.5%, (<i>P</i> = 0.097) LT-2 1.6 g = 56.1%, (<i>P</i> = 0.097) LT-2 3.2 g = 51.4%, (<i>P</i> = 0.097) Pooled LT-02 groups 55.2 (<i>P</i> = 0.098)

UC: Ulcerative colitis; OCTAVE: Oral Clinical Trials for tofacitinib in ulcerative colitis.

TOUCHSTONE study^[41], a randomised, double-blind, placebo-controlled phase II trial that recruited 197 patients with moderate to severe active UC, tested the efficacy and safety of ozanimod through induction and maintenance. Patients were randomised in a 1:1:1 ratio to receive once daily oral ozanimod at 1 mg (*n* = 67) and 0.5 mg (*n* = 65) concentrations or placebo (*n* = 65) for 8 wk (induction phase). Flexible sigmoidoscopy, with blinded central reading, was performed at screening and at week 8 and 32. The primary endpoint was clinical remission (defined as Mayo score ≤ 2 and no subscore > 1) at week 8. One of the exploratory secondary endpoints was MH (defined as an endoscopy subscore ≤ 1). Although ozanimod provided some benefits, most endpoints did not reach statistical significance. At 8 wk, 16% and 57% of patients receiving 1 mg daily ozanimod achieved clinical remission and clinical response, respectively, vs 6% and 37% of the placebo group, respectively. At 8 wk, significant endoscopic improvements were observed in patients receiving all doses of ozanimod compared with placebo. MH occurred

in 18/65 patients (28%) in the 0.5 mg group (*P* = 0.03), and in 23/67 patients (34%) in the 1 mg group (*P* = 0.002) vs 8/65 patients (12%) in the placebo group. However, no significant differences emerged in histological remission. The 32 wk double-blind maintenance phase included 103/197 (52.3%) patients who had been recruited in the induction phase and wanted to continue with their original treatment, with 91 (88.3%) patients completing maintenance. Explorative outcome measures at week 32 included clinical response, histological remission, clinical remission and MH. At weeks 8 and 32, MH was observed in 32% (0.5 mg) and 33% (1 mg) of patients, respectively, compared with 12% in each placebo group, however these differences did not reach statistical significance. One limitation of the study was the time point for primary outcome analysis, since 8 wk might not have been long enough for ozanimod to target lymphocyte trafficking. Moreover, the long-term safety profile could not be assessed because the cohort of patients was relatively small and the follow-up was short. Larger studies with longer follow-ups

are therefore needed. Since ozanimod displayed some potential benefits and the results appeared promising, two phase III studies for induction and maintenance therapy are currently underway to further evaluate the potential role of ozanimod in moderate to severe UC^[42,43].

Other S1P modulators

Etrasimod (APD334), a S1P-R₁ modulator, is currently being investigated in a phase 2 study as a potential therapeutic agent for UC patients^[44].

SMALL-MOLECULE $\alpha 4$ INTEGRIN ANTAGONISTS

AJM300

AJM300, a new, orally active small molecule, is classified as a phenylalanine derivative and is currently being developed for UC^[45]. Both the efficacy and safety of AJM300 were tested in a Japanese randomized, double-blind, placebo-controlled phase IIa study^[46] conducted on 102 patients with moderately active UC who were intolerant or showed an inappropriate response to mesalazine or steroids. For 8 wk, patients were orally administered 960 mg of AJM300 or placebo 3 times daily. The primary endpoint was clinical response. Secondary endpoints were clinical remission (defined as a Mayo Clinic score of 2 or lower and no sub-score higher than 1) and MH (defined as an endoscopic sub-score of 0 or 1, and a partial Mayo Clinic score). Endoscopic assessment with biopsy was performed at baseline and at week 8, and the endoscopic sub-scores were analysed by a central evaluation committee. In this study, 62.7% of patients receiving AJM300 and 25.5% of the placebo group had a clinical response at week 8. MH was achieved by 58.8% of patients (30/51) in the active treatment arm and by 29.4% (15/51) in the placebo group. Although the difference was not significant, more patients in the active treatment arm achieved endoscopic subscores of 0 at week 8 than in the placebo group.

The most concerning adverse event of an $\alpha 4$ integrin blockade is the development of progressive multifocal leukoencephalopathy, a demyelinating central nervous system disorder caused by JC viral infection and reactivation. However, neither infection nor neurological symptoms were observed in this study. These data demonstrated the feasibility of AJM300 treatment, particularly when it is delivered in a gut-specific manner. A phase III Study of AJM300 in UC patients is currently ongoing^[47]. The results of AJM300 treatment for UC patients are summarized in Table 2.

SUBSTITUTION OF PHOSPHATIDYLCHOLINE

LT02

Phosphatidylcholine, which prevents bacterial invasion,

is reduced by up to 70% in the colonic mucus of UC patients^[48]. Therefore, phosphatidylcholine substitution in the colonic mucus might be an interesting future therapeutic approach^[49]. In a double-blind, randomized, placebo-controlled phase IIa study, 60 patients with UC were treated with 6 g of phosphatidylcholine-rich phospholipids for 3 mo^[50]. The phospholipids were released in the distal ileum in a pH-dependent manner. Significant improvements in clinical remission and clinical response, the primary endpoints, were observed compared with placebo, together with significant positive effects in endoscopic and histological assessments. However, MH was not formally assessed.

LT-02, a novel modified-release phosphatidylcholine agent, was investigated for mucosal barrier enhancement in UC. In a double-blinded, randomized, placebo-controlled, multi-centre phase II study^[51], LT-02 was administered to a total of 156 patients with an inadequate response to mesalazine, characterized by a disease activity score ≥ 5 [Simple Clinical Colitis Activity Index (SCCAI)] and bloody diarrhea. The patients were randomized into three treatment groups orally receiving 0.8, 1.6 or 3.2 g of LT-02 or placebo. The primary endpoint was clinical response after 3 mo therapy, as indicated by changes in SCCAI from baseline to the end of treatment. Data analysis showed a 33.3% SCCAI drop in the placebo group compared with 44.3% in the 0.8 g LT-02 group ($P > 0.05$) and 40.7% in the 1.6 g group ($P > 0.05$). The 3.2 g group improved by 51.7%, falling from 8.5 to 4.1 ($P = 0.030$ vs placebo). The remission rate was 15% (6/40) in the placebo group vs 31.4% (11/35) in the highest LT-02 dose group ($P = 0.089$). MH was achieved in 32.5% of the placebo group vs 47.4% in the pooled LT-02 groups ($P = 0.098$). The histological healing rate (histological index = 1) was 20.0% in the placebo cohort vs 35.3% in the LT-02 groups ($P = 0.016$). In a second analysis, considering dropouts as failures, endoscopic remission but not clinical remission reached statistical significance. Histological remission was reached significantly more often in the treatment groups. No serious adverse events were observed and there were no deviations in adverse events in the treatment groups. The authors concluded that, compared with placebo, LT-02 is useful for reducing disease activity in UC and is associated with a good safety profile. The results of such treatments for UC patients are summarized in Table 2.

CONCLUSION

The new oral-targeted therapies seem to be effective for UC patients. They share some common characteristics, such as shorter half-lives, potential off-target effects, relatively narrow dosing windows and lack of immunogenicity. The mechanisms of action of the four classes of these oral synthetic drugs include: (1) Jak-inhibitors, which reduce the production of several cytokines, (2) AJM300, which blocks lymphocyte

trafficking from blood vessels into the lamina propria, (3) ozanimod, which prevents egression of lymphocytes from lymph nodes by following the S1P gradient *via* receptor internalization, and (4) LT-02, a substitute of phosphatidylcholine. Further studies are ongoing and will establish the value of these agents for the treatment of UC patients in clinical practice. They could potentially offer three major advantages: (1) As an alternative for patients who mount immunogenic responses to biologics, (2) in association to other drugs, as innovative combination strategies, and (3) to investigate stop and start therapeutic strategies. Moreover, with convenient storage, they might be potentially transported into the site of action and act as topical therapy. On the other hand, multiple daily dosing, uncertainties about bioavailability at the right target site and adverse events may constitute the potential disadvantages of this therapeutic approach.

ACKNOWLEDGMENTS

We are warmly indebted to Ms. Geraldine Anne Boyd of our Faculty, Lecturer in Scientific English, for the revision of the English form of the manuscript.

REFERENCES

- 1 **Feuerstein JD**, Cheifetz AS. Ulcerative colitis: epidemiology, diagnosis, and management. *Mayo Clin Proc* 2014; **89**: 1553-1563 [PMID: 25199861 DOI: 10.1016/j.mayocp.2014.07.002]
- 2 **Matsuoka K**, Kobayashi T, Ueno F, Matsui T, Hirai F, Inoue N, Kato J, Kobayashi K, Kobayashi K, Koganei K, Kunisaki R, Motoya S, Nagahori M, Nakase H, Omata F, Saruta M, Watanabe T, Tanaka T, Kanai T, Noguchi Y, Takahashi KI, Watanabe K, Hibi T, Suzuki Y, Watanabe M, Sugano K, Shimosegawa T. Evidence-based clinical practice guidelines for inflammatory bowel disease. *J Gastroenterol* 2018; **53**: 305-353 [PMID: 29429045 DOI: 10.1007/s00535-018-1439-1]
- 3 **Pouillon L**, Bossuyt P, Peyrin-Biroulet L. Considerations, challenges and future of anti-TNF therapy in treating inflammatory bowel disease. *Expert Opin Biol Ther* 2016; **16**: 1277-1290 [PMID: 27329436 DOI: 10.1080/14712598.2016.1203897]
- 4 **Narula N**, Peerani F, Meserve J, Kochhar G, Chaudrey K, Hartke J, Chilukuri P, Koliiani-Pace J, Winters A, Katta L, Shmidt E, Hirtner R, Faleck D, Parikh MP, Whitehead D, Boland BS, Singh S, Sagi SV, Fischer M, Chang S, Barocas M, Luo M, Lasch K, Bohm M, Lukin D, Sultan K, Swaminath A, Hudesman D, Gupta N, Shen B, Kane S, Loftus EV, Siegel CA, Sands BE, Colombel JF, Sandborn WJ, Dulai PS. Vedolizumab for Ulcerative Colitis: Treatment Outcomes from the VICTORY Consortium. *Am J Gastroenterol* 2018; **113**: 1345-1354 [PMID: 29946178 DOI: 10.1038/s41395-018-0162-0]
- 5 **Bevino G**, Monteleone G. Advances in understanding the role of cytokines in inflammatory bowel disease. *Expert Rev Gastroenterol Hepatol* 2018; **12**: 907-915 [PMID: 30024302 DOI: 10.1080/17474124.2018.1503053]
- 6 **Hindryckx P**, Vande Casteele N, Novak G, Khanna R, D'Haens G, Sandborn WJ, Danese S, Jairath V, Feagan BG. The Expanding Therapeutic Armamentarium for Inflammatory Bowel Disease: How to Choose the Right Drug[s] for Our Patients? *J Crohns Colitis* 2018; **12**: 105-119 [PMID: 28961959 DOI: 10.1093/ecco-jcc/jjx117]
- 7 **Orlando A**, Guglielmi FW, Cottone M, Orlando E, Romano C, Sinagra E. Clinical implications of mucosal healing in the management of patients with inflammatory bowel disease. *Dig Liver Dis* 2013; **45**: 986-991 [PMID: 23993738 DOI: 10.1016/j.dld.2013.07.005]
- 8 **Villanacci V**, Antonelli E, Geboes K, Casella G, Bassotti G. Histological healing in inflammatory bowel disease: a still unfulfilled promise. *World J Gastroenterol* 2013; **19**: 968-978 [PMID: 23467585 DOI: 10.3748/wjg.v19.i7.968]
- 9 **Mazzuoli S**, Guglielmi FW, Antonelli E, Salemm M, Bassotti G, Villanacci V. Definition and evaluation of mucosal healing in clinical practice. *Dig Liver Dis* 2013; **45**: 969-977 [PMID: 23932331 DOI: 10.1016/j.dld.2013.06.010]
- 10 **Goetz M**. Endoscopic Surveillance in Inflammatory Bowel Disease. *Visc Med* 2018; **34**: 66-71 [PMID: 29594172 DOI: 10.1159/000485019]
- 11 **Vuitton L**, Peyrin-Biroulet L, Colombel JF, Pariente B, Pineton de Chambrun G, Walsh AJ, Panes J, Travis SP, Mary JY, Marteau P. Defining endoscopic response and remission in ulcerative colitis clinical trials: an international consensus. *Aliment Pharmacol Ther* 2017; **45**: 801-813 [PMID: 28112419 DOI: 10.1111/apt.13948]
- 12 **Peyrin-Biroulet L**, Ferrante M, Magro F, Campbell S, Franchimont D, Fidler H, Strid H, Ardizzone S, Veeraman-Wauters G, Chevaux JB, Allez M, Danese S, Sturm A; Scientific Committee of the European Crohn's and Colitis Organization. Results from the 2nd Scientific Workshop of the ECCO. I: Impact of mucosal healing on the course of inflammatory bowel disease. *J Crohns Colitis* 2011; **5**: 477-483 [PMID: 21939925 DOI: 10.1016/j.crohns.2011.06.009]
- 13 **Boal Carvalho P**, Cotter J. Mucosal Healing in Ulcerative Colitis: A Comprehensive Review. *Drugs* 2017; **77**: 159-173 [PMID: 28078646 DOI: 10.1007/s40265-016-0676-y]
- 14 **Mohammed Vashist N**, Samaan M, Mosli MH, Parker CE, MacDonald JK, Nelson SA, Zou GY, Feagan BG, Khanna R, Jairath V. Endoscopic scoring indices for evaluation of disease activity in ulcerative colitis. *Cochrane Database Syst Rev* 2018; **1**: CD011450 [PMID: 29338066 DOI: 10.1002/14651858.CD011450.pub2]
- 15 **Schroeder KW**, Tremaine WJ, Ilstrup DM. Coated oral 5-aminosalicylic acid therapy for mildly to moderately active ulcerative colitis. A randomized study. *N Engl J Med* 1987; **317**: 1625-1629 [PMID: 3317057 DOI: 10.1056/NEJM198712243172603]
- 16 **Travis SP**, Schnell D, Krzeski P, Abreu MT, Altman DG, Colombel JF, Feagan BG, Hanauer SB, Lichtenstein GR, Marteau PR, Reinisch W, Sands BE, Yacyszyn BR, Schnell P, Bernhardt CA, Mary JY, Sandborn WJ. Reliability and initial validation of the ulcerative colitis endoscopic index of severity. *Gastroenterology* 2013; **145**: 987-995 [PMID: 23891974 DOI: 10.1053/j.gastro.2013.07.024]
- 17 **Lee JS**, Kim ES, Moon W. Chronological Review of Endoscopic Indices in Inflammatory Bowel Disease. *Clin Endosc* 2018 [PMID: 30130840 DOI: 10.5946/ce.2018.042]
- 18 **Frøslie KF**, Jahnsen J, Moum BA, Vatn MH; IBSEN Group. Mucosal healing in inflammatory bowel disease: results from a Norwegian population-based cohort. *Gastroenterology* 2007; **133**: 412-422 [PMID: 17681162 DOI: 10.1053/j.gastro.2007.05.051]
- 19 **Hanauer SB**, Sandborn WJ, Dallaire C, Archambault A, Yacyszyn B, Yeh C, Smith-Hall N. Delayed-release oral mesalamine 4.8 g/day (800 mg tablets) compared to 2.4 g/day (400 mg tablets) for the treatment of mildly to moderately active ulcerative colitis: The ASCEND I trial. *Can J Gastroenterol* 2007; **21**: 827-834 [PMID: 18080055]
- 20 **Rizzello F**, Gionchetti P, D'Arienzo A, Manguso F, Di Matteo G, Annese V, Valpiani D, Casetti T, Adamo S, Prada A, Castiglione GN, Varoli G, Campieri M. Oral beclomethasone dipropionate in the treatment of active ulcerative colitis: a double-blind placebo-controlled study. *Aliment Pharmacol Ther* 2002; **16**: 1109-1116 [PMID: 12030952]
- 21 **Ardizzone S**, Maconi G, Russo A, Imbesi V, Colombo E, Bianchi Porro G. Randomised controlled trial of azathioprine and 5-aminosalicylic acid for treatment of steroid dependent ulcerative colitis. *Gut* 2006; **55**: 47-53 [PMID: 15972298]
- 22 **Laharie D**, Filippi J, Roblin X, Nancey S, Chevaux JB, Hébuterne X, Flourie B, Capdepon M, Peyrin-Biroulet L. Impact of mucosal

- healing on long-term outcomes in ulcerative colitis treated with infliximab: a multicenter experience. *Aliment Pharmacol Ther* 2013; **37**: 998-1004 [PMID: 23521659 DOI: 10.1111/apt.12289]
- 23 **D'Amico F**, Fiorino G, Furfaro F, Allocca M, Danese S. Janus kinase inhibitors for the treatment of inflammatory bowel diseases: developments from phase I and phase II clinical trials. *Expert Opin Investig Drugs* 2018; **27**: 595-599 [PMID: 29938545 DOI: 10.1080/13543784.2018.1492547]
 - 24 **Hirahara K**, Schwartz D, Gadina M, Kanno Y, O'Shea JJ. Targeting cytokine signaling in autoimmunity: back to the future and beyond. *Curr Opin Immunol* 2016; **43**: 89-97 [PMID: 27821272 DOI: 10.1016/j.coi.2016.10.001]
 - 25 **Flanagan ME**, Blumenkopf TA, Brissette WH, Brown MF, Casavant JM, Shang-Poa C, Doty JL, Elliott EA, Fisher MB, Hines M, Kent C, Kudlacz EM, Lillie BM, Magnuson KS, McCurdy SP, Munchhof MJ, Perry BD, Sawyer PS, Strelevitz TJ, Subramanyam C, Sun J, Whipple DA, Changelian PS. Discovery of CP-690,550: a potent and selective Janus kinase (JAK) inhibitor for the treatment of autoimmune diseases and organ transplant rejection. *J Med Chem* 2010; **53**: 8468-8484 [PMID: 21105711 DOI: 10.1021/jm1004286]
 - 26 **Dowty ME**, Lin J, Ryder TF, Wang W, Walker GS, Vaz A, Chan GL, Krishnaswami S, Prakash C. The pharmacokinetics, metabolism, and clearance mechanisms of tofacitinib, a janus kinase inhibitor, in humans. *Drug Metab Dispos* 2014; **42**: 759-773 [PMID: 24464803 DOI: 10.1124/dmd.113.054940]
 - 27 Pfizer: XELJANZ gets marketing authorization in EU for ulcerative colitis. Available from: URL: <http://www.rttnews.com/2921111/pfizer-xeljanz-gets-marketing-authorization-in-eu-for-ulcerative-colitis.aspx>
 - 28 **Sandborn WJ**, Ghosh S, Panes J, Vranic I, Su C, Rousell S, Niezychowski W; Study A3921063 Investigators. Tofacitinib, an oral Janus kinase inhibitor, in active ulcerative colitis. *N Engl J Med* 2012; **367**: 616-624 [PMID: 22894574 DOI: 10.1056/NEJMoa1112168]
 - 29 **Sandborn WJ**, Panés J, Zhang H, Yu D, Niezychowski W, Su C. Correlation Between Concentrations of Fecal Calprotectin and Outcomes of Patients With Ulcerative Colitis in a Phase 2 Trial. *Gastroenterology* 2016; **150**: 96-102 [PMID: 26376350 DOI: 10.1053/j.gastro.2015.09.001]
 - 30 **Sandborn WJ**, Su C, Sands BE, D'Haens GR, Vermeire S, Schreiber S, Danese S, Feagan BG, Reinisch W, Niezychowski W, Friedman G, Lawendy N, Yu D, Woodworth D, Mukherjee A, Zhang H, Healey P, Panés J, OCTAVE Induction 1, OCTAVE Induction 2, and OCTAVE Sustain Investigators. Tofacitinib as Induction and Maintenance Therapy for Ulcerative Colitis. *N Engl J Med* 2017; **376**: 1723-1736 [PMID: 28467869 DOI: 10.1056/NEJMoa1606910]
 - 31 **Motoya S**, Watanabe M, Kim HJ, Kim YH, Han DS, Yuasa H, Tabira J, Isogawa N, Arai S, Kawaguchi I, Hibi T. Tofacitinib induction and maintenance therapy in East Asian patients with active ulcerative colitis: subgroup analyses from three phase 3 multinational studies. *Intest Res* 2018; **16**: 233-245 [PMID: 29743836 DOI: 10.5217/ir.2018.16.2.233]
 - 32 Long-term study of CP-690, 550 In subjects with ulcerative colitis (OCTAVE). ClinicalTrials.gov Identifier: NCT01470612. Available from: URL: <https://clinicaltrials.gov/ct2/show/study/NCT01470612>
 - 33 **Sands BE**, Moss AC, Armuzzi A, Marshall JK, Lindsay JO, Sandborn WJ, Danese S, Tsikos K, Lawendy N, Zhang H, Friedman GS, Chan G, Krichbaum DW, Su C. Efficacy and safety of dose escalation to tofacitinib 10 mg BID for patients with ulcerative colitis following loss of response on tofacitinib 5 mg BID maintenance therapy: results from OCTAVE open. *J Crohn's Colitis* 2018 **12** (suppl): S049-S049
 - 34 **Roskoski R Jr.** Janus kinase (JAK) inhibitors in the treatment of inflammatory and neoplastic diseases. *Pharmacol Res* 2016; **111**: 784-803 [PMID: 27473820 DOI: 10.1016/j.phrs.2016.07.038]
 - 35 **Sands BE**, Sandborn WJ, Feagan BG, Lichtenstein GR, Zhang H, Strauss R, Szapary P, Johanns J, Panes J, Vermeire S, O'Brien CD, Yang Z, Bertelsen K, Marano C; Peficitinib-UC Study Group. Peficitinib, an Oral Janus Kinase Inhibitor, in Moderate-to-severe Ulcerative Colitis: Results From a Randomised, Phase 2 Study. *J Crohn's Colitis* 2018; **12**: 1158-1169 [PMID: 29917064 DOI: 10.1093/ecco-jcc/jjy085]
 - 36 A Study to Evaluate the Safety and Efficacy of Upadacitinib (ABT-494) for Induction and Maintenance Therapy in Subjects With Moderately to Severely Active Ulcerative Colitis (UC). Available from: URL: <https://clinicaltrials.gov/ct2/show/NCT02819635?term=upadacitinib&cond=Ulcerative+Colitis>. ClinicalTrials.gov Identifier: NCT02819635
 - 37 A Study to Evaluate the Long-Term Safety and Efficacy of Upadacitinib (ABT-494) in Subjects With Ulcerative Colitis (UC). ClinicalTrials.gov Identifier: NCT03006068. Available from: URL: <https://clinicaltrials.gov/ct2/show/NCT03006068?term=upadacitinib&cond=Ulcerative+Colitis&rank=1>
 - 38 **Pyne NJ**, Pyne S. Sphingosine 1-Phosphate Receptor 1 Signaling in Mammalian Cells. *Molecules* 2017; **22** [PMID: 28241498 DOI: 10.3390/molecules22030344]
 - 39 **Peyrin-Biroulet L**, Christopher R, Behan D, Lassen C. Modulation of sphingosine-1-phosphate in inflammatory bowel disease. *Autoimmun Rev* 2017; **16**: 495-503 [PMID: 28279838 DOI: 10.1016/j.autrev.2017.03.007]
 - 40 **White JR**, Phillips F, Monaghan T, Fateen W, Samuel S, Ghosh S, Moran GW. Review article: novel oral-targeted therapies in inflammatory bowel disease. *Aliment Pharmacol Ther* 2018; **47**: 1610-1622 [PMID: 29672874 DOI: 10.1111/apt.14669]
 - 41 **Sandborn WJ**, Feagan BG, Wolf DC, D'Haens G, Vermeire S, Hanauer SB, Ghosh S, Smith H, Cravets M, Frohna PA, Aranda R, Gujrathi S, Olson A; TOUCHSTONE Study Group. Ozanimod Induction and Maintenance Treatment for Ulcerative Colitis. *N Engl J Med* 2016; **374**: 1754-1762 [PMID: 27144850 DOI: 10.1056/NEJMoa1513248]
 - 42 Safety and efficacy trial of RPC1063 for moderate to severe ulcerative colitis. ClinicalTrials.gov Identifier: NCT02435992. Available from: URL: <https://clinicaltrials.gov/ct2/show/NCT02435992>
 - 43 Open-label extension of RPC1063 as therapy for moderate to severe ulcerative colitis. ClinicalTrials.gov Identifier: NCT02531126. Available from: URL: <https://clinicaltrials.gov/ct2/show/NCT02531126>
 - 44 Safety and efficacy of etrasimod (APD334) in patients with ulcerative colitis. ClinicalTrials.gov Identifier: NCT02447302. Available from: URL: <https://clinicaltrials.gov/ct2/show/NCT02447302>
 - 45 **Park SC**, Jeon YT. Anti-integrin therapy for inflammatory bowel disease. *World J Gastroenterol* 2018; **24**: 1868-1880 [PMID: 29740202 DOI: 10.3748/wjg.v24.i17.1868]
 - 46 **Yoshimura N**, Watanabe M, Motoya S, Tominaga K, Matsuoka K, Iwakiri R, Watanabe K, Hibi T; AJM300 Study Group. Safety and Efficacy of AJM300, an Oral Antagonist of $\alpha 4$ Integrin, in Induction Therapy for Patients With Active Ulcerative Colitis. *Gastroenterology* 2015; **149**: 1775-1783.e2 [PMID: 26327130 DOI: 10.1053/j.gastro.2015.08.044]
 - 47 A study to evaluate the safety and efficacy of AJM300 in participants with active ulcerative colitis. ClinicalTrials.gov Identifier: NCT03531892. Available from: URL: <https://clinicaltrials.gov/ct2/show/NCT03531892>
 - 48 **Ehehalt R**, Wagenblast J, Erben G, Lehmann WD, Hinz U, Merle U, Stremmel W. Phosphatidylcholine and lysophosphatidylcholine in intestinal mucus of ulcerative colitis patients. A quantitative approach by nanoElectrospray-tandem mass spectrometry. *Scand J Gastroenterol* 2004; **39**: 737-742 [PMID: 15513358 DOI: 10.1080/00365520410006233]
 - 49 **Schneider H**, Braun A, Füllekrug J, Stremmel W, Ehehalt R. Lipid based therapy for ulcerative colitis-modulation of intestinal mucus membrane phospholipids as a tool to influence inflammation. *Int J Mol Sci* 2010; **11**: 4149-4164 [PMID: 21152327 DOI: 10.3390/ijms11104149]
 - 50 **Stremmel W**, Merle U, Zahn A, Autschbach F, Hinz U, Ehehalt R. Retarded release phosphatidylcholine benefits patients with chronic active ulcerative colitis. *Gut* 2005; **54**: 966-971 [PMID: 15951544 DOI: 10.1136/gut.2004.052316]

- 51 **Karner M**, Kocjan A, Stein J, Schreiber S, von Boyen G, Uebel P, Schmidt C, Kupcinskas L, Dina I, Zuelch F, Keilhauer G, Stremmel W. First multicenter study of modified release phosphatidylcholine

“LT-02” in ulcerative colitis: a randomized, placebo-controlled trial in mesalazine-refractory courses. *Am J Gastroenterol* 2014; **109**: 1041-1051 [PMID: 24796768 DOI: 10.1038/ajg.2014.104]

P- Reviewer: Efthymiou A, Martin-Villa JM, Yokoyama K
S- Editor: Wang XJ **L- Editor:** Filipodia **E- Editor:** Huang Y



Percutaneous ablation for perivascular hepatocellular carcinoma: Refining the current status based on emerging evidence and future perspectives

Tae Wook Kang, Hyo Keun Lim, Dong Ik Cha

Tae Wook Kang, Hyo Keun Lim, Dong Ik Cha, Department of Radiology and Center for Imaging Science, Samsung Medical Center, Sungkyunkwan University School of Medicine, Seoul 135-710, South Korea

Hyo Keun Lim, Department of Health Sciences and Technology, SAIHST, Sungkyunkwan University, Seoul 135-710, South Korea

ORCID number: Tae Wook Kang (0000-0002-0725-8317); Hyo Keun Lim (0000-0003-3269-7503); Dong Ik Cha (0000-0002-9116-3803).

Author contributions: Lim HK and Kang TW contributed to concept and writing of the article; Cha DI and Kang TW contributed to critical review and final approval of the article.

Supported by Nano-Convergence Foundation, the Ministry of Science, ICT and Future Planning (MSIP, South Korea) and the Ministry of Trade, Industry and Energy (MOTIE, South Korea), No. R201603110.

Conflict-of-interest statement: The authors do not have any conflicts of interest to declare.

Open-Access: This article is an open-access article which was selected by an in-house editor and fully peer-reviewed by external reviewers. It is distributed in accordance with the Creative Commons Attribution Non Commercial (CC BY-NC 4.0) license, which permits others to distribute, remix, adapt, build upon this work non-commercially, and license their derivative works on different terms, provided the original work is properly cited and the use is non-commercial. See: <http://creativecommons.org/licenses/by-nc/4.0/>

Manuscript source: Invited manuscript

Corresponding author to: Hyo Keun Lim, MD, PhD, Professor, Department of Radiology, Samsung Medical Center, Sungkyunkwan University School of Medicine, Irwon-ro 81, Gangnam-gu, Seoul 135-710, South Korea. rfalim@skku.edu
Telephone: +82-2-34102505

Fax: +82-2-34102559

Received: September 19, 2018

Peer-review started: September 19, 2018

First decision: October 16, 2018

Revised: October 24, 2018

Accepted: November 2, 2018

Article in press: November 2, 2018

Published online: December 21, 2018

Abstract

Various therapeutic modalities including radiofrequency ablation, cryoablation, microwave ablation, and irreversible electroporation have attracted attention as energy sources for effective locoregional treatment of hepatocellular carcinoma (HCC); these are accepted non-surgical treatments that provide excellent local tumor control and favorable survival. However, in contrast to surgery, tumor location is a crucial factor in the outcomes of locoregional treatment because such treatment is mainly performed using a percutaneous approach for minimal invasiveness; accordingly, it has a limited range of ablation volume. When the index tumor is near large blood vessels, the blood flow drags thermal energy away from the targeted tissue, resulting in reduced ablation volume through a so-called "heat-sink effect". This modifies the size and shape of the ablation zone considerably. In addition, serious complications including infarction or aggressive tumor recurrence can be observed during follow-up after ablation for perivascular tumors by mechanical or thermal damage. Therefore, perivascular locations of HCC adjacent to large intrahepatic vessels can affect post-treatment outcomes. In this review, we primarily focus on physical properties of perivascular tumor location, characteristics of perivascular HCC,

potential complications, and clinical outcomes after various locoregional treatments; moreover, we discuss the current status and future perspectives regarding percutaneous ablation for perivascular HCC.

Key words: Hepatocellular carcinoma; Perivascular; Radiofrequency ablation; Liver; Cryoablation; Microwave ablation; Irreversible electroporation

© **The Author(s) 2018.** Published by Baishideng Publishing Group Inc. All rights reserved.

Core tip: Recently safety concerns have been raised regarding the risks of radiofrequency (RF) ablation for perivascular hepatocellular carcinomas (HCCs), due to the risks of ischemic complications and intravascular tumor spread during treatment. To overcome these potential risks, a modified RF ablation technique, cryoablation, combined treatment with transarterial chemoembolization, or microwave ablation could be problem-solving tools for the treatment of perivascular HCCs. However, the effectiveness of these techniques should be validated with further prospective studies due to the lack of current evidence.

Kang TW, Lim HK, Cha DI. Percutaneous ablation for perivascular hepatocellular carcinoma: Refining the current status based on emerging evidence and future perspectives. *World J Gastroenterol* 2018; 24(47): 5331-5337
URL: <https://www.wjgnet.com/1007-9327/full/v24/i47/5331.htm>
DOI: <https://dx.doi.org/10.3748/wjg.v24.i47.5331>

INTRODUCTION

Image-guided tumor ablation is an evolving and growing treatment option for patients with hepatocellular carcinoma (HCC). This local treatment offers significant advantages, as it is less invasive than surgery and demonstrates a low risk of major complications^[1]. In contrast to surgical resection with a laparoscopic or open approach, tumor location is a crucial factor in the outcomes of local ablation therapy, because it is primarily performed by using a percutaneous approach for minimal invasiveness^[2].

Although ablation technology has evolved and grown rapidly during the past decades, such that it can help improve clinical outcomes and safety profiles^[3], high-risk locations of HCC adjacent to extrahepatic vital organs or large intrahepatic vessels exhibit increased risks of complications after local ablation therapy^[4]. In particular, there remain controversies regarding the outcomes of local treatment because of the heat-sink effect, which can considerably modify the size of the ablation zone, in patients with perivascular tumors^[5,6]. In addition, perivascular HCC exhibits different underlying tumor characteristics, which can have profound effects on the resulting poor prognosis after local ablation

therapy^[7]. A previous study also suggested that the iatrogenic transportal tumor spread may occur during radiofrequency (RF) ablation for periportal tumors^[8] because these local therapies cannot remove a hepatic segment confined to tumor-bearing portal tributaries, unlike anatomical surgical resection.

For improvement of patient outcomes with respect to perivascular HCCs, a modified RF ablation technique and other new energy sources for ablation therapies have recently been introduced. An understanding of these new aspects is important for optimizing clinical results. In particular, combining an understanding of the specific characteristics of each ablation modality with an understanding of the characteristics of perivascular HCC, and then selecting the most appropriate ablation modality available for each patient, can have a remarkable effect on patient outcomes. This review can help physicians to plan state-of-the-art local ablation treatment for patients with perivascular HCC.

Definition of perivascular HCC

To date, there is no universal consensus definition regarding perivascular HCC. The optimal threshold of the contacting vessel size has been based on the results of an experimental study that used pigs^[9]. Notably, most veins greater than 3 mm remained patent after RF ablation; there was an invagination of residual viable tissue between vessels and the RF ablation zone, known as the "heat-sink effect". Many subsequent clinical studies^[5-7,10,11] adopted corresponding definitions of perivascular tumor; an index tumor was characterized by any contact with first or second degree branches of a portal or hepatic vein that are 3 mm or greater in diameter.

Specific ablation environment in perivascular HCC

Unlike *en bloc* tissue removal by surgical resection, RF or microwave ablation uses thermal energy from the RF electric current or microwave field to destroy cancer cells^[12]. However, when the index tumor is near large blood vessels, the blood flow carries thermal energy away from the targeted tissue, resulting in reduced ablation volume; this considerably modifies the size and shape of the ablation zone, especially during RF ablation^[9]. Similarly, the same phenomenon can happen during cryoablation. The convective influx of circulating warm blood into a frozen tumor would theoretically make the ablation of perivascular tumor tissue insufficient^[13].

Specific tumor environment for perivascular HCC

According to recent Barcelona Clinic Liver Cancer guidelines^[1], macroscopic vascular invasion into the portal or hepatic vein is a key factor for staging in patients with HCC due to poor prognosis, despite curative treatment. In addition, microvascular invasion of HCC, which cannot be easily diagnosed by preoperative imaging studies, is another important

indicator of poor prognosis after surgical resection^[14] and liver transplantation^[15]. Thus, perivascular tumors are more likely to be exposed to these substantial risks of vascular invasion, compared with non-perivascular tumors; this difference may lead to poor patient outcomes. Although some researchers^[16] have shown that post-operative adjuvant transarterial chemoembolization (TACE) after surgical resection improved outcomes among patients who exhibit HCC with microvascular invasion, there remains uncertainty with respect to adjuvant therapy after curative treatment for HCC, with either micro- or macro-vascular invasion because a potent anticancer drug for HCC is not well established in clinical practice.

RF ablation

The mechanism of RF ablation uses electric current to rapidly oscillate tissue ions, creating frictional heating in areas of high current density adjacent to the electrode^[12]. Thus, growth of the ablation zone primarily depends on thermal diffusion; this process could be limited by the "heat-sink effect" from peritumoral vessels. Previous studies^[5,11] showed a significant correlation between the presence of peritumoral vessel and poor local tumor control during RF ablation for HCCs. Among these investigations, Lu *et al.*^[11] reported that the presence of a peritumoral vessel is a significant factor for incomplete treatment in RF ablation (53% in perivascular HCC vs 12% in non-perivascular HCC), as verified during histologic examination of explanted liver after transplantation. In contrast to the aforementioned studies, several other studies^[6,10,17,18] investigating the same topic reported similar therapeutic outcomes between perivascular and non-perivascular HCCs; the presence of a peritumoral vessel was not an independent factor associated with incomplete tumor ablation. Improvements in the outcomes of more recent studies of RF ablation for perivascular HCC may be attributed to advances in technical factors, including RF ablation strategies such as the no-touch technique, the use of multiple or large electrodes, a more powerful generator, or advancements in power deploy algorithms^[19].

Regarding clinical outcomes associated with specific types of peritumoral vessels in RF ablation, Lee *et al.*^[7] demonstrated a significant interaction effect between RF ablation and type of peritumoral vessel, with respect to extrahepatic recurrence or overall survival. Although this study did not reveal the cause of different outcomes according to the type of peritumoral vessel, these results could support an increased risk of extrahepatic recurrence when performing RF ablation for periportal HCCs, compared with RF ablation for perivenous HCCs; this increased risk may affect survival outcome. The hemodynamics of blood flow differ considerably between the two types of hepatic vessels^[20]; this could lead to a different ablation environment when performing RF ablation for HCC. Therefore, future

studies should consider the type of peritumoral vessel during assessment of the outcomes of RF ablation in patients with perivascular HCCs.

With respect to tumor location, Kang *et al.*^[8] reported that periportal tumor location was a risk factor for aggressive intrasegmental recurrence after RF ablation (Figure 1). Although the exact mechanism of this type of tumor recurrence remains unclear, intravascular tumor spread along the peritumoral portal vein may be a primary cause of such complications. During insertion of the RF electrode, abnormal communication of an iatrogenic arteriportal fistula may develop; this may enable cancer cells to spread into the peripheral liver due to ablation-related mechanical injury^[21]. In addition, rapid heating of a HCC can lead to a sudden increase in the internal pressure of ablated tissue, which may cause unintentional scattering of tumor cells around the ablation zone^[22,23]. To prevent this potential vascular complication, potential approaches include the no-touch multi-polar ablation technique without direct puncture of the index tumor^[24,25], longer ablation times with stepwise power increment at lower power^[23], combined RF ablation treatments with TACE^[26], or cryoablation^[13]; these problem solving tools may be especially effective in patients with periportal HCCs. The effectiveness of these techniques should be validated with further prospective studies.

Cryoablation

Despite the absence of thermal injury and superb visualization of the procedure process, cryoablation for HCC has been used much less frequently than RF ablation. This is because large cryoprobes with bulky liquid nitrogen systems under laparotomy setting were used in the early era of cryoablation^[27]. Thus, although serious complications were rare, excessive bleeding and cryoshock related to the procedure were reported^[28]. However, a new generation of cryoablation systems with thin cryoprobes that use argon-helium has been introduced^[29] and recent randomized controlled trials showed that they were equally safe and effective compared with RF ablation^[30]. Cryoablation systems use the Joule-Thomson theory of expanding gases within a needlelike cryoprobe^[12]. The mechanism of cell death with ice-ball formation involves cell membrane disruption and an associated release of intracellular contents^[31]. Unlike RF ablation, cryoablation for perivascular HCC could show a better safety profile with respect to vascular complications, such as hepatic infarction or peritumoral vessel thrombosis, because the ablation zone is rapidly reperused after the ice ball has melted. A previous study^[6] regarding hepatic infarction after RF ablation reported an incidence of 5% in patients with HCC, due to the frequent development of thrombosis in peritumoral vessels by thermal injury (Figure 2). However, Kim *et al.*^[13] reported that persistent thrombosis of peritumoral vessels was 3.4%; no case of hepatic infarction was observed in

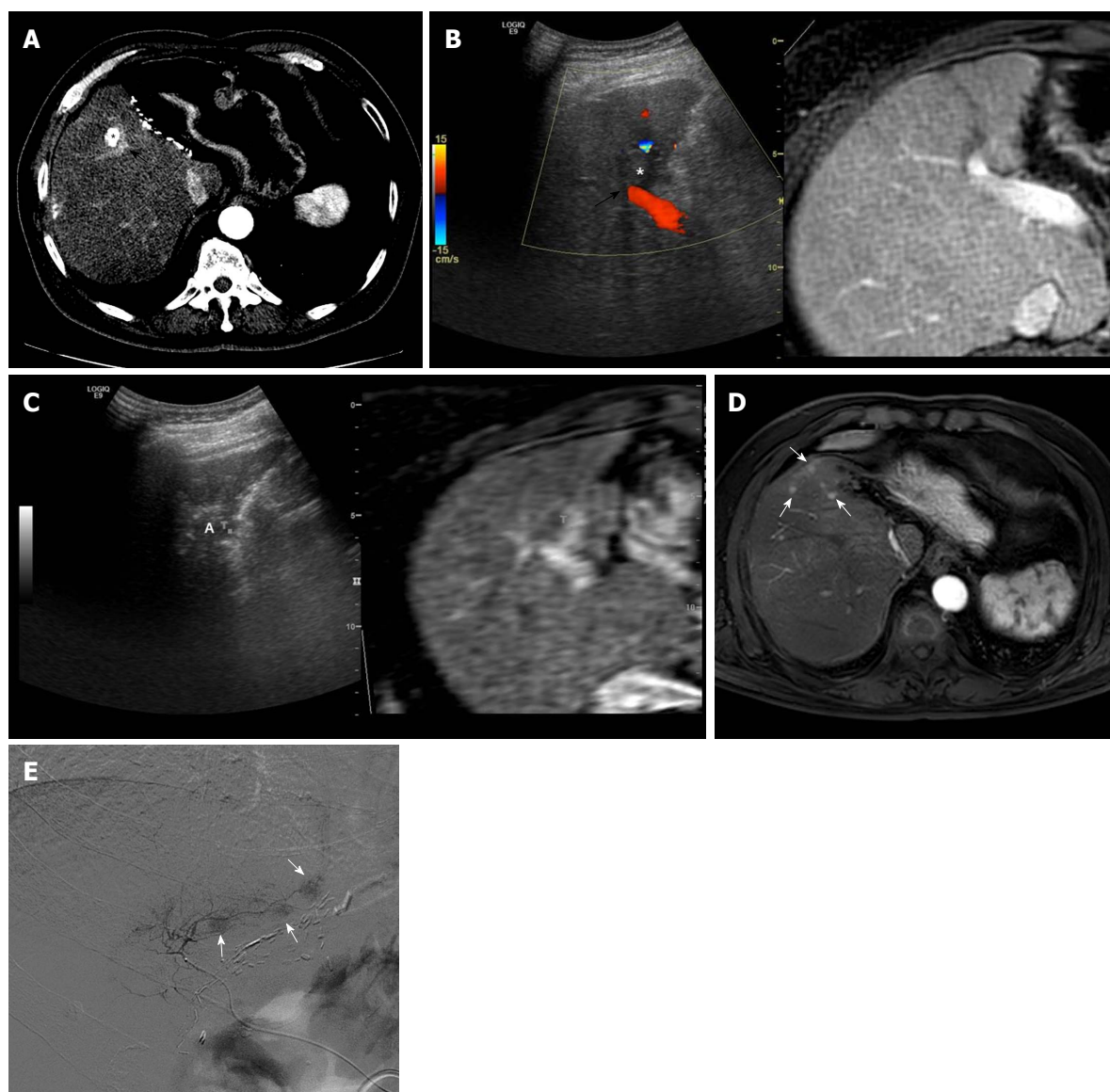


Figure 1 Images demonstrating aggressive intrasegmental recurrence after radiofrequency ablation for perivascular hepatocellular carcinoma. A: Axial computed tomography image obtained during hepatic arterial phase shows viable hepatocellular carcinoma (HCC) within the partially lipiodolized nodule (asterisk) in segment V before radiofrequency (RF) ablation. The index tumor is in contact with the right portal vein (black arrow); B: On planning ultrasonography (US), using fusion imaging with color Doppler US and magnetic resonance imaging (MRI), the low echogenic incident tumor (asterisk) is in contact with a right portal vein (black arrow); C: During RF ablation with the US fusion system, the ablation zone (A) is covered with viable enhancing tumor foci, indicating T marker on real time US/fused MR image; D: MRI scan obtained during the hepatic arterial phase 9 mo after RF ablation shows multiple small arterial enhancing nodules (white arrows) of consistent size, representing recurrent tumors. These recurrent tumors developed simultaneously in a peripheral area of the treated segment, fed by the previous peritumoral portal vein; E: The patient underwent transarterial chemoembolization for tumor control considering tumor multiplicity. Multiple small nodular tumors were detected along the portal tract on hepatic angiogram.

patients who underwent cryoablation for perivascular HCCs. In clinical practice, local ablation therapy is preferred when the patient exhibits recurrent tumors after surgical resection, because more limited hepatic functional reserve is expected^[32]. In these particular scenarios, cryoablation may be the most effective local ablation modality in patients with limited hepatic reserve due to the very low risk of procedure-related vascular complications, including hepatic infarction. In addition, to the best of our knowledge, there have been no reports regarding aggressive tumor recurrence after cryoablation for perivascular HCC. Based on the

absence of thermal expansion of ablation zones, as is observed in RF or microwave ablation, cryoablation theoretically might constitute a safer ablation method with respect to the possibility of tumor spread through an increase in the internal pressure of ablated tissue. However, insufficient data are available and further studies are required to validate the long-term safety of cryoablation for perivascular HCCs.

Microwave ablation

Although previous first- or second-generation microwave ablation system was limited due to lack of active antenna

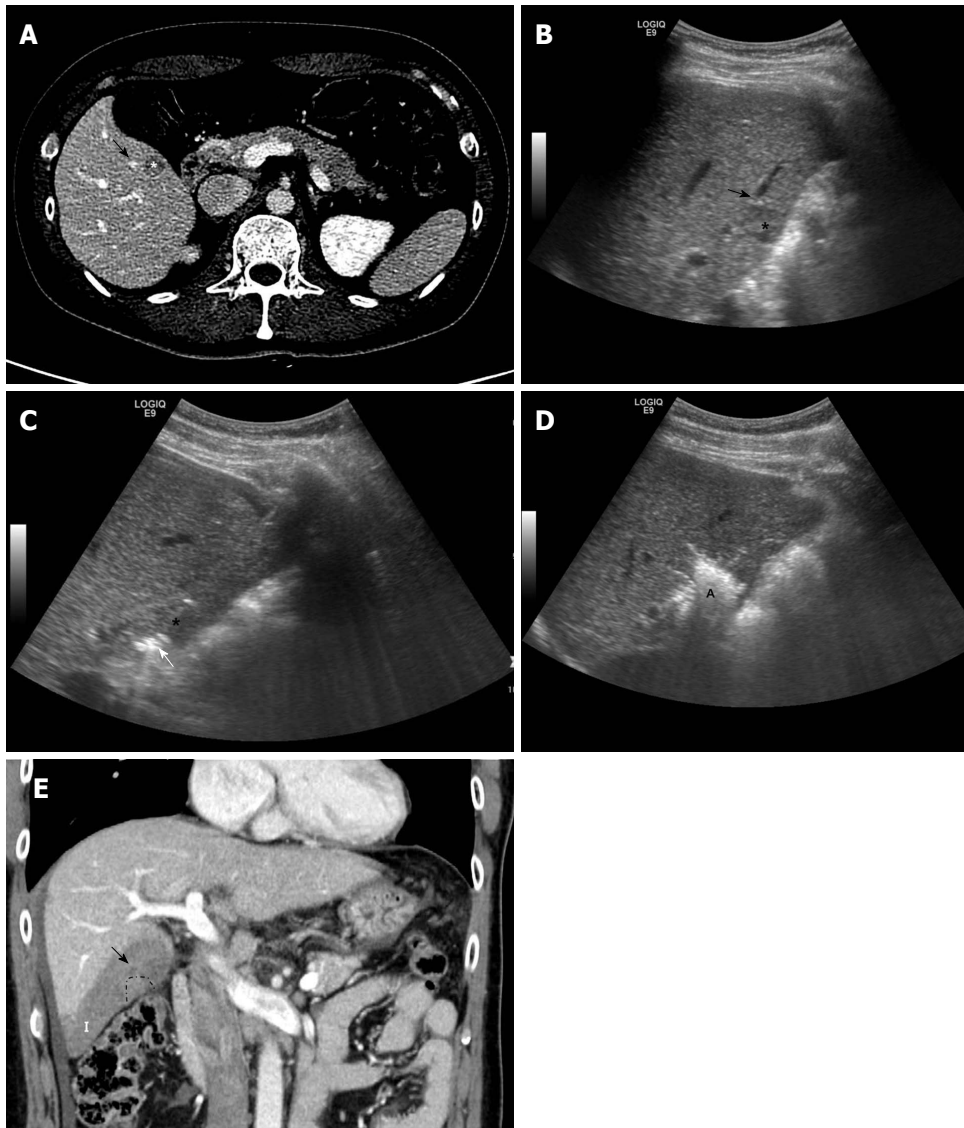


Figure 2 Images showing subsegmental hepatic infarction after radiofrequency ablation for perivascular hepatocellular carcinoma. A: Axial computed tomography image obtained during equilibrium phase shows 1.3-cm hepatocellular carcinoma (asterisk) in segment V before radiofrequency (RF) ablation. The index tumor is in contact with the right portal vein (black arrow); B: Planning ultrasound image obtained before RF ablation shows the low-echoic-index tumor (asterisk) in contact with a right portal vein (black arrow); C: During RF ablation, the RF electrode (white arrow) is inserted into the index tumor (asterisk), evading the adjacent portal vein; D: At the end of the procedure, a hyperechoic ablation zone (A) completely covered the index tumor; E: Thrombosis within the peritumoral portal vein (black arrow) developed around the index tumor (dotted line), shown on coronal computed tomography images obtained immediately after RF ablation. This led to subsegmental infarction (I) in the peripheral area of hepatic segment VI.

cooling and low power generator, recent third-generation systems incorporate antenna cooling and high power generators^[12]. In microwave heating, polar molecules continuously realign with the oscillating microwave field, effectively increasing kinetic energy and tissue temperature^[12]. As a result, microwave energy may possess several advantages, compared with RF ablation; these include faster heating with a larger ablation volume, higher intratumoral temperatures, and less dependence on the electrical conductivities of tissue^[33]. These characteristics of microwave ablation may render it less affected by the "heat-sink effect" present in perivascular tissue^[34]. In addition, combined TACE and microwave ablation could increase local tumor control for perivascular tumor resulting from the complementary

nature of the two different treatments^[35]. To be specific, TACE can decrease blood flow and thereby decrease perfusion-mediated cooling, allowing the creation of larger ablation zones even in perivascular tumor location^[36]. Furthermore, there could be substantial synergistic effect of applying thermal ablation to a chemotherapeutic agent-laden tumor^[30]. Recent report showed that local tumor control, overall survival, and major complications in the perivascular and non-perivascular groups are not significantly different when performing microwave ablation for HCCs. However, there has been no study directly comparing RF ablation and microwave ablation for perivascular HCCs. In addition, whether the ability of microwave ablation to induce a broader ablation zone can lead to a real survival benefit

remains unclear. Although randomized controlled trials are difficult to perform in such a rapidly evolving field, additional trials are required to confirm these debates.

Irreversible electroporation

Irreversible electroporation (IRE) is a novel, non-thermal form of tumor ablation that uses high-current electrical pulses to induce pore formation in the cell lipid bilayer, resulting in cell death^[37]. Thus, it is not affected by the “heat-sink effect” and may cause less collateral damage based on its mechanism of action. Through several studies investigating IRE for hepatic tumors^[38-40], IRE has been shown to be safe and acceptable for local tumor control, especially with regard to use within close proximity to the venous systems of the liver; this is a notable advantage for IRE. However, given the paucity of long-term data demonstrating safety and efficacy for the treatment of HCC, IRE largely serves as a niche technology for the ablation of small (< 3 cm), unresectable tumors, which are not amenable to thermal ablation due to the abutment of major vessels or hilar structures^[41].

CONCLUSION

Image-guided tumor ablation is becoming increasingly accepted for the treatment of very early and early stage HCC. Ablative treatments, particularly RF ablation, currently represent the first-line option for patients with unresectable early-stage HCC. However, safety concerns have been raised regarding the risks of RF ablation for perivascular HCCs, due to the risks of ischemic complications and intravascular tumor spread during treatment. To overcome these potential risks, a modified RF ablation technique, cryoablation, microwave ablation, or combined treatment with TACE have been used recently. Especially, microwave ablation has potential physical advantages over RF ablation and it may be beneficial in treating perivascular tumors. However, additional prospective studies are needed to assess whether the recent technical advances of RF ablation and ablation therapies with new energy sources can translate into better clinical outcomes for patients with perivascular HCC, compared with conventional RF ablation. We hope that understanding the characteristics of perivascular tumor locations and the current status of each ablation modality could help overcome difficulties related to the treatment of perivascular HCCs, and ultimately provide meaningful improvements in patient outcomes.

REFERENCES

- 1 **European Association for the Study of the Liver.** European Association for the Study of the Liver. EASL Clinical Practice Guidelines: Management of hepatocellular carcinoma. *J Hepatol* 2018; **69**: 182-236 [PMID: 29628281 DOI: 10.1016/j.jhep.2018.03.019]
- 2 **Mulier S, Ni Y, Jamart J, Ruers T, Marchal G, Michel L.** Local recurrence after hepatic radiofrequency coagulation: multivariate meta-analysis and review of contributing factors. *Ann Surg* 2005; **242**: 158-171 [PMID: 16041205 DOI: 10.1097/01.sla.0000171032.99149.fe]
- 3 **Kang TW, Rhim H.** Recent Advances in Tumor Ablation for Hepatocellular Carcinoma. *Liver Cancer* 2015; **4**: 176-187 [PMID: 26674766 DOI: 10.1159/000367740]
- 4 **Teratani T, Yoshida H, Shiina S, Obi S, Sato S, Tateishi R, Mine N, Kondo Y, Kawabe T, Omata M.** Radiofrequency ablation for hepatocellular carcinoma in so-called high-risk locations. *Hepatology* 2006; **43**: 1101-1108 [PMID: 16628706 DOI: 10.1002/hep.21164]
- 5 **Lu DS, Raman SS, Limanond P, Aziz D, Economou J, Busuttill R, Sayre J.** Influence of large peritumoral vessels on outcome of radiofrequency ablation of liver tumors. *J Vasc Interv Radiol* 2003; **14**: 1267-1274 [PMID: 14551273 DOI: 10.1097/01.RVI.0000092666.72261.6B]
- 6 **Kang TW, Lim HK, Lee MW, Kim YS, Choi D, Rhim H.** Perivascular versus nonperivascular small HCC treated with percutaneous RF ablation: retrospective comparison of long-term therapeutic outcomes. *Radiology* 2014; **270**: 888-899 [PMID: 24475820 DOI: 10.1148/radiol.13130753]
- 7 **Lee S, Kang TW, Cha DI, Song KD, Lee MW, Rhim H, Lim HK, Sinn DH, Kim JM, Kim K.** Radiofrequency ablation vs. surgery for perivascular hepatocellular carcinoma: Propensity score analyses of long-term outcomes. *J Hepatol* 2018; **69**: 70-78 [PMID: 29524532 DOI: 10.1016/j.jhep.2018.02.026]
- 8 **Kang TW, Lim HK, Lee MW, Kim YS, Rhim H, Lee WJ, Gwak GY, Paik YH, Lim HY, Kim MJ.** Aggressive Intrahepatic Recurrence of Hepatocellular Carcinoma after Radiofrequency Ablation: Risk Factors and Clinical Significance. *Radiology* 2015; **276**: 274-285 [PMID: 25734550 DOI: 10.1148/radiol.15141215]
- 9 **Lu DS, Raman SS, Vodopich DJ, Wang M, Sayre J, Lassman C.** Effect of vessel size on creation of hepatic radiofrequency lesions in pigs: assessment of the “heat sink” effect. *AJR Am J Roentgenol* 2002; **178**: 47-51 [PMID: 11756085 DOI: 10.2214/ajr.178.1.1780047]
- 10 **Ng KK, Poon RT, Lam CM, Yuen J, Tso WK, Fan ST.** Efficacy and safety of radiofrequency ablation for perivascular hepatocellular carcinoma without hepatic inflow occlusion. *Br J Surg* 2006; **93**: 440-447 [PMID: 16470712 DOI: 10.1002/bjs.5267]
- 11 **Lu DS, Yu NC, Raman SS, Limanond P, Lassman C, Murray K, Tong MJ, Amado RG, Busuttill RW.** Radiofrequency ablation of hepatocellular carcinoma: treatment success as defined by histologic examination of the explanted liver. *Radiology* 2005; **234**: 954-960 [PMID: 15681691 DOI: 10.1148/radiol.2343040153]
- 12 **Hinshaw JL, Lubner MG, Ziemlewicz TJ, Lee FT Jr, Brace CL.** Percutaneous tumor ablation tools: microwave, radiofrequency, or cryoablation--what should you use and why? *Radiographics* 2014; **34**: 1344-1362 [PMID: 25208284 DOI: 10.1148/rg.345140054]
- 13 **Kim R, Kang TW, Cha DI, Song KD, Lee MW, Rhim H, Lim HK, Sinn DH.** Percutaneous cryoablation for perivascular hepatocellular carcinoma: Therapeutic efficacy and vascular complications. *Eur Radiol* 2018; Epub ahead of print [PMID: 30043160 DOI: 10.1007/s00330-018-5617-6]
- 14 **Sumie S, Kuromatsu R, Okuda K, Ando E, Takata A, Fukushima N, Watanabe Y, Kojiro M, Sata M.** Microvascular invasion in patients with hepatocellular carcinoma and its predictable clinicopathological factors. *Ann Surg Oncol* 2008; **15**: 1375-1382 [PMID: 18324443 DOI: 10.1245/s10434-008-9846-9]
- 15 **Iguchi T, Shirabe K, Aishima S, Wang H, Fujita N, Ninomiya M, Yamashita Y, Ikegami T, Uchiyama H, Yoshizumi T, Oda Y, Maehara Y.** New Pathologic Stratification of Microvascular Invasion in Hepatocellular Carcinoma: Predicting Prognosis After Living-donor Liver Transplantation. *Transplantation* 2015; **99**: 1236-1242 [PMID: 25427164 DOI: 10.1097/TP.0000000000000489]
- 16 **Sun JJ, Wang K, Zhang CZ, Guo WX, Shi J, Cong WM, Wu MC, Lau WY, Cheng SQ.** Postoperative Adjuvant Transcatheter Arterial Chemoembolization After R0 Hepatectomy Improves Outcomes of Patients Who have Hepatocellular Carcinoma with Microvascular

- Invasion. *Ann Surg Oncol* 2016; **23**: 1344-1351 [PMID: 26714945 DOI: 10.1245/s10434-015-5008-z]
- 17 **Lam VW**, Ng KK, Chok KS, Cheung TT, Yuen J, Tung H, Tso WK, Fan ST, Poon RT. Incomplete ablation after radiofrequency ablation of hepatocellular carcinoma: analysis of risk factors and prognostic factors. *Ann Surg Oncol* 2008; **15**: 782-790 [PMID: 18095030 DOI: 10.1245/s10434-007-9733-9]
 - 18 **Thanos L**, Mylona S, Galani P, Pomoni M, Pomoni A, Koskinas I. Overcoming the heat-sink phenomenon: successful radiofrequency thermal ablation of liver tumors in contact with blood vessels. *Diagn Interv Radiol* 2008; **14**: 51-56 [PMID: 18306146]
 - 19 **Nault JC**, Sutter O, Nahon P, Ganne-Carrié N, Sèror O. Percutaneous treatment of hepatocellular carcinoma: State of the art and innovations. *J Hepatol* 2017 Epub ahead of print [PMID: 29031662 DOI: 10.1016/j.jhep.2017.10.004]
 - 20 **McNaughton DA**, Abu-Yousef MM. Doppler US of the liver made simple. *Radiographics* 2011; **31**: 161-188 [PMID: 21257940 DOI: 10.1148/rg.311105093]
 - 21 **Nicoli N**, Casaril A, Abu Hilal M, Mangiante G, Marchiori L, Ciola M, Invernizzi L, Campagnaro T, Mansueto G. A case of rapid intrahepatic dissemination of hepatocellular carcinoma after radiofrequency thermal ablation. *Am J Surg* 2004; **188**: 165-167 [PMID: 15249243 DOI: 10.1016/j.amjsurg.2003.12.061]
 - 22 **Mori Y**, Tamai H, Shingaki N, Moribata K, Shiraki T, Deguchi H, Ueda K, Enomoto S, Magari H, Inoue I, Maekita T, Iguchi M, Yanaoka K, Oka M, Ichinose M. Diffuse intrahepatic recurrence after percutaneous radiofrequency ablation for solitary and small hepatocellular carcinoma. *Hepatol Int* 2009; **3**: 509-515 [PMID: 19669252 DOI: 10.1007/s12072-009-9131-4]
 - 23 **Kotoh K**, Nakamuta M, Morizono S, Kohjima M, Arimura E, Fukushima M, Enjoji M, Sakai H, Nawata H. A multi-step, incremental expansion method for radio frequency ablation: optimization of the procedure to prevent increases in intra-tumor pressure and to reduce the ablation time. *Liver Int* 2005; **25**: 542-547 [PMID: 15910491 DOI: 10.1111/j.1478-3231.2005.01051.x]
 - 24 **Seror O**, N'kontchou G, Nault JC, Rabahi Y, Nahon P, Ganne-Carrié N, Grando V, Zentar N, Beaugrand M, Trinchet JC, Diallo A, Sellier N. Hepatocellular Carcinoma within Milan Criteria: No-Touch Multibipolar Radiofrequency Ablation for Treatment-Long-term Results. *Radiology* 2016; **280**: 611-621 [PMID: 27010381 DOI: 10.1148/radiol.2016150743]
 - 25 **Hocquelet A**, Aubé C, Rode A, Cartier V, Sutter O, Manichon AF, Boursier J, N'kontchou G, Merle P, Blanc JF, Trillaud H, Seror O. Comparison of no-touch multi-bipolar vs. monopolar radiofrequency ablation for small HCC. *J Hepatol* 2017; **66**: 67-74 [PMID: 27422750 DOI: 10.1016/j.jhep.2016.07.010]
 - 26 **Song KD**, Lee MW, Rhim H, Kim YS, Kang TW, Shin SW, Cho SK. Aggressive Intrasegmental Recurrence of Hepatocellular Carcinoma After Combined Transarterial Chemoembolization and Radiofrequency Ablation. *AJR Am J Roentgenol* 2016; **207**: 1122-1127 [PMID: 27575338 DOI: 10.2214/AJR.16.16080]
 - 27 **Hu KQ**. Advances in clinical application of cryoablation therapy for hepatocellular carcinoma and metastatic liver tumor. *J Clin Gastroenterol* 2014; **48**: 830-836 [PMID: 25148553 DOI: 10.1097/MCG.0000000000000201]
 - 28 **Seifert JK**, Stewart GJ, Hewitt PM, Bolton EJ, Junginger T, Morris DL. Interleukin-6 and tumor necrosis factor-alpha levels following hepatic cryotherapy: association with volume and duration of freezing. *World J Surg* 1999; **23**: 1019-1026 [PMID: 10512941]
 - 29 **Lee SM**, Won JY, Lee DY, Lee KH, Lee KS, Paik YH, Kim JK. Percutaneous cryoablation of small hepatocellular carcinomas using a 17-gauge ultrathin probe. *Clin Radiol* 2011; **66**: 752-759 [PMID: 21513923 DOI: 10.1016/j.crad.2011.02.015]
 - 30 **Wang C**, Wang H, Yang W, Hu K, Xie H, Hu KQ, Bai W, Dong Z, Lu Y, Zeng Z, Lou M, Wang H, Gao X, Chang X, An L, Qu J, Li J, Yang Y. Multicenter randomized controlled trial of percutaneous cryoablation versus radiofrequency ablation in hepatocellular carcinoma. *Hepatology* 2015; **61**: 1579-1590 [PMID: 25284802 DOI: 10.1002/hep.27548]
 - 31 **Rui J**, Tatsutani KN, Dahiya R, Rubinsky B. Effect of thermal variables on human breast cancer in cryosurgery. *Breast Cancer Res Treat* 1999; **53**: 185-192 [PMID: 10326796]
 - 32 **Song KD**, Lim HK, Rhim H, Lee MW, Kim YS, Lee WJ, Paik YH, Gwak GY, Kim JM, Kwon CH, Joh JW. Repeated Hepatic Resection versus Radiofrequency Ablation for Recurrent Hepatocellular Carcinoma after Hepatic Resection: A Propensity Score Matching Study. *Radiology* 2015; **275**: 599-608 [PMID: 25559235 DOI: 10.1148/radiol.14141568]
 - 33 **Lubner MG**, Brace CL, Hinshaw JL, Lee FT Jr. Microwave tumor ablation: mechanism of action, clinical results, and devices. *J Vasc Interv Radiol* 2010; **21**: S192-S203 [PMID: 20656229 DOI: 10.1016/j.jvir.2010.04.007]
 - 34 **Wright AS**, Sampson LA, Warner TF, Mahvi DM, Lee FT Jr. Radiofrequency versus microwave ablation in a hepatic porcine model. *Radiology* 2005; **236**: 132-139 [PMID: 15987969 DOI: 10.1148/radiol.2361031249]
 - 35 **Smolock AR**, Cristescu MM, Hinshaw A, Woo KM, Wells SA, Ziemlewicz TJ, Lubner MG, Dalvie PS, Louis Hinshaw J, Brace CL, Ozkan OS, Lee FT Jr, Laeseke P. Combination transarterial chemoembolization and microwave ablation improves local tumor control for 3- to 5-cm hepatocellular carcinoma when compared with transarterial chemoembolization alone. *Abdom Radiol (NY)* 2018; **43**: 2497-2504 [PMID: 29450606 DOI: 10.1007/s00261-018-1464-9]
 - 36 **Chinn SB**, Lee FT Jr, Kennedy GD, Chinn C, Johnson CD, Winter TC 3rd, Warner TF, Mahvi DM. Effect of vascular occlusion on radiofrequency ablation of the liver: results in a porcine model. *AJR Am J Roentgenol* 2001; **176**: 789-795 [PMID: 11222227 DOI: 10.2214/ajr.176.3.1760789]
 - 37 **Charpentier KP**, Wolf F, Noble L, Winn B, Resnick M, Dupuy DE. Irreversible electroporation of the liver and liver hilum in swine. *HPB (Oxford)* 2011; **13**: 168-173 [PMID: 21309933 DOI: 10.1111/j.1477-2574.2010.00261.x]
 - 38 **Niessen C**, Igl J, Pregler B, Beyer L, Noeva E, Dollinger M, Schreyer AG, Jung EM, Stroszczynski C, Wiggermann P. Factors associated with short-term local recurrence of liver cancer after percutaneous ablation using irreversible electroporation: a prospective single-center study. *J Vasc Interv Radiol* 2015; **26**: 694-702 [PMID: 25812712 DOI: 10.1016/j.jvir.2015.02.001]
 - 39 **Dollinger M**, Müller-Wille R, Zeman F, Haimerl M, Niessen C, Beyer LP, Lang SA, Teufel A, Stroszczynski C, Wiggermann P. Irreversible Electroporation of Malignant Hepatic Tumors - Alterations in Venous Structures at Subacute Follow-Up and Evolution at Mid-Term Follow-Up. *PLoS One* 2015; **10**: e0135773 [PMID: 26270651 DOI: 10.1371/journal.pone.0135773]
 - 40 **Dollinger M**, Beyer LP, Haimerl M, Niessen C, Jung EM, Zeman F, Stroszczynski C, Wiggermann P. Adverse effects of irreversible electroporation of malignant liver tumors under CT fluoroscopic guidance: a single-center experience. *Diagn Interv Radiol* 2015; **21**: 471-475 [PMID: 26359870 DOI: 10.5152/dir.2015.14442]
 - 41 **Zimmerman A**, Grand D, Charpentier KP. Irreversible electroporation of hepatocellular carcinoma: patient selection and perspectives. *J Hepatocell Carcinoma* 2017; **4**: 49-58 [PMID: 28331845 DOI: 10.2147/JHC.S129063]

P- Reviewer: Iannitti DA, Sartori S, Shousha HI

S- Editor: Ma RY **L- Editor:** A **E- Editor:** Huang Y



Basic Study

***Piwi like RNA-mediated gene silencing 1* gene as a possible major player in gastric cancer**

Taíssa Araújo, André Khayat, Luciana Quintana, Danielle Calcagno, Ronald Mourão, Antônio Modesto, Juliana Paiva, Adhara Lima, Fabiano Moreira, Edivaldo Oliveira, Michel Souza, Moneeb Othman, Thomas Liehr, Eliana Abdelhay, Renata Gomes, Sidney Santos, Paulo Assumpção

Taíssa Araújo, André Khayat, Luciana Quintana, Danielle Calcagno, Ronald Mourão, Antônio Modesto, Juliana Paiva, Adhara Lima, Fabiano Moreira, Sidney Santos, Paulo Assumpção, Núcleo de Pesquisas em Oncologia, Universidade Federal do Pará, Belém 66073-000, Brazil

Edivaldo Oliveira, Michel Souza, Laboratório de Cultura de Tecidos e Citogenética, Instituto Evandro Chagas, Belém 66087-082, Brazil

Moneeb Othman, Thomas Liehr, Institute of Human Genetics, Universitätsklinikum Jena, Jena 07747, Germany

Eliana Abdelhay, Renata Gomes, Laboratório de Célula Tronco, Centro de Transplante de Medula Óssea, Instituto Nacional de Câncer José Alencar Gomes da Silva, Rio de Janeiro 20230-130, Brazil

ORCID number: Taíssa Araújo (0000-0002-1716-4445); André Khayat (000-0002-3451-6369); Luciana Quintana (0000-0003-3261-910X); Danielle Calcagno (0000-0002-4429-2573); Ronald Mourão (0000-0001-5582-4961); Antônio Modesto (0000-0003-1854-0358); Juliana Paiva (0000-0002-2082-2250); Adhara Lima (0000-0001-6315-2392); Fabiano Moreira (0000-0002-2799-3546); Edivaldo Oliveira (0000-0001-6315-3352); Michel Souza (0000-0003-1038-6448); Moneeb Othman (0000-0002-0743-1191); Thomas Liehr (0000-0003-1672-3054); Eliana Abdelhay (0000-0001-5166-0832); Renata Gomes (0000-0001-7590-0335); Sidney Santos (0000-0002-8622-9417); Paulo Assumpção (0000-0003-3846-8445).

Author contributions: Araújo T and Khayat A contributed equally to this work; Araújo T and Khayat A performed the majority of experiments; Moreira F, Oliveira E and Souza M analyzed the data; Modesto A, Paiva J and Lima A performed the molecular investigations; Quintana L, Calcagno D and Mourão R participated equally in cell culture management; Othman M and Liehr T performed molecular cytogenetics experiments; Abdelhay E and Gomes R performed proteomic assay; Santos S and Assumpção P designed and coordinated the research; Araújo T, Khayat A and Quintana L wrote the paper.

Supported by Fundação Amazônia de Amparo a Estudos e Pesquisa (FAPESPA), No. 174/2014.

Conflict-of-interest statement: The authors declare that they have no conflicts of interest.

Data sharing statement: No additional data are available.

Open-Access: This article is an open-access article which was selected by an in-house editor and fully peer-reviewed by external reviewers. It is distributed in accordance with the Creative Commons Attribution Non Commercial (CC BY-NC 4.0) license, which permits others to distribute, remix, adapt, build upon this work non-commercially, and license their derivative works on different terms, provided the original work is properly cited and the use is non-commercial. See: <http://creativecommons.org/licenses/by-nc/4.0/>

Manuscript source: Unsolicited manuscript

Corresponding author to: Paulo Assumpção, MD, MSc, PhD, Academic Research, Adjunct Professor, Surgical Oncologist, Núcleo de Pesquisas em Oncologia, Universidade Federal do Pará, Rua dos Mundurucus 4487, Belém 66073-000, Brazil. assumpcaopp@gmail.com
Telephone: +55-91-984171112

Received: August 14, 2018

Peer-review started: August 14, 2018

First decision: August 31, 2018

Revised: September 7, 2018

Accepted: October 5, 2018

Article in press: October 5, 2018

Published online: December 21, 2018

Abstract

AIM

To establish a permanent *piwi like RNA-mediated gene*

silencing 1 (PIWIL1) gene knockout in AGP01 gastric cancer cell line using CRISPR-Cas9 system and analyze phenotypic modifications as well as gene expression alterations.

METHODS

CRISPR-Cas9 system used was purchased from Dharmacon GE Life Sciences (Lafayette, CO, United States) and permanent knockout was performed according to manufacturer's recommendations. Wound-healing assay was performed to investigate the effect of *PIWIL1* knockout on migration capability of cells and Boyden chamber invasion assay was performed to investigate the effect on invasion capability. For the gene expression analysis, a one-color microarray-based gene expression analysis kit (Agilent Technologies, Santa Clara, CA, United States) was used according to the protocol provided by the manufacturer.

RESULTS

PIWIL1 gene knockout caused a significant decrease in AGP01 migration capacity as well as a significant decrease in cell invasiveness. Moreover, functional analysis based on grouping of all differentially expressed mRNAs identified a total of 35 genes (5 up-regulated and 30 down-regulated) encoding proteins involved in cellular invasion and migration. According to current literature, 9 of these 35 genes (*DOCK2*, *ZNF503*, *PDE4D*, *ABL1*, *ABL2*, *LPAR1*, *SMAD2*, *WASF3* and *DACH1*) are possibly related to the mechanisms used by *PIWIL1* to promote carcinogenic effects related to migration and invasion, since their functions are consistent with the changes observed (being up- or down-regulated after knockout).

CONCLUSION

Taken together, these data reinforce the idea that *PIWIL1* plays a crucial role in the signaling pathway of gastric cancer, regulating several genes involved in migration and invasion processes; therefore, its use as a therapeutic target may generate promising results in the treatment of gastric cancer.

Key words: Gastric cancer; *Piwi like RNA-mediated gene silencing 1*; CRISPR-Cas9; Migration; Invasion

© The Author(s) 2018. Published by Baishideng Publishing Group Inc. All rights reserved.

Core tip: *Piwi like RNA-mediated gene silencing 1 (PIWIL1)* gene emerged as an interesting target for gastric cancer, as it is expressed in cancer, stem and germ cells, but it is absent in normal somatic tissue. Our results propose that *PIWIL1* plays a crucial role in the signaling pathway of gastric cancer, regulating several genes involved in migration and invasion processes; therefore, its use as a therapeutic target may generate promising results in the treatment of gastric cancer.

Liehr T, Abdelhay E, Gomes R, Santos S, Assumpção P. *Piwi like RNA-mediated gene silencing 1* gene as a possible major player in gastric cancer. *World J Gastroenterol* 2018; 24(47): 5338-5350
URL: <https://www.wjgnet.com/1007-9327/full/v24/i47/5338.htm>
DOI: <https://dx.doi.org/10.3748/wjg.v24.i47.5338>

INTRODUCTION

Gastric cancer is a major contributor to global cancer burden, being the third leading cause of cancer death worldwide and in both sexes^[1]. This type of cancer is thought to be consequence of a multi-step process, resulting from different genetic and epigenetic changes. Specifically, dysfunction of oncogenes and tumor suppressor genes contributes to this malignant disease, and many candidate genes have been implicated to serve as gastric cancer biomarkers^[2].

In this context, the *piwi like RNA-mediated gene silencing 1 (PIWIL1)* gene, located in 12q24.33 and having 22 exons, became an attractive target for gastric cancer treatment. *PIWIL1* protein is expressed at increased levels in cancer tissues, stem cells and germ cells, but it has been shown to be absent in normal somatic tissues. This means that it could be a potential target for therapy, since most non-cancer cells would not be affected by cytotoxic effects^[3-7].

PIWIL1 plays a key role in tumor cell viability, migration and invasion, and its expression is associated with the maintenance of stem-like characteristics of tumors, which in turn contribute to more severe histological grade, advanced stage and worse clinical outcome^[8-10].

Wang *et al.*^[11] showed that expression of *PIWIL1* in gastric cancer tissue was significantly higher than in adjacent-to-tumor tissue (tumor front). They also demonstrated that patients with a lower expression of *PIWIL1* presented a significant better overall survival rate compared to patients with a higher expression levels. Additionally, the 5-year survival rate of patients with a higher expression level of *PIWIL1* was significantly lower (36.5% vs 67.6%).

Liu *et al.*^[12] reported that expression of *PIWIL1* progressively increases during cancer development. The expression ratio in normal gastric tissues, atrophic gastritis, intestinal metaplasia and gastric cancers varied from 10% to 76%.

To further investigate the potential functions of the *PIWIL1* gene, Liu *et al.*^[12] also silenced *PIWIL1* by antisense or short hairpin RNA and noted that suppression of this gene inhibited the growth of gastric cancer cells and induced G2/M arrest. Although relevant information regarding the possible role of *PIWIL1* in gastric cancer carcinogenesis is provided by the current literature, the exact molecular mechanisms involved in this carcinogenic process remain unclear.

A recently introduced technology, based on the adaptive immune system of prokaryotes and known as type II clustered, regularly interspaced, short palindromic

Araújo T, Khayat A, Quintana L, Calcagno D, Mourão R, Modesto A, Paiva J, Lima A, Moreira F, Oliveira E, Souza M, Othman M,

repeats (CRISPR)/associated protein (Cas), has been demonstrated to cleave double-stranded DNA and has emerged as a relevant genome editing tool^[13-15].

This technology can be used both to perform permanent gene knockouts and the site-specific integration of a gene (knock-in)^[16-19]. Importantly, it allows for the permanent silencing of the target gene, and it also creates a stable and permanent cell line with the desired modification^[14,16].

Here we applied CRISPR/Cas9 technology for the first time to knockout *PIWIL1* gene in a gastric cancer cell line and analyzed its phenotypic modifications.

MATERIALS AND METHODS

Cell lines

The human gastric cancer cell line AGP01 was maintained in DMEM-F12 medium supplemented with 10% fetal bovine serum. The cell culture grew attached to a plastic flask in a monolayer in a humidified incubator maintained at 37 °C and 5% CO₂.

The AGP01 cell line was established by our research group in 2009^[20] from cancer cells present in the ascitic fluid of a female individual with intestinal gastric cancer, located at the antrum and the body region of the stomach, and staged as T3N2M1. The cell line was tested and authenticated by conventional cytogenetics^[20]. Recently, the AGP01 cell line was tested by multicolor-fluorescence *in situ* hybridization (FISH), and results are presented here.

24-color-FISH using all human whole chromosome painting probes

24-color-FISH using simultaneous all human whole chromosome painting (WCP) probes was done as previously reported^[21,22]. A total of 20 metaphases was analyzed, using a fluorescence microscope (Axio Imager Z1 mot; Carl Zeiss AG, Oberkochen, Germany) equipped with appropriate filter sets to discriminate between a maximum of five fluorochromes and the counterstain DAPI; the latter was used to induce a GTG-like banding pattern. Image capturing and processing were carried out using ISIS imaging system (MetaSystems, Altlussheim, Germany).

Targeted knockout of *PIWIL1* using the CRISPR-Cas9 system

The CRISPR-Cas9 system used was purchased from Dharmacon GE Life Sciences (Lafayette, CO, United States). First, 1×10^4 AGP01 cells/well were seeded in DMEM-F12 medium to a 96-well plate for 24 h. Subsequently, transfection was performed using CR-0046-03-005 (Dharmacon GE Life Sciences) for 48 h. For the transfection procedure, a solution containing 1 µL of the CRISPR RNAs (crRNAs) mixed with the trans-activating small RNA, 2 µL of Cas9 and 7 µL of DMEM-F12 medium (for each well) was prepared first. In another tube, 0.4 µL of DharmaftecDUO and 9.6 µL of DMEM-F12 medium (to each well) were added.

The solutions were then incubated for 5 min at room temperature before being combined. After combining, the solution was incubated for 20 min at room temperature, and finally 80 µL of DMEM-F12 medium/10% fetal calf serum (FCS) (per well) was added. At the end of the transfection, all contents (from each well) were transferred to a 24-well plate containing DMEM-F12 medium/10% FCS/1% pen-strep.

After 24 h, samples were treated with 6 µg/mL of puromycin for 72 h to select the resistant clones. Next, 40 cells were plated per well in a 6-well plate to isolate the clones by the filter paper method.

This method consists of using a cut and autoclaved piece of filter paper so that it, after being soaked in trypsin, can be positioned above a single colony of cells that has grown from an isolated cell, allowing for the collection of this clone. Subsequently, each clone grew in a separate well in a 6-well plate, so it could reach the confluence needed to perform DNA extraction and sequencing.

Sequencing

DNA was extracted using the Wizard Genomic DNA Purification Kit (Promega Corporation, Madison, WI, United States) according to the manufacturer's instructions. For PCR, specific primers targeting the binding region of the purchased crRNA were constructed using the online program Primer3 (Supplementary Table 1).

The quantities of the reagents used in the PCR for a final volume of 12 µL were as follows: 6.25 µL of nuclease-free H₂O, 0.5 µL of forward primer (10 ng/µL), 0.5 µL of reverse primer (ng/µL), 4.25 µL of GoTaq Colorless Master Mix 2× (Promega Corporation) and 1 µL of DNA (10 ng/µL).

The conditions using the MasterCycler Gradient thermal cycler (Eppendorf, Hamburg, Germany) were 1 cycle at 95 °C for 3 min for initial denaturation followed by 35 cycles consisting of denaturation at 94 °C for 2 min, primer annealing at 59 °C for 1 min and extension at 70 °C for 2 min, ending with 1 cycle at 70 °C for a final extension for 30 min.

For direct sequencing of the PCR product, the quantities of the reagents used for a final volume of 20 µL were as follows: 15 µL of nuclease-free water, 0.5 µL of forward or reverse primer (10 ng/µL), 0.5 µL of Big Dye, 3 µL of Save Money and 1 µL of the PCR reaction. For this reaction, the ABI PRISM Big Dye Terminator 3.1 Cycle Sequencing Kit (Applied Biosystems, Hercules, CA, United States) was used.

The sequencing was performed using the MasterCycler Gradient (Eppendorf) thermal cycler according to the following 25-cycle thermocycling conditions: denaturation at 96 °C for 50 s, primer annealing at 59 °C for 1 min and extension at 60 °C for 4 min, ending with 1 cycle at 4 °C for 5 min.

After this procedure, a precipitation step was carried out in order to purify the product of the reaction before continuing. For this step, samples were washed with

70% isopropanol and 70% ethanol. Subsequently, sequencing was performed using the ABI Prism 3500 DNA Sequencer (Applied Biosystems). The methodology used was based on the biochemical synthesis of the DNA strand by the Sanger method.

Sequencing analysis

Reference sequence for exon 15 in the *PIWIL1* gene was obtained from the National Center for Biotechnology Information (NCBI) and compared with the DNA sequence of the modified cell line as well as the negative control (cell line without the gene knockout). To infer the effect of changes in protein synthesis, we applied Gene Runner v.3.05 (Hastings Software Inc., Hastings, NY, United States; <http://www.generunner.com>).

Wound-healing assay

Cells were grown in 12-well plates at a density of 2×10^5 cells/well and maintained for 24 h in 5% CO₂ at 37 °C. After this period, cells were injured with a 10 µL tip in the center of each well. The medium was then removed to eliminate suspended cells, and wells were washed with $1 \times$ phosphate buffered saline before fresh DMEM-F12 medium/10% FCS/1% pen-strep was added again.

The behavior of cells was observed and photographed immediately after injury and at 6 h, 12 h and 24 h after injury. All experiments were performed in triplicate.

Boyden chamber invasion assay

Boyden inserts (8 µm pores) (BD Biosciences™, Franklin Lakes, NJ, United States) were coated with 200 µL of Matrigel (10-13 mg/mL) in 12-well plates. Cells (2×10^5) were seeded in the upper chamber in 1 mL of DMEM without fetal bovine serum. In the lower chamber, DMEM-F12 medium/10% FCS/1% pen-strep was added, functioning as a chemoattractant for the cells present in the upper chamber.

After 48 h, the remaining cells above the filter were removed by scraping with a sterile swab. The cells at the bottom of the filter were fixed with 4% paraformaldehyde and stained with Giemsa. Cells were photographed and analyzed using a light microscope and counted in optical fields (100 \times). All experiments were performed in triplicate.

Total RNA extraction

The mRNA extraction was performed using Promega's Total RNA Isolation System kit, according to the manufacturer's specifications. AGP01 and AGP01 *PIWIL1* knockout cells were prepared for mRNA extraction. Samples were lysed with lysis buffer containing beta-mercaptoethanol and then diluted in RNA dilution buffer. The samples were centrifuged for 10 min at maximum speed. Then, 95% ethanol was added to ensure adequate membrane binding conditions.

The samples were then transferred to centrifuge

columns where the RNA could bind the membrane of the column, facilitating washing to eliminate possible contaminants as well as favoring the extraction of high quality of total RNA.

At the end of the procedure, the RNA was diluted in 60 µL of nuclease-free water. The total RNA was quantified using a Nanodrop spectrophotometer ND-1000 UV-VIS version 3.2.1 (Nanodrop Technologies, Wilmington, DE, United States). The RNA quality was also evaluated by analyzing the A₂₆₀/A₂₈₀ ratio according to the manufacturer's specifications. Purified RNA was stored at -80 °C for the microarray expression assay.

Microarray expression

For the microarray assay, a one-color microarray-based gene expression analysis kit (Agilent Technologies, Santa Clara, CA, United States) was used according to the protocol provided by the manufacturer. The gene expression profile was evaluated in both cell lines (AGP01 with and without *PIWIL1* knockout).

The total RNA obtained during the extraction phase was used as the template for the synthesis of the first cDNA strand by reverse transcription using T7 RNA polymerase. Synthesis of the second cDNA strand was used as the template for the *in vitro* transcription reaction for cRNA production. The cRNA was then incorporated into the fluorochrome 3-cyanine (Cy-3) using the Low Input Quick Amp Labeling kit (Agilent Technologies) according to the protocol provided by the manufacturer. Thereafter, the cRNA purification process was carried out.

The cRNA was quantified by a spectrophotometer (pmol/L), by which it was possible to analyze the absorbance ratio (260 nm/280 nm) and the cRNA (ng/µL) concentration in each sample. After, hybridization was performed for 17 h in a hybridization chamber at 65 °C at 10 rpm. After this period, the slide was washed and immediately scanned in the Agilent G4900DA SureScan Microarray System.

The following setup was used to scan the microarray slides for one color: scan region of 61 mm \times 21.6 mm, 5 µm scan resolution, dye channel of green. Next, the images were obtained by using Feature Extraction v10.10 software, and the data were analyzed with GeneSpring GX 9.0 and IPATHWAYGUIDE (Advaita Bioinformatics Company, Plymouth, MI, United States) programs. Gene identification followed a restriction criterion with a fold-change of > 2 .

Differential expression and gene ontology enrichment analysis

To identify differentially expressed (DE) mRNAs, we compared the probes' expression profiles before and after *PIWIL1* knockout. Probes with a mean fold-change < 0.5 and a mean fold-change of > 2 [$|\text{Log}_2(\text{fold-change})| > 1$] were selected for differential analysis. Student's *t* test was performed in 1222 selected probes, false discovery rate adjustment^[23] was performed,

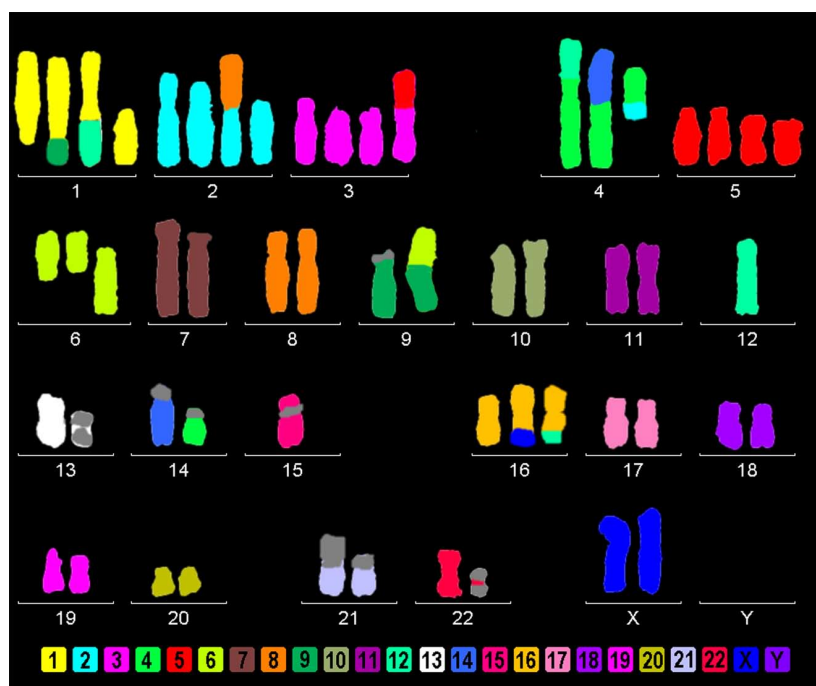


Figure 1 AGP01 cell line multicolor-FISH showing several chromosomal changes, including the monosomy of chromosome 12, where the *PIWIL1* gene is located.

and genes with an adjusted *P*-value of < 0.05 were tagged as DE. For the volcano plot, the fold-change and the *P*-value of all probes were used, and probes were tagged as DE following the previous criteria. Gene ontology enrichment was performed using org. Hs.eg.db^[24] and Gostats^[25] R libraries. All graphical and statistical analyses were performed in the R platform (R Core Team, 2017, Vienna, Austria; <https://www.R-project.org/>).

RESULTS

24-color-FISH using all human WCP probes

24-color-FISH using all human WCP probes revealed in AGP01 cell line a complex karyotype as follows: 63,XX,inv(1)(p12q43),der(1)(1pter->1 p 1 2 : : 1 q 4 3 -> 1 p 1 2 : : 9 p 1 2 ->9pter),+der(1)t(1;12)(q21;q12),+del(1)(p12),+del(2)(p12),+der(2)t(2;8)(p12;q11.2),inv(3)(p21q13)x2,+inv(3)(p21q13),+der(3)t(3;5)(p14;q13),t(4;14)(p12;q11.2),dic(4;12)(p15;q12),+der(4)t(2;4)(p or q;q12),del(5)(p13)x2,+der(5)x2,del(6)(q12)x2,+del(6)(p21),inv(7)(p12;q11.2),der(7),der(9)t(9;acro)(p21;p12),der(9)t(6;9)(p12;p12),t(13;13)(p10),der(15)(:q13->p11::p11->qter),-15,der(16)t(X;16)(q or p;q23),+der(16)t(12;16)(q12;q23),21p+,t(22;22)(p10) (Figure 1).

From the analysis, we verified that the unique chromosome 12 (where *PIWIL1* gene is located) remains intact, without translocations or derivative chromosomes. It is important to note that the monosomy of chromosome 12 agrees with the sequencing result, since the 7 bp insert sequence was observed in hemizygous status.

Targeted knockout of the *PIWIL1* gene using the CRISPR-Cas9 system

PIWIL1 gene knockout was successful, as determined by Sanger sequencing. The latter revealed an insertion of 7 adenines in the *PIWIL1* gene sequence (Figure 2), which caused a frameshift mutation that impaired protein synthesis.

Prediction of the encoded protein indicated a premature stop codon (Figure 3), suggesting that this insertion generates a truncated protein consisting of 573 amino acids (the wild-type contains 861) with a loss-of-function phenotype, which means that knockout was efficient.

Notably, the *PIWIL1* knockout cell line remained viable and could be used for further experiments.

Wound-healing assay

The *PIWIL1* gene knockout caused a significant decrease in AGP01 migration capacity after 24 h ($P < 0.01$; Figure 4), which is consistent with the fact that this protein is related to various pathways that regulate cell motility.

Boyden chamber invasion assay

Also, *PIWIL1* gene knockout caused a significant decrease in AGP01 invasiveness ($P < 0.001$; Figure 5), which is also consistent with the fact that this protein is related to various pathways that regulate cell motility.

mRNA array and gene ontology enrichment

Differential analysis: By comparing expression profiles after *PIWIL1* permanent knockout in the AGP01 cell line, a total of 251 mRNA were found to be DE

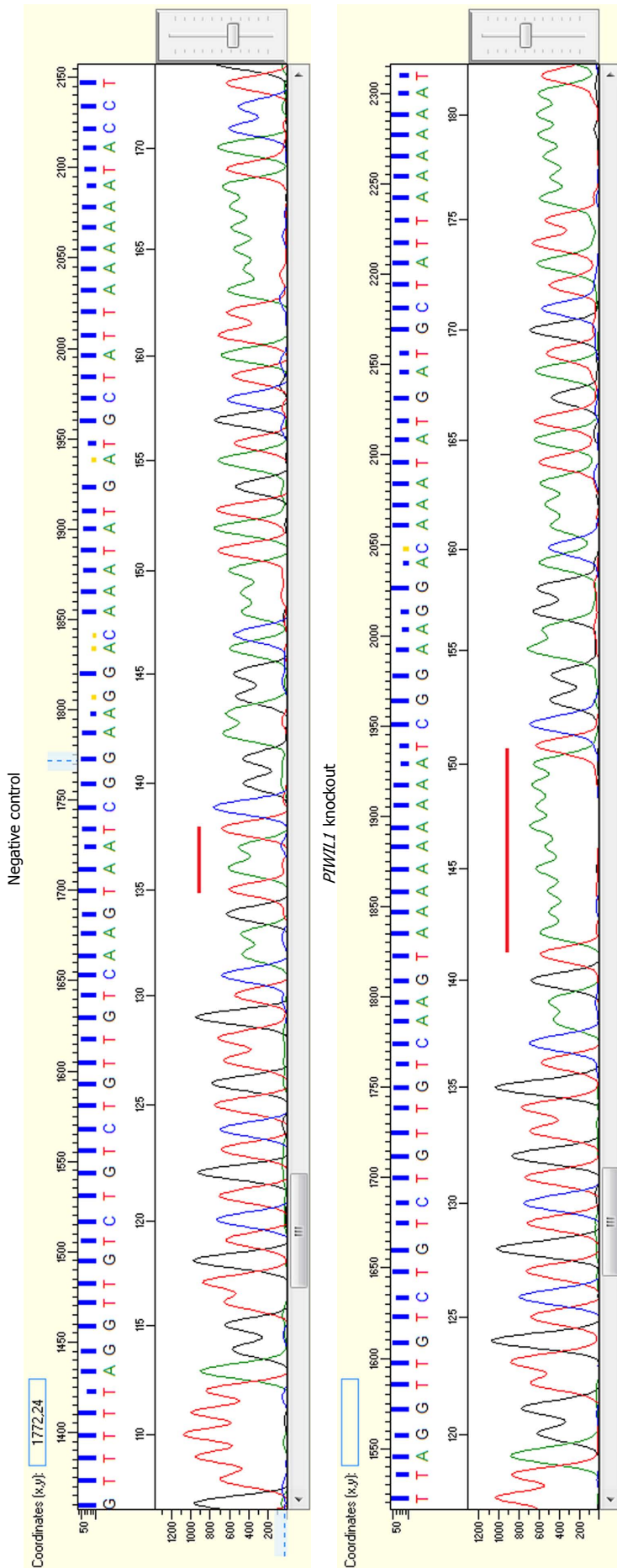


Figure 2 Electropherograms showing the insertion of seven adenines in the *PIWIL1* gene sequence after using the CRISPR-Cas9 system (B) in comparison with the reference sequence of the negative control (A).

[adjusted P -value of < 0.05 and $|\log_2(\text{Fold-Change})| > 1$]. A total of 43 mRNA probes were up-regulated and 208 were down-regulated (Figure 6). The DE genes are described in Supplementary Table 2.

We performed a functional analysis by grouping all DE mRNAs. This approach revealed that a total of 35 genes (five up-regulated and 30 down-regulated) encoded proteins involved in invasion and migration cellular processes (Supplementary Figure 1; Supplementary Tables 3 and 4).

According to the current literature, 9 of these 35 genes (*DOCK2*, *ZNF503*, *PDE4D*, *ABL1*, *ABL2*, *LPAR1*, *SMAD2*, *WASF3* and *DACH1*) are possibly related to the mechanisms used by *PIWIL1* to promote carcinogenic effects related to migration and invasion, since their functions are consistent with the changes observed (being up- or down-regulated after knockout).

DISCUSSION

Evidence indicating that *PIWIL1* is an oncogene that regulates several cellular mechanisms important for the carcinogenic process of many types of cancers is rising in recent years. *PIWIL1* seems to be especially implicated in proliferating activity of cancer cells^(8,10,26,27).

Here, we introduce a new gastric cell line, *i.e.*, AGP01, and provide a first description of its karyotype. As is usual for cancer cell lines, there were slight changes from

861 aa
3591
nucleotides,
1196 amino
acids

```

1 YWAYGVQTRG RRPGGGVHPP GKRAVARCP RVPGLSLGNA PKARWARAEG GPGRSAARRD
61 LRGSRWGCPW RAEVQGPGLG RGQRSKK*KT MTGRARARAR GRARGQETAQ LVGSTASQQP
121 GYIQPRPQPP PAEGELFGRG RQRGTAGGTA KSQGLQISAG FQELSLAERG GRRRDFHDLG
181 VNTRQNLDHV KESKTGSSGI IVRLSTNHFR LTRPQWALY QYHIDYNPL EARRLSALL
241 FQHEDLIGKC HAFDGTILFL PKRLQQKYTE VFSKTRNGED VRITITLTNE LPPTSPTCLQ
301 FYNIIFFRLL KIMNLQQIGR NYNPNPID IPSHRLVIWP GFTTSILQYE NSIMLCTDVS
361 HKVLRSETVL DFMFNFYHQT EEHKFQEQVS KELIGLVVLT KYNNKTYRVD DIDWDQNPKS
421 TFKKADGSEV SFLEYRKQY NQEITDLKQP VLVSQPKRRR GPGGTLPGPA MLIPELCYLT
481 GLTDKMRNDF NVNKDLAVHT RLTPQQRRE VGRLLIDYHK NDNVQRELRLD WGLSFDSNLL
541 SFSGRILQTE KIHQGGKTFD YNPQFADWSK ETRGAPLISV KPLDNWLLIY TRRNYEAANS
601 LIQNLFKVTP AMGMQMRKAI MIEVDDRTEA YLRVLQKKVT ADTQIVVCLL SSNRKDKYDA
661 IKKYLCTDCP TPSQCVVART LGKQQTVMAI ATKIALQNC KNGGELWRVD IPLKLVIVG
721 IDCYHDMTAG RRSIAGFVAS INEGMTRWFS RCIFQDRGQE LVDGLKVCLQ AALRAWNSCN
781 EYMPRIIVY RDGVGDGQLK TLVNYEVPQF LDCLKSIGRG YNPLTVIVV KKRNVTRFFA
841 QSGGRLQNP L PGTVIDVEVT RPEWYDFFIV SQAVRSQSVS PTHYNYIYDV SGLKPDHIQR
901 LTYKLCHIIY NWPGVIRVPA PCQYAHKLAFL LVGQSIHREP NLSLSNRLYY L*PAEDDAAA
961 FLFEMTLGFF *AFIYFFNC YLSG*NLGRG LGDLAFYF*H CYPASLFYT *KLRFYILSS
1021 CFS*IFCEHF FVYFEEMWIR YLVV*NRLSE SI*NVFGDLL KRTFRSEQVL LINLY*LYF*
1081 DTCFEFGKDK RRVKGCCLQP *VGFQLIS*R *KVLNLYNT RYRRKYA*FL FGRGARLYGS
1141 KKNIEFN*IV QRNLRFLFNK KGHE*ISILT LLFILFWNWD MIFLVK*N* CDCHLI

```

Amino acids sequence in
the wild-type *PIWIL1*

Stop codon of wild-type
PIWIL1

Wild-type *PIWIL1* protein sequence

573 aa
3598
nucleotides,
1199 amino
acids

```

1 YWAYGVQTRG RRPGGGVHPP GKRAVARCP RVPGLSLGNA PKARWARAEG GPGRSAARRD
61 LRGSRWGCPW RAEVQGPGLG RGQRSKK*KT MTGRARARAR GRARGQETAQ LVGSTASQQP
121 GYIQPRPQPP PAEGELFGRG RQRGTAGGTA KSQGLQISAG FQELSLAERG GRRRDFHDLG
181 VNTRQNLDHV KESKTGSSGI IVRLSTNHFR LTRPQWALY QYHIDYNPL EARRLSALL
241 FQHEDLIGKC HAFDGTILFL PKRLQQKYTE VFSKTRNGED VRITITLTNE LPPTSPTCLQ
301 FYNIIFFRLL KIMNLQQIGR NYNPNPID IPSHRLVIWP GFTTSILQYE NSIMLCTDVS
361 HKVLRSETVL DFMFNFYHQT EEHKFQEQVS KELIGLVVLT KYNNKTYRVD DIDWDQNPKS
421 TFKKADGSEV SFLEYRKQY NQEITDLKQP VLVSQPKRRR GPGGTLPGPA MLIPELCYLT
481 GLTDKMRNDF NVNKDLAVHT RLTPQQRRE VGRLLIDYHK NDNVQRELRLD WGLSFDSNLL
541 SFSGRILQTE KIHQGGKTFD YNPQFADWSK ETRGAPLISV KPLDNWLLIY TRRNYEAANS
601 LIQNLFKVTP AMGMQMRKAI MIEVDDRTEA YLRVLQKKVT ADTQIVVCLL SSKKKSEGQI
661 RCY*KIPVYR LPYPKSVCGG PNLRTQANCH GHCKYDCPTD ELQDGRRALE GGHPPPEARDD
721 RWHRLLP*HD SWAEVNRRIC CQHQRDDPL VTLTHISG*R TGAGRWAQSL PASGSEGLE*
781 LQ*VHAQPDH RVPRWRRRRP AENTGELRSA TVFGLSKIHW *RLQP*TNGN CGEEKSEHQI
841 FCSVWRKTSE STSWNSY*CR GYQTRV*LF YREPGCEKW* CFSHTLQCHL *QQRPEARPH
901 TALDLQAVPH LLQLARCHSC SCCLPVRPQA GFSCWPEYSQ RAKSVTVKPP LLPLTCRRRC
961 SRSF*NDFF IFLSFYLLFF *LLSFW*KLK KGIRRSSILF LALLFTGFLI LYVKIKILYF
1021 IRLFLIDL* AFFCLF*RNVD DKILGSIKQT L*EYLKCVWR FT*TYFQE*A SPTYKPIITL
1081 FLRYLF*I*R R*EA*SRMLT TTIGGVSAHI LKIKGTII*P IHKIQEKICL IFIWQGG*VV
1141 WE*KKH*KFL NCPKKHFKTL *QKRP*VNLY INITIYFVLE LGHDSICYKI KLM*LSPYL

```

Premature
stop codon

Alteration in amino
acid sequence

Predict sequence of *PIWIL1* after knockout

Figure 3 Amino acid sequences of the wild-type *PIWIL1* protein and the *PIWIL1* protein after the insertion of seven adenines by the CRISPR-Cas9 system.

cell to cell concerning number of chromosomes or single cell chromosomal rearrangements^[28]. The here-given karyotype was the most frequently observed one. Interestingly, inversions, dicentrics and reciprocal translocations of homologous acrocentric (#13, #15, #22) was observed. Overall, gain of the following regions was present: #1, #3, large parts of #2 and #5, 8q11.2 to 8qter, 12pter to 12q12. Besides, the following regions were under-represented: 2pter to 2p12, 9pter to 9p12, 15q12 to 15qter. These imbalances are in concordance with the literature^[29].

In AGP01, we performed for the first time an *in*

vitro knockout experiment of *PIWIL1* gene using the CRISPR-Cas9 system. It could be shown that absence of this gene significantly impairs migration and invasion capacity of AGP01 cells. Thus, the AGP01 cell line behaves like that previously reported for gastric cancer cells^[12] or lung adenocarcinoma^[26]. Together, these studies suggest that *PIWIL1* expression is strongly associated with an increased aggressiveness of cancer cells.

According to Wang *et al.*^[30], one of the mechanisms by which *PIWIL1* regulates the migration and invasion of cancer cells is by promoting the expression of MMP2

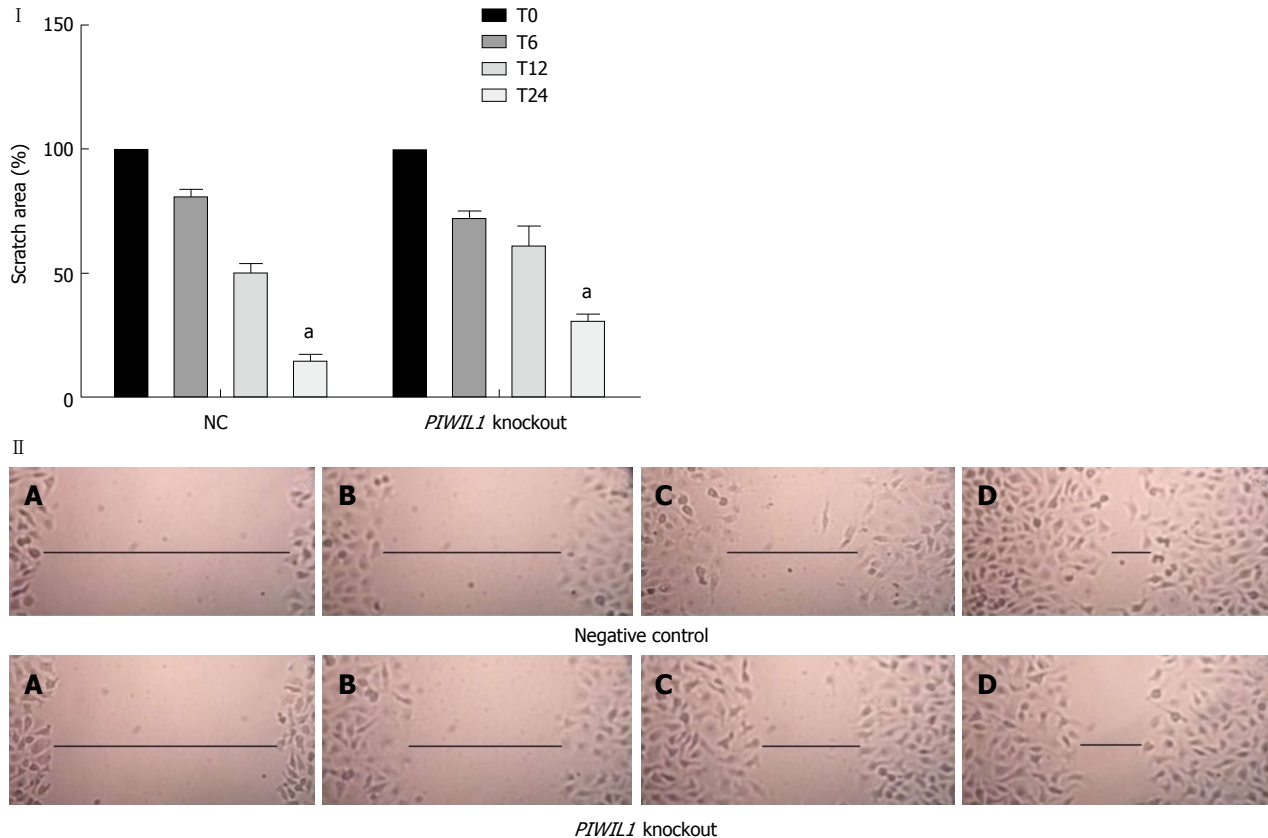


Figure 4 Analysis of the migration capacity of the AGP01 cell line with and without *PIWIL1* gene knockout. T0: Immediately after injury; T6: 6 h after injury; T12: 12 h after injury; T24: 24 h after injury. NC: Negative control. ^a $P < 0.01$. Two-way ANOVA, Bonferroni post-test. Photomicrography of AGP01 cell migration. A: Immediately after injury; B: 6 h after injury; C: 12 h after injury; D: 24 h after injury. The black lines represent approximation of the edges over time, demonstrating the migration capacity of the cells.

and MMP9, two important metalloproteinases involved in the degradation of the extracellular matrix, thereby creating paths for the locomotion of cancer cells^[31].

Additionally, Amaar *et al.*^[32] demonstrated that the over-expression of *PIWIL1* down-regulates the tumor suppressor gene *IGFBP5*, a member of the insulin-like growth factor binding protein family and whose expression is implicated in suppressing epithelial-mesenchymal transition and reducing the expression of E-cadherin and HIF1 α , indicating that it is critically related to cancer progression^[33,34].

Data obtained from our gene expression experiments also provided corroborating evidence that the *PIWIL1* gene plays a key role in cancer cell migration and invasion because several genes involved in these cellular processes were observed as DE when the cell lines were compared before and after *PIWIL1* knockout.

Many studies have demonstrated the oncogenic activities of the *DOCK2*, *ZNF503*, *PDE4D*, *ABL1*, *ABL2*, *LPAR1*, *SMAD2* and *WASF3* genes and their relation to tumor aggressiveness in several types of cancer, including gastric cancer^[35-58]. Interestingly, *PIWIL1* knockout led to a decreased expression of these genes as well as an increased expression of the tumor suppressor gene *DACH1*, demonstrating that *PIWIL1* plays a crucial role in the pathway of development and progression of gastric cancer, and is likely a promising

candidate for therapeutic intervention.

Zhu *et al.*^[53] reported that the over-expression of *DACH1* impaired the proliferation and invasion ability of lung adenocarcinoma cells *in vitro* via the down-regulation of PRX3, an oncoprotein required for the maintenance of mitochondrial function and tumorigenesis^[59]. *DACH1* expression also inhibited epithelial-mesenchymal transition and metastasis by affecting TGF- β signaling and decreased proliferation of cancer cells by inducing cell cycle arrest at the G2/M phase^[60,61].

Regarding the reported oncogenes, Rahrmann *et al.*^[37] observed that *PDE4D* is over-expressed in human prostate cancer and demonstrated that the knockdown of this gene reduced the growth and migration of prostate cancer cells *in vitro* as well as the growth and proliferation rate of prostate cancer xenografts *in vivo*^[38]. Delyon *et al.*^[39] demonstrated that *PDE4D* is also over-expressed in melanoma cell lines and pinpointed this gene as a regulator of cell invasion by interacting with *FAK* through *RACK1*, constituting a signaling pathway that when activated promotes tumor progression and metastasis^[43].

Recent studies have determined the role of ABL members from the tyrosine kinase family, *ABL1* and *ABL2*, in the development of many types of solid tumors. These proteins induce the activation of actin polymerization machinery by modulating the expression

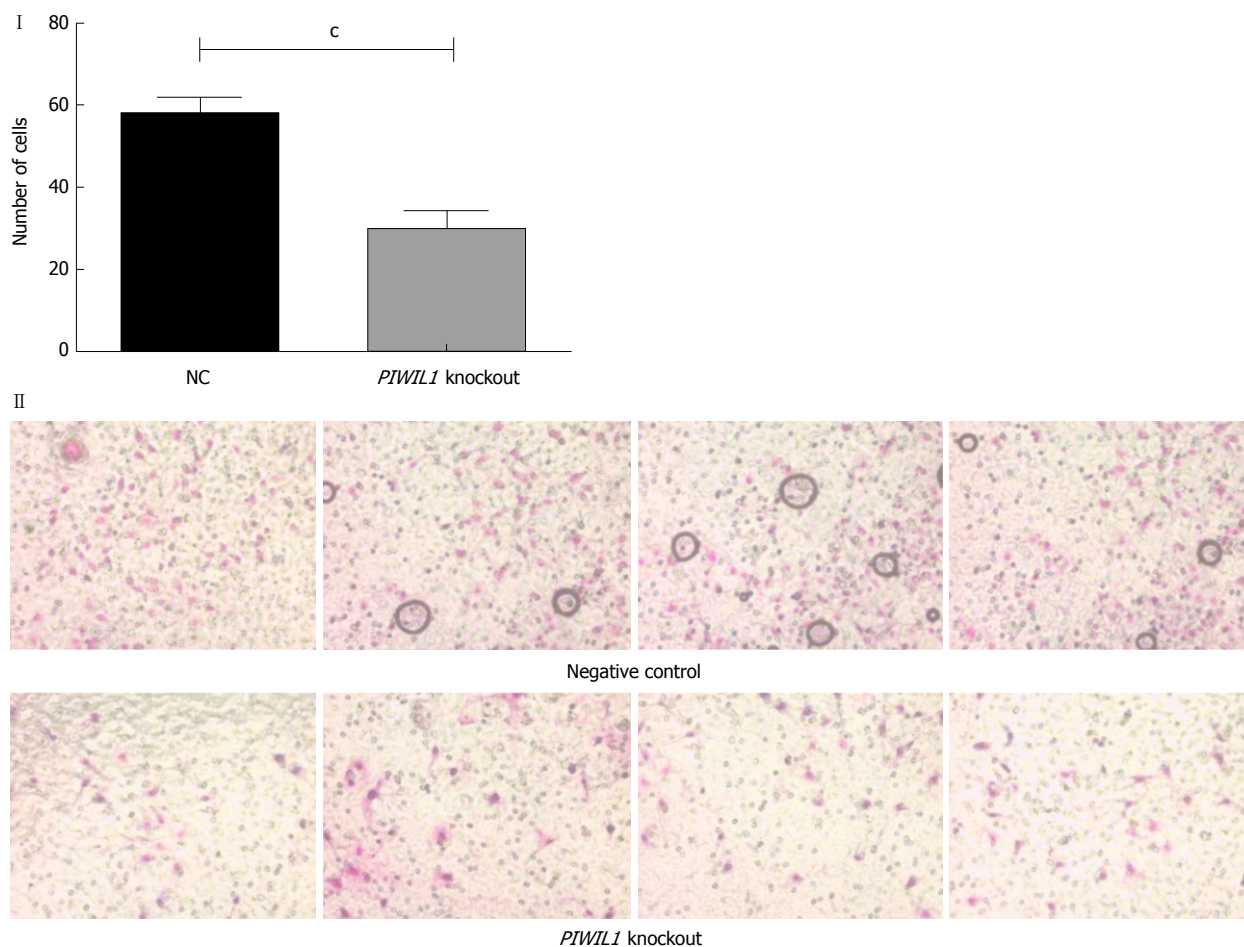


Figure 5 Analysis of the invasion capacity of the AGP01 cell line with and without the *PIWIL1* gene knockout. Statistically significant difference between groups was shown by the Student's *t* test ($P < 0.001$). Photomicrography of the cell invasion assay demonstrating the decrease in the number of cells that invaded when *PIWIL1* was knocked out. NC: Negative control.

of several MMPs to promote morphological changes, including the formation of membrane protrusions and altered cell adhesion. Consequently, activation of ABL1 and ABL2 in cancer cells promote enhanced proliferation, migration and invasion, as well as drug resistance^[39-42].

DOCK2 (dedicator of cytokinesis) belongs to the *DOCK* family of proteins and is expressed in hematopoietic cells^[44]. According to Kulkarni *et al.*^[45], *DOCK2* has been reported to activate Rac, which is known to regulate several crucial processes, including lymphocyte migration, activation and differentiation of T cells^[46]. Wang *et al.*^[47] knocked out *DOCK2* in a B-cell lymphoma cell line and observed a decrease in Rac1 expression. Additionally, analysis of the growth curves of both cell lines demonstrated that the *DOCK2* knockout grew less than *DOCK2*, as evidenced by the lower cell proliferation.

ZNF503 is expressed in the mammary gland and other tissues, and there is a high incidence of association between this gene deregulation and tumor aggressiveness in several kinds of tissues, such as lung, kidney and intestine^[49]. Shahi *et al.*^[48] performed scratch and 3D Matrigel culture assays in two mammary

epithelial cell lines to analyze the cell motility and migration. Both assays demonstrated that cell lines with *ZNF503* knockout migrated less, did not close the gaps, and inhibited invasiveness when compared to the control cells. These data indicate that *ZNF503* promotes cellular invasion and migration, and high levels of this gene are closely related with poor patient survival, breast cancer progression and increased metastasis.

Yu *et al.*^[50] demonstrated that the *lysophosphatidic acid receptor 1 (LPAR1)* gene is related to migration and invasion in ascites from ovarian cancer and is expressed at higher levels in metastatic cell lines, when compared to non-metastatic cell lines. They also observed that the presence of high levels of lysophosphatidic acid are directly connected to cell migration stimulation, and *LPAR1* silencing reduced lysophosphatidic acid-induced invasion. Additionally, in breast tumors, a higher expression of *LPAR1* is related to a worse lung metastasis-free survival rate^[51].

Wiskott-Aldrich syndrome protein family 3 (*WASF3*) is an important gene, which has C-terminal domains that are responsible for actin polymerization activation, playing a role in cell proliferation and migration. The *WASF3* gene is normally over-expressed in several types

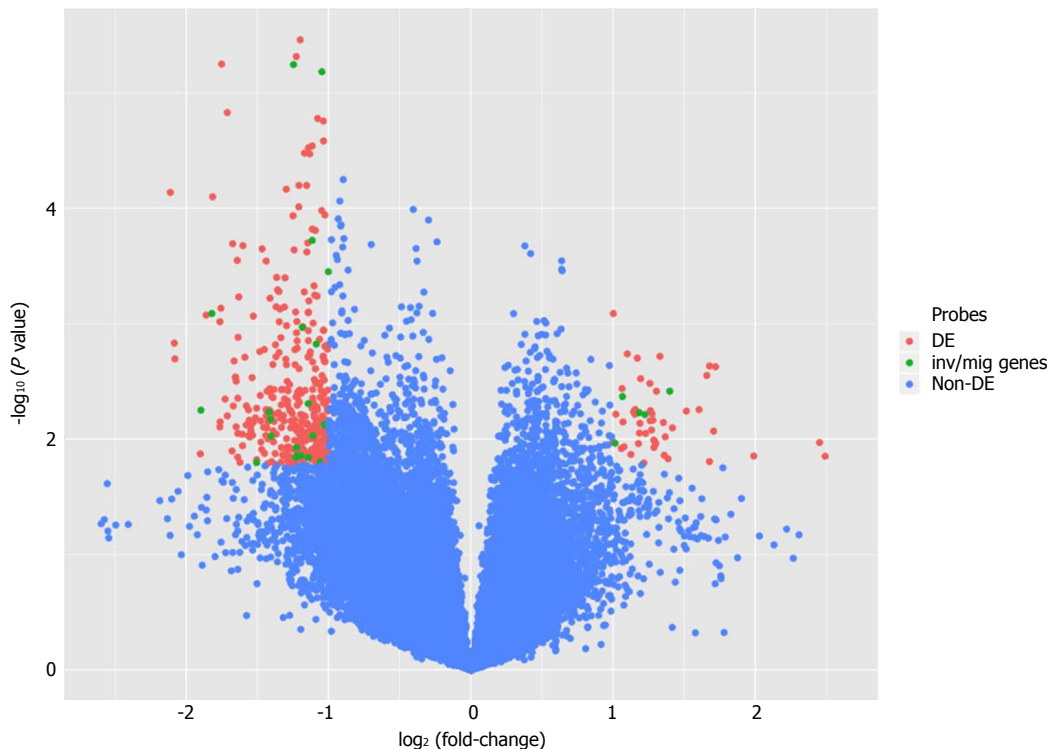


Figure 6 Volcano plot comparing gene expression after *PIWIL1* permanent knockout in the gastric cancer AGP01 cell line. Differentially expressed probes [adjusted *P*-value of < 0.05 and |Log₂(Fold-Change)| > 1] are on superior left and right areas (red). mRNAs involved in invasion and migration processes are in green.

of tumors, such as breast cancer, osteosarcoma and prostate cancer^[52,53]. In gastric cancer, little is known about this gene; however, since micro (mi)RNAs and their targets are considered potential biomarkers for gastric cancer, Wang *et al.*^[54] performed a luciferase assay and western blotting to investigate the relationship between miR-218 and *WASF3*. Their results demonstrated that over-expression of *WASF3* harms miR-218 and results in the inhibition of cell proliferation and migration, suggesting that *WASF3* is over-expressed in gastric cancer and induces cell proliferation and migration. Additionally, in qRT-PCR, *WASF3* mRNA expression levels were higher when compared to normal gastric cell lines.

Smad2 is the first intracellular protein in the signaling cascade of the TGF- β 1 signaling pathway, which is involved in the progression of gastric cancer. In advanced stages of cancer, TGF- β 1 acts as an oncogene, regulating multiple cellular functions, including stimulation of proliferation, differentiation and the inhibition of apoptosis^[55,57].

Interestingly, Lv *et al.*^[56] observed that TGF- β 1 levels in peritoneal lavage fluid are directly connected to peritoneal metastasis. Corroborating evidence was provided by Shinto *et al.*^[58], whose experiments demonstrated that p-Smad2 expression was higher in diffuse-type tumors and in peritoneal metastasis cases. Notably, the AGP01 cell line used to perform the *PIWIL1* knockout in our study was obtained from a patient with peritoneal metastasis, and we found *SMAD2* was over-expressed.

Taken together, these data reinforce the idea that *PIWIL1* plays a crucial role in the signaling pathway

of gastric cancer, regulating several genes involved in migration and invasion processes; therefore, its use as a therapeutic target may generate promising results in the treatment of gastric cancer, mainly in patients with peritoneal carcinomatosis, which is a condition associated with poor prognosis and a decreased overall survival.

ARTICLE HIGHLIGHTS

Research background

Gastric cancer (GC) remains a major public health problem, having the third highest incidence of death worldwide. *Piwi like RNA-mediated gene silencing 1* (*PIWIL1*) is involved in regulation of widespread biological processes, including stem cell proliferation, embryogenesis, growth, and development, and has been found to be frequently over-expressed in various tumor types, including GC. Previous studies have demonstrated that *PIWIL1* is implicated in improving tumor malignant behavior. *PIWIL1* expression has been shown to be absent in normal somatic tissues, making it a very intriguing target for therapy. We attempted to investigate the role of *PIWIL1* on the migration and invasion capacity of metastatic GC cells, using the AGP01 cell line, as well as checking the expression status of genes and proteins involved in these cellular processes, in order to elucidate the mechanisms by which *PIWIL1* provokes tumorigenic effects and to shed light on potential new strategies to target *PIWIL1*.

Research motivation

Many aspects of gastric carcinogenesis remain elusive, and much effort has been made to improve patient prognosis. The *PIWIL1* has been identified as a novel extremely highly expressed gene in many types of cancer and its expression in GC tissue is related to poorer overall survival, suggesting that high expression of *PIWIL1* is associated with poor prognosis and that it could be used as a predictive marker or even a target for therapy. Although *PIWIL1* has been correlated with worse outcome, the involved mechanisms remain

unclear, and many hypotheses are being tested. Once the upstream and downstream signaling pathways of *PIWIL1* are elucidated, it will be possible to create new therapeutic strategies for gastric carcinogenesis, in order to improve the overall health of patients affected by this disease.

Research objectives

We performed permanent knockout of the *PIWIL1* gene to verify phenotypic modifications in the AGP01 metastatic GC cell line, as well as alterations in expression level of mRNA and protein, in an attempt to better understand the mechanisms by which *PIWIL1* promotes tumor malignant behavior. This research demonstrates the importance of studying *PIWIL1* in GC, since data obtained through the achievement of our objectives showed that this protein has a crucial role in gastric carcinogenesis, promoting molecular and phenotypic alterations compatible with enhanced tumor aggressiveness. The elucidation of the role of *PIWIL1* protein in cancer cell invasion and migration will pave the way for developing potential clinical interventions, aiming to control GC dissemination.

Research methods

We applied CRISPR/Cas9 technology to knockout the *PIWIL1* gene in a metastatic GC cell line, and analyzed its phenotypic modifications, as well as alterations in gene and protein expression. CRISPR-Cas9 technology was considered in 2015 as one of the most important technological advances of science. Mainly, it allows permanent silencing of the target gene and also creates a stable and permanent cell line with the desired modification. By this way, multiple experiments can be carried on, including long term evaluation of the downstream events caused by the molecular alteration, as well as discovering potential pathways influenced by the studied gene. Therefore, after permanent knockout of *PIWIL1* in the AGP01 cell line, we analyzed phenotypic modifications by performing wound-healing and Boyden chamber invasion assays, to assess migration and invasion, respectively. Moreover, aiming to shed light on the molecular mechanisms used by *PIWIL1* to make changes in the migration and invasion capability of cells, we carried out proteomic and microarray assays, using multidimensional protein identification technology (commonly known as MudPIT) and a one-color microarray-based gene expression analysis kit, respectively.

Research results

PIWIL1 gene knockout was successfully performed and confirmed by Sanger sequencing, which revealed an insertion of seven adenines in the *PIWIL1* gene sequence. *In silico* prediction of the encoded protein pointed to the appearance of a premature termination codon, suggesting that this insertion generates a truncated protein with a loss-of-function phenotype. *PIWIL1* knockout promoted a significant decrease in cell migration and invasion capacity ($P < 0.01$ and $P < 0.001$, respectively), which is consistent with data present in the literature demonstrating that this protein is implicated in several signaling pathways that regulate cell motility. By comparing expression profiles after *PIWIL1* knockout, a total of 251 mRNA were found to be differentially expressed, with 43 up-regulated and 208 down-regulated mRNA. A functional analysis grouping all differentially expressed mRNAs demonstrated that 35 genes encoded proteins were involved in invasion and migration cellular processes. After extensive review of data presented in the literature, we selected 9 of these 35 genes (*DOCK2*, *ZNF503*, *PDE4D*, *ABL1*, *ABL2*, *LPAR1*, *SMAD2*, *WASF3* and *DACH1*) as possibly related to the mechanisms used by *PIWIL1* to promote carcinogenic effects related to migration and invasion, since their functions are consistent with the changes observed (being up- or down-regulated after knockout). Additionally, the analysis of proteomic data revealed that *PIWIL1* knockout caused modification in the expression of 27 proteins involved in epithelial-mesenchymal transition (EMT). Twenty-two oncoproteins related to EMT promotion, including *FGFR1*, *PCNA*, *ACTN4*, *GSN* and *TUBB3*, were expressed in the AGP01 cell line before knockout and reduced to a level that were not detectable by the technique after knockout. On the other hand, *PIWIL1* knockout caused an increase in the expression of six proteins implicated in EMT suppression, such as *ACSM3*, *ADGRG1* and *ANPEP*, that were absent in AGP01 before knockout. To the best of our knowledge, this is the first report describing molecular alteration compatible with phenotypic alterations after permanent knockout of *PIWIL1* in GC. Detailed mechanisms leading to *PIWIL1* over-expression in cancer as well as the pathways by which this protein

improves the malignant phenotype should be further investigated.

Research conclusions

In the current study, we pioneered the performance of an *in vitro* knockout of the *PIWIL1* gene by using the CRISPR-Cas9 system, and found that absence of this gene significantly impaired the migration and invasion capacity of the AGP01 cell line, besides modifying mRNA and protein expression of potential molecular targets involved in the EMT process. The results of such experiments contributed to understanding of the mechanisms used by *PIWIL1* to promote alteration in migration and invasion capacity of gastric cells during tumorigenesis, and also revealed the participation of new players related to *PIWIL1* expression, such as *FGFR1*, *PCNA*, *ACTN4*, *PDE4D* and *SMAD2*. Our results demonstrated that knockout of *PIWIL1* promotes several changes in cell phenotype, suggesting the critical role of the *PIWIL1* oncogene in GC, and confirmed the hypothesis that *PIWIL1* expression provokes migration, invasiveness and EMT as potential mechanisms of improved tumor aggressiveness. The presented findings open new perspectives for molecular interventions in GC.

Research perspectives

Definite silencing of *PIWIL1* by the CRISPR-Cas9 system resulted in robust findings favoring the discovery of new mechanisms involved in gastric carcinogenesis. The presented results must be validated by other researchers, and if confirmed, might lead to innovative interventions aiming to treat GC.

REFERENCES

- 1 Ferlay J, Soerjomataram I, Dikshit R, Eser S, Mathers C, Rebelo M, Parkin DM, Forman D, Bray F. Cancer incidence and mortality worldwide: sources, methods and major patterns in GLOBOCAN 2012. *Int J Cancer* 2015; **136**: E359-E386 [PMID: 25220842 DOI: 10.1002/ijc.29210]
- 2 Wu HH, Lin WC, Tsai KW. Advances in molecular biomarkers for gastric cancer: miRNAs as emerging novel cancer markers. *Expert Rev Mol Med* 2014; **16**: e1 [PMID: 24456939 DOI: 10.1017/erm.2013.16]
- 3 Assumpção CB, Calcagno DQ, Araújo TM, Santos SE, Santos ÂK, Riggins GJ, Burbano RR, Assumpção PP. The role of piRNA and its potential clinical implications in cancer. *Epigenomics* 2015; **7**: 975-984 [PMID: 25929784 DOI: 10.2217/epi.15.37]
- 4 Navarro A, Tejero R, Viñolas N, Cordeiro A, Marrades RM, Fuster D, Caritg O, Moises J, Muñoz C, Molins L, Ramirez J, Monzo M. The significance of PIWI family expression in human lung embryogenesis and non-small cell lung cancer. *Oncotarget* 2015; **6**: 31544-31556 [PMID: 25742785 DOI: 10.18632/oncotarget.3003]
- 5 Tan Y, Liu L, Liao M, Zhang C, Hu S, Zou M, Gu M, Li X. Emerging roles for PIWI proteins in cancer. *Acta Biochim Biophys Sin (Shanghai)* 2015; **47**: 315-324 [PMID: 25854579 DOI: 10.1093/abbs/gmv018]
- 6 Siddiqi S, Matushansky I. Piwis and piwi-interacting RNAs in the epigenetics of cancer. *J Cell Biochem* 2012; **113**: 373-380 [PMID: 21928326 DOI: 10.1002/jcb.23363]
- 7 Siddiqi S, Terry M, Matushansky I. Hiwi mediated tumorigenesis is associated with DNA hypermethylation. *PLoS One* 2012; **7**: e33711 [PMID: 22438986 DOI: 10.1371/journal.pone.0033711]
- 8 Litwin M, Szczepańska-Buda A, Piotrowska A, Dzięgiel P, Witkiewicz W. The meaning of PIWI proteins in cancer development. *Oncol Lett* 2017; **13**: 3354-3362 [PMID: 28529570 DOI: 10.3892/ol.2017.5932]
- 9 Li C, Zhou X, Chen J, Lu Y, Sun Q, Tao D, Hu W, Zheng X, Bian S, Liu Y, Ma Y. *PIWIL1* destabilizes microtubule by suppressing phosphorylation at Ser16 and RLIM-mediated degradation of Stathmin1. *Oncotarget* 2015; **6**: 27794-27804 [PMID: 26317901 DOI: 10.18632/oncotarget.4533]
- 10 Chen Z, Che Q, He X, Wang F, Wang H, Zhu M, Sun J, Wan X. Stem cell protein Piwil1 endowed endometrial cancer cells with stem-like properties via inducing epithelial-mesenchymal transition. *BMC Cancer* 2015; **15**: 811 [PMID: 26506848 DOI: 10.1186/

- s12885-015-1794-8]
- 11 **Wang Y**, Liu Y, Shen X, Zhang X, Chen X, Yang C, Gao H. The PIWI protein acts as a predictive marker for human gastric cancer. *Int J Clin Exp Pathol* 2012; **5**: 315-325 [PMID: 22670175]
 - 12 **Liu X**, Sun Y, Guo J, Ma H, Li J, Dong B, Jin G, Zhang J, Wu J, Meng L, Shou C. Expression of hiwi gene in human gastric cancer was associated with proliferation of cancer cells. *Int J Cancer* 2006; **118**: 1922-1929 [PMID: 16287078 DOI: 10.1002/ijc.21575]
 - 13 **Riordan SM**, Heruth DP, Zhang LQ, Ye SQ. Application of CRISPR/Cas9 for biomedical discoveries. *Cell Biosci* 2015; **5**: 33 [PMID: 26137216 DOI: 10.1186/s13578-015-0027-9]
 - 14 **Hsu PD**, Lander ES, Zhang F. Development and applications of CRISPR-Cas9 for genome engineering. *Cell* 2014; **157**: 1262-1278 [PMID: 24906146 DOI: 10.1016/j.cell.2014.05.010]
 - 15 **Jinek M**, Chylinski K, Fonfara I, Hauer M, Doudna JA, Charpentier E. A programmable dual-RNA-guided DNA endonuclease in adaptive bacterial immunity. *Science* 2012; **337**: 816-821 [PMID: 22745249 DOI: 10.1126/science.1225829]
 - 16 **Chen S**, Sun H, Miao K, Deng CX. CRISPR-Cas9: from Genome Editing to Cancer Research. *Int J Biol Sci* 2016; **12**: 1427-1436 [PMID: 27994508 DOI: 10.7150/ijbs.17421]
 - 17 **Kawahara A**, Hisano Y, Ota S, Taimatsu K. Site-Specific Integration of Exogenous Genes Using Genome Editing Technologies in Zebrafish. *Int J Mol Sci* 2016; **17** [PMID: 27187373 DOI: 10.3390/ijms17050727]
 - 18 **Maeder ML**, Gersbach CA. Genome-editing Technologies for Gene and Cell Therapy. *Mol Ther* 2016; **24**: 430-446 [PMID: 26755333 DOI: 10.1038/mt.2016.10]
 - 19 **Travis J**. Breakthrough of the Year: CRISPR makes the cut. *Science Magazine* 2015; Available from: URL: <http://www.sciencemag.org/news/2015/12/and-science-s-breakthrough-year>
 - 20 **Leal MF**, Martins do Nascimento JL, da Silva CE, Vita Lamarão MF, Calcagno DQ, Khayat AS, Assumpção PP, Cabral IR, de Arruda Cardoso Smith M, Burbano RR. Establishment and conventional cytogenetic characterization of three gastric cancer cell lines. *Cancer Genet Cytogenet* 2009; **195**: 85-91 [PMID: 19837275 DOI: 10.1016/j.cancergencyto.2009.04.020]
 - 21 **Liehr T**, Heller A, Starke H, Rubtsov N, Trifonov V, Mrasek K, Weise A, Kuechler A, Claussen U. Microdissection based high resolution multicolor banding for all 24 human chromosomes. *Int J Mol Med* 2002; **9**: 335-339 [PMID: 11891523]
 - 22 **Liehr T**. The Standard FISH Procedure. Fluorescence In Situ Hybridization (FISH) - Application Guide. Berlin: *Springer* 2017; 109-118
 - 23 **Benjamini Y**, Hochberg Y. Controlling the false discovery rate: a practical and powerful approach to multiple testing. *J Royal Stat Soc* 1995; **57**: 289-300
 - 24 **Carlson M**. org.Hs.eg.db: Genome wide annotation for Human. 2017; R package version 3.5.0
 - 25 **Falcon S**, Gentleman R. Using GOSTats to test gene lists for GO term association. *Bioinformatics* 2007; **23**: 257-258 [PMID: 17098774 DOI: 10.1093/bioinformatics/btl567]
 - 26 **Xie K**, Zhang K, Kong J, Wang C, Gu Y, Liang C, Jiang T, Qin N, Liu J, Guo X, Huo R, Liu M, Ma H, Dai J, Hu Z. Cancer-testis gene PIWIL1 promotes cell proliferation, migration, and invasion in lung adenocarcinoma. *Cancer Med* 2018; **7**: 157-166 [PMID: 29168346 DOI: 10.1002/cam4.1248]
 - 27 **Sun R**, Gao CL, Li DH, Li BJ, Ding YH. Expression Status of PIWIL1 as a Prognostic Marker of Colorectal Cancer. *Dis Markers* 2017; **2017**: 1204937 [PMID: 28634417 DOI: 10.1155/2017/1204937]
 - 28 **Bloomfield M**, Duesberg P. Karyotype alteration generates the neoplastic phenotypes of SV40-infected human and rodent cells. *Mol Cytogenet* 2015; **8**: 79 [PMID: 26500699 DOI: 10.1186/s13039-015-0183-y]
 - 29 **Gebhart E**, Liehr T. Patterns of genomic imbalances in human solid tumors (Review). *Int J Oncol* 2000; **16**: 383-399 [PMID: 10639584]
 - 30 **Wang X**, Tong X, Gao H, Yan X, Xu X, Sun S, Wang Q, Wang J. Silencing HIWI suppresses the growth, invasion and migration of glioma cells. *Int J Oncol* 2014; **45**: 2385-2392 [PMID: 25269862 DOI: 10.3892/ijo.2014.2673]
 - 31 **Rundhaug JE**. Matrix metalloproteinases and angiogenesis. *J Cell Mol Med* 2005; **9**: 267-285 [PMID: 15963249]
 - 32 **Amaar YG**, Baylink DJ, Mohan S. Ras-association domain family 1 protein, RASSF1C, is an IGFBP-5 binding partner and a potential regulator of osteoblast cell proliferation. *J Bone Miner Res* 2005; **20**: 1430-1439 [PMID: 16007340 DOI: 10.1359/JBMR.050311]
 - 33 **Wang J**, Ding N, Li Y, Cheng H, Wang D, Yang Q, Deng Y, Yang Y, Li Y, Ruan X, Xie F, Zhao H, Fang X. Insulin-like growth factor binding protein 5 (IGFBP5) functions as a tumor suppressor in human melanoma cells. *Oncotarget* 2015; **6**: 20636-20649 [PMID: 26010068 DOI: 10.18632/oncotarget.4114]
 - 34 **Güllü G**, Karabulut S, Akkiprik M. Functional roles and clinical values of insulin-like growth factor-binding protein-5 in different types of cancers. *Chin J Cancer* 2012; **31**: 266-280 [PMID: 22313597 DOI: 10.5732/cjc.011.10405]
 - 35 **Henry C**, Llamas E, Knipprath-Meszaros A, Schoetza A, Obermann E, Fuenfschilling M, Caduff R, Fink D, Hacker N, Ward R, Heinzelmann-Schwarz V, Ford C. Targeting the ROR1 and ROR2 receptors in epithelial ovarian cancer inhibits cell migration and invasion. *Oncotarget* 2015; **6**: 40310-40326 [PMID: 26515598 DOI: 10.18632/oncotarget.5643]
 - 36 **Henry CE**, Llamas E, Djordjevic A, Hacker NF, Ford CE. Migration and invasion is inhibited by silencing ROR1 and ROR2 in chemoresistant ovarian cancer. *Oncogenesis* 2016; **5**: e226 [PMID: 27239958 DOI: 10.1038/ncis.2016.32]
 - 37 **Rahrmann EP**, Collier LS, Knutson TP, Doyal ME, Kuslak SL, Green LE, Malinowski RL, Roethe L, Akagi K, Waknitz M, Huang W, Largaespada DA, Marker PC. Identification of PDE4D as a proliferation promoting factor in prostate cancer using a Sleeping Beauty transposon-based somatic mutagenesis screen. *Cancer Res* 2009; **69**: 4388-4397 [PMID: 19401450 DOI: 10.1158/0008-5472.CAN-08-3901]
 - 38 **Delyon J**, Servy A, Laugier F, André J, Ortonne N, Battistella M, Mourah S, Bensussan A, Lebbé C, Dumaz N. PDE4D promotes FAK-mediated cell invasion in BRAF-mutated melanoma. *Oncogene* 2017; **36**: 3252-3262 [PMID: 28092671 DOI: 10.1038/onc.2016.469]
 - 39 **Greuber EK**, Smith-Pearson P, Wang J, Pendergast AM. Role of ABL family kinases in cancer: from leukaemia to solid tumours. *Nat Rev Cancer* 2013; **13**: 559-571 [PMID: 23842646 DOI: 10.1038/nrc3563]
 - 40 **Wang J**, Pendergast AM. The Emerging Role of ABL Kinases in Solid Tumors. *Trends Cancer* 2015; **1**: 110-123 [PMID: 26645050 DOI: 10.1016/j.trecan.2015.07.004]
 - 41 **Gu JJ**, Rouse C, Xu X, Wang J, Onaitis MW, Pendergast AM. Inactivation of ABL kinases suppresses non-small cell lung cancer metastasis. *JCI Insight* 2016; **1**: e89647 [PMID: 28018973 DOI: 10.1172/jci.insight.89647]
 - 42 **Wang J**, Rouse C, Jasper JS, Pendergast AM. ABL kinases promote breast cancer osteolytic metastasis by modulating tumor-bone interactions through TAZ and STAT5 signaling. *Sci Signal* 2016; **9**: ra12 [PMID: 26838548 DOI: 10.1126/scisignal.aad3210]
 - 43 **Sulzmaier FJ**, Jean C, Schlaepfer DD. FAK in cancer: mechanistic findings and clinical applications. *Nat Rev Cancer* 2014; **14**: 598-610 [PMID: 25098269 DOI: 10.1038/nrc3792]
 - 44 **Tajiri H**, Urano T, Shirai T, Takaya D, Matsunaga S, Setoyama D, Watanabe M, Kukimoto-Niino M, Oisaki K, Ushijima M, Sanematsu F, Honma T, Terada T, Oki E, Shirasawa S, Maehara Y, Kang D, Côté JF, Yokoyama S, Kanai M, Fukui Y. Targeting Ras-Driven Cancer Cell Survival and Invasion through Selective Inhibition of DOCK1. *Cell Rep* 2017; **19**: 969-980 [PMID: 28467910 DOI: 10.1016/j.celrep.2017.04.016]
 - 45 **Kulkarni K**, Yang J, Zhang Z, Barford D. Multiple factors confer specific Cdc42 and Rac protein activation by dedicator of cytokinesis (DOCK) nucleotide exchange factors. *J Biol Chem* 2011; **286**: 25341-25351 [PMID: 21613211 DOI: 10.1074/jbc.M111.236455]
 - 46 **Wu M**, Small D, Duffield AS. DOCK2: A novel FLT3/ITD

- leukemia drug target. *Oncotarget* 2017; **8**: 88253-88254 [PMID: 29179430 DOI: 10.18632/oncotarget.21390]
- 47 **Wang L**, Nishihara H, Kimura T, Kato Y, Tanino M, Nishio M, Obara M, Endo T, Koike T, Tanaka S. DOCK2 regulates cell proliferation through Rac and ERK activation in B cell lymphoma. *Biochem Biophys Res Commun* 2010; **395**: 111-115 [PMID: 20350533 DOI: 10.1016/j.bbrc.2010.03.148]
- 48 **Shahi P**, Slorach EM, Wang CY, Chou J, Lu A, Ruderisch A, Werb Z. The Transcriptional Repressor ZNF503/Zeppo2 Promotes Mammary Epithelial Cell Proliferation and Enhances Cell Invasion. *J Biol Chem* 2015; **290**: 3803-3813 [PMID: 25538248 DOI: 10.1074/jbc.M114.611202]
- 49 **Shahi P**, Wang CY, Lawson DA, Slorach EM, Lu A, Yu Y, Lai MD, Gonzalez Velozo H, Werb Z. ZNF503/Zpo2 drives aggressive breast cancer progression by down-regulation of GATA3 expression. *Proc Natl Acad Sci USA* 2017; **114**: 3169-3174 [PMID: 28258171 DOI: 10.1073/pnas.1701690114]
- 50 **Yu X**, Zhang Y, Chen H. LPA receptor 1 mediates LPA-induced ovarian cancer metastasis: an in vitro and in vivo study. *BMC Cancer* 2016; **16**: 846 [PMID: 27809800 DOI: 10.1186/s12885-016-2865-1]
- 51 **Sahay D**, Leblanc R, Grunewald TG, Ambatipudi S, Ribeiro J, Clézardin P, Peyruchaud O. The LPA1/ZEB1/miR-21-activation pathway regulates metastasis in basal breast cancer. *Oncotarget* 2015; **6**: 20604-20620 [PMID: 26098771 DOI: 10.18632/oncotarget.3774]
- 52 **Teng Y**, Ghoshal P, Ngoka L, Mei Y, Cowell JK. Critical role of the WASF3 gene in JAK2/STAT3 regulation of cancer cell motility. *Carcinogenesis* 2013; **34**: 1994-1999 [PMID: 23677069 DOI: 10.1093/carcin/bgt167]
- 53 **Zhu Z**, Chen W, Yin X, Lai J, Wang Q, Liang L, Wang W, Wang A, Zheng C. WAVE3 Induces EMT and Promotes Migration and Invasion in Intrahepatic Cholangiocarcinoma. *Dig Dis Sci* 2016; **61**: 1950-1960 [PMID: 26971088 DOI: 10.1007/s10620-016-4102-9]
- 54 **Wang G**, Fu Y, Liu G, Ye Y, Zhang X. miR-218 Inhibits Proliferation, Migration, and EMT of Gastric Cancer Cells by Targeting WASF3. *Oncol Res* 2017; **25**: 355-364 [PMID: 27642088 DOI: 10.3727/096504016X14738114257367]
- 55 **Lv ZD**, Wang HB, Li FN, Wu L, Liu C, Nie G, Kong B, Qu HL, Li JG. TGF- β 1 induces peritoneal fibrosis by activating the Smad2 pathway in mesothelial cells and promotes peritoneal carcinomatosis. *Int J Mol Med* 2012; **29**: 373-379 [PMID: 22139024 DOI: 10.3892/ijmm.2011.852]
- 56 **Lv ZD**, Na D, Ma XY, Zhao C, Zhao WJ, Xu HM. Human peritoneal mesothelial cell transformation into myofibroblasts in response to TGF- β 1 in vitro. *Int J Mol Med* 2011; **27**: 187-193 [PMID: 21152863 DOI: 10.3892/ijmm.2010.574]
- 57 **Wu Y**, Li Q, Zhou X, Yu J, Mu Y, Munker S, Xu C, Shen Z, Müllenbach R, Liu Y, Li L, Gretz N, Zieker D, Li J, Matsuzaki K, Li Y, Dooley S, Weng H. Decreased levels of active SMAD2 correlate with poor prognosis in gastric cancer. *PLoS One* 2012; **7**: e35684 [PMID: 22539990 DOI: 10.1371/journal.pone.0035684]
- 58 **Shinto O**, Yashiro M, Toyokawa T, Nishii T, Kaizaki R, Matsuzaki T, Noda S, Kubo N, Tanaka H, Doi Y, Ohira M, Muguruma K, Sawada T, Hirakawa K. Phosphorylated smad2 in advanced stage gastric carcinoma. *BMC Cancer* 2010; **10**: 652 [PMID: 21110833 DOI: 10.1186/1471-2407-10-652]
- 59 **Song IS**, Jeong YJ, Jeong SH, Heo HJ, Kim HK, Bae KB, Park YH, Kim SU, Kim JM, Kim N, Ko KS, Rhee BD, Han J. FOXM1-Induced PRX3 Regulates Stemness and Survival of Colon Cancer Cells via Maintenance of Mitochondrial Function. *Gastroenterology* 2015; **149**: 1006-1016.e9 [PMID: 26091938 DOI: 10.1053/j.gastro.2015.06.007]
- 60 **Bu XN**, Qiu C, Wang C, Jiang Z. Inhibition of DACH1 activity by short hairpin RNA represses cell proliferation and tumor invasion in pancreatic cancer. *Oncol Rep* 2016; **36**: 745-754 [PMID: 27278537 DOI: 10.3892/or.2016.4843]
- 61 **Yan W**, Wu K, Herman JG, Brock MV, Zhou Y, Lu Y, Zhang Z, Yang Y, Guo M. Epigenetic silencing of DACH1 induces the invasion and metastasis of gastric cancer by activating TGF- β signalling. *J Cell Mol Med* 2014; **18**: 2499-2511 [PMID: 24912879 DOI: 10.1111/jcmm.12325]

P- Reviewer: Chen Z, Kimura A, Matowicka-Karna J, Park WS
S- Editor: Wang XJ **L- Editor:** Filipodia **E- Editor:** Huang Y



Basic Study

Relationship between *Fusobacterium nucleatum*, inflammatory mediators and microRNAs in colorectal carcinogenesis

Marcela Alcântara Proença, Joice Matos Biselli, Maysa Succi, Fábio Eduardo Severino, Gustavo Noriz Berardinelli, Alaor Caetano, Rui Manuel Reis, David J Hughes, Ana Elizabete Silva

Marcela Alcântara Proença, Joice Matos Biselli, Maysa Succi, Ana Elizabete Silva, Department of Biology, UNESP, Univ. Estadual Paulista, Campus of São José do Rio Preto, São José do Rio Preto, São Paulo 15054-000, Brazil

Fábio Eduardo Severino, Department of Surgery and Orthopedics, Faculty of Medicine, UNESP, Univ. Estadual Paulista, Campus of Botucatu, Botucatu, São Paulo 18618-687, Brazil

Alaor Caetano, Endoscopy Center of Rio Preto, São José do Rio Preto, São Paulo 15015-700, Brazil

Gustavo Noriz Berardinelli, Rui Manuel Reis, Molecular Oncology Research Center, Barretos Cancer Hospital, Barretos, São Paulo 14784-400, Brazil

Rui Manuel Reis, Life and Health Sciences Research Institute, University of Minho, Campus Gualtar, Braga 4710-057, Portugal

Rui Manuel Reis, ICVS/3B's-PT Government Associate Laboratory, Campus Gualtar, Braga 4710-057, Portugal

David J Hughes, Cancer Biology and Therapeutics Group, UCD Conway Institute, University College Dublin, Dublin D04 V1W8, Ireland

ORCID number: Marcela Alcântara Proença (0000-0002-9583-0917); Joice Matos Biselli (0000-0001-5105-9537); Maysa Succi (0000-0001-8911-9208); Fábio Eduardo Severino (0000-0002-2304-3404); Gustavo Noriz Berardinelli (0000-0001-5404-9748); Alaor Caetano (0000-0003-2412-9370); Rui Manuel Reis (0000-0002-9639-7940); David J Hughes (0000-0003-1668-8770); Ana Elizabete Silva (0000-0003-1491-8878).

Author contributions: Proença MA performed the research and experiments, collected the data, performed statistical analyses, and wrote the paper; Biselli JM performed statistical analyses and quantification of *Fusobacterium nucleatum*; Severino FE constructed the microRNA:mRNA interaction network; Caetano A and Succi M collected the samples; Berardinelli GN and Reis RM performed the KRAS mutation and MSI status experiments; Hughes DJ designed the research experiments and reviewed the paper; Silva AE designed the research experiments, wrote the

paper, and reviewed the paper; all authors read and approved the final manuscript.

Supported by São Paulo Research Foundation (FAPESP), No. 2012/15036-8; and National Council for Scientific and Technological Development (CNPq), No. 474.776/2013-1.

Institutional review board statement: This work was approved by the Ethics in Research Committee of CEP/IBILCE/UNESP, No. 1.452.373.

Conflict-of-interest statement: No conflict-of-interest.

Data sharing statement: Participants gave written informed consent for data sharing.

Open-Access: This article is an open-access article which was selected by an in-house editor and fully peer-reviewed by external reviewers. It is distributed in accordance with the Creative Commons Attribution Non Commercial (CC BY-NC 4.0) license, which permits others to distribute, remix, adapt, build upon this work non-commercially, and license their derivative works on different terms, provided the original work is properly cited and the use is non-commercial. See: <http://creativecommons.org/licenses/by-nc/4.0/>

Manuscript source: Invited manuscript

Corresponding author to: Ana Elizabete Silva, PhD, Adjunct Professor, Teacher, Department of Biology, UNESP São Paulo State University, Rua Cristóvão Colombo 2265, São José do Rio Preto, São Paulo 15054-000, Brazil. ae.silva@unesp.br
Telephone: +55-17-322122384
Fax: +55-17-322212390

Received: October 30, 2018
Peer-review started: October 30, 2018
First decision: November 6, 2018
Revised: November 29, 2018
Accepted: December 13, 2018
Article in press: December 13, 2018
Published online: December 21, 2018

Abstract

AIM

To examine the effect of *Fusobacterium nucleatum* (*F. nucleatum*) on the microenvironment of colonic neoplasms and the expression of inflammatory mediators and microRNAs (miRNAs).

METHODS

Levels of *F. nucleatum* DNA, cytokine gene mRNA (*TLR2*, *TLR4*, *NFKB1*, *TNF*, *IL1B*, *IL6* and *IL8*), and potentially interacting miRNAs (miR-21-3p, miR-22-3p, miR-28-5p, miR-34a-5p, miR-135b-5p) were measured by quantitative polymerase chain reaction (qPCR) TaqMan® assays in DNA and/or RNA extracted from the disease and adjacent normal fresh tissues of 27 colorectal adenoma (CRA) and 43 colorectal cancer (CRC) patients. *KRAS* mutations were detected by direct sequencing and microsatellite instability (MSI) status by multiplex PCR. Cytoscape v3.1.1 was used to construct the postulated miRNA:mRNA interaction network.

RESULTS

Overabundance of *F. nucleatum* in neoplastic tissue compared to matched normal tissue was detected in CRA (51.8%) and more markedly in CRC (72.1%). We observed significantly greater expression of *TLR4*, *IL1B*, *IL8*, and miR-135b in CRA lesions and *TLR2*, *IL1B*, *IL6*, *IL8*, miR-34a and miR-135b in CRC tumours compared to their respective normal tissues. Only two transcripts for miR-22 and miR-28 were exclusively downregulated in CRC tumour samples. The mRNA expression of *IL1B*, *IL6*, *IL8* and miR-22 was positively correlated with *F. nucleatum* quantification in CRC tumours. The mRNA expression of miR-135b and *TNF* was inversely correlated. The miRNA:mRNA interaction network suggested that the upregulation of miR-34a in CRC proceeds *via* a *TLR2/TLR4*-dependent response to *F. nucleatum*. Finally, *KRAS* mutations were more frequently observed in CRC samples infected with *F. nucleatum* and were associated with greater expression of miR-21 in CRA, while *IL8* was upregulated in MSI-high CRC.

CONCLUSION

Our findings indicate that *F. nucleatum* is a risk factor for CRC by increasing the expression of inflammatory mediators through a possible miRNA-mediated activation of *TLR2/TLR4*.

Key words: Colorectal cancer; Colorectal adenoma; *Fusobacterium nucleatum*; Inflammation; Cytokines; MicroRNAs

© The Author(s) 2018. Published by Baishideng Publishing Group Inc. All rights reserved.

Core tip: We examined the influence of *Fusobacterium nucleatum* (*F. nucleatum*) in colorectal adenoma (CRA) and colorectal cancer (CRC) on the mRNA expression of inflammatory mediators and the association with microRNA (miRNA) levels, *KRAS* mutation, and micro-

satellite instability (MSI). We suggest that *F. nucleatum* contributes to CRC development by increasing the expression of inflammatory mediators through a possible miRNA-mediated activation of *TLR2/TLR4*. The miRNA:mRNA interaction network suggests an upregulation of miR-34a in CRC *via* a *TLR2/TLR4*-dependent response to *F. nucleatum*. *KRAS* mutations were more frequent in *F. nucleatum*-infected CRC and were associated with a greater expression of miR-21 in CRA, while *IL8* was upregulated in MSI-high CRC.

Proença MA, Biselli JM, Succi M, Severino FE, Berardinelli GN, Caetano A, Reis RM, Hughes DJ, Silva AE. Relationship between *Fusobacterium nucleatum*, inflammatory mediators and microRNAs in colorectal carcinogenesis. *World J Gastroenterol* 2018; 24(47): 5351-5365

URL: <https://www.wjgnet.com/1007-9327/full/v24/i47/5351.htm>
DOI: <https://dx.doi.org/10.3748/wjg.v24.i47.5351>

INTRODUCTION

Colorectal cancer (CRC) is one of the three leading causes of cancer-related deaths and the third most frequently diagnosed cancer worldwide, with 1849518 new cases and 880792 deaths estimated in 2018^[1]. In Brazil, CRC is the third most frequent cancer in men and the second most frequent cancer in women^[2]. CRC is associated with chronic inflammation and oxidative processes that can induce malignant cell transformation and activate carcinogenic processes such as proliferation and angiogenesis^[3].

The human intestinal microbiota is composed of many species that may play an important role in inflammatory gastrointestinal diseases, such as inflammatory bowel disease and CRC. Among the microbiota, *Fusobacterium nucleatum* (*F. nucleatum*) has emerged as a potential factor in CRC aetiology^[4-7]. This bacterium is a gram-negative anaerobic commensal pathogen that is associated with several human diseases, especially those related to the oral and intestinal tracts^[5,8]. Some studies suggest that *F. nucleatum* can cause a pro-inflammatory microenvironment in the intestine through deregulating inflammatory and immune responses, thereby promoting a microenvironment propitious for tumour initiation and CRC progression^[5,6,9]. However, the mechanisms involved in this proposed tumourigenic process are still under discussion.

Studies have shown an abundance of *F. nucleatum* in tumour tissues and stool samples from CRC patients compared to adjacent normal tissues, colorectal adenomas (CRA) or even healthy subjects, and this observation was also correlated with shorter post-diagnosis overall survival^[6,10-12]. These results reinforce the importance of *F. nucleatum* detection to assist in the identification of risk groups and early detection of CRC with implications for disease prognosis as well.

The interaction of microorganisms with the intestinal epithelium initially involves recognition by Toll-like receptors (TLRs)^[13] and activation of the nuclear factor-kappa B (NF-κB) pathway, which is the main signalling pathway regulating inflammatory responses implicated in colorectal tumorigenesis^[14]. NF-κB may facilitate tumour progression through the expression of pro-inflammatory cytokines^[15], which have different roles in colorectal carcinogenesis. These pro-inflammatory cytokines include interleukin (IL) IL1B, which can induce tumour cell proliferation^[16]; IL6 and IL8, which are related to tumour growth, angiogenesis and metastasis^[17]; and tumour necrosis factor (TNF) A, which can decrease cell death^[16,18].

F. nucleatum infection has also been associated with common CRC tumour genetic and epigenetic alterations, such as microsatellite instability (MSI), CpG island methylator phenotype (CIMP), and mutations in the *BRAF* and *KRAS* genes^[19-21]. These alterations are thought to be due to *F. nucleatum*-mediated inflammatory responses influencing the molecular pathways of colorectal carcinogenesis *via* generation of reactive oxygen species (ROS) and greater pro-inflammatory gene expression, resulting in aberrant DNA methylation and DNA damage.

MicroRNAs (miRNAs) have a well-established role in inflammatory processes and can serve as molecular markers for diagnosis, prognosis, and treatment response^[22]. Several miRNAs have been associated with CRC development and progression^[23-25], including investigations of *F. nucleatum*-induced inflammation and CRC^[26-28].

However, the interaction and (dys)regulation between inflammatory genes and miRNAs in potential *F. nucleatum*-induced colorectal carcinogenesis has not previously been elucidated. Thus, we investigated the association of *F. nucleatum* abundance in CRA and CRC tissues with the expression of inflammatory genes (*TLR2*, *TLR4*, *NFKB1*, *TNF*, *IL1B*, *IL6* and *IL8*) and miRNAs (miR-21-3p, miR-22-3p, miR-28-5p, miR-34a-5p and miR-135b-5p). These genes and miRNAs were selected due to their proposed involvement in the inflammatory process or colorectal carcinogenesis from the literature and public databases (TarBase v7.0 and miRBase 2.1)^[29,30]. Our findings suggest that the host inflammatory response to *F. nucleatum* contributes to the neoplastic progression of CRA to CRC through *TLR2* and *TLR4* activation of the pro-inflammatory cytokines *IL1B*, *IL6* and *IL8* in a potentially miRNA-dependent process.

MATERIALS AND METHODS

Clinical samples

This study was approved by the Research Ethics Committee of IBILCE/UNESP, São José do Rio Preto (SP), Brazil (reference 1.452.373). Written informed consent was obtained from all individuals, and all samples were coded to protect patient anonymity.

A total of 43 fresh-frozen CRC tissue samples and the matched adjacent normal tissue (N-CRC) as well as 27 CRA tissue samples and the matched adjacent normal tissue (N-CRA) were collected from the Proctology Service of Hospital de Base and Endoscopy Center Rio Preto, both in SP (Brazil) during the period of 2010 to 2012.

All required information on demographic and clinical histopathological parameters was obtained from the patients' medical records. The inclusion criteria were patients with a confirmed diagnosis of pre-cancerous adenomas or sporadic CRC by standard clinical histopathological measures without previous chemotherapy and radiotherapy, and the exclusion criterion was patients with hereditary CRC.

Acid nucleic extraction and cDNA reverse transcription

Simultaneous extraction of total RNA and DNA from colorectal tissue samples was performed using the TRIzol reagent (Ambion, Carlsbad, CA, United States) and corresponding protocol from the manufacturer. A reverse transcriptase reaction was performed using a High Capacity cDNA Reverse Transcription Kit (Applied Biosystems, Foster City, CA, United States) as described previously^[31]. The synthesis of cDNA to the miRNAs was carried out with a TaqMan® MicroRNA Reverse Transcription Kit (Applied Biosystems, Foster City, CA, United States) according to the manufacturer's protocol.

Quantification of *F. nucleatum*

Quantification of *F. nucleatum* was performed in CRA, CRC and the respective adjacent normal DNA samples by quantitative real-time PCR (qPCR). TaqMan® Gene Expression Assays (Applied Biosystems, Foster City, CA, United States) with specific probes for the bacterial gene target *NusG* (5'-TCAGCAACTTGCTCTTCTTGATCTTTAAATGAACC-3' TAMRA probe FAM) and the human gene *PGT* (5'-CCATCCATGTCCTCATCTC-3' TAMRA probe FAM) as a reference were assayed by StepOnePlus Real-Time PCR (Applied Biosystems, Foster City, CA, United States). The reactions were performed separately for each gene at a 12 µL final volume using 20 ng of genomic DNA, 400 nmol/L primer (*NusG* sequences: 5'-CAACCATTACTTTAACTCTACCATGTTCA-3' and 3'-GTTGACTTTACAGAAGGAGATTATGTAAAAATC-5', *PGT*: 5'-ATCCCCAAAGCACCTGGTTT-3' and 3'-AGAGGCCAAGATAGTCCTGGTAA-5') (Invitrogen, Carlsbad, California, United States), 400 nmol/L probe and GoTaq probe 1 × qPCR Master Mix (Promega, Madison, Wisconsin, United States). The reaction was subjected to temperatures of 50 °C for 2 min, 95 °C for 10 min, then 60 cycles of 95 °C for 15 s and 57 °C for 1 min^[10]. All reactions were performed in duplicate, and all experiments had a no-template control that was used to confirm no contamination in samples. Cq (cycle quantification) values were calculated after adjusting the threshold by StepOne software (v. 2.2.2) (Applied

Biosystems, Foster City, CA, United States), and all samples with a resulting Cq value were considered positive. Relative quantification (RQ) for the *F. nucleatum* gene (*NusG*) was calculated based on the $2^{-\Delta\Delta C_t}$ method^[32] and was expressed for each group relative to the respective normal tissue samples both in an unpaired way, using the mean of adjacent normal samples as a calibrator for each group, and in a paired way, using the respective adjacent normal of each sample as its specific calibrator.

Relative quantification of inflammatory mediator genes and miRNAs

Relative quantifications for the expression of 7 inflammatory genes [*TLR2* (Hs00610101_m1), *TLR4* (Hs01060206_m1), *NFKB1* (Hs00765730_m1), *IL1B* (Hs01555410_m1), *IL6* (Hs00985639_m1), *IL8* (Hs00174103_m1) and *TNF* (Hs00174128_m1)] and 5 miRNAs [*hsa-miR-21-3p* (TM002438), *hsa-miR-22-3p* (TM000398), *hsa-miR-28-5p* (TM000411), *hsa-miR-34a-5p* (TM000426), and *hsa-miR-135b-5p* (TM002261)] were performed in 27 CRA and 43 CRC cDNA samples. Adjacent normal tissue samples of each lesion (CRA and CRC) were studied as a sample pool with the same amount of cDNA. The qPCRs were performed using the TaqMan® Gene Expression Assays (Applied Biosystems, Foster City, CA, United States) with specific probes for each gene according to the instructions from the manufacturer, in a final volume of 10 µL using 25 ng of cDNA for the cytokine genes and 0.66 ng for the miRNAs. All reactions were performed in duplicate, and all experiments had a no-template control. The reactions were subjected to the StepOne Plus Real-Time PCR System (Applied Biosystems, Foster City, CA, United States). Cq values were calculated after adjusting the threshold by the StepOne software (v.2.2.2) (Applied Biosystems, Foster City, CA, United States). For the mRNA analyses, the *ACTB* and *GAPDH* genes were used as reference genes, as validated in a previous study^[31]. For the miRNA analysis, the method of global normalization was employed^[33]. RQ values were calculated using the $2^{-\Delta\Delta C_t}$ method^[32], considering the pool of the respective adjacent normal samples as the calibrator and considering the Cq mean of CRA expression for the CRC samples.

miRNA-mRNA interaction networks

Prediction of targets regulated by miRNAs was performed using the miRNA Data Integration Portal bioinformatics tool (<http://ophid.utoronto.ca/mirDIP/>)^[34]. A protein-protein interaction network was generated via the String database (version 9.1) using the target genes as an input^[35]. The identified miRNAs and target genes were integrated into interaction networks by Cytoscape software (version 3.1.1)^[36]. The biological function of the identified genes in the network was defined using the BiNGO tool in Cytoscape (version 3.0.2)^[37]. Cytoscape software also provides a graphical visualization of the

network with the nodes representing the genes, miRNAs, and/or proteins and the edges representing their interactions.

KRAS mutation

KRAS (codons 12 and 13) hotspot mutation regions were analysed by PCR, followed by direct sequencing, as previously described^[38]. PCR was performed at a final volume of 15 µL under the following conditions: 1.5 µL of buffer (Qiagen, Venlo, The Netherlands), 2 mmol/L MgCl₂ (Qiagen, Venlo, The Netherlands), 100 mmol/L dNTPs (Invitrogen, Carlsbad, California, United States), forward and reverse primers at 0.2 mmol/L (Sigma Aldrich), 1 unit of HotStarTaq DNA polymerase (Qiagen, Venlo, The Netherlands) and 1 µL of DNA at 50 ng/µL. The *KRAS* primers used were 5'-GTGTGACATGTTCTAATATAGTCA-3' (forward) and 3'-GAATGGTCTGCACCAAGTAA-5' (reverse)^[39].

PCR products were purified with ExoSAP (GE Technology, IL, United States) and then added to a sequencing reaction mix containing 1 µL of BigDye (Applied Biosystems, Foster City, CA, United States), 1.5 µL of sequencing buffer (Applied Biosystems, Foster City, CA, United States) and 1 µL of primer, followed by post-sequencing purification with a BigDye XTerminator Purification Kit (Applied Biosystems, Foster City, CA, United States) according to the instructions from the manufacturer. Direct sequencing was performed on a 3500 xL Genetic Analyzer (Applied Biosystems, Foster City, CA, United States). All mutations were confirmed in a second, independent PCR experiment.

MSI status

MSI evaluation was performed using a multiplex PCR comprising six quasimonomorphic mononucleotide repeat markers (NR-27, NR-21, NR-24, BAT-25, BAT-26 and HSP110), as previously described^[40,41]. Primer sequences, as described^[41,42], were each reverse primer end-labelled with a fluorescent dye as follows: 6-carboxyfluorescein (6-FAM) for BAT-26 and NR-21; 20-chloro-70-phenyl-1,4-dichloro-6-carboxyfluorescein (VIC) for BAT-25, NR-27 and HSP110; and 2,7,8-benzo-5-fluoro-2,4,7-trichloro-5-carboxyfluorescein (NED) for NR-24. PCR was performed using a Qiagen Multiplex PCR Kit (Qiagen, Venlo, The Netherlands) with 0.5 µL of DNA at 50 ng/µL and the following thermocycling conditions: 15 min at 95 °C; 40 cycles of 95 °C for 30 s, 55 °C for 90 s and 72 °C for 30 s; and a final extension at 72 °C for 60 min. Fragment analyses were performed on a 3500 xL Genetic Analyser (Applied Biosystems, Foster City, CA, United States) according to the instructions from the manufacturer, and the results were analysed using GeneMapper v4.1 (Applied Biosystems, Foster City, CA, United States). Cases exhibiting instability at two or more markers were considered to have high MSI (MSI-H), cases with instability at one marker were defined as having low MSI (MSI-L) and cases that showed no instability were defined as microsatellite

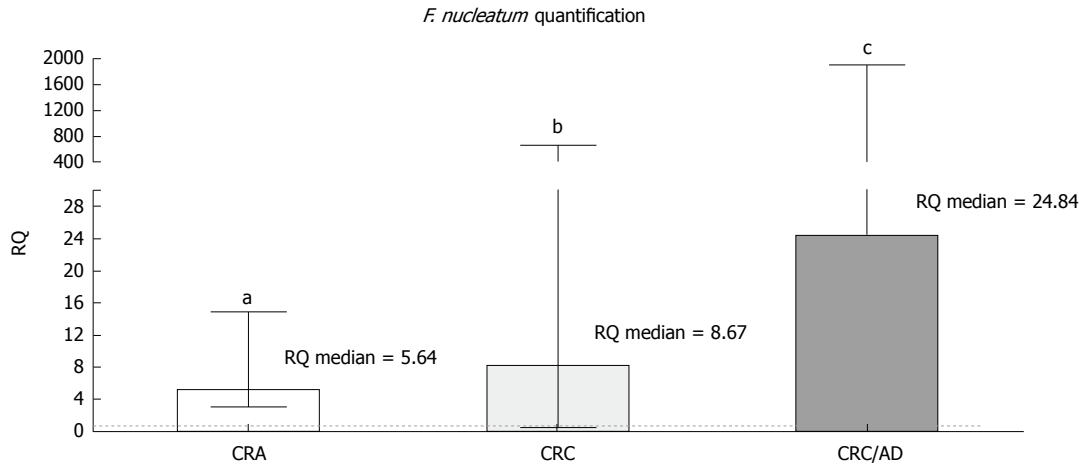


Figure 1 Relative quantification of the *Fusobacterium nucleatum* NusG gene in adenoma and colorectal cancer samples compared to adjacent normal tissues and colorectal cancer compared to adenoma tissue. Statistically significant differences, according to the Wilcoxon signed-rank test, were as follows: colorectal adenoma: ^a $P = 0.0002$, colorectal cancer: ^b $P = 0.0002$, colorectal cancer/adenoma: ^c $P < 0.0001$. Median with interquartile range graph. CRA: Colorectal adenoma; CRC: Colorectal cancer; CRC/AD: Colorectal cancer/adenoma; RQ: Relative quantification; *F. nucleatum*: *Fusobacterium nucleatum*.

stable (MSS)^[40].

Statistical analysis

KRAS mutation and MSI status were compared between groups using Fisher's exact test. The distribution of continuous data was evaluated using the D'Agostino-Pearson normality test. The Wilcoxon signed-rank test was used to test the significance of the RQ of the measured genes from the qPCR experiments. Spearman's rank correlation coefficient test was performed to compare the *F. nucleatum* quantification with the expression of the inflammatory genes and miRNAs. For all analyses, $P < 0.05$ was considered statistically significant. The analysis was performed by GraphPad Prism software (version 6.01).

RESULTS

Quantification of *F. nucleatum* in CRA and CRC tissues

Among 43 CRC and 27 CRA samples and their respective normal adjacent mucosa (N-CRC and N-CRA, respectively) quantified for *F. nucleatum*, 33 (76.7%) CRC samples, 31 (72.1%) N-CRC samples, 14 (51.8%) CRA samples, and 13 (48.1%) N-CRA samples were positive for bacterial DNA. Of these samples, the presence of the bacterium was observed in both the lesion and its matched normal mucosa for 6 CRA samples and 27 CRC samples. A significant increase in bacterial DNA was found for both CRA (RQ = 5.64) and CRC (RQ = 8.67) tissues compared to the respective normal adjacent tissues (Figure 1).

In addition, the analysis of *F. nucleatum* quantification for the CRC group was also performed in a paired way, using the respective adjacent normal tissue of each sample as its specific calibrator. This result was consistent with the unpaired analysis showing more *F. nucleatum* in tumour tissues (RQ = 17.71, $P = 0.0002$). For the CRA samples, this paired analysis was not performed due to the low potential of analysing the available 6 paired

samples.

A comparison of CRC samples with CRA samples, using the Cq mean of CRA rather than the normal mucosa as a calibrator for the analysis, estimated the quantification of *F. nucleatum* as 24.84 times greater in CRC samples than in CRA samples ($P < 0.0001$) (Figure 1).

Gene expression of inflammatory mediators

Gene expression of inflammatory mediators in CRA samples and CRC samples relative to adjacent normal tissue samples showed significantly increased mRNA levels for *TLR4* (RQ = 2.27, $P = 0.0003$), *IL1B* (RQ = 2.27, $P = 0.0047$) and *IL8* (RQ = 3.33, $P = 0.0006$) in CRA tissues (Table 1, Figure 2A) and for *TLR2* (RQ = 2.36, $P < 0.0001$), *IL1B* (RQ = 4.13, $P < 0.0001$), *IL6* (RQ = 6.67, $P < 0.0001$) and *IL8* (RQ = 6.36, $P < 0.0001$) in CRC tumours (Table 1, Figure 2B).

Additionally, elevated expression of *TLR2* (RQ = 1.68, $P < 0.0001$), *IL1B* (RQ = 4.79, $P < 0.0001$), *IL6* (RQ = 9.40, $P < 0.0001$) and *IL8* (RQ = 12.12, $P < 0.0001$) was observed in CRC tumours compared to CRA tissues (Table 1, Figure 2C).

miRNA gene expression

A similar estimation of miRNA relative gene expression was performed for CRA and CRC samples, in which miRNAs (miR-21, miR-22, miR-28, miR-34a, miR-135b) were quantified in each neoplastic tissue sample relative to a pool of the adjacent normal tissue. For the CRA group, only miR-135b was upregulated (RQ = 2.19, $P = 0.0074$) (Table 2, Figure 3A). However, for CRC samples, while miR-34a (RQ = 1.38, $P = 0.0029$) and miR-135b (RQ = 9.31, $P < 0.0001$) were upregulated, miR-22 (RQ = 0.27, $P < 0.0001$) and miR-28 (RQ = 0.65, $P = 0.0045$) were downregulated (Table 2, Figure 3B). Relative to the CRA group, CRC samples also presented a significant increase in the gene expression of miR-34a (RQ = 1.26, $P = 0.01$) and miR-135b (RQ =

Table 1 Relative quantification of mRNA expression of the inflammatory genes in adenoma and colorectal cancer samples compared with adjacent normal tissue samples and colorectal cancer samples relative to the adenoma group

	<i>TLR2</i>	<i>TLR4</i>	<i>NFKB1</i>	<i>IL1B</i>	<i>IL6</i>	<i>IL8</i>	<i>TNF</i>
CRA							
RQ median	0.87	2.27	1.02	2.27	1.12	3.33	0.75
RQ Range	0.36-10.80	0.32-11.25	0.45-3.38	0.14-76.76	0.09-80.41	0.10-874.50	0.14-2.60
P value	0.2940	0.0003 ^a	0.5360	0.0047 ^a	0.2473	0.0006 ^a	0.0527
CRC							
RQ median	2.36	0.74	0.90	4.13	6.67	6.36	0.72
RQ Range	0.31-35.80	0.20-23.42	0.31-8.49	0.13-245.70	0.09-192.80	0.16-194.20	0.06-31.76
P value	< 0.0001 ^a	0.4476	0.9855	< 0.0001 ^a	< 0.0001 ^a	< 0.0001 ^a	0.2391
CRC/CRA							
RQ median	1.68	0.54	0.78	4.79	9.40	12.14	0.70
RQ Range	0.22-25.49	0.15-17.22	0.27-7.35	0.15-284.80	0.13-271.80	0.31-370.60	0.06-30.77
P value	< 0.0001 ^a	0.0608	0.1237	< 0.0001 ^a	< 0.0001 ^a	< 0.0001 ^a	0.1560

Wilcoxon signed rank test. ^aP value < 0.05 were considered statistically significant. CRA: Colorectal adenoma; CRC: Colorectal cancer; RQ: Relative quantification; TNF: Tumour necrosis factor; IL: Interleukin; NFKB: Nuclear factor kappa B; TLR: Toll-like receptor.

Table 2 Relative quantification of microRNAs in adenoma and colorectal cancer samples compared with adjacent normal tissue samples and colorectal cancer samples relative to the adenoma group

	miR-21	miR-22	miR-28	miR-34a	miR-135b
CRA					
RQ median	0.75	0.85	0.73	0.97	2.19
RQ Range	0.15-13.91	0.10-3.05	0.08-2.17	0.12-4.74	0.10-25.13
P value	0.6349	0.1747	0.1904	0.3306	0.0074 ^a
CRC					
RQ median	0.53	0.27	0.65	1.38	9.31
RQ Range	0.08-12.53	0.026-2.78	0.11-7.27	0.20-30.0	0.45-74.00
P value	0.1725	< 0.0001 ^a	0.0045 ^a	0.0029 ^a	< 0.0001 ^a
CRC/CRA					
RQ median	1.01	0.59	0.77	1.26	2.64
RQ Range	0.15-23.91	0.06-6.07	0.14-8.79	0.18-27.51	0.13-20.96
P value	0.0969	0.5770	0.1271	0.0101 ^a	< 0.0001 ^a

Wilcoxon signed rank test. ^aP value < 0.05 were considered statistically significant. CRA: Colorectal adenoma; CRC: Colorectal cancer; RQ: Relative quantification.

2.64, $P < 0.0001$) (Table 2, Figure 3C).

Interactions between *F. nucleatum* abundance with the expression of inflammatory mediator genes and miRNAs

A correlation analysis was performed between the RQ values of inflammatory genes (*TLR2*, *TLR4*, *NFKB1*, *TNF*, *IL1B*, *IL6* and *IL8*) and *F. nucleatum* DNA levels in all neoplasms. For the CRA group, the only significant finding was a negative correlation between *TLR4* and *F. nucleatum* quantification ($r = -0.62$, $P = 0.0235$). However, for CRC, significant positive correlations were observed for bacterial DNA levels with cytokines *IL1B* ($r = 0.46$, $P = 0.0066$), *IL6* ($r = 0.47$, $P = 0.0059$), and *IL8* ($r = 0.54$, $P = 0.0013$) (Table 3).

In the miRNA analysis, while no significant correlations were observed for the CRA group, there was a significant positive correlation between miR-22 expression and *F. nucleatum* ($r = 0.38$, $P = 0.0331$) in the CRC group (Table 3).

miRNA-mRNA correlation and interaction networks

Finally, independent of considerations of *F. nucleatum*

levels, we also performed a correlation analysis between the RQ values of miRNAs and inflammatory genes in both CRA and CRC samples. For CRA samples, there was a positive correlation of *IL8* with miR-21 ($r = 0.40$, $P = 0.0466$), miR-34a ($r = 0.44$, $P = 0.0296$) and miR-135b ($r = 0.46$, $P = 0.0200$) (Table 4). Regarding CRC, several positive correlations were observed between miR-21, miR-22, and miR-28 and most of the inflammatory genes evaluated, and there was also a significant inverse correlation between miR-135b and *TNF* ($r = -0.32$, $P = 0.0411$) (Table 4).

Additionally, we identified *in silico* a miRNA:mRNA interaction network that may be deregulated in CRC (Figure 4). This analysis demonstrated the interrelations of the inflammatory mediator genes alone and with their miRNA moderators (e.g., miR-28 and miR-34a targeting *TLR4*, miR-22 targeting *TLR2* and miR-135b targeting *IL6*). The negative correlation of the expression of miR-135b and *TNF* found in this study (Table 4) was also demonstrated in this *in silico* a miRNA:mRNA interaction network, although not functionally validated in our study and not yet predicted by public databases^[34] (Figure 4).

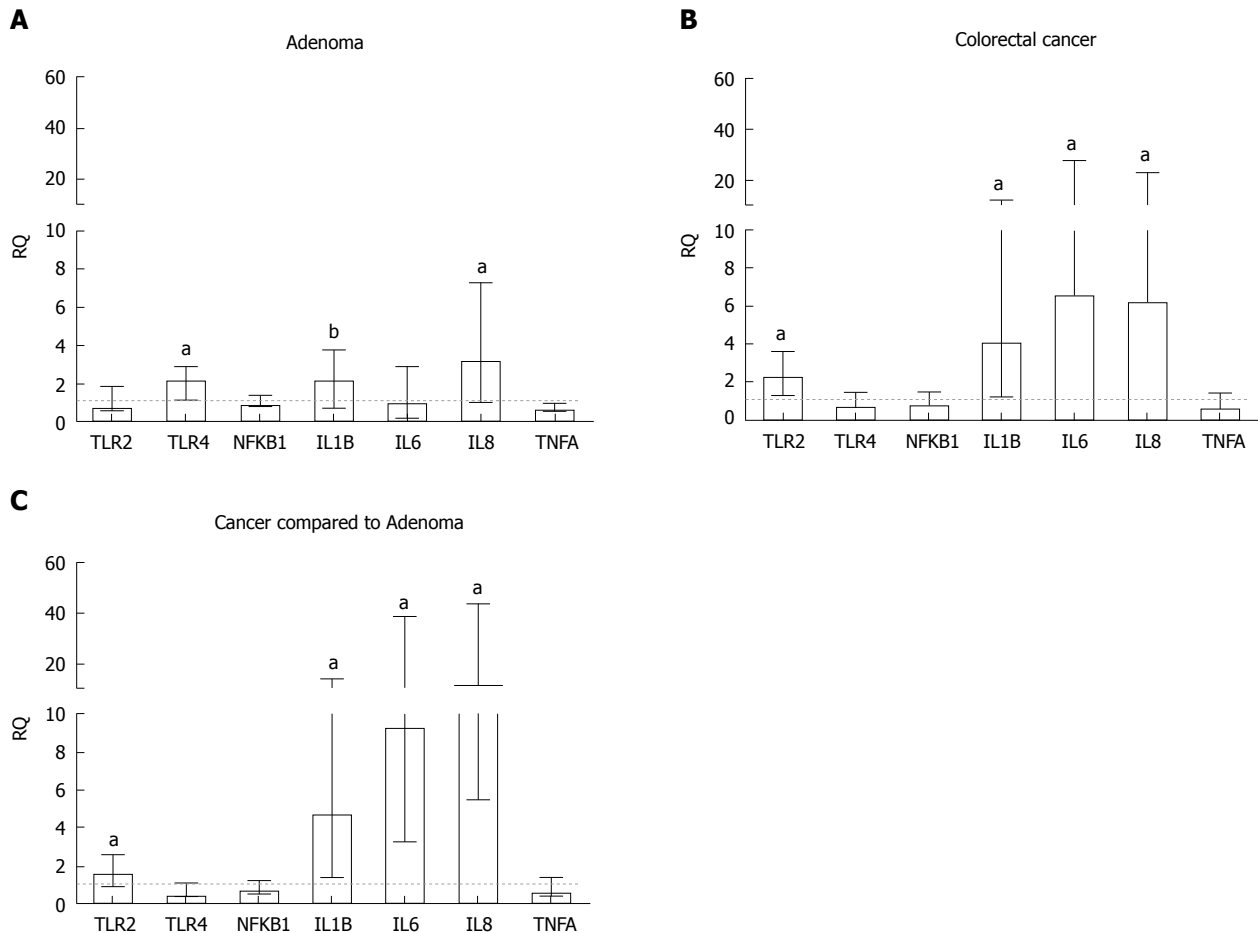


Figure 2 Relative quantification of inflammatory genes in (A) adenoma and (B) colorectal tumour tissue samples compared to a pool of respective adjacent normal tissue samples and (C) colorectal tumour tissue samples compared to adenoma samples. All samples were normalized to the reference genes *ACTB* and *GAPDH*. Statistically significant differences, according to the Wilcoxon signed-rank test, were ^a $P \leq 0.001$ and ^b $P \leq 0.01$. Median with interquartile range graph. RQ: Relative quantification.

KRAS mutation and MSI status in CRA and CRC tissues

Mutations in codons 12 and 13 of the *KRAS* gene were detected in 8/27 (30%) of CRA tissues and 11/43 (26%) of CRC tissues ($P = 0.7854$), of which p.Gly12Asp (G12D) and p.Gly13Asp (G13D) were the most frequent changes in both CRA and CRC tissues (Table 5). Regarding the MSI status, all the CRAs were microsatellite stable or MSI-low, while 7/43 (16%) of CRC samples were MSI-high ($P = 0.0382$; Table 5). The *KRAS* mutation was associated with *F. nucleatum* presence in CRC tumours ($P = 0.0432$) and had greater expression of miR-21 in CRA samples ($P = 0.0409$). The MSI-high tumour status was associated with increased expression of *IL8* ($P = 0.0171$). Other comparisons of the association between *KRAS* mutations and MSI status with *F. nucleatum* levels or cytokine gene and miRNA expressions showed no significant differences.

DISCUSSION

To better understand the possible mechanistic relationship between *F. nucleatum* presence and the immune response in CRC development, we evaluated

the association between *F. nucleatum* quantification and the expression of cytokines and miRNAs involved in the inflammatory stress response in CRA and CRC tissues from a South American patient study. Our results corroborated previous studies showing that *F. nucleatum* is present in greater amounts in tumours compared to both CRA and matched normal tissues. Importantly, our work further suggests that the abundance of *F. nucleatum* can affect cytokine expression possibly via recognition by *TLR4* and *TLR2* with regulation by miRNAs such as miR-34a, miR-135b and miR-22.

Several studies in North American, European and Asian populations showed the overabundance of *F. nucleatum* when comparing CRC tissues with normal adjacent tissues, healthy subjects^[5,10,11,37,40,43-45] or CRA tissues^[10,43]. A recent meta-analysis concluded that intestinal *F. nucleatum* is a valuable diagnostic marker for CRC^[46]. A different Brazilian study with a small sample size, also in the southeast region, previously showed greater levels of *F. nucleatum* in CRC (DNA levels in faecal samples of CRC patients were compared to those of healthy subjects)^[47]. Our study of fresh tissue samples from Brazilian CRA and CRC patients

Table 3 Correlation analysis between the relative quantification of the inflammatory genes and microRNAs with the quantification of *Fusobacterium nucleatum* in adenoma and colorectal cancer samples

Spearman correlation coefficient (r)	CRA	CRC
<i>TLR2</i>	0.42	0.09
<i>P</i> value	0.1557	0.6335
<i>TLR4</i>	-0.62	-0.01
<i>P</i> value	0.0235 ^a	0.9587
<i>NFKB1</i>	-0.40	-0.04
<i>P</i> value	0.1809	0.8045
<i>IL1B</i>	0.31	0.46
<i>P</i> value	0.3064	0.0066 ^a
<i>IL6</i>	0.01	0.47
<i>P</i> value	0.9716	0.0059 ^a
<i>IL8</i>	-0.07	0.54
<i>P</i> value	0.8166	0.0013 ^a
<i>TNF</i>	0.30	0.23
<i>P</i> value	0.3156	0.2027
miR-21	-0.21	0.26
<i>P</i> value	0.4643	0.1467
miR-22	0.17	0.38
<i>P</i> value	0.5528	0.0331 ^a
miR-28	0.04	0.01
<i>P</i> value	0.8872	0.9413
miR-34a	0.17	0.00
<i>P</i> value	0.5630	0.9905
miR-135b	-0.05	0.22
<i>P</i> value	0.8637	0.2163

Spearman correlation test. ^a*P* value < 0.05 were considered statistically significant. CRA: Colorectal adenoma; CRC: Colorectal cancer; TNF: Tumour necrosis factor; IL: Interleukin; NFKB: Nuclear factor kappa B; TLR: Toll-like receptor.

provided more evidence of the increasing abundance of *F. nucleatum* in the progression from adenoma to cancer.

The mechanism by which *F. nucleatum* functionally contributes to colorectal tumorigenesis has been investigated in several studies. It has been shown that this bacterium causes an inflammatory microenvironment more favourable to CRC development among other bacteria that colonize at the tumour site^[6]. A carcinogenic mechanism proposed is that *F. nucleatum* promotes an oncogenic and inflammatory response via FadA, the main virulence factor of *F. nucleatum*, binding to E-cadherin and activating the B-catenin pathway^[48]. In addition, the *F. nucleatum* lectin Fap2 binds to the Gal-GalNAc polysaccharide expressed by CRC cells, likely increasing immune-mediated inflammation^[9]. Moreover, the presence of *F. nucleatum* in the gut affects tumour-related cytokines and activates the JAK/STAT and MAPK/ERK pathways involved in CRC tumour progression^[49] (Figure 5).

In our study, in CRA disease tissues, we found that the mRNA expression of *TLR4*, *IL1B*, and *IL8* was increased, as was the expression of miR-135b. In CRC tumour tissues, the *TLR2* receptor and the IL genes *IL1B*, *IL6* and *IL8* were significantly upregulated when compared to adjacent normal tissues and to CRA tissues. miRNA levels of miR-34a and miR-135b were

more highly expressed in CRC tumours, while miR-22 and miR-28 were downregulated (Figure 5). These findings indicate that several of these genes are already dysregulated in early CRA stages of colorectal neoplasia as well as in CRC; thus, these genes may contribute to inflammatory stresses that drive the progression from CRA to CRC. Greater *TLR2* expression appears to be a later event in colorectal carcinogenesis, as also indicated by our recent study showing increased mRNA and protein expression of *TLR2* in CRC tissues^[31].

Recent studies have demonstrated that the *TLR4*/MYD88/NF-κB pathway is activated by *F. nucleatum* infection, which stimulates the overexpression of miR-21^[28]. Moreover, the *TLR4*/MYD88 innate immune signalling and the miR-18a and miR-4802 expression in CRC patients with a high amount of *F. nucleatum* activate the autophagy pathway to control CRC chemoresistance^[50]. In summary, these findings suggest the involvement of both *TLR2* and *TLR4* in *F. nucleatum* immune recognition.

Correlations of both inflammatory genes and miRNA expression with *F. nucleatum* levels showed positive associations with *IL1B*, *IL6*, and *IL8* as well as with miR-22 in CRC tissues. Increased expression of *IL1B*, *IL6* and *TNF* has also been reported by *in vitro* and animal model studies after *F. nucleatum* infection^[51,52].

Together with existing data, our results are consistent with a scenario in which *F. nucleatum* triggers an increased expression of *IL1B*, *IL6* and *IL8*, which further adds to inflammatory pressures fuelling the progression of colorectal neoplasia. Our work suggests that this phenomenon may proceed by an alternative pathway involving the recognition by the *TLR2* receptor (Figure 5) to that pathway previously shown for the invasion of epithelial cells via FadA^[48].

To date, several studies evaluated the abundance of *F. nucleatum* with miRNA expression in CRC^[26-28]. In our study, we found a positive correlation between miR-22 and the abundance of *F. nucleatum* in CRC. miR-22 suppresses the expression of the *p38* gene, which can impair the production of dendritic cells in tumours^[53]. As dendritic cells are important in the TLR-mediated recognition of microorganisms^[54], patients with upregulated miR-22 may have a compromised immune system due to fewer dendritic cells, favouring the proliferation of microorganisms such as *F. nucleatum*. Therefore, this positive correlation observed between miR-22 and *F. nucleatum* levels may be related to its role in the immune response and should be further investigated.

In addition, we also observed associations between both the *KRAS* mutation and MSI status and the expression of inflammatory genes or miRNAs in CRA and CRC tissues. Interestingly, we observed a greater expression of miR-21 associated with the *KRAS* mutation in the CRA tissues, but not in CRC tissues. In non-small cell lung cancer (NSCLC), the overexpression of wild type *KRAS* or mutated *KRAS* (G12D) was

Table 4 Correlation analysis between the relative quantification of microRNAs with the inflammatory genes in adenoma and colorectal cancer samples

Spearman correlation coefficient (<i>r</i>)	miR-21	miR-22	miR-28	miR-34a	miR-135b
CRA					
<i>TLR2</i>	0.09	0.29	0.31	0.23	0.09
<i>P</i> value	0.6608	0.1655	0.1266	0.2606	0.6714
<i>TLR4</i>	0.18	0.06	0.18	0.41	0.38
<i>P</i> value	0.3892	0.7926	0.3955	0.0431	0.0598
<i>NFKB1</i>	-0.01	-0.17	-0.21	-0.19	-0.20
<i>P</i> value	0.9796	0.4252	0.3191	0.3650	0.3454
<i>IL1B</i>	0.29	0.15	0.09	0.45	0.38
<i>P</i> value	0.1667	0.4834	0.6555	0.0232	0.0610
<i>IL6</i>	0.30	0.08	0.05	0.26	0.24
<i>P</i> value	0.1430	0.7148	0.8237	0.2136	0.2417
<i>IL8</i>	0.40	0.18	0.17	0.44	0.46
<i>P</i> value	0.0466 ^a	0.4017	0.4273	0.0296 ^a	0.0200 ^a
<i>TNF</i>	-0.21	-0.04	-0.03	-0.05	-0.11
<i>P</i> value	0.3083	0.8638	0.9012	0.8152	0.6084
CRC					
<i>TLR2</i>	0.29	0.53	0.18	0.19	-0.14
<i>P</i> value	0.0777	0.0005 ^a	0.2790	0.2408	0.3923
<i>TLR4</i>	0.07	0.34	0.33	0.26	0.05
<i>P</i> value	0.668	0.0377 ^a	0.0401 ^a	0.1216	0.7586
<i>NFKB1</i>	0.18	0.31	0.02	-0.10	-0.30
<i>P</i> value	0.2779	0.0499 ^a	0.8958	0.5462	0.0574
<i>IL1B</i>	0.53	0.43	0.13	0.22	-0.10
<i>P</i> value	0.0004 ^a	0.0055 ^a	0.4139	0.1668	0.5248
<i>IL6</i>	0.54	0.57	0.18	0.21	0.05
<i>P</i> value	0.0004 ^a	0.0002 ^a	0.2813	0.2095	0.7680
<i>IL8</i>	0.53	0.37	0.09	0.23	0.13
<i>P</i> value	0.0005 ^a	0.0180 ^a	0.5734	0.1506	0.4314
<i>TNF</i>	0.26	0.42	0.03	0.08	-0.32
<i>P</i> value	0.1094	0.0071 ^a	0.8406	0.6264	0.0411 ^a

Spearman correlation test. ^a*P* value < 0.05 were considered statistically significant. CRA: Colorectal adenoma; CRC: Colorectal cancer; TNF: Tumour necrosis factor; IL: Interleukin; NFKB: Nuclear factor kappa B; TLR: Toll-like receptor.

reported to modulate the expression of miRNAs, including miR-21 and miR-30c^[55]. The authors showed that miR-30c and miR-21 were specifically activated by *KRAS* and played an important role in lung cancer development and chemoresistance by targeting crucial tumour suppressor genes. Moreover, we also observed a positive association between the expression of *IL8* mRNA and MSI-H colorectal carcinoma, independent of the presence and abundance of *F. nucleatum*. Recently, Hamada *et al.*^[20] reported an association of *F. nucleatum* levels with the immune response to colorectal carcinoma according to the tumour MSI status, suggesting an interplay between *F. nucleatum*, MSI status, and immune cells in the CRC tumour microenvironment. MSI-H colorectal carcinomas generate immunogenic peptides due to a mismatch repair deficiency, resulting in a strong anti-tumour immune response thought to underlie the reported favourable prognosis and better response to immunotherapies of this molecular subtype of CRC^[20].

We also evaluated the correlation between the expression of miRNAs and inflammatory mediator genes, and we formulated a miRNA:mRNA interaction network based on predicted database targets^[34]. The correlations were mainly positive, including miR-21,

miR-34a and miR-135b with *IL8* in CRA tissues and between miR-21, miR-22 and miR-28 with most of the inflammatory mediator genes studied in CRC tissues. However, a negative correlation was observed between miR-135b and *TNF*.

miR-135b has been previously associated with an increased expression in CRC and CRA tissues^[56-58] and has been proposed to be an oncomiR targeting several tumour suppressor genes^[56,58]. Studies have proposed that the detection of miR-135b in stool samples can be used as a non-invasive biomarker for CRC and CRA^[59], and silencing miR-135b may be considered a possible therapy for CRC^[56,58]. Data showing that miR-135b indirectly inhibits the production of LPS (lipopolysaccharide)-induced *TNF* by suppressing the production of ROS and the activation of *NF-κB* in human macrophages^[60] support the negative correlation found between miR-135b and *TNF* in this study. Although this proposed miRNA-mRNA relationship is not yet predicted by the major miRNA public databases^[34], *TNF* may have an indirect immune regulation by miR-135b.

Regarding the role of miR-34a in CRC, studies demonstrated that it acts as both an oncomiR that is upregulated^[61,62] and as a tumour suppressor that displays reduced expression^[63-66]. According to our

Table 5 *KRAS* mutation and microsatellite instability status in adenoma and colorectal cancer groups

<i>KRAS</i> status/mutation type	CRA, <i>n</i> = 27 (%)	CRC, <i>n</i> = 43 (%)	<i>P</i> value
WT	19 (70.4)	32 (74.5)	0.7854
Mutation	8	11	
p.Gly12Ala (G12A)	1 (3.7)	0	
p.Gly12Ser (G12S)	1 (3.7)	1 (2.3)	
p.Gly12Val (G12V)	1 (3.7)	2 (4.6)	
p.Gly12Asp (G12D)	3 (11.1)	4 (9.3)	
p.Gly13Asp (G13D)	2 (7.4)	4 (9.3)	
MSI status			0.0382 ^a
MSS + MSI-L	25 + 2 (100)	34 + 2 (83.7)	
MSI-H	0	7 (16.3)	

Fisher's exact test. ^a*P* value < 0.05 were considered statistically significant. WT: Wild; MSI: Microsatellite instability; MSS: Microsatellite stable; MSI-L: Microsatellite instability low; MSI-H: Microsatellite instability high; CRA: Colorectal adenoma; CRC: Colorectal cancer.

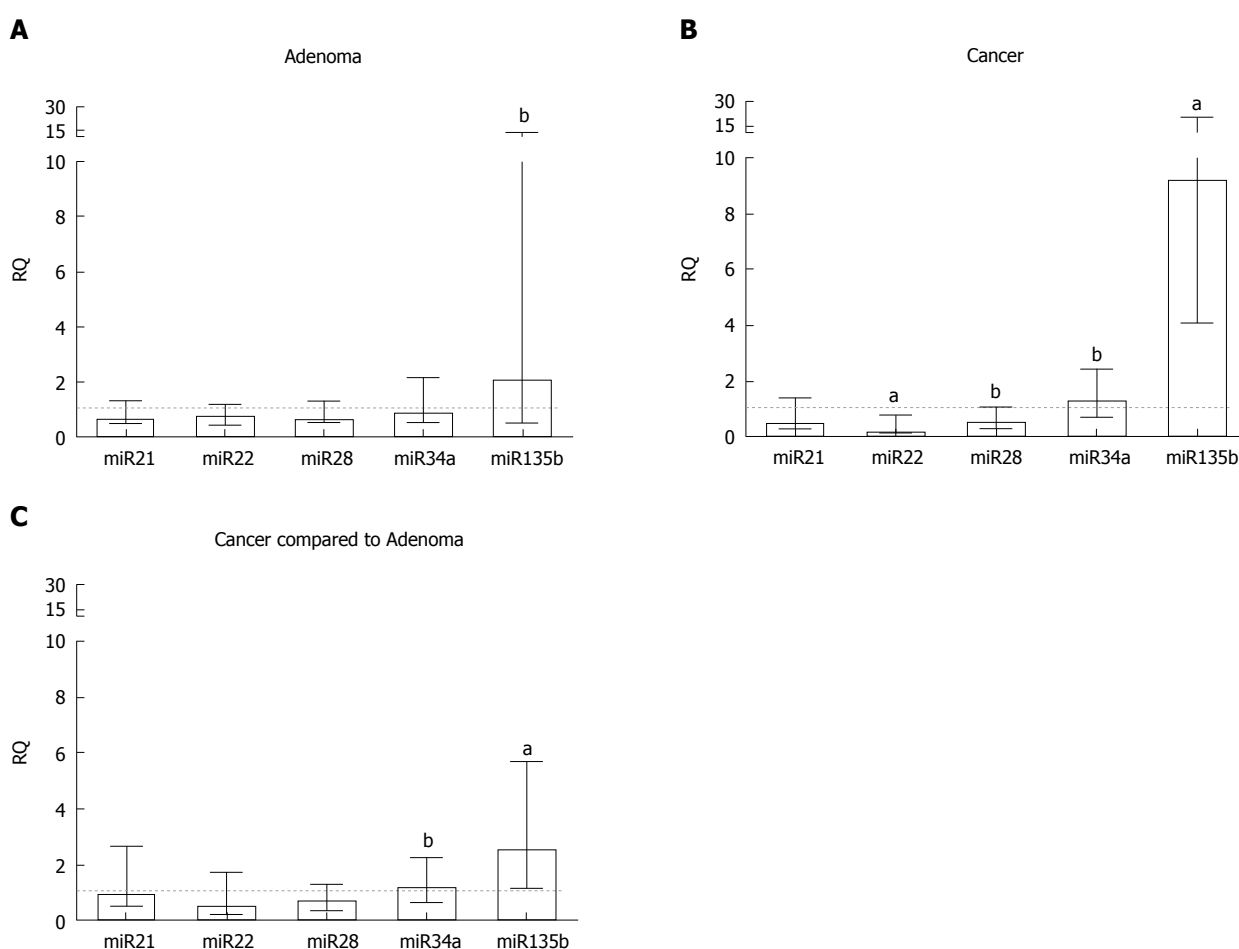


Figure 3 Relative quantification of microRNA genes in (A) adenoma and (B) colorectal tumour tissue samples compared to a pool of respective adjacent normal tissue samples and (C) colorectal tumour tissue samples compared to adenoma samples. Statistically significant differences, according to the Wilcoxon signed-rank test, were ^a*P* ≤ 0.001 and ^b*P* ≤ 0.01. Median with interquartile range graph. RQ: Relative quantification.

miRNA:mRNA interaction network analysis, miR-34a can target *TLR4* (Figure 4). This may explain the low expression of *TLR4* in CRC samples and overexpression in CRA samples, in which miR-34a had basal expression. Our data, together with that of previous studies, showed an increased expression of *TLR2* in CRC samples. Therefore, in CRC, a significant mechanism for the recognition of *F. nucleatum* may operate via *TLR2*, with consequent activation of ILs *IL1B*, *IL6* and *IL8* via NF-κB.

Moreover, *TLR2* is a predicted target of miR-22, which was downregulated in the CRC samples evaluated in our study (Figure 5).

Evidence suggests that miR-22 and miR-28 function as tumour suppressors. miR-22 can target key oncogenes for tumour invasion, metastasis and angiogenesis in CRC^[67,68]. A recent study showed reduced expression of miR-28 in the tissues of CRC liver metastases^[69]. However, the activity of this miRNA differs

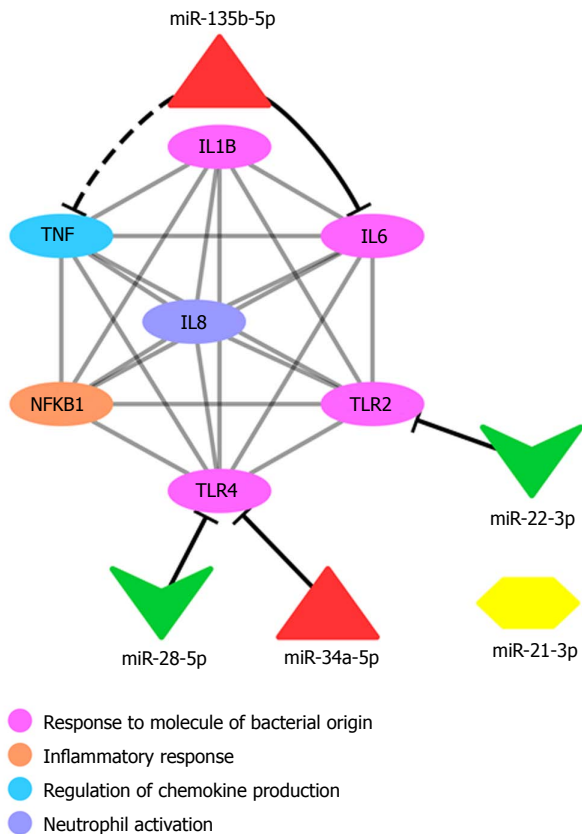


Figure 4 Protein interaction network showing microRNAs and their predicted gene targets. The protein interaction network (grey lines) shows the interaction between proteins encoded by target genes that are predicted to be regulated by microRNAs (miRNAs). Predicted interactions between miRNAs and target genes are shown by black lines. The dashed black line represents the possible interaction suggested in this study for *miR-135b-5p* and *TNF*. Ellipses represent target genes and/or proteins; red triangles represent upregulated miRNAs; green triangles represent downregulated miRNAs. *TNF*: Tumour necrosis factor; *IL*: Interleukin; *NFKB*: Nuclear factor kappa B; *TLR*: Toll-like receptor.

by 3p or 5p strand translation. *miR-28-3p* has been implicated in increased tumour migration and invasion, while *miR-28-5p*, analysed in our study, was reported to play a role in reducing tumour proliferation, migration and invasion in CRC^[70].

Our results showed a greater level of *F. nucleatum* in CRA and CRC tissues, which was more striking for CRC samples, suggesting an expansion of *F. nucleatum* colonization during the progression from adenoma to adenocarcinoma. Our gene expression data suggested that this phenomenon may lead to increased inflammatory pressures during CRC development based on the high expression of pro-inflammatory ILs *IL1B*, *IL6* and *IL8* and the correlation with *F. nucleatum* levels. Immune recognition of *F. nucleatum* may be mainly mediated by *TLR2* and/or *TLR4* and dependent on interactions with differently regulated miRNAs. Together, these findings provide further potential mechanistic rationale for the immune-comprised pro-inflammatory role of *F. nucleatum* in colorectal carcinogenesis. Efforts to develop early detection strategies for CRC could

include these biological interactors as potential functional biomarkers of *F. nucleatum*-mediated disease in addition to overall measures of *F. nucleatum* levels.

ARTICLE HIGHLIGHTS

Research background

Recently, *Fusobacterium nucleatum* (*F. nucleatum*), an anaerobic bacterial component of the oral and gut commensal flora, has emerged as a risk factor for colorectal cancer (CRC) development. Several studies have observed an association between overabundance of *F. nucleatum* in colonic tumor tissue compared to the normal matched mucosa. However, despite progress in this field the molecular mechanisms of how the bacterium etiologically contributes to carcinogenesis are still unclear.

Research motivation

We previously observed an association of the *TLR2*-196 to -174del genetic variant with increased CRC risk, together with an increased expression of *TLR2* mRNA and protein in tumor tissues^[31]. The major postulated mechanism of *F. nucleatum*-mediated colorectal tumorigenesis involves immune related inflammatory responses. Therefore, we decided to extend our previous work by measuring the transcript levels of important mediators in the pathogen-activated immune and inflammatory response, including *TLR2* / *TLR4* receptor and cytokine genes, and then evaluating the association of their expression with *F. nucleatum* levels in colorectal tumors. As microRNAs have been shown to be epigenetic regulators of inflammatory responses, we further examined the involvement of miRNAs in modulating the bacterial - cytokine interaction.

Research objectives

The main objective of this study was to investigate the association between inflammatory genes and *F. nucleatum* in colorectal carcinogenesis, by examining tissues from the major colorectal neoplasms of adenoma and adenocarcinomas. A secondary objective was to examine the interaction of the bacterial mediated immune response with microRNA (miRNA) regulation. The elucidation of likely mechanisms whereby *F. nucleatum* may contribute to inflammatory mediated colorectal carcinogenesis will help to better understand the molecular pathways activated by this bacterium and where prevention and treatment strategies can be best targeted.

Research methods

Robust techniques were used for DNA quantification of *F. nucleatum* and RNA transcript measures of the inflammatory genes and miRNAs in normal and tumor tissues. For this purpose, we used TaqMan gene expression assays (Applied Biosystems, Foster City, CA, United States) with specific probes for each gene and miRNA for relative quantification. The reactions were analyzed using the StepOnePlus real-time PCR System (Applied Biosystems, Foster City, CA, United States). Mutation testing of the *KRAS* gene was performed by direct sequencing and microsatellite instability (MSI) evaluation was performed using a multiplex PCR. In addition, we also used a bioinformatic tool 'miRNA Data Integration Portal' (<http://ophid.utoronto.ca/mirDIP/>)^[34] to build an miRNA: mRNA interaction network by using Cytoscape software (version 3.1.1)^[36].

Research results

Ours results confirm the overabundance of *F. nucleatum* in adenoma and tumor neoplasms compared to their respective matched normal tissues, as previously found in several populations. We further suggest that this bacterial load increases the expression of *TLR2* and *TLR4* receptors and consequently of pro-inflammatory interleukins *IL1B*, *IL6* and *IL8*. This immune-modulation of the inflammatory response to *F. nucleatum* colonic invasion also affects the expression of miRNA regulators of the inflammatory response. In particular, these miRNA:mRNA interactions network indicate a mechanism of colorectal carcinogenesis where altered expression of *miR-34a*, *miR-135b*, and *miR-22*, previously associated with CRC, occurs via a *TLR2/TLR4* dependent response to *F. nucleatum*. In analyses stratified by tumor molecular characteristics, we observed that *KRAS* was more frequently mutated in tumors with *F. nucleatum*, and that an increased *IL-8* expression was associated with MSI-

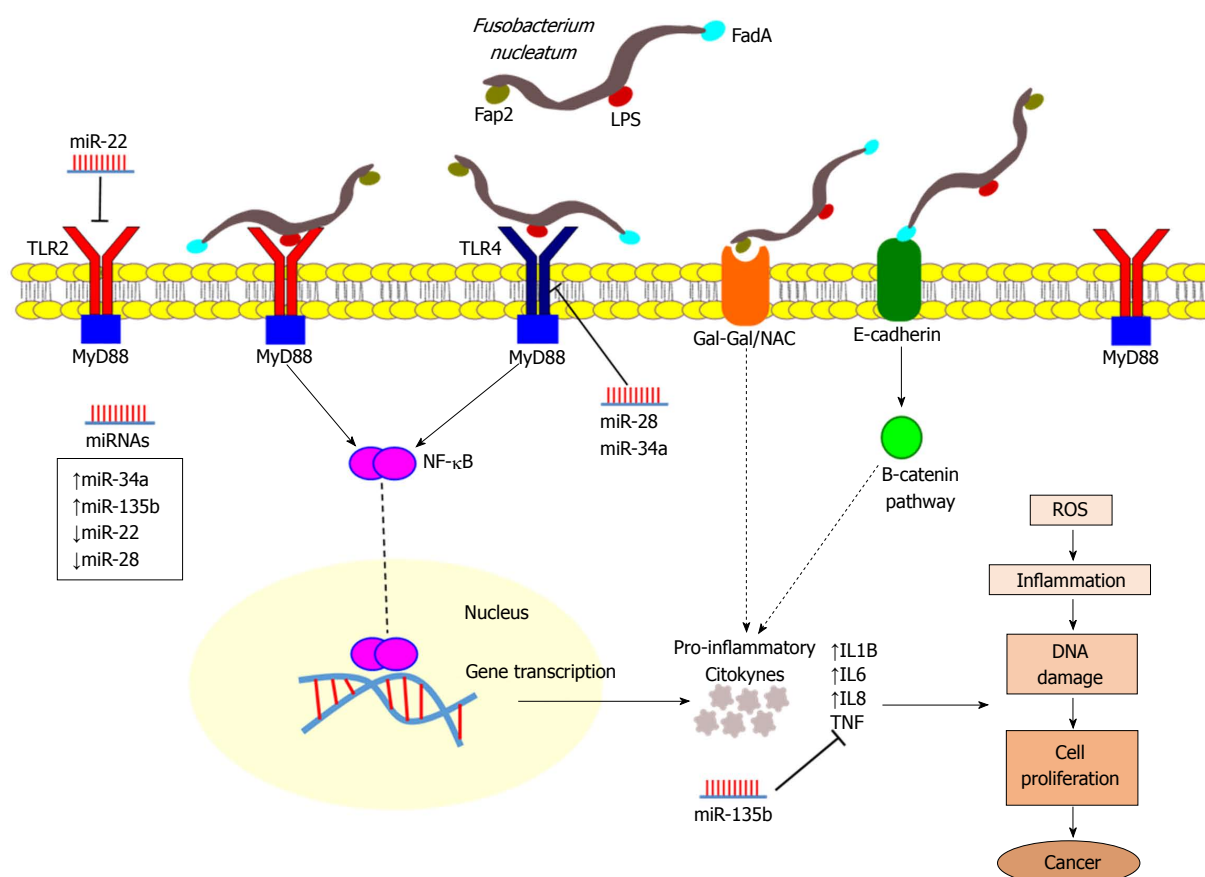


Figure 5 Representation illustrating the interactions of *Fusobacterium nucleatum* in colorectal cancer. *Fusobacterium nucleatum* (*F. nucleatum*) presents the virulence factors FadA and Fap2 and lipopolysaccharide (LPS), which are recognized by Toll-like receptors (TLR2 and TLR4) mediating *F. nucleatum* invasion and the promotion of colorectal cancer (CRC). FadA, a surface adhesion protein, can bind to E-cadherin on CRC cells, activating B-catenin signalling. Fap2, a galactose-sensitive haemagglutinin and adhesion protein binding to Gal-GalNAc, contributes to the invasive ability of *F. nucleatum*. The TLR2/TLR4/MyD88 pathway is activated in response to *F. nucleatum*, leading to the activation of NF- κ B, a transcription factor that is involved in regulating the expression of many genes, leading to elevated expression levels of oncogenes and pro-inflammatory cytokines, mainly interleukin (IL)1B, IL6, IL8 and tumour necrosis factor, inducing the production of reactive oxygen species, which subsequently lead to inflammation and DNA damage that promotes tumour growth and progression. Furthermore, these pathways may be under the regulation of differentially expressed microRNAs. ROS: Reactive oxygen species; TNF: Tumour necrosis factor; IL: Interleukin; NF- κ B: Nuclear factor kappa B; TLR: Toll-like receptor; miRNA: MicroRNA.

high status. Therefore, more studies of gene function and regulation within the inflammatory pathways impacted by *F. nucleatum* invasion are needed, along with consideration of tumor molecular subtypes.

Research conclusions

Our findings reinforce the increasing invasion of *F. nucleatum* during the colorectal adenoma to cancer development. This appears to increase expression of pro-inflammatory mediators and dysregulation of miRNA expression, leading to a more carcinogenic microenvironment alongside genetic alterations such as *KRAS* mutation and MSI-high. Therefore, together with other studies, our results suggest that *F. nucleatum* is involved in CRC development through immune responses to inflammatory stresses. Further work is needed to functionally demonstrate these postulated tumorigenic mechanisms, and also for early CRC detection and diagnosis strategies using biomarkers of *F. nucleatum* presence or the consequent immune response.

Research perspectives

The intestinal microbiota is very diverse and important for the maintenance of epithelial homeostasis. Disturbances of this microbiome balance appears to be a major factor in CRC etiology. *F. nucleatum* has been implicated in recent years, by *in vitro* and in mouse models, as a carcinogenic bacterium through generation of a microenvironment conducive to cancer development. Considering that *F. nucleatum* has been found to be highly abundant in both adenoma and CRC neoplasms, it may have uses as a tissue or non-invasive

biomarker in faeces (or possibly mouth-rinse samples) for CRC and the early detection of adenomas (which may help define a higher risk group for CRC development due to the presences of the bacterium). However, further investigations are needed to understand the molecular mechanisms in the immuno-inflammatory response to the increased invasion of this bacterium into developing neoplasms, and if this can promote genetic and epigenetic alterations that may culminate in CRC development.

ACKNOWLEDGMENTS

We thank Lucas Trevizani Rasmussen for kindly donating some miRNA probes. We are grateful to the São Paulo Research Foundation (FAPESP, NO. 2015/21464-0) for the support for English revision, the Coordination for the Improvement of Higher Education Personnel (CAPES) for the doctoral scholarship, and the National Council for Scientific and Technological Development (CNPq, NO. 310120/2015-2) for the productivity research scholarship.

REFERENCES

- 1 Ferlay J, Colombet M, Soerjomataram I, Mathers C, Parkin DM,

- Piñeros M, Znaor A, Bray F. Estimating the global cancer incidence and mortality in 2018: GLOBOCAN sources and methods. *Int J Cancer* 2018; Epub ahead of print [PMID: 30350310 DOI: 10.1002/ijc.31937]
- 2 **Ministério da Saúde**, Instituto Nacional de Câncer José Alencar Gomes da Silva. Estimativa 2018 - Incidência de câncer no Brasil. 2018. Accessed October 24, 2018 Available from: URL: <http://www.inca.gov.br/estimativa/2018/index.asp>
 - 3 **Landskron G**, De la Fuente M, Thuwajit P, Thuwajit C, Hermoso MA. Chronic inflammation and cytokines in the tumor microenvironment. *J Immunol Res* 2014; **2014**: 149185 [PMID: 24901008 DOI: 10.1155/2014/149185]
 - 4 **Leung A**, Tsoi H, Yu J. *Fusobacterium* and *Escherichia*: models of colorectal cancer driven by microbiota and the utility of microbiota in colorectal cancer screening. *Expert Rev Gastroenterol Hepatol* 2015; **9**: 651-657 [PMID: 25582922 DOI: 10.1586/17474124.2015.1001745]
 - 5 **Castellarin M**, Warren RL, Freeman JD, Dreolini L, Krzywinski M, Strauss J, Barnes R, Watson P, Allen-Vercos E, Moore RA, Holt RA. *Fusobacterium nucleatum* infection is prevalent in human colorectal carcinoma. *Genome Res* 2012; **22**: 299-306 [PMID: 22009989 DOI: 10.1101/gr.126516.111]
 - 6 **Kostic AD**, Chun E, Robertson L, Glickman JN, Gallini CA, Michaud M, Clancy TE, Chung DC, Lochhead P, Hold GL, El-Omar EM, Brenner D, Fuchs CS, Meyerson M, Garrett WS. *Fusobacterium nucleatum* potentiates intestinal tumorigenesis and modulates the tumor-immune microenvironment. *Cell Host Microbe* 2013; **14**: 207-215 [PMID: 23954159 DOI: 10.1016/j.chom.2013.07.007]
 - 7 **Shang FM**, Liu HL. *Fusobacterium nucleatum* and colorectal cancer: A review. *World J Gastrointest Oncol* 2018; **10**: 71-81 [PMID: 29564037 DOI: 10.4251/wjgo.v10.i3.71]
 - 8 **Han YW**. *Fusobacterium nucleatum*: a commensal-turned pathogen. *Curr Opin Microbiol* 2015; **23**: 141-147 [PMID: 25576662 DOI: 10.1016/j.mib.2014.11.013]
 - 9 **Liu Y**, Baba Y, Ishimoto T, Iwatsuki M, Hiyoshi Y, Miyamoto Y, Yoshida N, Wu R, Baba H. Progress in characterizing the linkage between *Fusobacterium nucleatum* and gastrointestinal cancer. *J Gastroenterol* 2018; Epub ahead of print [PMID: 30244399 DOI: 10.1007/s00535-018-1512-9]
 - 10 **Flanagan L**, Schmid J, Ebert M, Soucek P, Kunicka T, Liska V, Bruha J, Neary P, Dezeew N, Tommasino M, Jenab M, Prehn JH, Hughes DJ. *Fusobacterium nucleatum* associates with stages of colorectal neoplasia development, colorectal cancer and disease outcome. *Eur J Clin Microbiol Infect Dis* 2014; **33**: 1381-1390 [PMID: 24599709 DOI: 10.1007/s10096-014-2081-3]
 - 11 **Li YY**, Ge QX, Cao J, Zhou YJ, Du YL, Shen B, Wan YJ, Nie YQ. Association of *Fusobacterium nucleatum* infection with colorectal cancer in Chinese patients. *World J Gastroenterol* 2016; **22**: 3227-3233 [PMID: 27004000 DOI: 10.3748/wjg.v22.i11.3227]
 - 12 **Hussan H**, Clinton SK, Roberts K, Bailey MT. *Fusobacterium*'s link to colorectal neoplasia sequenced: A systematic review and future insights. *World J Gastroenterol* 2017; **23**: 8626-8650 [PMID: 29358871 DOI: 10.3748/wjg.v23.i48.8626]
 - 13 **Marietta E**, Rishi A, Taneja V. Immunogenetic control of the intestinal microbiota. *Immunology* 2015; **145**: 313-322 [PMID: 25913295 DOI: 10.1111/imm.12474]
 - 14 **Sakamoto K**, Maeda S. Targeting NF-kappaB for colorectal cancer. *Expert Opin Ther Targets* 2010; **14**: 593-601 [PMID: 20367537 DOI: 10.1517/14728221003769903]
 - 15 **de Koning HD**, Simon A, Zeeuwen PL, Schalkwijk J. Pattern recognition receptors in infectious skin diseases. *Microbes Infect* 2012; **14**: 881-893 [PMID: 22516809 DOI: 10.1016/j.micinf.2012.03.004]
 - 16 **Koorts AM**, Levay PF, Becker PJ, Viljoen M. Pro- and anti-inflammatory cytokines during immune stimulation: modulation of iron status and red blood cell profile. *Mediators Inflamm* 2011; **2011**: 716301 [PMID: 21547258 DOI: 10.1155/2011/716301]
 - 17 **Morandini AC**, Chaves Souza PP, Ramos-Junior ES, Brozoski DT, Sipert CR, Souza Costa CA, Santos CF. Toll-like receptor 2 knockdown modulates interleukin (IL)-6 and IL-8 but not stromal derived factor-1 (SDF-1/CXCL12) in human periodontal ligament and gingival fibroblasts. *J Periodontol* 2013; **84**: 535-544 [PMID: 22680301 DOI: 10.1902/jop.2012.120177]
 - 18 **Mager LF**, Wasmer MH, Rau TT, Krebs P. Cytokine-Induced Modulation of Colorectal Cancer. *Front Oncol* 2016; **6**: 96 [PMID: 27148488 DOI: 10.3389/fonc.2016.00096]
 - 19 **Mima K**, Sukawa Y, Nishihara R, Qian ZR, Yamauchi M, Inamura K, Kim SA, Masuda A, Nowak JA, Noshok K, Kostic AD, Giannakis M, Watanabe H, Bullman S, Milner DA, Harris CC, Giovannucci E, Garraway LA, Freeman GJ, Dranoff G, Chan AT, Garrett WS, Huttenhower C, Fuchs CS, Ogino S. *Fusobacterium nucleatum* and T Cells in Colorectal Carcinoma. *JAMA Oncol* 2015; **1**: 653-661 [PMID: 26181352 DOI: 10.1001/jamaoncol.2015.1377]
 - 20 **Hamada T**, Zhang X, Mima K, Bullman S, Sukawa Y, Nowak JA, Kosumi K, Masugi Y, Twombly TS, Cao Y, Song M, Liu L, da Silva A, Shi Y, Gu M, Li W, Koh H, Noshok K, Inamura K, Keum N, Wu K, Meyerhardt JA, Kostic AD, Huttenhower C, Garrett WS, Meyerson M, Giovannucci EL, Chan AT, Fuchs CS, Nishihara R, Giannakis M, Ogino S. *Fusobacterium nucleatum* in Colorectal Cancer Relates to Immune Response Differentially by Tumor Microsatellite Instability Status. *Cancer Immunol Res* 2018; **6**: 1327-1336 [PMID: 30228205 DOI: 10.1158/2326-6066.CIR-18-0174]
 - 21 **Koi M**, Okita Y, Carethers JM. *Fusobacterium nucleatum* Infection in Colorectal Cancer: Linking Inflammation, DNA Mismatch Repair and Genetic and Epigenetic Alterations. *J Anus Rectum Colon* 2018; **2**: 37-46 [PMID: 30116794 DOI: 10.23922/jarc.2017-055]
 - 22 **Li X**, Nie J, Mei Q, Han WD. MicroRNAs: Novel immunotherapeutic targets in colorectal carcinoma. *World J Gastroenterol* 2016; **22**: 5317-5331 [PMID: 27340348 DOI: 10.3748/wjg.v22.i23.5317]
 - 23 **Okayama H**, Schetter AJ, Harris CC. MicroRNAs and inflammation in the pathogenesis and progression of colon cancer. *Dig Dis* 2012; **30** Suppl 2: 9-15 [PMID: 23207927 DOI: 10.1159/000341882]
 - 24 **Mohammadi A**, Mansoori B, Baradaran B. The role of microRNAs in colorectal cancer. *Biomed Pharmacother* 2016; **84**: 705-713 [PMID: 27701052 DOI: 10.1016/j.biopha.2016.09.099]
 - 25 **Qu A**, Yang Y, Zhang X, Wang W, Liu Y, Zheng G, Du L, Wang C. Development of a preoperative prediction nomogram for lymph node metastasis in colorectal cancer based on a novel serum miRNA signature and CT scans. *EBioMedicine* 2018; Epub ahead of print [PMID: 30314890 DOI: 10.1016/j.ebiom.2018.09.052]
 - 26 **Ito M**, Kanno S, Noshok K, Sukawa Y, Mitsuhashi K, Kurihara H, Igarashi H, Takahashi T, Tachibana M, Takahashi H, Yoshii S, Takenouchi T, Hasegawa T, Okita K, Hirata K, Maruyama R, Suzuki H, Imai K, Yamamoto H, Shinomura Y. Association of *Fusobacterium nucleatum* with clinical and molecular features in colorectal serrated pathway. *Int J Cancer* 2015; **137**: 1258-1268 [PMID: 25703934 DOI: 10.1002/ijc.29488]
 - 27 **Noshok K**, Sukawa Y, Adachi Y, Ito M, Mitsuhashi K, Kurihara H, Kanno S, Yamamoto I, Ishigami K, Igarashi H, Maruyama R, Imai K, Yamamoto H, Shinomura Y. Association of *Fusobacterium nucleatum* with immunity and molecular alterations in colorectal cancer. *World J Gastroenterol* 2016; **22**: 557-566 [PMID: 26811607 DOI: 10.3748/wjg.v22.i2.557]
 - 28 **Yang Y**, Weng W, Peng J, Hong L, Yang L, Toiyama Y, Gao R, Liu M, Yin M, Pan C, Li H, Guo B, Zhu Q, Wei Q, Moyer MP, Wang P, Cai S, Goel A, Qin H, Ma Y. *Fusobacterium nucleatum* Increases Proliferation of Colorectal Cancer Cells and Tumor Development in Mice by Activating Toll-Like Receptor 4 Signaling to Nuclear Factor-kB, and Up-regulating Expression of MicroRNA-21. *Gastroenterology* 2017; **152**: 851-866.e24 [PMID: 27876571 DOI: 10.1053/j.gastro.2016.11.018]
 - 29 **Vlachos IS**, Paraskevopoulou MD, Karagkouni D, Georgakilas G, Vergoulis T, Kanellos I, Anastasopoulos IL, Maniou S, Karathanou K, Kalfakakou D, Fevgas A, Dalamagas T, Hatzigeorgiou AG. DIANA-TarBase v7.0: indexing more than half a million experimentally supported miRNA:mRNA interactions. *Nucleic Acids Res* 2015; **43**: D153-D159 [PMID: 25416803 DOI: 10.1093/nar/gku1215]

- 30 **Kozomara A**, Griffiths-Jones S. miRBase: annotating high confidence microRNAs using deep sequencing data. *Nucleic Acids Res* 2014; **42**: D68-D73 [PMID: 24275495 DOI: 10.1093/nar/gkt1181]
- 31 **Proença MA**, de Oliveira JG, Cadamuro AC, Succi M, Netinho JG, Goloni-Bertolo EM, Pavarino EC, Silva AE. TLR2 and TLR4 polymorphisms influence mRNA and protein expression in colorectal cancer. *World J Gastroenterol* 2015; **21**: 7730-7741 [PMID: 26167073 DOI: 10.3748/wjg.v21.i25.7730]
- 32 **Livak KJ**, Schmittgen TD. Analysis of relative gene expression data using real-time quantitative PCR and the 2(-Delta Delta C(T)) Method. *Methods* 2001; **25**: 402-408 [PMID: 11846609 DOI: 10.1006/meth.2001.1262]
- 33 **Mestdagh P**, Van Vlierberghe P, De Weer A, Muth D, Westermann F, Speleman F, Vandesompele J. A novel and universal method for microRNA RT-qPCR data normalization. *Genome Biol* 2009; **10**: R64 [PMID: 19531210 DOI: 10.1186/gb-2009-10-6-r64]
- 34 **Shirdel EA**, Xie W, Mak TW, Jurisica I. NAViGaTing the microne--using multiple microRNA prediction databases to identify signalling pathway-associated microRNAs. *PLoS One* 2011; **6**: e17429 [PMID: 21364759 DOI: 10.1371/journal.pone.0017429]
- 35 **Franceschini A**, Szklarczyk D, Frankild S, Kuhn M, Simonovic M, Roth A, Lin J, Minguez P, Bork P, von Mering C, Jensen LJ. STRING v9.1: protein-protein interaction networks, with increased coverage and integration. *Nucleic Acids Res* 2013; **41**: D808-D815 [PMID: 23203871 DOI: 10.1093/nar/gks1094]
- 36 **Chen R**, Mias GI, Li-Pook-Than J, Jiang L, Lam HY, Chen R, Miriami E, Karczewski KJ, Hariharan M, Dewey FE, Cheng Y, Clark MJ, Im H, Habegger L, Balasubramanian S, O'Huallachain M, Dudley JT, Hillenmeyer S, Harakasingh R, Sharon D, Euskirchen G, Lacroix P, Bettinger K, Boyle AP, Kasowski K, Grubert F, Seki S, Garcia M, Whirl-Carrillo M, Gallardo M, Blasco MA, Greenberg PL, Snyder P, Klein TE, Altman RB, Butte AJ, Ashley EA, Gerstein M, Nadeau KC, Tang H, Snyder M. Personal omics profiling reveals dynamic molecular and medical phenotypes. *Cell* 2012; **148**: 1293-1307 [PMID: 22424236 DOI: 10.1016/j.cell.2012.02.009]
- 37 **Maere S**, Heymans K, Kuiper M. BiNGO: a Cytoscape plugin to assess overrepresentation of gene ontology categories in biological networks. *Bioinformatics* 2005; **21**: 3448-3449 [PMID: 15972284 DOI: 10.1093/bioinformatics/bti551]
- 38 **Yamane LS**, Scapulatempo-Neto C, Alvarenga L, Oliveira CZ, Berardinelli GN, Almodova E, Cunha TR, Fava G, Colaiacovo W, Melani A, Fregnano JH, Reis RM, Guimarães DP. KRAS and BRAF mutations and MSI status in precursor lesions of colorectal cancer detected by colonoscopy. *Oncol Rep* 2014; **32**: 1419-1426 [PMID: 25050586 DOI: 10.3892/or.2014.3338]
- 39 **Martinho O**, Gouveia A, Viana-Pereira M, Silva P, Pimenta A, Reis RM, Lopes JM. Low frequency of MAP kinase pathway alterations in KIT and PDGFRA wild-type GISTs. *Histopathology* 2009; **55**: 53-62 [PMID: 19614767 DOI: 10.1111/j.1365-2559.2009.03323.x]
- 40 **Campanella NC**, Berardinelli GN, Scapulatempo-Neto C, Viana D, Palmero EI, Pereira R, Reis RM. Optimization of a pentaplex panel for MSI analysis without control DNA in a Brazilian population: correlation with ancestry markers. *Eur J Hum Genet* 2014; **22**: 875-880 [PMID: 24193342 DOI: 10.1038/ejhg.2013.256]
- 41 **Berardinelli GN**, Scapulatempo-Neto C, Durães R, Antônio de Oliveira M, Guimarães D, Reis RM. Advantage of *HSP110* (T17) marker inclusion for microsatellite instability (MSI) detection in colorectal cancer patients. *Oncotarget* 2018; **9**: 28691-28701 [PMID: 29983889 DOI: 10.18632/oncotarget.25611]
- 42 **Buhard O**, Cattaneo F, Wong YF, Yim SF, Friedman E, Flejou JF, Duval A, Hamelin R. Multipopulation analysis of polymorphisms in five mononucleotide repeats used to determine the microsatellite instability status of human tumors. *J Clin Oncol* 2006; **24**: 241-251 [PMID: 16330668 DOI: 10.1200/JCO.2005.02.7227]
- 43 **Mira-Pascual L**, Cabrera-Rubio R, Ocon S, Costales P, Parra A, Suarez A, Moris F, Rodrigo L, Mira A, Collado MC. Microbial mucosal colonic shifts associated with the development of colorectal cancer reveal the presence of different bacterial and archaeal biomarkers. *J Gastroenterol* 2015; **50**: 167-179 [PMID: 24811328 DOI: 10.1007/s00535-014-0963-x]
- 44 **Wei Z**, Cao S, Liu S, Yao Z, Sun T, Li Y, Li J, Zhang D, Zhou Y. Could gut microbiota serve as prognostic biomarker associated with colorectal cancer patients' survival? A pilot study on relevant mechanism. *Oncotarget* 2016; **7**: 46158-46172 [PMID: 27323816 DOI: 10.18632/oncotarget.10064]
- 45 **Repas J**, Maherali N, Owen K; Reproducibility Project: Cancer Biology; Reproducibility Project Cancer Biology. Registered report: *Fusobacterium nucleatum* infection is prevalent in human colorectal carcinoma. *Elife* 2016; **5** [PMID: 26882501 DOI: 10.7554/eLife.10012]
- 46 **Peng BJ**, Cao CY, Li W, Zhou YJ, Zhang Y, Nie YQ, Cao YW, Li YY. Diagnostic Performance of Intestinal *Fusobacterium nucleatum* in Colorectal Cancer: A Meta-Analysis. *Chin Med J (Engl)* 2018; **131**: 1349-1356 [PMID: 29786050 DOI: 10.4103/0366-6999.232814]
- 47 **Fukugaiti MH**, Ignacio A, Fernandes MR, Ribeiro Júnior U, Nakano V, Avila-Campos MJ. High occurrence of *Fusobacterium nucleatum* and *Clostridium difficile* in the intestinal microbiota of colorectal carcinoma patients. *Braz J Microbiol* 2015; **46**: 1135-1140 [PMID: 26691472 DOI: 10.1590/S1517-838246420140665]
- 48 **Rubinstein MR**, Wang X, Liu W, Hao Y, Cai G, Han YW. *Fusobacterium nucleatum* promotes colorectal carcinogenesis by modulating E-cadherin/ β -catenin signaling via its FadA adhesin. *Cell Host Microbe* 2013; **14**: 195-206 [PMID: 23954158 DOI: 10.1016/j.chom.2013.07.012]
- 49 **Yu YN**, Yu TC, Zhao HJ, Sun TT, Chen HM, Chen HY, An HF, Weng YR, Yu J, Li M, Qin WX, Ma X, Shen N, Hong J, Fang JY. Berberine may rescue *Fusobacterium nucleatum*-induced colorectal tumorigenesis by modulating the tumor microenvironment. *Oncotarget* 2015; **6**: 32013-32026 [PMID: 26397137 DOI: 10.18632/oncotarget.5166]
- 50 **Yu T**, Guo F, Yu Y, Sun T, Ma D, Han J, Qian Y, Kryczek I, Sun D, Nagarsheth N, Chen Y, Chen H, Hong J, Zou W, Fang JY. *Fusobacterium nucleatum* Promotes Chemoresistance to Colorectal Cancer by Modulating Autophagy. *Cell* 2017; **170**: 548-563.e16 [PMID: 28753429 DOI: 10.1016/j.cell.2017.07.008]
- 51 **Velsko IM**, Chukkapalli SS, Rivera-Kweh MF, Chen H, Zheng D, Bhattacharyya I, Gangula PR, Lucas AR, Kesavalu L. *Fusobacterium nucleatum* Alters Atherosclerosis Risk Factors and Enhances Inflammatory Markers with an Atheroprotective Immune Response in ApoE(null) Mice. *PLoS One* 2015; **10**: e0129795 [PMID: 26079509 DOI: 10.1371/journal.pone.0129795]
- 52 **Martinho FC**, Leite FR, Nóbrega LM, Endo MS, Nascimento GG, Darveau RP, Gomes BP. Comparison of *Fusobacterium nucleatum* and *Porphyromonas gingivalis* Lipopolysaccharides Clinically Isolated from Root Canal Infection in the Induction of Pro-Inflammatory Cytokines Secretion. *Braz Dent J* 2016; **27**: 202-207 [PMID: 27058385 DOI: 10.1590/0103-6440201600572]
- 53 **Liang Q**, Chiu J, Chen Y, Huang Y, Higashimori A, Fang J, Brim H, Ashktorab H, Ng SC, Ng SSM, Zheng S, Chan FKL, Sung JJY, Yu J. Fecal Bacteria Act as Novel Biomarkers for Noninvasive Diagnosis of Colorectal Cancer. *Clin Cancer Res* 2017; **23**: 2061-2070 [PMID: 27697996 DOI: 10.1158/1078-0432.CCR-16-1599]
- 54 **Legitimo A**, Consolini R, Failli A, Orsini G, Spisni R. Dendritic cell defects in the colorectal cancer. *Hum Vaccin Immunother* 2014; **10**: 3224-3235 [PMID: 25483675 DOI: 10.4161/hv.29857]
- 55 **Shi L**, Middleton J, Jeon YJ, Magee P, Veneziano D, Laganà A, Leong HS, Sahoo S, Fassan M, Booton R, Shah R, Crosbie PAJ, Garofalo M. KRAS induces lung tumorigenesis through microRNAs modulation. *Cell Death Dis* 2018; **9**: 219 [PMID: 29440633 DOI: 10.1038/s41419-017-0243-9]
- 56 **Valeri N**, Braconi C, Gasparini P, Murgia C, Lampis A, Paulus-Hock V, Hart JR, Ueno L, Grivennikov SI, Lovat F, Paone A, Cascione L, Sumani KM, Veronese A, Fabbri M, Carasi S, Alder H, Lanza G, Gafa' R, Moyer MP, Ridgway RA, Cordero J, Nuovo GJ, Frankel WL, Rugge M, Fassan M, Groden J, Vogt PK, Karin M, Sansom OJ, Croce CM. MicroRNA-135b promotes cancer progression by acting as a downstream effector of oncogenic pathways in colon cancer. *Cancer Cell* 2014; **25**: 469-483 [PMID: 24735923 DOI: 10.1016/j.ccr.2014.03.006]

- 57 **Wu W**, Wang Z, Yang P, Yang J, Liang J, Chen Y, Wang H, Wei G, Ye S, Zhou Y. MicroRNA-135b regulates metastasis suppressor 1 expression and promotes migration and invasion in colorectal cancer. *Mol Cell Biochem* 2014; **388**: 249-259 [PMID: 24343340 DOI: 10.1007/s11010-013-1916-z]
- 58 **He Y**, Wang J, Wang J, Yung VY, Hsu E, Li A, Kang Q, Ma J, Han Q, Jin P, Xing R, Lu Y, Sheng J. MicroRNA-135b regulates apoptosis and chemoresistance in colorectal cancer by targeting large tumor suppressor kinase 2. *Am J Cancer Res* 2015; **5**: 1382-1395 [PMID: 26101704]
- 59 **Wu CW**, Ng SC, Dong Y, Tian L, Ng SS, Leung WW, Law WT, Yau TO, Chan FK, Sung JJ, Yu J. Identification of microRNA-135b in stool as a potential noninvasive biomarker for colorectal cancer and adenoma. *Clin Cancer Res* 2014; **20**: 2994-3002 [PMID: 24691020 DOI: 10.1158/1078-0432.CCR-13-1750]
- 60 **Li P**, Fan JB, Gao Y, Zhang M, Zhang L, Yang N, Zhao X. miR-135b-5p inhibits LPS-induced TNF α production via silencing AMPK phosphatase Ppm1e. *Oncotarget* 2016; **7**: 77978-77986 [PMID: 27793001 DOI: 10.18632/oncotarget.12866]
- 61 **Kara M**, Yumrutas O, Ozcan O, Celik OI, Bozgeyik E, Bozgeyik I, Tasdemir S. Differential expressions of cancer-associated genes and their regulatory miRNAs in colorectal carcinoma. *Gene* 2015; **567**: 81-86 [PMID: 25925209 DOI: 10.1016/j.gene.2015.04.065]
- 62 **Aherne ST**, Madden SF, Hughes DJ, Pardini B, Naccarati A, Levy M, Vodicka P, Neary P, Dowling P, Clynes M. Circulating miRNAs miR-34a and miR-150 associated with colorectal cancer progression. *BMC Cancer* 2015; **15**: 329 [PMID: 25924769 DOI: 10.1186/s12885-015-1327-5]
- 63 **Lai M**, Du G, Shi R, Yao J, Yang G, Wei Y, Zhang D, Xu Z, Zhang R, Li Y, Li Z, Wang L. MiR-34a inhibits migration and invasion by regulating the SIRT1/p53 pathway in human SW480 cells. *Mol Med Rep* 2015; **11**: 3301-3307 [PMID: 25585539 DOI: 10.3892/mmr.2015.3182]
- 64 **Li C**, Wang Y, Lu S, Zhang Z, Meng H, Liang L, Zhang Y, Song B. MiR-34a inhibits colon cancer proliferation and metastasis by inhibiting platelet-derived growth factor receptor α . *Mol Med Rep* 2015; **12**: 7072-7078 [PMID: 26324236 DOI: 10.3892/mmr.2015.4263]
- 65 **Chandrasekaran KS**, Sathyanarayanan A, Karunakaran D. Downregulation of HMGB1 by miR-34a is sufficient to suppress proliferation, migration and invasion of human cervical and colorectal cancer cells. *Tumour Biol* 2016; **37**: 13155-13166 [PMID: 27456356 DOI: 10.1007/s13277-016-5261-1]
- 66 **Almeida AL**, Bernardes MV, Feitosa MR, Peria FM, Tirapelli DP, Rocha JJ, Feres O. Serological under expression of microRNA-21, microRNA-34a and microRNA-126 in colorectal cancer. *Acta Cir Bras* 2016; **31** Suppl 1: 13-18 [PMID: 27142899 DOI: 10.1590/S0102-86502016001300004]
- 67 **Li B**, Song Y, Liu TJ, Cui YB, Jiang Y, Xie ZS, Xie SL. miRNA-22 suppresses colon cancer cell migration and invasion by inhibiting the expression of T-cell lymphoma invasion and metastasis 1 and matrix metalloproteinases 2 and 9. *Oncol Rep* 2013; **29**: 1932-1938 [PMID: 23440286 DOI: 10.3892/or.2013.2300]
- 68 **Yamakuchi M**, Yagi S, Ito T, Lowenstein CJ. MicroRNA-22 regulates hypoxia signaling in colon cancer cells. *PLoS One* 2011; **6**: e20291 [PMID: 21629773 DOI: 10.1371/journal.pone.0020291]
- 69 **Vychytilova-Faltejskova P**, Pesta M, Radova L, Liska V, Daum O, Kala Z, Svoboda M, Kiss I, Slaby O. Genome-wide microRNA Expression Profiling in Primary Tumors and Matched Liver Metastasis of Patients with Colorectal Cancer. *Cancer Genomics Proteomics* 2016; **13**: 311-316 [PMID: 27365381]
- 70 **Almeida MI**, Nicoloso MS, Zeng L, Ivan C, Spizzo R, Gafã R, Xiao L, Zhang X, Vannini I, Fanini F, Fabbri M, Lanza G, Reis RM, Zweidler-McKay PA, Calin GA. Strand-specific miR-28-5p and miR-28-3p have distinct effects in colorectal cancer cells. *Gastroenterology* 2012; **142**: 886-896.e9 [PMID: 22240480 DOI: 10.1053/j.gastro.2011.12.047]

P- Reviewer: Li YY, Roncucci L **S- Editor:** Ma RY **L- Editor:** A
E- Editor: Huang Y



Basic Study

Bypassing major venous occlusion and duodenal lesions in rats, and therapy with the stable gastric pentadecapeptide BPC 157, L-NAME and L-arginine

Fedor Amic, Domagoj Drmic, Zdenko Bilic, Ivan Krezic, Helena Zizek, Marina Peklic, Robert Kliceck, Alen Pajtak, Enio Amic, Tinka Vidovic, Mislav Rakic, Marija Milkovic Perisa, Katarina Horvat Pavlov, Antonio Kokot, Ante Tvrdeic, Alenka Boban Blagaic, Mario Zovak, Sven Seiwert, Predrag Sikiric

Fedor Amic, Domagoj Drmic, Zdenko Bilic, Ivan Krezic, Helena Zizek, Marina Peklic, Robert Kliceck, Alen Pajtak, Enio Amic, Tinka Vidovic, Mislav Rakic, Marija Milkovic Perisa, Katarina Horvat Pavlov, Antonio Kokot, Ante Tvrdeic, Alenka Boban Blagaic, Mario Zovak, Sven Seiwert, Predrag Sikiric, Department of Pharmacology, Medical Faculty, University of Zagreb, Zagreb 10000, Croatia

Fedor Amic, Domagoj Drmic, Zdenko Bilic, Ivan Krezic, Helena Zizek, Marina Peklic, Robert Kliceck, Alen Pajtak, Enio Amic, Tinka Vidovic, Mislav Rakic, Marija Milkovic Perisa, Katarina Horvat Pavlov, Antonio Kokot, Ante Tvrdeic, Alenka Boban Blagaic, Mario Zovak, Sven Seiwert, Predrag Sikiric, Department of Pathology, Medical Faculty, University of Zagreb, Zagreb 10000, Croatia

ORCID number: Fedor Amic (0000-0002-5914-4565); Domagoj Drmic (0000-0002-1081-7175); Zdenko Bilic (0000-0003-2503-7179); Ivan Krezic (0000-0001-7994-5645); Helena Zizek (0000-0001-9863-4164); Marina Peklic (0000-0002-1232-3777); Robert Kliceck (0000-0001-5532-6989); Alen Pajtak (0000-0002-7217-7425); Enio Amic (0000-0003-0331-7962); Tinka Vidovic (0000-0003-0092-9365); Mislav Rakic (0000-0003-3367-6739); Marija Milkovic Perisa (0000-0002-9530-9208); Katarina Horvat Pavlov (0000-0002-2661-7346); Antonio Kokot (0000-0002-4836-7536); Ante Tvrdeic (0000-0002-8881-2278); Alenka Boban Blagaic (0000-0003-1266-3402); Mario Zovak (0000-0002-8603-5022); Sven Seiwert (0000-0002-5894-419X); Predrag Sikiric (0000-0002-7952-2252).

Author contributions: Amic F, Drmic D, Bilic Z, Krezic I, Zizek H, Peklic M, Kliceck R, Pajtak A, Amic E, Vidovic T, Rakic M, Milkovic Perisa M, Horvat Pavlov K, Kokot A, Tvrdeic A and Boban Blagaic A performed experiments; Amic F, Drmic D, Bilic Z, Krezic I, Zizek H, Peklic M, Kliceck R, Pajtak A, Amic E, Vidovic T, Rakic M, Milkovic Perisa M, Horvat Pavlov K, Kokot

A, Tvrdeic A, Boban Blagaic A, Zovak M, Seiwert S and Sikiric P analyzed data; Seiwert S and Sikiric P contributed reagents and analytic tools; Amic F, Tvrdeic A, Seiwert S and Sikiric P wrote the manuscript.

Institutional review board statement: The study was reviewed and approved by the Department of Veterinary, Ministry of Agriculture, Republic of Croatia, No: UP/I 322-01/07-01/210.

Institutional animal care and use committee statement: All procedures involving animals were reviewed and approved by the Institutional Animal Care and Use Committee of the Uprava Za Veterinarstvo (NN 135/06).

Conflict-of-interest statement: The authors state that they have no conflicts of interest.

Data sharing statement: No additional data are available.

ARRIVE guidelines statement: The authors have checked the manuscript according to the ARRIVE guidelines.

Open-Access: This article is an open-access article which was selected by an in-house editor and fully peer-reviewed by external reviewers. It is distributed in accordance with the Creative Commons Attribution Non Commercial (CC BY-NC 4.0) license, which permits others to distribute, remix, adapt, build upon this work non-commercially, and license their derivative works on different terms, provided the original work is properly cited and the use is non-commercial. See: <http://creativecommons.org/licenses/by-nc/4.0/>

Manuscript source: Unsolicited manuscript

Corresponding author to: Predrag Sikiric, MD, PhD, Professor, Department of Pharmacology, Medical Faculty,

University of Zagreb, Salata 11, POB 916, Zagreb 10000, Croatia. sikiric@mef.hr
 Telephone: +385-1-4566833
 Fax: +385-1-4920050

Received: August 8, 2018
 Peer-review started: August 9, 2018
 First decision: October 5, 2018
 Revised: November 26, 2018
 Accepted: November 30, 2018
 Article in press: November 30, 2018
 Published online: December 21, 2018

Abstract

AIM

To investigate whether duodenal lesions induced by major venous occlusions can be attenuated by BPC 157 regardless nitric oxide (NO) system involvement.

METHODS

Male Wistar rats underwent superior anterior pancreaticoduodenal vein (SAPDV)-ligation and were treated with a bath at the ligated SAPDV site (BPC 157 10 µg, 10 ng/kg per 1 mL bath/rat; L-NAME 5 mg/kg per 1 mL bath/rat; L-arginine 100 mg/kg per 1 mL bath/rat, alone and/or together; or BPC 157 10 µg/kg instilled into the rat stomach, at 1 min ligation-time). We recorded the vessel presentation (filled/appearance or emptied/disappearance) between the 5 arcade vessels arising from the SAPDV on the ventral duodenum side, the inferior anterior pancreaticoduodenal vein (IAPDV) and superior mesenteric vein (SMV) as bypassing vascular pathway to document the duodenal lesions presentation; increased NO- and oxidative stress [malondialdehyde (MDA)]-levels in duodenum.

RESULTS

Unlike the severe course in the SAPDV-ligated controls, after BPC 157 application, the rats exhibited strong attenuation of the mucosal lesions and serosal congestion, improved vessel presentation, increased interconnections, increased branching by more than 60% from the initial value, the IAPDV and SMV were not congested. Interestingly, after 5 min and 30 min of L-NAME and L-arginine treatment alone, decreased mucosal and serosal duodenal lesions were observed; their effect was worsened at 24 h, and no effect on the collateral vessels and branching was seen. Together, L-NAME+L-arginine antagonized each other's response, and thus, there was an NO-related effect. With BPC 157, all SAPDV-ligated rats receiving L-NAME and/or L-arginine appeared similar to the rats treated with BPC 157 alone. Also, BPC 157 in SAPDV-ligated rats normalized levels of NO and MDA, two oxidative stress markers, in duodenal tissues.

CONCLUSION

BPC 157, rapidly bypassing occlusion, rescued the original duodenal flow through IAPDV to SMV flow, an

effect related to the NO system and reduction of free radical formation.

Key words: Major venous occlusion; Duodenal lesions; BPC 157; L-NAME; Bypassing; L-arginine; Reduction of free radical formation; Rats

© **The Author(s) 2018.** Published by Baishideng Publishing Group Inc. All rights reserved.

Core tip: Up to now, application of prototype cytoprotective agent BPC 157 induced bypassing of occlusion, in rats underwent vessels occlusions, through rapid collaterals presentation, and lesions and whole consequent syndrome (ischemic colitis; deep vein thrombosis, Virchow triad) were attenuated. In rats underwent superior anterior pancreaticoduodenal vein-ligation, medication was with BPC 157, L-NAME; L-arginine, saline given alone and/or together at 1 min ligation time. Unlike severe course in controls, BPC 157 rats commonly exhibited strong attenuation of mucosal lesion and serosal congestion, since BPC 157 rescued original duodenal flow through inferior anterior pancreaticoduodenal vein to superior mesenteric vein flow.

Amic F, Drmic D, Bilic Z, Krezic I, Zizek H, Peklic M, Klicek R, Pajtak A, Amic E, Vidovic T, Rakic M, Milkovic Perisa M, Horvat Pavlov K, Kokot A, Tvrdeic A, Boban Blagaic A, Zovak M, Seiwerth S, Sikiric P. Bypassing major venous occlusion and duodenal lesions in rats, and therapy with the stable gastric pentadecapeptide BPC 157, L-NAME and L-arginine. *World J Gastroenterol* 2018; 24(47): 5366-5378

URL: <https://www.wjgnet.com/1007-9327/full/v24/i47/5366.htm>
 DOI: <https://dx.doi.org/10.3748/wjg.v24.i47.5366>

INTRODUCTION

We focused on major venous occlusions and duodenal lesions in the rat and treatment with the stable gastric pentadecapeptide BPC 157, which is a prototype cytoprotective agent used in ulcerative colitis and multiple sclerosis trials (LD1 not achieved) and is known to counteract duodenal lesions^[1-10]. Rat duodenal lesion research is mostly based on cysteamine and acetic acid models^[11-14]; investigations are sparse on the impact of major venous obstruction and whether recruitment of blood vessels to bypass obstruction may occur quickly, and if so, whether it may be facilitated by a suitable therapy. On the other hand, in rats that underwent other vessel occlusions (*i.e.*, left colic artery and vein, infrarenal inferior caval vein^[15,16]), after application of stable gastric pentadecapeptide BPC 157, the bypassing occurs through a rapid collateral presentation, and the lesions and consequent syndrome were largely attenuated. Rapidly reestablished arcade vessel interconnections upon BPC 157 application mitigated the harm in two ligations of the left colic artery and vein

and consequently alleviated ischemic colitis as well^[15]. In rats with infrarenal inferior caval vein occlusion, the therapeutic effect occurs through the immediate presentation of the left ovarian vein (LOV) and other veins, bypassing the obstruction, and counteracting all the symptoms of Virchow's triad^[16]. The normalized levels of two oxidative stress markers, nitric oxide (NO) and malondialdehyde (MDA), in tissues as well as the reduced L-NAME and L-arginine effects showed BPC 157 effectiveness over the NO-system background^[15,16].

These findings were related^[15,16] to the cytoprotective agents, to the effects originally noted in the stomach, which is the rapid endothelial protection. Using BPC 157 as a prototype cytoprotective agent^[15,16], these mechanisms can prevent and resolve adjacent ischemic mucosal lesions^[17-21] providing activation of the collateral circulation^[15,16]. This activation is specific and can circumvent obstructions^[15,16]. That factor had not been considered in vascular studies of ischemic colitis or deep vein thrombosis^[22-25]. As a result exerted within the immediate post-injury time in vascular studies of ischemic colitis or deep vein thrombosis^[15,16], it reestablishes the continuity of blood flow, in particular^[15,16]. Also, this effect was shown to be a long-lasting effect^[15,16]. It was also applicable in the later period, even after additional colon or major vein obstruction had occurred^[15,16].

This will also resolve mucosal lesions that would appear with disturbed duodenal circulation, if the cytoprotection/endothelium protection is essential^[15,16] to quickly restore blood supply to the ischemic area, and if the application of BPC 157 may offer a fundamental treatment with the rapid and successful recruitment of blood vessels during harmful events. In support, various harmful conditions, all overwhelmed, such as vascular obstruction, short-lasting blood deprivation, reperfusion, long-lasting blood deprivation and additional bowel obstruction, verify that BPC 157 can rapidly activate collaterals as we suggested^[15,16].

We treated occluded superior anterior pancreaticoduodenal veins (SPDAVs) and duodenal lesions (that would otherwise rapidly appear and sustainably progress) with the stable gastric pentadecapeptide BPC 157, L-NAME and L-arginine. Namely, interaction between BPC 157 and NO-system goes in different systems and species. This was also demonstrated using both L-NAME and L-arginine as individual agents or in combination^[1-5] in cytoprotection studies. Furthermore, venous obstruction may be more damaging to the intestine than corresponding artery occlusions and rapidly induces mucosal lesions (*i.e.*, within 5 min in the case of the superior mesenteric vein)^[26]. Thus, bypassing one or more of the vascular obstructions and thereby achieving a therapeutic effect^[15,16] appears, if BPC 157 rapidly activates collaterals due to its particular direct and rapid effect on vessel presentation. The main focus of the intervention was parallel with the findings in the colon and venous tissues^[15,16]. Levels of oxidative stress MDA

and NO were also assessed in duodenal tissue, and the results showed NO- and MDA- duodenal tissue levels and relative to the ligation course or therapeutic effects.

MATERIALS AND METHODS

Animals

We used male Albino Wistar rats, 200 g b.w., randomly assigned to groups with at least 7 rats per group. Local ethics committee approved all of the experiments. Rats had access to food and water *ad libitum* before the procedure and until the end of the experiment. The surgical procedure was performed as well as the assessments were performed by a blinded observer.

Drugs

We used the pentadecapeptide Gly-Glu-Pro-Pro-Pro-Gly-Lys-Pro-Ala-Asp-Asp-Ala-Gly-Leu-Val, M.W. 1419, named BPC 157 (Diagen, Ljubljana, Slovenia), freely soluble in water at pH 7.0 and in saline, prepared as previously described^[1-10]. L-NAME (Sigma, United States) and L-arginine (Sigma, United States) were used as previously described^[1-10].

Experimental procedure and assessment

Surgery: The surgery was conducted in deeply anesthetized rats. The SAPDV was occluded by ligation (Premilene 7/0, Braun) of 5 arcade vessels at the duodenal serosa within the SAPDV branches. The 30-mm blood-flow affecting a duodenum segment was marked (Figure 1).

Medication: We used two regimens of BPC 157 application: 10 µg, 10 ng/kg per 1 mL bath/rat or 10 µg/kg instilled into the rat stomach, at 1 min ligation-time. To investigate the effect of NO-agents [L-NAME (NO-system-blockade), L-arginine (NO-system over-stimulation); L-NAME+L-arginine (NO-system immobilization)] we used L-NAME 5 mg/kg per 1 mL bath/rat; L-arginine 100 mg/kg per 1 mL bath/rat, alone and/or together. Controls received a saline bath of equal volume at 1 min of ligation time or an equal volume of saline instilled into the stomach of the SAPDV-ligated rats.

Assessment: Considering the point immediately before therapy (as 100%) [see the assessment shown in Figure 1 (SAPDV rats)], we scored the vessel presentation {recorded filled/appearance or emptied/disappearance [camera attached to a USB microscope (Veho discovery VMS-004 deluxe)]} between the 5 arcade vessels arising from the SAPDV on the ventral duodenum side (as described before^[15]), the IAPDV, SMV as bypassing vascular pathway. Scoring 0-3 was as follows: 0, presentation similar to healthy rats; 1, mild congestion; 2, moderate congestion; and 3, severe congestion, after 5 min; then, at 30 min, at 24 h. Likewise, upon the duodenum opening and after

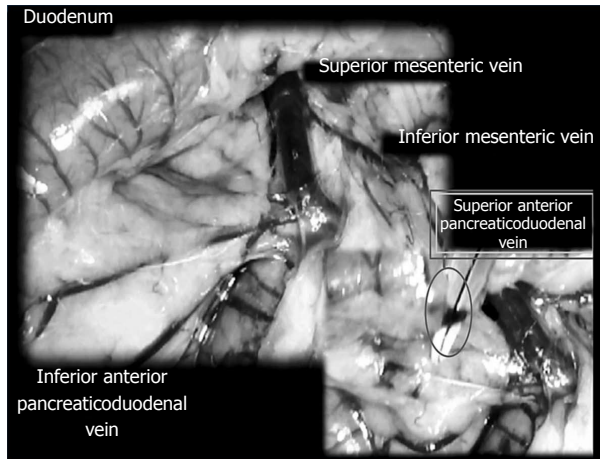


Figure 1 Model illustration of major venous obstruction and duodenal lesions in rat. The major venous obstruction and duodenal lesions in rat, and therapy solution with the stable gastric pentadecapeptide BPC 157, model illustration. Superior anterior pancreaticoduodenal vein (SAPDV) was occluded by ligation (Premilene 7/0, Braun), 5 arcade vessels at duodenal serosa within the SAPDV tributaries, the 30-mm blood-flow disturbed duodenum segment was the marked area; inferior anterior pancreaticoduodenal vein and superior mesenteric vein as bypassing loop.

sacrifice, we assessed the congested hemorrhagic areas as the sum of the largest lesion diameters^[21,27-29]. As described previously^[1-10,15,30], we processed the representative tissue sections for further histological analysis.

Oxidative stress

As described before^[15,16,31,32], at the end of the experiment and at 5 min, 30 min and 24 h of ligation time in SAPDV-ligated rats, we assessed the oxidative stress in the collected tissue samples by quantifying thiobarbituric acid-reactive species (TBARS) as MDA equivalents (results expressed in nmol per mg of protein). Briefly, we homogenized the tissue samples [in PBS (pH 7.4) containing 0.1 mmol/L butylated hydroxytoluene (BHT) (TissueRuptor, Qiagen, United States)] and sonicated [for 30 s in an ice bath (Ultrasonic bath, Branson, United States)], added trichloroacetic acid (TCA, 10%) to the homogenate, centrifuged the mixture (at 3000 rpm for 5 min), and collected the supernatant. Then, we added 1% TBA, boiled the samples (95 °C, 60 min), and kept the tubes on ice for 10 min. Following centrifugation (14000 rpm, 10 min), we determined the absorbance of the mixture at the wavelength of 532 nm. We assessed the concentration of MDA from a standard calibration curve plotted using 1,1,3,3'-tetraethoxypropane (TEP). We express the extent of lipid peroxidation as MDA using a molar extinction coefficient for MDA of 1.56×10^5 mol/L per cm and determined protein concentration using a commercial kit.

NO determination in duodenum tissue

In SAPDV-ligated rats, as described before^[15,16,31,32], at the end of the experiment and at 5 min, 30 min and 24

h ligation time, we determined the NO levels ($\mu\text{mol/mg}$ protein) in the duodenum tissue samples using the Griess reaction (Griess Reagent System, Promega, United States). Briefly, we added sulfanilamide to the homogenized tissue; we incubated the mixture, and added N-1-naphthylethylenediamine dihydrochloride. We measured absorbance at 540 nm using a sodium nitrite solution as a standard. We determined protein concentrations using a commercial kit (BioRad Protein DR Assay Reagent Kit, United States).

Statistical analysis

We used parametric one-way ANOVA with a *post hoc* Newman-Keuls test, nonparametric Kruskal-Wallis and subsequent Mann-Whitney *U*-test to compare the groups. We considered $P < 0.05$ to be statistically relevant.

RESULTS

The regular perilous course in rats with SAPDV occlusion

Failure progressed in control SAPDV-ligated rats (5-30 min - 24 h). Lesions were more than 30 mm in diameter and included hemorrhagic mucosal lesions, serosal congestion (Figures 2-4) with deteriorating vessels, losing collaterals, and branching was present in 30% or less of the initial value at the end of the experiment (Figure 5). IAPDV and SMV were both congested (Figures 2 and 6).

Microscopically (Figure 7), the lesions progressed from mild villous edema with mild lymphocytic infiltrate (5 min ligation time) toward denuded villous tops with marked villous edema and submucosal capillary congestion (30 min ligation time) to the substantial subepithelial space with abundant lifting of epithelial layer from lamina propria extending down sides of villi, villous edema with capillary congestion, submucosal congestion and lymphocytic infiltrate (24 h ligation time) (Figure 7).

Oxidative stress and NO determination in duodenum tissue

The negative chain of events was first characterized by decreased NO levels and increased MDA levels in the duodenum tissue, followed by excessive NO release and increased MDA levels in the duodenum tissue (Figure 8).

The regular course in rats with SAPDV occlusion counteracted with BPC 157 therapy

In contrast, after BPC 157 therapy (applied directly to the duodenum as a bath, or instilled into the stomach), only a few treated rats exhibited more than 10 mm-diameter mucosal lesions and serosal congestion (Figures 2-4). Frequently, vessel presentation was markedly improved with increased interconnections, and branching increased more than 60% from the initial value (Figure 5). IAPDV and SMV were both non-

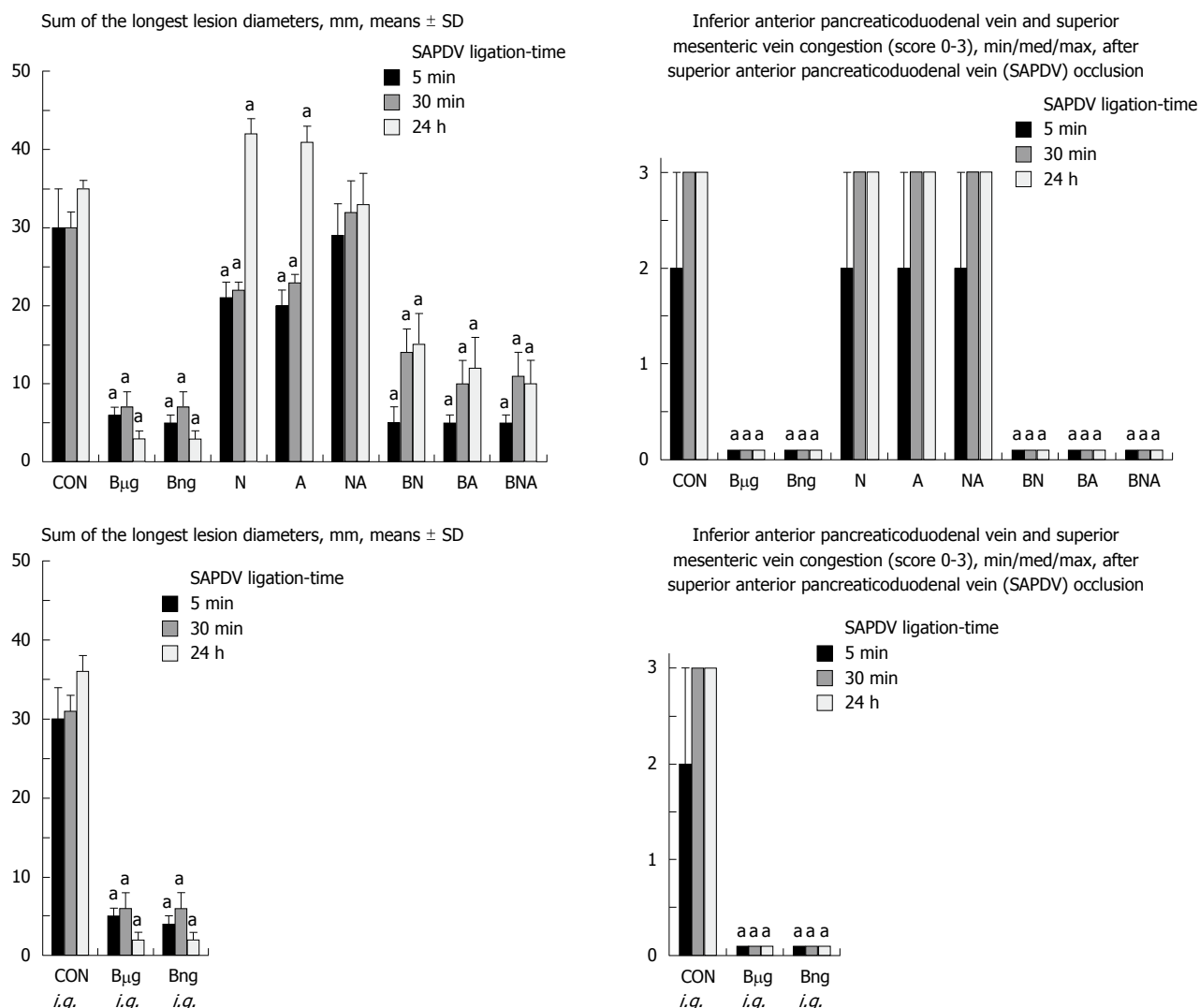


Figure 2 Duodenal lesions as a sum of the longest lesions diameters (left); Inferior anterior pancreaticoduodenal vein and superior mesenteric vein congestion, scored 0-3 (right). The gross appearance of the tissue was recorded using a USB microscope camera. At 1 min post-injury, medication [BPC 157, 10 μ g/kg (B μ g), 10 ng/kg (Bng), L-NAME, 5 mg/kg (N), L-arginine, 100 mg/kg (A) alone and/or together (NA, BN, BA, BNA) 1 mL bath/rat] or an equal volume of a saline was applied to the duodenum of the superior anterior pancreaticoduodenal vein (SAPDV)-ligated rats (upper); alternatively, at 1 min post-injury, medication was B μ g i.g., Bng i.g., 1 mL instillation into the stomach or an equal volume of a saline instilled into the stomach of the SAPDV-ligated rats (CON i.g.) (lower). The rats were sacrificed 5 min, 30 min or 24 h later. ^a*P* < 0.05 vs saline. Bng: BPC 157, 10 ng/kg; B μ g: BPC 157, 10 μ g/kg; N: L-NAME, 5 mg/kg; A: L-arginine, 100 mg/kg; NA: L-NAME+L-arginine; BN: BPC 157+L-NAME; BA: BPC 157+L-arginine; BNA: BPC 157+L-NAME+L-arginine; SAPDV: Superior anterior pancreaticoduodenal vein.

congested (Figures 2 and 6). Thereby, the treatment rescued the original duodenal flow through IAPDV to SMV flow, and the duodenal lesions largely diminished.

Microscopically, BPC 157 rats exhibited intestinal preservation with only mild villous edema and mild lymphocytic infiltrates. The elevation of the epithelium from the lamina propria was found only on the apical portion of the villi (after 24 h of ligation) (Figure 7).

Oxidative stress and NO determination in the duodenum tissue with BPC 157 revealed an increase in the duodenal NO values up to the normal values, but normal MDA-values compared to the excessively increased values seen in the controls (Figure 8).

L-NAME and L-arginine, given alone or together; BPC 157 treatment

L-NAME and L-arginine treatment alone decreased

mucosal and serosal duodenal lesions at 5 min and 30 min. Their effects were less at 24 h, but they did not further influence the loss of the collateral vessels and branching. Together, L-NAME+L-arginine antagonized each other's response at any treatment point, and thus, NO-related effects were seen. When treated with BPC 157, all SAPDV-ligated rats receiving L-NAME and/or L-arginine responded similarly to the rats treated with BPC 157 alone (Figures 2, 5 and 6).

Thus, it seems that BPC 157 rescues SAPDV failure and duodenum lesions, and its effect is related to the NO system.

DISCUSSION

We attempted to alleviate major venous obstruction and duodenal lesions in rats with stable gastric

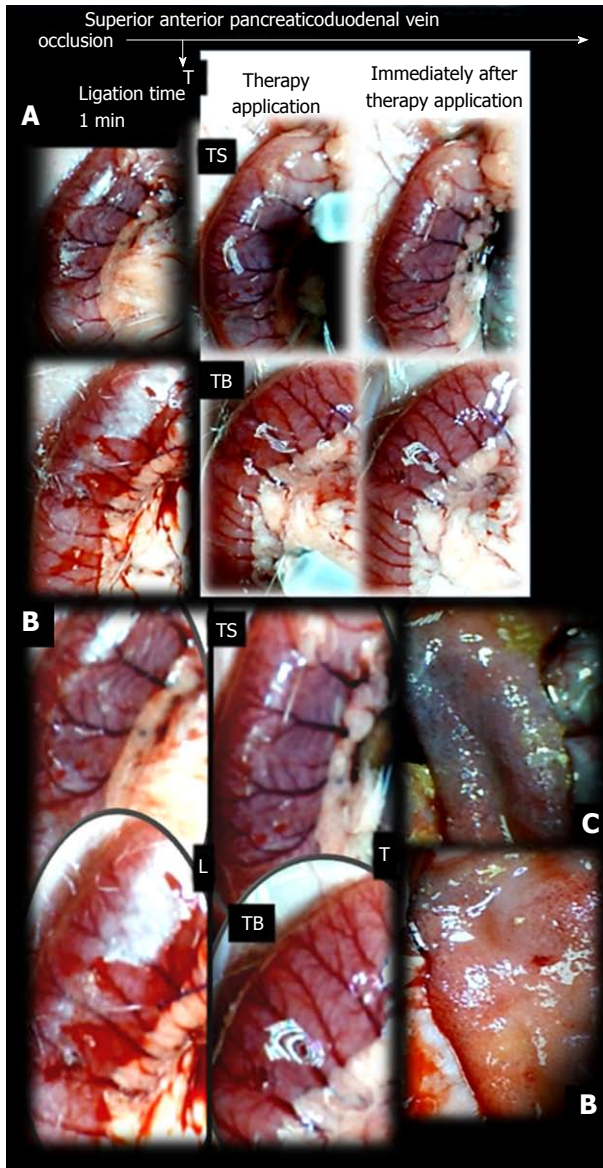


Figure 3 Characteristic appearance of the duodenum in superior anterior pancreaticoduodenal vein-ligated rats. A: The characteristic appearance of the duodenum in superior anterior pancreaticoduodenal vein (SAPDV)-ligated rats after ligation (before therapy), and then with therapy: during and immediately after medication bath [saline (upper); BPC 157 (lower) application; duodenum opening before sacrifice at 5 min ligation-time; USB microscope camera]. Therapy with saline bath. Congested duodenal serosa and duodenal arcades with few vessels branching before, during and after medication saline bath. The congested haemorrhagic area was observed upon duodenal opening after saline bath treatment in rats that underwent obstruction of the SAPDV for 5 min. Therapy with BPC 157 bath. Immediately with BPC 157 medication applied as a bath apparently not congested serosa and vessels with increased branching replaced congested duodenal serosa and duodenal arcades with few vessel branching. Area without apparent congestion and haemorrhage was observed upon duodenal opening after BPC 157 bath treatment in rats that underwent obstruction of the SAPDV for 5 min; B: High magnification of presentation with ligation, and presentation of the moment immediately with therapy application, as saline bath as medication, or BPC 157 bath medication. L: Ligation; T: Therapy; TS: Therapy with saline bath; TB: Therapy with BPC 157 bath; C: Congested haemorrhagic area; B: Area without apparent congestion and haemorrhage.

pentadecapeptide BPC 157 treatment and to investigate its relation to the NO system^[1-10]. In duodenal lesion

development, the occlusion of the SAPDV appears as the key failure (before other vessel occlusions: *i.e.*, left colic artery and vein ligation, and inferior caval vein ligation)^[15,16] that could never be spontaneously alleviated, even though well-placed vessels or additional therapy with NO agents [NOS-over-activation (L-arginine) and/or NOS-blockade (L-NAME)]. On the other hand, BPC 157 therapy resulted in promptly alleviated vascular presentation and then alleviated a perilous course of duodenal lesions in rats with SAPDV occlusions. We documented again “running” toward the bypassing vessel occlusion(s)^[15,16] and that BPC 157 after SAPDV occlusion quickly restores the blood supply to the ischemically injured area. BPC 157 rapidly activates collaterals much like a fundamental treatment that counteracted the injurious course (ischemic colitis^[15]; the syndrome resulting from inferior caval vein infrarenal-ligation^[16]) and this effect involves the NO system and reduction of free radical formation^[15,16].

The SAPDV-ligated rats treated with BPC 157 exhibited a complete reduction of the SAPDV-occlusion syndrome: improved vessel presentation, increased interconnections, duodenal arcade branching increased up to 60% from the initial value, and uncongested IAPDV and SMV. Thereby, BPC 157 treatment rescued the original duodenal flow through IAPDV to SMV flow and largely mitigated the duodenal lesions (Figures 2-6). The results provide consistent evidence for the beneficial effects of a rapid and sustained BPC 157 μg and ng regimen.

In addition, we clarified the distinction between BPC 157 and NO-agent activity. We assumed that a prolonged occlusion would result in a more severe lesion and that a persisting and powerful defensive process would oppose these injuries and assure long-lasting protection. Thus, BPC 157 therapy, along with the findings mentioned before^[15,16], exhibited a special “bypassing” effect (through arcade vessels and/or minor and major vessels^[15,16]) making vascular occlusion harmless and reorganizing the blood flow to counteract the duodenal lesions in rats with SAPDV-ligation. Similar to occlusion of the other vessels^[15,16], this study indicates the early positive outcome (“bypassing” effect) of BPC 157 that may be crucial for its persisting beneficial effect, even with continuous occlusions. The effect of BPC 157 in rats with SAPDV-ligation and rats with left colic artery and vein ligations may indicate that the action of BPC 157 overlaps in the duodenum and colon^[15,16]. BPC 157 plays an important role in with respect to the “bypassing” effect that maintains duodenum and colon mucosal integrity^[15,16] and interacts with the NO system (L-NAME and L-arginine exhibited parallel effects (lesion worsening), which mitigated each other) in SAPDV, left colic artery and vein circulation, and duodenal and colon lesions^[15,16]. Together, the “bypassing” effect combined with duodenum (and colon) mucosal integrity as the revealed phenomenon could be quite complex^[15,16] as it was

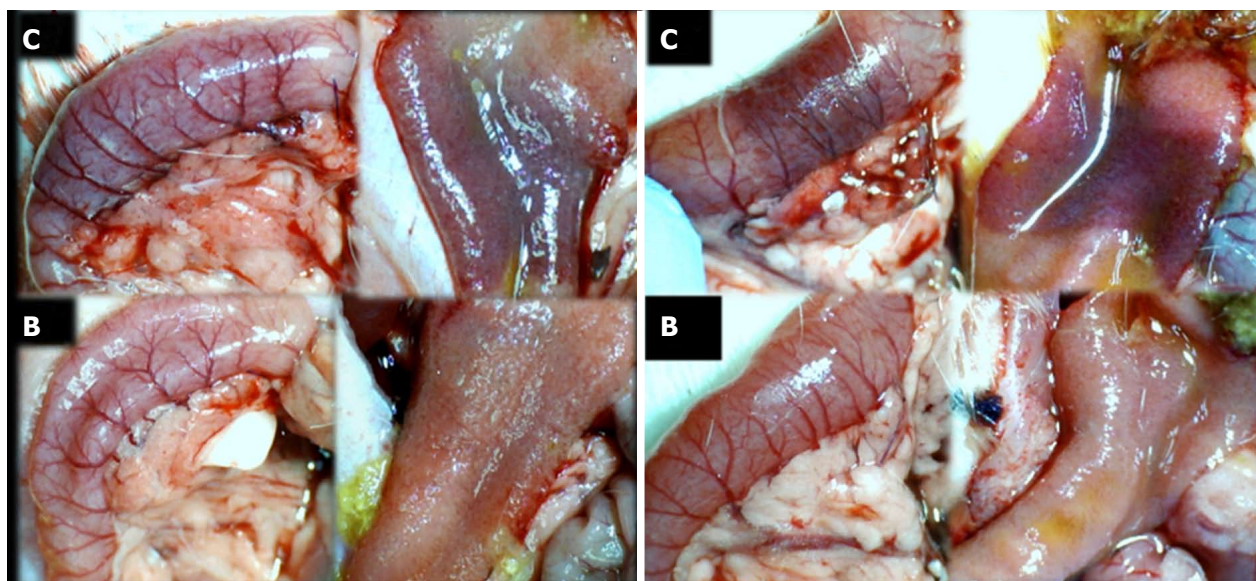


Figure 4 Characteristic appearance of the duodenum in superior anterior pancreaticoduodenal vein-ligated rats at 30 min (left) or 24 h (right) ligation-time. After medication bath [saline (upper) (C); BPC 157 (lower) (B) application]; duodenum opening before sacrifice at 30 min (left) or 24 h (right) ligation-time; USB microscope camera. Control: 30 min. Congested duodenal serosa and duodenal arcades with few vessel branching. Congested haemorrhagic upon duodenal opening. 24 h. Severely congested duodenal serosa and duodenal arcades with few vessel branching. Severely congested haemorrhagic upon duodenal opening. BPC 157 therapy: 30 min. Not congested serosa and vessels with increased branching. Area without apparent congestion and haemorrhage was observed upon duodenal opening; 24 h. Not congested serosa and vessels with increased branching. Area without apparent congestion and haemorrhage was observed upon duodenal opening. C: Control; B: BPC 157.

seen with respect to the L-NAME (NOS blockade) and L-arginine (NOS over-activity) treatments, which given alone and/or together (NO-system immobilized) never exhibited the “bypassing” effect and did not provide any mucosal protection^[15,16]. However, when given together with BPC 157 (L-NAME+BPC 157; L-arginine+BPC 157; L-NAME+L-arginine+BPC 157), with either SAPDV-ligation or left colic artery and vein ligation, the BPC 157 beneficial effect was observed, compensating either the L-NAME and L-arginine effects, while mucosal protection was seen at a higher level.

It is possible that the environment created by vessel(s) occlusion is responsible for the “bypassing” effect (SAPDV-duodenal arcade vessel interconnections-IAPDV-SMV required for adequate compensation and duodenal mucosal protection consistently obtained by BPC 157 administration) and remains outside the regular L-NAME or L-arginine influence on blood vessels but inside BPC 157 influence on NO-agent effects. L-NAME and L-arginine were given in doses necessary to instantly induce hypertension or hypotension^[33], while both effects were counteracted by BPC 157 administration^[33]. Providing a complex beneficial effect, BPC 157 did not affect normal blood pressure^[33]; in addition to counteracting L-NAME induced hypertension and L-arginine induced hypotension^[33], when BPC 157 counteracted arterial^[34] or venous hypertension^[16] or systemic hypotension^[16], it also counteracted other disturbances, which may be related to blood pressure disturbances (*i.e.*, potassium-overload induced arrhythmias^[34]; Virchow’s triad^[16]; chronic heart failure induced by doxorubicin in hypotensive rats and mice^[35];

venous hypertension in systemically hypotensive rats with inferior caval vein occlusion^[16]). Therefore, in SAPDV-ligated rats, venous occlusion alone causes severe congestion and increased intravascular pressure^[26]; the vessels hampered with occlusions would fail to respond to either NO agent. On the other hand, this complete failure is not present in left colic artery and vein ligated rats^[15] (arterial occlusion results only in reduced inflow perfusion with normal outflow^[26], arteriovenous occlusion balances inflow and outflow alteration). Thus, the arteriovenous occlusion, intravascular pressure and tone equilibrium^[26] (left colic artery and vein ligated rats^[15]) still permits NO-agents activity, unlike the venous occlusion, severe congestion and increased intravascular pressure^[26] (SAPDV-ligated rats). Syndrome in left colic artery and vein ligated rats^[15] [the decrease (L-NAME) or increase (L-arginine) in vessels], but without the vessel interconnection and bypassing effect, worsening the mucosal lesions (even after the initial short-lasting protective effect) accords with the more severe syndrome in SAPDV-ligated rats (vessels unresponsive to NO-agents) (Figure 5).

The common failure to heal SAPDV or left colic artery and vein occlusions^[15], parallelism much like in other models^[15,35,36], substantiates particular aspect of a NO system dual (L-NAME vs L-arginine) role (vs combination) (for review, see^[1-5]). Parallel L-NAME/L-arginine activity, which was noted as parallel outcomes, as a specific point (much like before^[15,35,36], L-NAME and L-arginine regularly attenuated or antagonized each other’s responses, presenting values comparable to the control), also appeared with two pharmacologically distinct

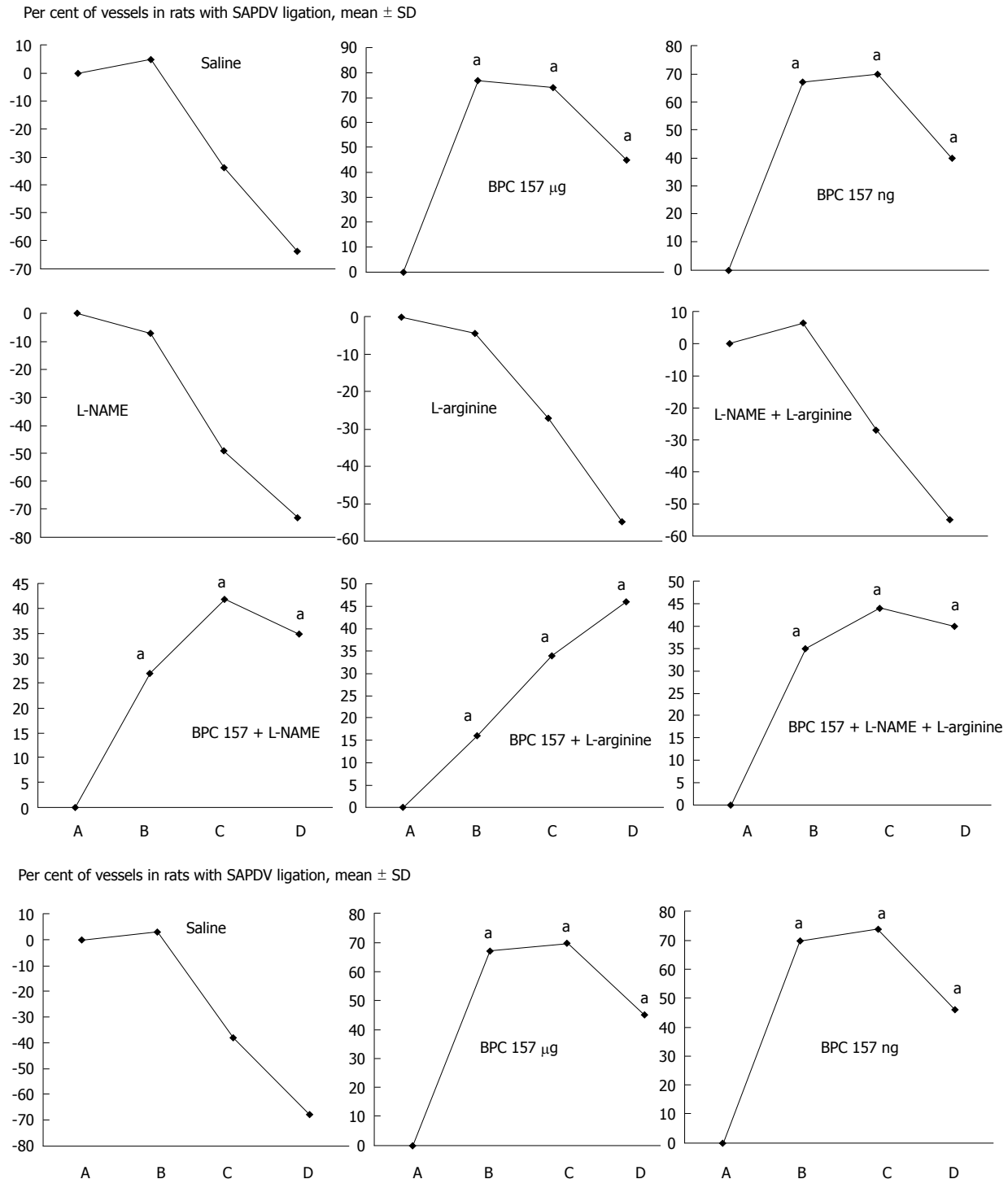


Figure 5 Percent of vessels present between 5 arcade vessels on the ventral side of the duodenum in different time points. Percent of vessels present between 5 arcade vessels on the ventral side of the duodenum 1 min following ligation before therapy (as 100%) (A); mean \pm SD. The gross appearance of the tissue was recorded using a USB microscope camera. The following time points were assessed: A: After ligation and before therapy (1 min); B: 5 min after the application of medication; C: 30 min after the application of medication; D: 24 h after the application of medication. At 1 min post-injury, medication [BPC 157, 10 μ g/kg (BPC 157 μ g), 10 ng/kg (BPC 157 ng), L-NAME, 5 mg/kg (L-NAME), L-arginine, 100 mg/kg (L-arginine) alone and/or together (L-NAME+L-arginine, BPC 157+L-NAME, BPC 157+L-arginine, BPC 157+L-NAME+L-arginine) 1 mL bath/rat] or an equal volume of a saline was applied to the duodenum of the SAPDV-ligated rats (upper); alternatively, at 1 min post-injury, medication was BPC 157 μ g, BPC 157 ng, 1 mL instillation into the stomach or an equal volume of a saline (saline) instilled into the stomach of the superior anterior pancreaticoduodenal vein-ligated rats (lower). The rats were sacrificed 5 min, 30 min or 24 h later. For clarity, the SD is not shown on the graph; the SD was never higher than 10% of the mean. ^a $P < 0.05$ vs saline. BPC 157 μ g: BPC 157, 10 μ g/kg; BPC 157 ng: BPC 157, 10 ng/kg; L-NAME: L-NAME, 5 mg/kg; L-arginine: L-arginine, 100 mg/kg.

mechanisms with opposing effects on the same signaling pathway (for review, see^[1-5]). In SAPDV-ligated rats, this parallelism is constant with also distinctive effects, lesion

attenuation (early intervals) vs lesion worsening (late interval), unless BPC 157 had been administered and the beneficial effect always attenuated the lesion^[15,35,36].

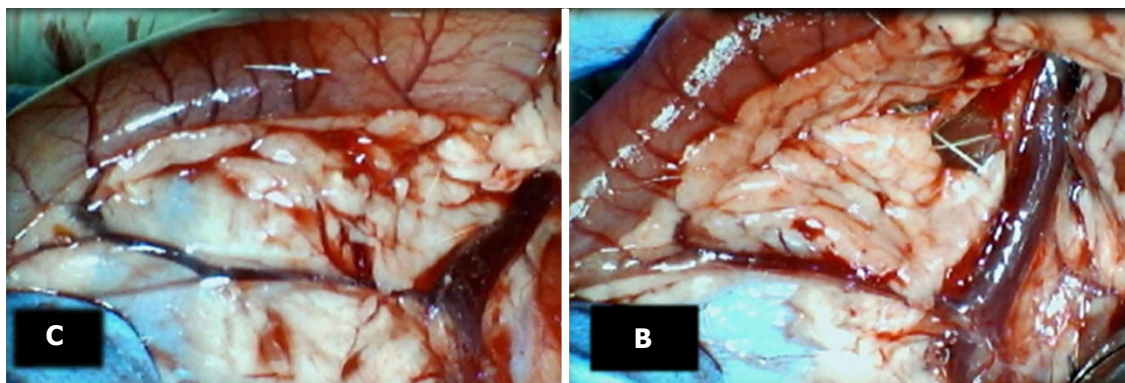


Figure 6 Characteristic appearance of inferior anterior pancreaticoduodenal and superior mesenteric vein presentation in superior anterior pancreaticoduodenal vein-ligated rats at 24 h ligation time. Control, left (C). Congested inferior anterior pancreaticoduodenal and superior mesenteric vein presentation along with duodenal serosa and arcade vessels. during and immediately after medication bath [saline (C); BPC 157, right (B)]. Presentation close to normal, unlike congested inferior anterior pancreaticoduodenal and superior mesenteric vein presentation along with duodenal serosa and arcade vessels in controls. C: Control; B: BPC 157.

Likewise, if the NO system immobilized (mutual actions of the combined L-NAME and L-arginine), it still produces the severe pathology in the L-NAME+L-arginine animals. If this remained severe pathology is further attenuated, it means that the other system(s) (likely cholinergic and BPC 157) functioned along with. In this view, the particular role of BPC 157 reestablished effectiveness (L-NAME+L-arginine → L-NAME+L-arginine+BPC 157). It means that BPC 157 is effective (L-NAME+L-arginine+BPC 157; L-arginine+BPC 157; L-NAME+ BPC 157) with all of the NO-system presentations [inactivated (L-NAME + L-arginine); overstimulated (L-arginine); or blocked (L-NAME)]^[15,35,36]. Thus, the three distinct NO-endpoints (NO-immobilization; -over-activity; -blockade) should be overwhelmed to achieve vessel presentation seen in rats that underwent BPC 157 treatment^[15,35,36]. BPC 157 may consolidate the NO system to produce more effective healing (*i.e.*, the stimulatory and inhibitory effects of the NO system promoted the interconnection of arcade vessels to bypass major obstructions) (a result not observed with L-NAME or L-arginine treatment)^[15].

This special BPC 157 role seems to be supported by the NO and MDA values seen in the duodenal tissues. The beneficial effects promptly counteract the full negative syndrome. Otherwise, after SAPDV-ligation, sudden decrease of blood supply appears. NO-levels decrease in the duodenum tissue. Heavy loss of endothelial cells occurs immediately from the vascular wall^[37]. A lower eNOS production ability^[37], oxidative stress appears as a result of the lysis of endothelial cells^[38,39]; and excessive NO release generated by the inducible isozyme damaging the vascular wall and other tissues cells, especially in combination with reactive oxygen intermediates, and failing endothelial production^[32,40,41]. The positive chain of events includes a BPC 157 treatment restored endothelial integrity and reversed most of the oxidative damage^[15,16,31,32] while interacting with the NO system^[1-5]. The positive endothelium syndrome (*i.e.*, increased duodenal NO-values, but normal MDA-values, indicative of adequate eNOS system function^[1-5]) appears with general

significance, and thereby, restored endothelial integrity and reversed most of the oxidative damage. With BPC 157, this recovery appears even during reperfusion (occurring while vessel occlusion is still present) much like during exaggerated reperfusion (occurring when vessel occlusion is removed)^[15].

There is evidence that BPC 157 also affects several other molecular pathways^[16,42-47], and thereby, the rapid recruitment of existing blood vessels following ongoing harmful events instead otherwise poor response to increased demands. Combined, these findings may substantiate the effects of which were seen at the later time point. In addition, this may accentuate the original cytoprotection understanding (endothelium maintenance → epithelium maintenance)^[17-21] to the complexity of reestablishing original flow by bypassing occlusion^[15,16]. And thereby, we documented recovery of SAPDV-occlusion by AIPDV → SMV, or ICV-occlusion by LOV and other veins^[16], or even two obstructions, the proximal and distal ligations in the left colic artery and vein through arcades within the ligations in rats with colitis^[15]. Furthermore, its subsequent strong angiogenic effect and its healing effects^[9,43-49] may be consequence of the specific activation of the collateral circulation that can circumvent obstructions and reestablish the continuity of blood flow^[15,16]. And thereby, its angiogenic effect and its healing effects^[9,43-49] may overcome those of standard anti-ulcer agents^[48]. Also, these effects are likely to be further extended. BPC 157 accelerates the blood flow recovery and vessel number in rats with hindlimb ischemia^[43]. BPC 157 upregulates VEGFR2 expression in rats with hindlimb ischemia and endothelial cell cultures and promotes VEGFR2 internalization in association with VEGFR2-Akt-eNOS activation^[43]. As mentioned, shared limitation of activity^[17-21,50], only prophylactic effectiveness of standard cytoprotective agents, is avoided. With both prophylactic and therapeutic abilities^[1-10], native and stable in human gastric juice BPC 157 as a novel mediator of Robert's cytoprotection^[1-10] maintains gastrointestinal mucosal integrity^[1-10]. In addition, the comparative effectiveness of BPC 157 when instilled into

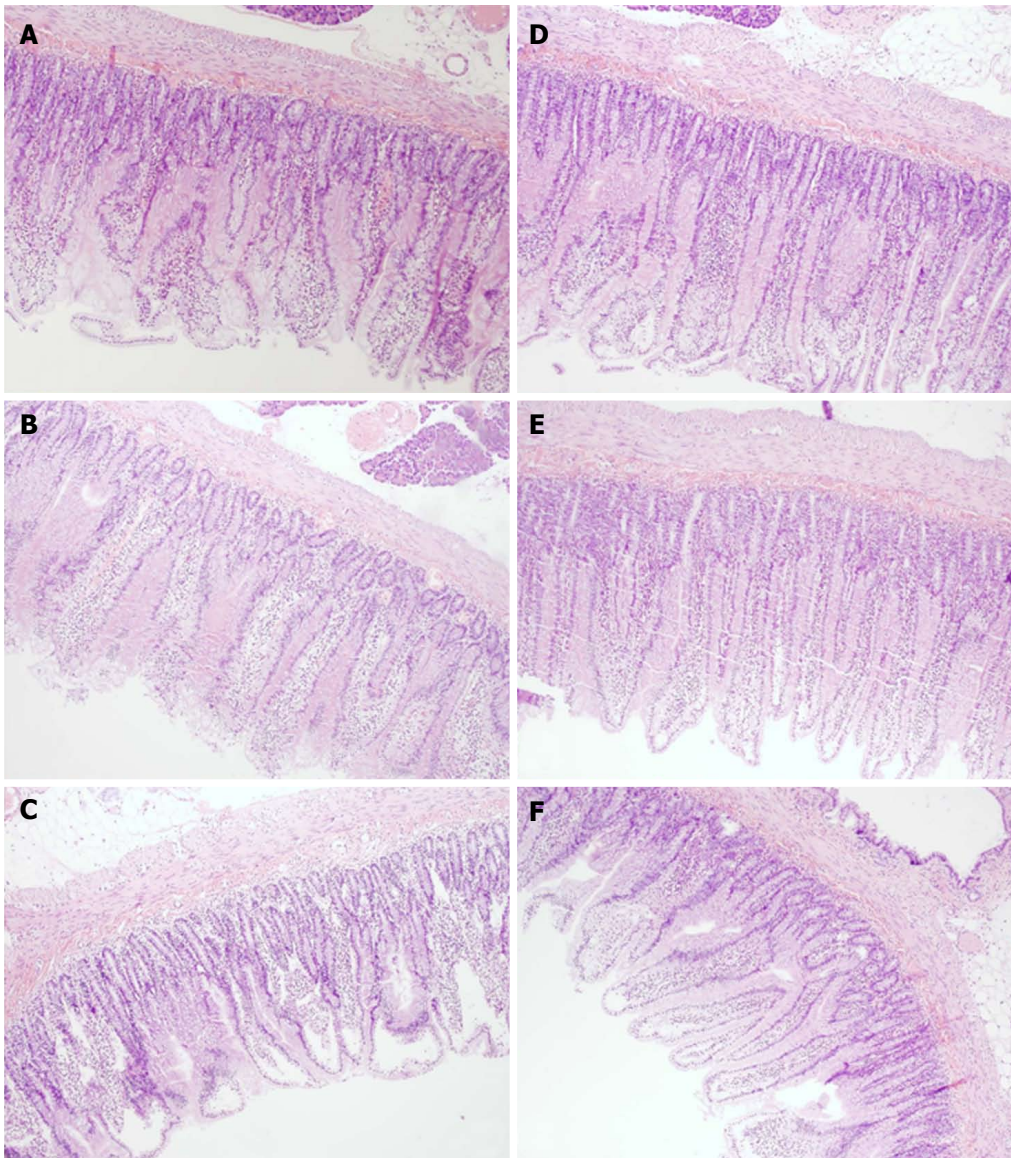


Figure 7 Microscopical presentation of duodenal lesions. Microscopically (Hex10), in controls the lesions progressed from mild villous edema with mild lymphocytic infiltrate (5 min ligation time) (A) toward denuded villous tops with marked villous edema and submucosal capillary congestion (30 min ligation time) (B) to the substantial subepithelial space with abundant lifting of epithelial layer from lamina propria extending down sides of villi, villous edema with capillary congestion, submucosal congestion and lymphocytic infiltrate (24 h ligation time) (C). BPC 157 rats (D, E, F) exhibited always intestinal preservation with only mild villous edema and mild lymphocytic infiltrate. Elevation of epithelium from lamina propria was found only on the apical portion of villi (24 h ligation time, F).

the stomach supports this contention of a prototype of a more effective class of cytoprotective agents.

In conclusion, this study provides evidence for a “bypassing” effect combined with mucosal integrity (*i.e.*, duodenum and colon) or major vessel obstruction made harmless^[15,16] as observed after BPC 157 treatment, which can be regarded as an implementation of the original cytoprotection concept in vascular occlusion therapy.

ARTICLE HIGHLIGHTS

Research background

The research background was our recent claim that treatment with the prototype cytoprotective agent, stable gastric pentadecapeptide BPC 157, induced

bypassing of occlusions in rats that underwent vessel occlusions through the rapid presentation of collaterals. In this study, we focused on the resolving of the duodenal lesions induced by major venous occlusions. These lesions can be counteracted by BPC 157 regardless of the involvement of the nitric oxide (NO) system while recruitment of blood vessels to bypass obstruction may occur quickly.

Research motivation

Research motivation was to resolve the major venous occlusions and duodenal lesions in the rat with the use of the stable gastric pentadecapeptide BPC 157 and/or NO-agents, L-NAME (NOS-blocker) and L-arginine (NOS-substrate). BPC 157 is a prototype cytoprotective agent used in ulcerative colitis and multiple sclerosis trials (LD1 not achieved) and is known to counteract duodenal lesions. Rat duodenal lesion research is mostly based on cysteamine and acetic acid models. Investigations are sparse on the impact of major venous obstruction and whether recruitment of blood vessels to bypass obstruction may occur quickly, and if so, whether it may be facilitated by a suitable therapy.

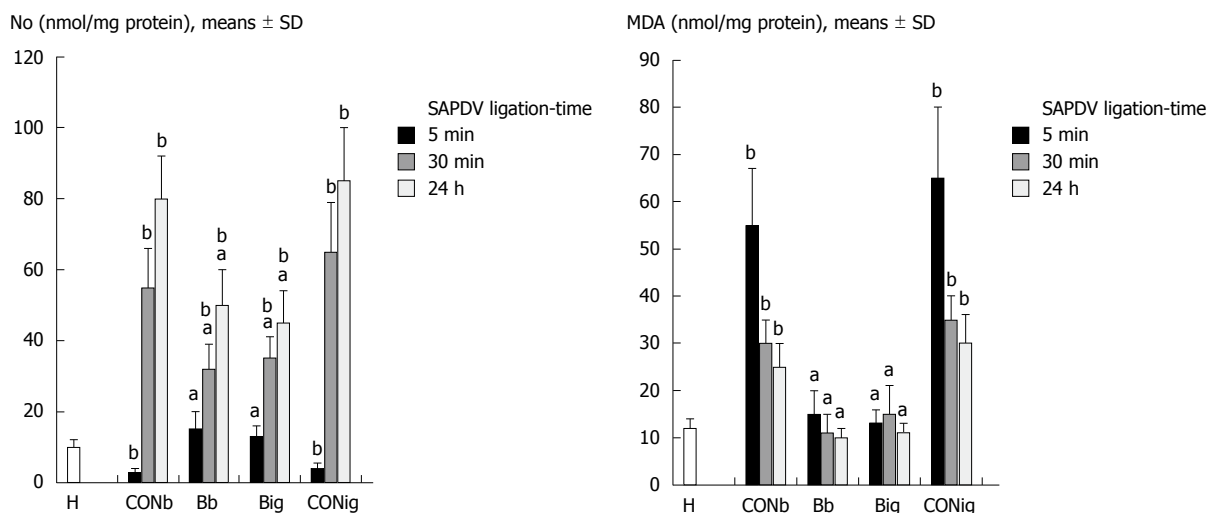


Figure 8 Nitric oxide levels and malondialdehyde levels in the duodenal tissue of superior anterior pancreaticoduodenal vein-ligated rats at 5 min, 30 min and 24 h ligation. BPC 157 [10 μ g/kg, 1 mL bath/rat (Bb), 1 mL instilled into the stomach (Big)] or an equal volume of a saline bath (CONb) or instillation in the stomach (CONig) (controls) was applied to superior anterior pancreaticoduodenal vein-ligated rats. ^a $P < 0.05$ vs saline; ^{*} $P < 0.05$ vs healthy duodenum. H: Healthy duodenum; Bb: BPC 157 10 μ g/kg, 1 mL bath/rat; Big: BPC 157 10 μ g/kg, 1 mL instilled into the stomach; CONb: 1 mL saline bath; CONig: 1 mL saline instillation in the stomach; NO: Nitric oxide; MDA: Malondialdehyde.

Research objectives

Research objectives were the occluded superior anterior pancreaticoduodenal vein (SAPDV) and duodenal lesions (congestion) and the recovering effect (rapidly activated collaterals bypassing vascular occlusion, absent lesions), the therapy effect of stable gastric pentadecapeptide BPC 157 vs harmful effect of NO-agents [L-NAME (NO-system-blockade), L-arginine (NO-system over-stimulation); L-NAME+L-arginine (NO-system immobilization)]. We recorded the vessel presentation (filled/appearance or emptied/disappearance) between the 5 arcade vessels arising from the SAPDV on the ventral duodenum side, the inferior anterior pancreaticoduodenal vein (IAPDV), superior mesenteric vein (SMV) as bypassing vascular pathway to document the duodenal lesions presentation. In duodenum, BPC 157 normalizes NO-levels and counteracts increased oxidative stress [malondialdehyde (MDA)]-levels.

Research methods

For research methods, we used rats with the occluded SAPDV and duodenal lesions (congestion) to reveal the recovering effect (rapidly activated collaterals bypassing vascular occlusion, absent lesions), at 5 min, 30 min and 24 h ligation time. Therapy effect of the stable gastric pentadecapeptide BPC 157 was achieved with two regimens (10 μ g, 10 ng/kg per 1 mL bath/rat or 10 μ g/kg instilled into the rat stomach), at 1 min ligation-time. Harmful effect of NO-agents [L-NAME (NO-system-blockade), L-arginine (NO-system over-stimulation); L-NAME+L-arginine (NO-system immobilization)] goes with L-NAME 5 mg/kg per 1 mL bath/rat; L-arginine 100 mg/kg per 1 mL bath/rat, alone and/or together. Considering the point immediately before therapy (as 100%), we scored the vessel presentation [recorded filled/appearance or emptied/disappearance (camera attached to a USB microscope)] between the 5 arcade vessels arising from the SAPDV on the ventral duodenum side, the IAPDV, SMV as bypassing vascular pathway. Upon the duodenum opening and after sacrifice, we assessed the congested hemorrhagic areas as the sum of the largest lesion diameters. In the collected duodenal tissue samples, we assessed NO-levels (Griess reaction) and oxidative stress [by quantifying thiobarbituric acid-reactive species (TBARS) as MDA equivalents].

Research results

For research results, we attempted to alleviate major venous obstruction and duodenal lesions in rats with stable gastric pentadecapeptide BPC 157 treatment and to investigate its relation to the NO system. In duodenal lesion development, the occlusion of the SAPDV appears as the key failure (before other vessel occlusions: *i.e.*, left colic artery and vein ligation, and inferior caval vein ligation) that could never be spontaneously alleviated, even though well-placed vessels or additional therapy with NO agents [NOS-over-activation

(L-arginine) and/or NOS-blockade (L-NAME)]. On the other hand, BPC 157 therapy resulted in promptly alleviated vascular presentation and then alleviated a perilous course of duodenal lesions in rats with SAPDV occlusions. We documented again "running" toward the bypassing vessel occlusion(s) and that BPC 157 after SAPDV occlusion quickly restores the blood supply to the ischemically injured area. BPC 157 rapidly activates collaterals much like a fundamental treatment that and counteracted the injurious course (ischemic colitis; the syndrome resulting from inferior caval vein infrarenal-ligation) and this effect involves the NO system and reduction of free radical formation.

Research conclusions

The new phenomena that were found through experiments in this study of the duodenal lesions with an obstructed major vein (SAPDV) offered is the early positive outcome ("bypassing" effect) of BPC 157. The hypotheses that were confirmed through experiments in this study are related to the cytoprotective agents, to the effects originally noted in the stomach, which is the rapid endothelial protection. Using BPC 157 as a prototype cytoprotective agent, these mechanisms can prevent and resolve adjacent ischemic mucosal lesions providing activation of the collateral circulation. This activation is specific and can circumvent obstructions. That effect may be crucial for its persisting beneficial effect, even with continuous occlusions. The effect of BPC 157 in rats with SAPDV-ligation and previously, in rats with left colic artery and vein ligations may indicate that the action of BPC 157 overlaps in the duodenum and colon. BPC 157 plays an important role in with respect to the "bypassing" effect that maintains duodenum and colon mucosal integrity and interacts with the NO system [L-NAME and L-arginine exhibited parallel effects (lesion worsening), which mitigated each other] in SAPDV, left colic artery and vein circulation, and duodenal and colon lesions. Thus, these findings can be regarded as an implementation of the original cytoprotection concept in vascular occlusion therapy.

Research perspectives

For research perspectives, we attempted to alleviate major venous obstruction and duodenal lesions in rats with stable gastric pentadecapeptide BPC 157 treatment and to investigate its relation to the NO system. In duodenal lesion development, the SAPDV occlusion appears as the key failure that could never be spontaneously alleviated, even though well-placed vessels or additional therapy with NO agents [NOS-overactivation (L-arginine) and/or NOS-blockade (L-NAME)]. Finally, BPC 157 therapy results in "bypassing" effect combined with mucosal integrity, or major vessel obstruction made harmless. These BPC 157 effects can be an implementation of the original cytoprotection concept in vascular occlusion therapy.

REFERENCES

- 1 **Sikirić P**, Seiwerth S, Rucman R, Drmic D, Stupnisek M, Kokot A, Sever M, Zoricic I, Zoricic Z, Batelja L, Ziger T, Luetic K, Vlaine J, Rasic Z, Bencic ML. Stress in gastrointestinal tract and stable gastric pentadecapeptide BPC 157. Finally, do we have a solution? *Curr Pharm Des* 2017; **23**: 4012-4028 [PMID: 28228068 DOI: 10.2174/1381612823666170220163219]
- 2 **Sikirić P**, Seiwerth S, Rucman R, Kolenc D, Vuletic LB, Drmic D, Grgic T, Strbe S, Zukanovic G, Crvenkovic D, Madzarac G, Rukavina I, Sucic M, Baric M, Starcevic N, Krstonijevic Z, Bencic ML, Filipic I, Rokotov DS, Vlaine J. Brain-gut axis and pentadecapeptide BPC 157: Theoretical and practical implications. *Curr Neuropharmacol* 2016; **14**: 857-865 [PMID: 27138887]
- 3 **Seiwerth S**, Breic L, Vuletic LB, Kolenc D, Aralica G, Misic M, Zenko A, Drmic D, Rucman R, Sikirić P. BPC 157 and blood vessels. *Curr Pharm Des* 2014; **20**: 1121-1125 [PMID: 23782145]
- 4 **Sikirić P**, Seiwerth S, Rucman R, Turkovic B, Rokotov DS, Breic L, Sever M, Klicek R, Radic B, Drmic D, Ilic S, Kolenc D, Aralica G, Stupnisek M, Suran J, Barisic I, Dzidic S, Vrcic H, Sebecic B. Stable gastric pentadecapeptide BPC 157-NO-system relation. *Curr Pharm Des* 2014; **20**: 1126-1135 [PMID: 23755725]
- 5 **Sikirić P**, Seiwerth S, Rucman R, Turkovic B, Rokotov DS, Breic L, Sever M, Klicek R, Radic B, Drmic D, Ilic S, Kolenc D, Aralica G, Safic H, Suran J, Rak D, Dzidic S, Vrcic H, Sebecic B. Toxicity by NSAIDs. Counteraction by stable gastric pentadecapeptide BPC 157. *Curr Pharm Des* 2013; **19**: 76-83 [PMID: 22950504]
- 6 **Sikirić P**, Seiwerth S, Rucman R, Turkovic B, Rokotov DS, Breic L, Sever M, Klicek R, Radic B, Drmic D, Ilic S, Kolenc D, Stambolija V, Zoricic Z, Vrcic H, Sebecic B. Focus on ulcerative colitis: stable gastric pentadecapeptide BPC 157. *Curr Med Chem* 2012; **19**: 126-132 [PMID: 22300085]
- 7 **Sikirić P**, Seiwerth S, Rucman R, Turkovic B, Rokotov DS, Breic L, Sever M, Klicek R, Radic B, Drmic D, Ilic S, Kolenc D, Vrcic H, Sebecic B. Stable gastric pentadecapeptide BPC 157: novel therapy in gastrointestinal tract. *Curr Pharm Des* 2011; **17**: 1612-1632 [PMID: 21548867 DOI: 10.2174/138161211796196954]
- 8 **Sikirić P**, Seiwerth S, Breic L, Sever M, Klicek R, Radic B, Drmic D, Ilic S, Kolenc D. Revised Robert's cytoprotection and adaptive cytoprotection and stable gastric pentadecapeptide BPC 157. Possible significance and implications for novel mediator. *Curr Pharm Des* 2010; **16**: 1224-1234 [PMID: 20166993 DOI: 10.2174/138161210790945977]
- 9 **Sikirić P**, Seiwerth S, Breic L, Blagaic AB, Zoricic I, Sever M, Klicek R, Radic B, Keller N, Sipos K, Jakir A, Udovicic M, Tonkic A, Kokic N, Turkovic B, Mise S, Anic T. Stable gastric pentadecapeptide BPC 157 in trials for inflammatory bowel disease (PL-10, PLD-116, PL 14736, Pliva, Croatia). Full and distended stomach, and vascular response. *Inflammopharmacology* 2006; **14**: 214-221 [PMID: 17186181 DOI: 10.1007/s10787-006-1531-7]
- 10 **Sikirić P**, Petek M, Rucman R, Seiwerth S, Grabarević Z, Rotkvić I, Turković B, Jagić V, Mildner B, Duvnjak M. A new gastric juice peptide, BPC. An overview of the stomach-stress-organoprotection hypothesis and beneficial effects of BPC. *J Physiol Paris* 1993; **87**: 313-327 [PMID: 8298609 DOI: 10.1016/0928-4257(93)90038-U]
- 11 **Szabo S**, Vincze A, Sandor Z, Jadas M, Gombos Z, Pedram A, Levin E, Hagar J, Iaquinio G. Vascular approach to gastroduodenal ulceration: new studies with endothelins and VEGF. *Dig Dis Sci* 1998; **43**: 40S-45S [PMID: 9753225]
- 12 **Szabo S**. Pathogenesis of duodenal ulcer disease. *Lab Invest* 1984; **51**: 121-147 [PMID: 6205219]
- 13 **Szabo S**. Dopamine disorder in duodenal ulceration. *Lancet* 1979; **2**: 880-882 [PMID: 90970]
- 14 **Okabe S**, Amagase K. An overview of acetic acid ulcer models--the history and state of the art of peptic ulcer research. *Biol Pharm Bull* 2005; **28**: 1321-1341 [PMID: 16079471]
- 15 **Duzel A**, Vlaine J, Antunovic M, Malekinusic D, Vrdoljak B, Samara M, Gojkovic S, Krezic I, Vidovic T, Bilic Z, Knezevic M, Sever M, Lojo N, Kokot A, Kolovrat M, Drmic D, Vukojevic J, Kralj T, Kasnik K, Siroglavic M, Seiwerth S, Sikirić P. Stable gastric pentadecapeptide BPC 157 in the treatment of colitis and ischemia and reperfusion in rats: New insights. *World J Gastroenterol* 2017; **23**: 8465-8488 [PMID: 29358856 DOI: 10.3748/wjg.v23.i48.8465]
- 16 **Vukojević J**, Siroglavić M, Kašnik K, Kralj T, Stanić D, Kokot A, Kolaric D, Drmic D, Sever AZ, Barišić I, Suran J, Bojić D, Patrlj MH, Sjekavica I, Pavlov KH, Vidović T, Vlaine J, Stupnisek M, Seiwerth S, Sikirić P. Rat inferior caval vein (ICV) ligation and particular new insights with the stable gastric pentadecapeptide BPC 157. *Vascul Pharmacol* 2018; **106**: 54-66 [PMID: 29510201 DOI: 10.1016/j.vph.2018.02.010]
- 17 **Szabo S**. Mechanisms of Mucosal Protection. In: Gastric Cytoprotection. Boston: Springer, 1989: 49-73
- 18 **Szabo S**, Trier J. Pathogenesis of acute gastric mucosal injury: Sulphydryls as a protector, adrenal cortex as a modulator, and vascular endothelium as a target. In: Allen A, Flemstrom G, Garner A, Silen W, Turnberg L. Mechanism of mucosal protection in the upper gastrointestinal tract. New York: Raven, 1984: 387-393
- 19 **Trier JS**, Szabo S, Allan CH. Ethanol-induced damage to mucosal capillaries of rat stomach. Ultrastructural features and effects of prostaglandin F2 beta and cysteamine. *Gastroenterology* 1987; **92**: 13-22 [PMID: 3781180]
- 20 **Szabo S**, Trier JS, Brown A, Schnoor J. Early vascular injury and increased vascular permeability in gastric mucosal injury caused by ethanol in the rat. *Gastroenterology* 1985; **88**: 228-236 [PMID: 3871087]
- 21 **Sikirić P**, Seiwerth S, Grabarević Z, Petek M, Rucman R, Turkovic B, Rotkvić I, Jagić V, Duvnjak M, Mise S. The beneficial effect of BPC 157, a 15 amino acid peptide BPC fragment, on gastric and duodenal lesions induced by restraint stress, cysteamine and 96% ethanol in rats. A comparative study with H2 receptor antagonists, dopamine promoters and gut peptides. *Life Sci* 1994; **54**: PL63-PL68 [PMID: 7904712]
- 22 **Turhan A**, Konerding MA, Tsuda A, Ravnic DJ, Hanidziar D, Lin M, Mentzer SJ. Bridging mucosal vessels associated with rhythmically oscillating blood flow in murine colitis. *Anat Rec (Hoboken)* 2008; **291**: 74-82 [PMID: 18085623 DOI: 10.1002/ar.20628]
- 23 **Konerding MA**, Turhan A, Ravnic DJ, Lin M, Fuchs C, Secomb TW, Tsuda A, Mentzer SJ. Inflammation-induced intussusceptive angiogenesis in murine colitis. *Anat Rec (Hoboken)* 2010; **293**: 849-857 [PMID: 20225210 DOI: 10.1002/ar.21110]
- 24 **Ravnic DJ**, Konerding MA, Tsuda A, Huss HT, Wolloscheck T, Pratt JP, Mentzer SJ. Structural adaptations in the murine colon microcirculation associated with hapten-induced inflammation. *Gut* 2007; **56**: 518-523 [PMID: 17114297 DOI: 10.1136/gut.2006.101824]
- 25 **Albadawi H**, Witting AA, Pershad Y, Wallace A, Fleck AR, Hoang P, Khademhosseini A, Oklu R. Animal models of venous thrombosis. *Cardiovasc Diagn Ther* 2017; **7**: S197-S206 [PMID: 29399523 DOI: 10.21037/cdt.2017.08.10]
- 26 **Guzmán-de la Garza FJ**, Cámara-Lemarroy CR, Alarcón-Galván G, Cordero-Pérez P, Muñoz-Espinosa LE, Fernández-Garza NE. Different patterns of intestinal response to injury after arterial, venous or arteriovenous occlusion in rats. *World J Gastroenterol* 2009; **15**: 3901-3907 [PMID: 19701970]
- 27 **Klicek R**, Kolenc D, Suran J, Drmic D, Breic L, Aralica G, Sever M, Holjevac J, Radic B, Turudic T, Kokot A, Patrlj L, Rucman R, Seiwerth S, Sikirić P. Stable gastric pentadecapeptide BPC 157 heals cysteamine-colitis and colon-colon-anastomosis and counteracts cuprizone brain injuries and motor disability. *J Physiol Pharmacol* 2013; **64**: 597-612 [PMID: 24304574]
- 28 **Mise S**, Tonkic A, Pesutic V, Tonkic M, Mise S, Capkun V, Batelja L, Blagaic AB, Kokic N, Zoricic I, Saifert D, Anic T, Seiwerth S, Sikirić P. The presentation and organization of adaptive cytoprotection in the rat stomach, duodenum, and colon. Dedicated to André Robert the founder of the concept of cytoprotection and adaptive cytoprotection. *Med Sci Monit* 2006; **12**: BR146-BR153 [PMID: 16572047]
- 29 **Bedekovic V**, Mise S, Anic T, Staresinic M, Gjurasin M, Kopljar M, Kalogjera L, Drvis P, Boban Blagaic A, Batelja L, Seiwerth S, Sikirić P. Different effect of antiulcer agents on rat cysteamine-

- induced duodenal ulcer after sialoadenectomy, but not gastrectomy. *Eur J Pharmacol* 2003; **477**: 73-80 [PMID: 14512101]
- 30 **Lojo N**, Rasic Z, Zenko Sever A, Kolenc D, Vukusic D, Drmic D, Zoricic I, Sever M, Seiwerth S, Sikiric P. Effects of diclofenac, L-NAME, L-arginine, and pentadecapeptide BPC 157 on gastrointestinal, liver and brain lesions, failed anastomosis, and intestinal adaptation deterioration in 24 hour-short-bowel rats. *PLoS One* 2016; **11**: e0162590 [PMID: 27627764 DOI: 10.1371/journal.pone.0162590]
 - 31 **Belosic Halle Z**, Vlainic J, Drmic D, Strinic D, Luetic K, Sucic M, Medvidovic-Grubisic M, Pavelic Turudic T, Petrovic I, Seiwerth S, Sikiric P. Class side effects: decreased pressure in the lower oesophageal and the pyloric sphincters after the administration of dopamine antagonists, neuroleptics, anti-emetics, L-NAME, pentadecapeptide BPC 157 and L-arginine. *Inflammopharmacology* 2017 [PMID: 28516373 DOI: 10.1007/s10787-017-0358-8]
 - 32 **Luetic K**, Sucic M, Vlainic J, Halle ZB, Strinic D, Vidovic T, Luetic F, Marusic M, Golic S, Pavelic TT, Kokot A, Seiwerth RS, Drmic D, Batelja L, Seiwerth S, Sikiric P. Cyclophosphamide induced stomach and duodenal lesions as a NO-system disturbance in rats: L-NAME, L-arginine, stable gastric pentadecapeptide BPC 157. *Inflammopharmacology* 2017; **25**: 255-264 [PMID: 28255738 DOI: 10.1007/s10787-017-0330-7]
 - 33 **Sikiric P**, Seiwerth S, Grabarevic Z, Rucman R, Petek M, Jagic V, Turkovic B, Rotkvic I, Mise S, Zoricic I, Konjevoda P, Perovic D, Jurina L, Separovic J, Hanzevacki M, Artukovic B, Bratulic M, Tisljar M, Gjurasin M, Miklic P, Stancic-Rokotov D, Slobodnjak Z, Jelovac N, Marovic A. The influence of a novel pentadecapeptide, BPC 157, on N(G)-nitro-L-arginine methylester and L-arginine effects on stomach mucosa integrity and blood pressure. *Eur J Pharmacol* 1997; **332**: 23-33 [PMID: 9298922]
 - 34 **Barisic I**, Balenovic D, Klicek R, Radic B, Nikitovic B, Drmic D, Udovicic M, Strinic D, Bardak D, Berkopic L, Djuzel V, Sever M, Cvjetko I, Romic Z, Sindic A, Bencic ML, Seiwerth S, Sikiric P. Mortal hyperkalemia disturbances in rats are NO-system related. The life saving effect of pentadecapeptide BPC 157. *Regul Pept* 2013; **181**: 50-66 [PMID: 23327997 DOI: 10.1016/j.regpep.2012.12.007]
 - 35 **Lovric-Bencic M**, Sikiric P, Hanzevacki JS, Seiwerth S, Rogic D, Kusec V, Aralica G, Konjevoda P, Batelja L, Blagaic AB. Doxorubicine-congestive heart failure-increased big endothelin-1 plasma concentration: reversal by amlodipine, losartan, and gastric pentadecapeptide BPC157 in rat and mouse. *J Pharmacol Sci* 2004; **95**: 19-26 [PMID: 15153646]
 - 36 **Medvidovic-Grubisic M**, Stambolija V, Kolenc D, Katancic J, Murselovic T, Plestina-Borjan I, Strbe S, Drmic D, Barisic I, Sindic A, Seiwerth S, Sikiric P. Hypermagnesemia disturbances in rats, NO-related: pentadecapeptide BPC 157 abrogates, L-NAME and L-arginine worsen. *Inflammopharmacology* 2017; **25**: 439-449 [PMID: 28210905 DOI: 10.1007/s10787-017-0323-6]
 - 37 **Berra-Romani R**, Avelino-Cruz JE, Raqeeb A, Della Corte A, Cinelli M, Montagnani S, Guerra G, Moccia F, Tanzi F. Ca²⁺-dependent nitric oxide release in the injured endothelium of excised rat aorta: a promising mechanism applying in vascular prosthetic devices in aging patients. *BMC Surg* 2013; **13** Suppl 2: S40 [PMID: 24266895 DOI: 10.1186/1471-2482-13-S2-S40]
 - 38 **Schiller HJ**, Reilly PM, Bulkley GB. Tissue perfusion in critical illnesses. Antioxidant therapy. *Crit Care Med* 1993; **21**: S92-102 [PMID: 8428505]
 - 39 **Rangan U**, Bulkley GB. Prospects for treatment of free radical-mediated tissue injury. *Br Med Bull* 1993; **49**: 700-718 [PMID: 8221033]
 - 40 **Matthys KE**, Bult H. Nitric oxide function in atherosclerosis. *Mediators Inflamm* 1997; **6**: 3-21 [PMID: 18472828 DOI: 10.1080/09629359791875]
 - 41 **Yousefipour Z**, Ranganna K, Newaz MA, Milton SG. Mechanism of acrolein-induced vascular toxicity. *J Physiol Pharmacol* 2005; **56**: 337-353 [PMID: 16204758]
 - 42 **Cesarec V**, Becejac T, Misic M, Djakovic Z, Olujic D, Drmic D, Brcic L, Rokotov DS, Seiwerth S, Sikiric P. Pentadecapeptide BPC 157 and the esophagocutaneous fistula healing therapy. *Eur J Pharmacol* 2013; **701**: 203-212 [PMID: 23220707 DOI: 10.1016/j.ejphar.2012.11.055]
 - 43 **Hsieh MJ**, Liu HT, Wang CN, Huang HY, Lin Y, Ko YS, Wang JS, Chang VH, Pang JS. Therapeutic potential of pro-angiogenic BPC157 is associated with VEGFR2 activation and up-regulation. *J Mol Med (Berl)* 2017; **95**: 323-333 [PMID: 27847966 DOI: 10.1007/s00109-016-1488-y]
 - 44 **Huang T**, Zhang K, Sun L, Xue X, Zhang C, Shu Z, Mu N, Gu J, Zhang W, Wang Y, Zhang Y, Zhang W. Body protective compound-157 enhances alkali-burn wound healing in vivo and promotes proliferation, migration, and angiogenesis in vitro. *Drug Des Devel Ther* 2015; **9**: 2485-2499 [PMID: 25995620 DOI: 10.2147/DDDT.S82030]
 - 45 **Chang CH**, Tsai WC, Hsu YH, Pang JH. Pentadecapeptide BPC 157 enhances the growth hormone receptor expression in tendon fibroblasts. *Molecules* 2014; **19**: 19066-19077 [PMID: 25415472 DOI: 10.3390/molecules191119066]
 - 46 **Chang CH**, Tsai WC, Lin MS, Hsu YH, Pang JH. The promoting effect of pentadecapeptide BPC 157 on tendon healing involves tendon outgrowth, cell survival, and cell migration. *J Appl Physiol* (1985) 2011; **110**: 774-780 [PMID: 21030672 DOI: 10.1152/japplphysiol.00945.2010]
 - 47 **Tkalcevic VI**, Cuzic S, Brajsa K, Mildner B, Bokulic A, Situm K, Perovic D, Glojnaric I, Parnham MJ. Enhancement by PL 14736 of granulation and collagen organization in healing wounds and the potential role of egr-1 expression. *Eur J Pharmacol* 2007; **570**: 212-221 [PMID: 17628536 DOI: 10.1016/j.ejphar.2007.05.072]
 - 48 **Sikiric P**, Separovic J, Anic T, Buljat G, Mikus D, Seiwerth S, Grabarevic Z, Stancic-Rokotov D, Pigac B, Hanzevacki M, Marovic A, Rucman R, Petek M, Zoricic I, Ziger T, Aralica G, Konjevoda P, Prkacin I, Gjurasin M, Miklic P, Artukovic B, Tisljar M, Bratulic M, Mise S, Rotkvic I. The effect of pentadecapeptide BPC 157, H2-blockers, omeprazole and sucralfate on new vessels and new granulation tissue formation. *J Physiol Paris* 1999; **93**: 479-485 [PMID: 10672992]
 - 49 **Brcic L**, Brcic I, Staresinic M, Novinscak T, Sikiric P, Seiwerth S. Modulatory effect of gastric pentadecapeptide BPC 157 on angiogenesis in muscle and tendon healing. *J Physiol Pharmacol* 2009; **60** Suppl 7: 191-196 [PMID: 20388964]
 - 50 **Robert A**. Cytoprotection by prostaglandins. *Gastroenterology* 1979; **77**: 761-767 [PMID: 38173]

P- Reviewer: Fu TL, Vukojevic J **S- Editor:** Ma RY **L- Editor:** A
E- Editor: Huang Y



Basic Study

Novel screening test for celiac disease using peptide functionalised gold nanoparticles

Anantdeep Kaur, Olga Shimoni, Michael Wallach

Anantdeep Kaur, Olga Shimoni, Institute for Biomedical Materials and Devices, Faculty of Science, University of Technology Sydney, Sydney 2007, Australia

Michael Wallach, School of Life Sciences, Faculty of Science, University of Technology Sydney, Sydney 2007, Australia

ORCID number: Anantdeep Kaur (0000-0003-4923-6332); Olga Shimoni (0000-0001-8822-1024).

Author contributions: Shimoni O and Wallach M designed research; Kaur A performed research, analysed data; Kaur A wrote the paper with critical revisions related to the intellectual content of the manuscript from Shimoni O and Wallach M; all authors approved the final version of the article to be published.

Supported by the Australian Government Research Training Program Scholarship, No. IH150100028; and Olga Shimoni acknowledges the Australian Research Council and National Health and Medical Research Council for financial support, No. APP1101258.

Institutional review board statement: This study was reviewed and approved by the University of Technology Sydney Research Ethics committee (UTS HREC ETH16 - 0841). The clinical samples were collected with informed consent and approval of Melbourne Health and WEHI Human Research Ethic Committees (2003.009 and 03/04) respectively.

Conflict-of-interest statement: The authors declare that they have no conflict of interest.

Data sharing statement: No additional data are available

Open-Access: This article is an open-access article which was selected by an in-house editor and fully peer-reviewed by external reviewers. It is distributed in accordance with the Creative Commons Attribution Non Commercial (CC BY-NC 4.0) license, which permits others to distribute, remix, adapt, build upon this work non-commercially, and license their derivative works on different terms, provided the original work is properly cited and the use is non-commercial. See: <http://creativecommons.org/licenses/by-nc/4.0/>

Manuscript source: Unsolicited manuscript

Corresponding author to: Olga Shimoni, BSc, MSc, PhD, Senior Lecturer, Institute for Biomedical Materials and Devices, Faculty of Science, University of Technology Sydney, PO Box 123, 15 Broadway, Ultimo, New South Wales, Sydney 2007, Australia. Olga.Shimoni@uts.edu.au
Telephone: +61-2-95142842

Received: July 13, 2018

Peer-review started: July 13, 2018

First decision: August 27, 2018

Revised: September 1, 2018

Accepted: October 5, 2018

Article in press: October 5, 2018

Published online: December 21, 2018

Abstract

AIM

To develop a screening test for celiac disease based on the coating of gold nanoparticles with a peptide sequence derived from gliadin, the protein that triggers celiac disease.

METHODS

20 nm gold nanoparticles were first coated with NeutrAvidin. A long chain Polyethylene glycol (PEG) linker containing Maleimide at the Ω -end and Biotin group at the α -end was used to ensure peptide coating to the gold nanoparticles. The maleimide group with the thiol (-SH) side chain reacted with the cysteine amino acid in the peptide sequence and the biotinylated and PEGylated peptide was added to the NeutrAvidin coated gold nanoparticles. The peptide coated gold nanoparticles were then converted into a serological assay. We used the peptide functionalised gold nanoparticle-based assay on thirty patient serum samples in a blinded assessment and compared our results with the previously run serological

and pathological tests on these patients.

RESULTS

A stable colloidal suspension of peptide coated gold nanoparticles was obtained without any aggregation. An absorbance peak shift as well as color change was caused by the aggregation of gold nanoparticles following the addition of anti-gliadin antibody to peptide coated nanoparticles at levels associated with celiac disease. The developed assay has been shown to detect anti-gliadin antibody not only in quantitatively spiked samples but also in a small-scale study on real non-hemolytic celiac disease patient's samples.

CONCLUSION

The study demonstrates the potential of gold nanoparticle-peptide based approach to be adapted for developing a screening assay for celiac disease diagnosis. The assay could be a part of an exclusion based diagnostic strategy and prove particularly useful for testing high celiac disease risk populations.

Key words: Celiac disease; Serological point-of-care; Gold nanoparticles; Diagnostic test; Autoantibodies

© The Author(s) 2018. Published by Baishideng Publishing Group Inc. All rights reserved.

Core tip: In the present study, we demonstrated that a peptide sequence derived from gliadin, a hydrophobic whole protein that induces celiac disease, in conjunction with gold nanoparticles can be used to detect a biomarker for celiac disease from serum. We confirmed our gold nanoparticle based serological assay can detect anti-gliadin antibody not only in quantitatively spiked samples but also in a small-scale study on real non-hemolytic celiac disease patient's samples.

Kaur A, Shimoni O, Wallach M. Novel screening test for celiac disease using peptide functionalised gold nanoparticles. *World J Gastroenterol* 2018; 24(47): 5379-5390
URL: <https://www.wjgnet.com/1007-9327/full/v24/i47/5379.htm>
DOI: <https://dx.doi.org/10.3748/wjg.v24.i47.5379>

INTRODUCTION

Sensing platforms based on the optical properties of gold nanoparticles (AuNPs) for the molecular detection and recognition of disease biomarkers is an important research challenge. Colorimetric sensors based on AuNPs have been applied for detecting targets, such as metal ions^[1-4], DNA^[5,6], protein conformations^[7] and enzyme activity^[8], where they have demonstrated high sensitivity and effectiveness.

In recent years, newer designs of nanoparticles with enhanced and controlled surface chemistry are being explored for sensing applications. Peptide-functionalized nanoparticles (PFNs) are one such emerging sensing

element. PFNs have previously been used for effective drug delivery for treating brain tumors and for pancreatic cancer treatment as well as for kinase inhibitor screening^[9,10,11-12]. Here we demonstrate the potential of PFNs as a colorimetric sensor for screening celiac disease.

Celiac disease (CD) is a small intestine enteropathy affecting genetically susceptible individuals, following the consumption of wheat prolamins (gliadin) and other prolamins of cereals^[13]. Population based studies have predicted a high prevalence rate for the disease, with a large number of CD sufferers remaining undiagnosed^[14]. The current diagnosis of CD is based on mucosal biopsy that remains the gold standard^[15]. Serological testing for gliadin-induced antibodies using an enzyme-linked immunosorbent assay is being widely applied^[16,17] and is usually the first line in clinical diagnosis for CD.

Gliadin antigenicity arises due to the higher content and repetitive arrangement of amino acids glutamine (~36 %) and proline (~17%-23%)^[18]. This acts as the substrate for the enzyme tissue transglutaminase (tTG: EC 2.3.2.13), resulting in deamidation and formation of an irreversible isopeptidyl bond^[19]. Human Leukocyte Antigen-DQ molecules (HLA-DQ2/8) present the deamidated gliadin peptides (DGP) to mucosal CD4⁺ T cells leading to an immunostimulatory effect^[20]. Gluten reactive helper T cells support the activated CD4⁺ T cells in the intestinal mucosa leading to the release of autoantibodies that act as the serological biomarkers^[21,22].

Non-treated CD patients have been shown to have increased concentration of anti-gliadin (AGA), tTG antibodies as well as Anti-DGP antibodies^[23,24]. A deamidated peptide sequence derived from α -gliadin amino acids 57-73 has also been identified as an immunogenic peptide sequence that can act as a trigger for CD^[25].

In this paper, we present a screening test for CD using gold nanoparticles (AuNPs) coated with a peptide sequence derived from the gliadin protein. We first established a stable suspension (without any significant level of aggregation) of peptide coated AuNPs, which enables us to translate it to a serological assay. We next assessed the sensitivity and specificity levels of the test using serum samples spiked with AGA. Furthermore, we tested our assay on thirty patient serum samples and found that the PFN-based assay could distinguish CD from non-CD patients.

This study highlights the potential of using immunodominant and biomarker specific peptide sequences that can be used for developing an efficient, easy to use screening test for pre-selecting CD cases, which can be then confirmed by mucosal biopsy for CD.

MATERIALS AND METHODS

Reagents: 20 nm citrate stabilized gold nanoparticles (AuNPs), bovine serum albumin (BSA), AGA from rabbit, IgG antibody from whole normal rabbit serum, 4-(2-hydroxyethyl)-1-piperazineethanesulfonic acid (HEPES), phosphate-buffered saline (PBS) were ob-

tained from Sigma-Aldrich (Australia). Poly (ethylene glycol) [*N*-(2-maleimidoethyl) carbamoyl] methyl ether 2-(biotinylamino) ethane (*i.e.*, Biotin-PEG₁₁-Maleimide) and NeutrAvidin were obtained from Thermo Fisher Scientific (Australia).

Peptide: The Peptide (QLQPFQPQLPYPQPQC) was synthesised from ChinaPeptides Co., Ltd. (China). The synthetic crude peptides were purified by reversed-phase liquid chromatography to give satisfactory peptide sequence (~90% homogeneity by analytical HPLC) with the correct amino acid sequences and mass spectra. The peptide contained residues 57-72 of α -gliadin and was designated as follows: Peptide: QLQPFQPQLPYPQPQC.

The peptide (QLQPFQPQLPYPQPQC) was coated on the surface of the AuNPs in two stages: First, coating with NeutrAvidin followed by a second step of binding of the peptide through a biotin-PEG₁₁-Maleimide linker molecule.

Preparation of the AuNPs coated with NeutrAvidin:

300 μ L of 20 nm AuNP were added dropwise to 200 μ L of NeutrAvidin dissolved in 10mM HEPES (1 mg/mL) while vortexing. The tube was incubated for 60 min at room temperature with repeated vortexing. The solution was centrifuged for 30 min at $4500 \times g$, supernatant discarded, and the pellet was re-suspended in 200 μ L MilliQ water. The process was repeated twice after which the pellet was re-suspended in 200 μ L HEPES buffer followed by centrifugation at $4500 \times g$ for 30 min using an Eppendorf® Microcentrifuge. The NeutrAvidin coated AuNPs were stored at 4 °C.

Binding of peptide to linker molecule: 300 μ L of 0.5 mg/mL peptide (QLQPFQPQLPYPQPQC) dissolved in MilliQ water was added dropwise to 700 μ L of 0.5 mg/mL Poly (ethylene glycol) [*N*-(2-maleimidoethyl) carbamoyl] methyl ether 2-(biotinylamino) ethane (*i.e.*, Biotin-PEG-Maleimide) dissolved in MilliQ water, (M_n 5400, MW 921 Da) having maleimide at the Ω -end and biotin at the α -end. This solution was left overnight at room temperature.

Preparation of the AuNPs coated with peptide using linker:

The NeutrAvidin coated AuNPs were centrifuged at $4500 \times g$ for 30 min using an Eppendorf® microcentrifuge, supernatant discarded, the pellet was re-suspended in 100 μ L of the peptide-linker solution. The tube was incubated for 60 min at room temperature with repeated vortexing. The solution was centrifuged for 5 min at $4500 \times g$, supernatant was discarded, and the pellet was re-suspended in 100 μ L of MilliQ water. The peptide coated AuNPs were stored at 4 °C for up to 4 wk.

Dynamic light scattering (DLS): The nanoparticle hydrodynamic radius was measured using Zetasizer Nano (Malvern Technologies, Inc.). Measurements were carried out at 25 °C in disposable cuvettes using a sample volume of 500 μ L. Each sample was measured in duplicates and the mean value was calculated.

Transmission electron microscopy: High-resolution transmission electron microscopy (TEM) micrographs were obtained using a FEI Tecnai TEM 200V fitted with a Gatan (Pleasantville, CA, United States) CCD camera. Samples were prepared by placing 2 μ L of AuNP coated with peptide onto a carbon-coated TEM grid (Agar Scientific, United Kingdom) and the film allowed to air dry for 15 min.

UV-vis measurements: UV-vis measurements were carried out using a Cary series UV-vis spectrophotometer (Agilent Technologies) using a standard 1 cm path-length quartz cuvette. Spectra were obtained from 200 nm to 800 nm. MilliQ water was used as the blank.

Anti-gliadin assay: The immunoassay used to assess the activity of AuNPs coated with peptide with the antibodies is outlined below. Assay steps were performed at room temperature. Briefly, 150 μ L of AuNPs coated with peptide were added to 1.5 mL low protein binding Eppendorf® tubes. AGA (1 mg/mL) from rabbit was added to each of the tubes corresponding to concentrations ranging from 2 μ g/mL to 20 μ g/mL (*i.e.*, 1 μ L to 10 μ L) to determine the specificity of the reaction between peptide coated AuNPs and AGA. IgG from normal rabbit serum (1 mg/mL) was used as a control antibody and added to 150 μ L of AuNPs coated with peptide in concentrations ranging from 2 μ g/mL to 20 μ g/mL (*i.e.*, 1 μ L to 10 μ L). MilliQ water was added to the tubes to bring the final volume in each Eppendorf tube up to 225 μ L. The UV-vis absorption spectra of solutions containing peptide coated gold nanoparticles and AGA at increasing dilutions (2 μ g/mL, 4 μ g/mL, 6 μ g/mL, 8 μ g/mL, 10 μ g/mL, 12 μ g/mL, 14 μ g/mL, 16 μ g/mL, 18 μ g/mL and 20 μ g/mL) were studied using a Cary Series UV-vis spectrophotometer. Readings were taken in triplicate and the student's *t*-test was used to determine the *P* value.

Anti-gliadin assay in spiked human serum: Normal human serum was diluted to 1:20 using 10 mmol/L HEPES buffer. 75 μ L of serum from the dilution was spiked with AGA at various dilutions comparable to that seen in celiac patients.

To prevent non-specific binding, 1 μ L of 20% BSA dissolved in MilliQ water and was added to 150 μ L of 20 nm AuNPs coated with peptide. The tubes were incubated for 30 min room temperature. 75 μ L of normal serum spiked with AGA at increasing dilutions of 2 μ g/mL, 4 μ g/mL, 6 μ g/mL, 8 μ g/mL and 10 μ g/mL, 12 μ g/mL, 14 μ g/mL, 16 μ g/mL, 18 μ g/mL and 20 μ g/mL was then added to AuNPs coated with peptide. The tubes were then incubated for 30 min room temperature.

Anti-gliadin assay in clinical human serum: Anonymous patient samples were provided by Dr Jason Tye-Din from the Walter and Eliza Hall Institute of Medical Research (WEHI Institute, Melbourne Parkville, Australia). They were collected with informed consent and approval of Melbourne Health and WEHI Human Research Ethic

Table 1 Comparison of the patient samples analysis using the AuNP-peptide-anti-gliadin test with previously existing histology and serological¹ results

Volunteer	Histology	tTG-IgA	DGP-IgG	AuNP-peptide-AGA test
n.1	CD	1 (< 4)	3 (< 20)	CD positive
n.2 ¹	Non-CD	0.1 (0-6)	0.2 (0-6)	CD positive
n.3	CD	> 100 (< 4)	33 (< 20)	CD positive
n.4	CD	121 (< 20)		CD positive
n.5	CD	> 100 (< 4)	> 100 (< 20)	CD positive
n.6	CD	217 (< 5)	> 150 (< 20)	CD positive
n.7 ²	CD	13 (0-6)	23 (0-6)	CD negative
n.8	CD	> 100 (< 5)	> 100 (< 20)	CD positive
n.9	CD	11 (0-6)	1.4 (0-6)	CD positive
n.10	CD	9 (< 4)	97 (< 20)	CD positive
n.11	CD	18.2 (0 < 20)	3 (0.20)	CD positive
n.12	CD	16 (0-20)	7 (< 20)	CD positive
n.13	Non-CD	4 (0-20)		Non-CD
n.14	CD	47 (< 5)	86 (< 5)	CD positive
n.15 ²	CD	74 (0-20)		CD negative
n.16	CD	145 (0-20)		CD positive
n.17	CD	57 (< 4)	93 (< 20)	CD positive
n.18	CD	149 (< 20)	63 (< 20)	CD positive
n.19	CD	> 100 (< 4)	> 100 (< 20)	CD positive
n.20 ¹	Non-CD	3.8 (< 6)	37 (< 6)	CD positive
n.21	Non-CD	< 5 (< 5)	< 20 (< 20)	Non-CD
n.22	CD	180 (0-6)	21 (0-6)	CD positive
n.23	CD	20 (0-6)	8.1 (0-6)	CD positive

¹False positive based on histology and tTG antibody titre, ²False negative based on histology and tTG antibody titre. Serology tTG (Tissue transglutaminase), deamidated gliadin peptides (deaminated gliadin peptides) results are indicated as IgA or IgG levels followed by normal reference ranges in brackets.

Table 2 Analysis of 7 samples with potential or latent celiac disease using the Peptide-AuNP-anti-gliadin test as compared with previously existing serology¹

Volunteer	Histology	tTG-IgA	DGP-IgG	Peptide-AuNP-AGA
n.24	Mucosal lesions	5 (< 20)	17 (< 20)	CD positive
n.25	Mucosal lesions	28 (0-6)	22 (0-6)	CD positive
n.26	Mucosal lesions	4.8 (0-6)	22 (0-6)	CD positive
n.27	Increased $\gamma\delta^+$ IELs	< 5 (< 5)	22 (< 20)	CD positive
n.28	Increased $\gamma\delta^+$ IELs	12 (0-6)	18 (0-6)	CD positive
n.29	Increased $\gamma\delta^+$ IELs	11 (0-6)	13 (0-6)	CD positive
n.30	Increased $\gamma\delta^+$ IELs	< 5 (< 5)	< 20 (< 20)	CD positive

¹Serology tTG (tissue transglutaminase), deamidated gliadin peptides (deaminated gliadin peptides) results are indicated as IgA or IgG levels followed by normal reference ranges in brackets. Cases are separated into those showing histological observations of irregular/patchy mucosal lesions or those with mucosal inflammation resulting from an increase in $\gamma\delta^+$ IELs.

Committees (2003.009 and 03/04) respectively. Ethical approval was also obtained from the University of Technology Sydney Research Ethics committee (UTS HREC ETH16 - 0841) before testing the clinical samples. The clinical samples consisted of 30 human serum samples that were analyzed in a blinded assessment. No prior knowledge of the CD status or any other clinical condition for any of the patient samples was known while testing. Samples were collected from patients with active CD (pre-treatment), treated CD (on a gluten free diet) and controls without CD (Tables 1 and 2). All cases of CD were medically diagnosed and based on typical small intestinal histology usually in conjunction with positive CD serology. The histological interpretation and the serology levels for each of the clinical sample tested using biopsy and the existing commercially available serology tests is

presented in Tables 1 and 2.

Prior to testing, each human serum sample was diluted to 1:10, 1:20 and 1:50 using 10 mmol/L HEPES buffer. 1 μ L of 20% BSA dissolved in MilliQ water was added to AuNPs coated with peptide to prevent non-specific binding. 75 μ L of serum from each of the dilutions and the tubes were incubated for 15 min at room temperature before the absorbance was measured using a UV-vis spectrophotometer.

Concentration of immunoglobulins in clinical human serum: 200 μ L of each human serum sample was centrifuged at $3200 \times g$ or 15 min. The supernatant was removed, and the serum samples were diluted with 200 μ L of 10 mmol/L PBS. An equal volume of saturated ammonium sulphate solution was added slowly to achi-

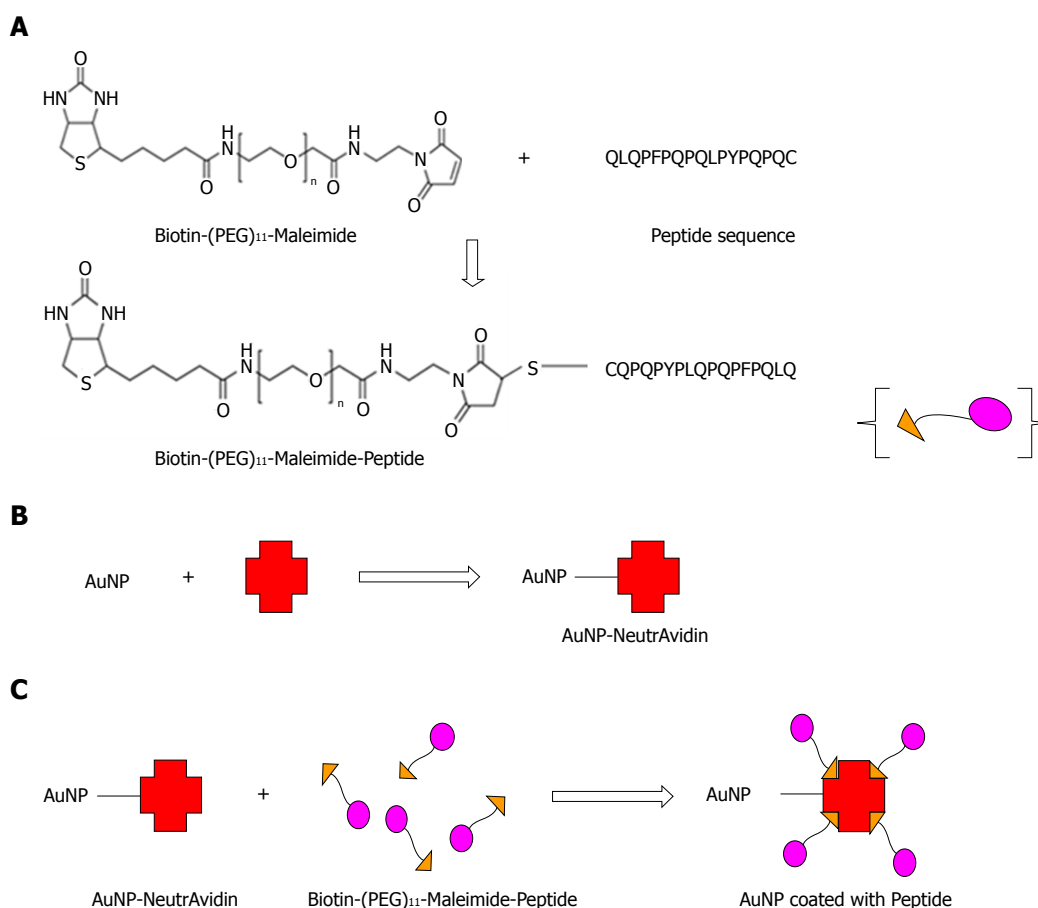


Figure 1 Schematic representation of preparation of peptide coated AuNPs. A: Maleimide groups of the linker reacted specifically with free (reduced) sulfhydryl's in the peptide sequence to form stable thio-ether bonds; B: NeutrAvidin was coated on the surface of the AuNPs to obtain NeutrAvidin-AuNP particles; C: The biotin end of the linker interacted with the NeutrAvidin-AuNPs resulting in the formation of peptide coated AuNPs.

even a 33% saturated (v/v) final concentration with continuous stirring of the tubes. Samples were kept at 4 °C for 30 min and then centrifuged again at 2500 × g for 15 min. The supernatant was removed, and the pellet was re-suspended by adding 200 µL of 10 mmol/L PBS. The concentrated serum solution was stored at 20 °C till further use.

Zeba™ Spin desalting columns (Thermo Scientific™) were used for the desalting of the immunoglobulins from the concentrated serum solution according to the manufacturer's instructions. The final concentration of the total immunoglobulins was measured using the NanoDrop and stored at -20 °C until further use.

Colorimetric response curve: A colorimetric response curve was plotted to represent the sensitivity values obtained for the different dilution values for both the AGA and the control antibody (IgG from rabbit serum). The assay sensitivity was determined based on the colorimetric response values calculated as colorimetric response = $I_{\text{max at 527 nm}} / I_{\text{at 550 nm}}$, i.e., spectral absorbance value obtained at 527 nm - the wavelength where AuNP coated with peptide show maximum absorbance by itself (no antibodies are added) - divided by the absorbance at 550 nm, where a shift in absorbance is observed following the interaction of the antibody to the AuNP coated with peptide.

The assay sensitivity in spiked serum was calculated as colorimetric response = $I_{\text{max at 580 nm}} / I_{\text{at 527 nm}}$, i.e., absorbance value obtained at 580 nm. This is the wavelength where a shift in absorbance is observed following the interaction of the antibody to the AuNP coated with peptide in serum divided by the maximum absorbance value of AuNP coated with peptide in serum.

RESULTS

To ensure the peptide coating on AuNPs, we used a long chain PEG linker containing Maleimide at the ω -end and Biotin group at the α -end. Following the reaction of maleimide group with the thiol (-SH) side chain of the cysteine amino acid in the peptide sequence, the biotinylated and PEGylated peptide was added to the NeutrAvidin coated AuNPs.

The coating of the peptide sequence to the colloidal AuNP using the Biotin-(PEG)₁₁-Maleimide linker is represented in the schematic (Figure 1).

The coating of peptide onto the AuNPs was characterized using the UV-vis spectrophotometer. It was observed that upon coating of peptide onto the AuNPs, there was a shift in absorbance maximum from 525 nm to 527 nm (red-shift) (Figure 2A). The DLS showed an increase in hydrodynamic diameter from 20 nm to 28 nm following coating with peptide (Figure 2B). The

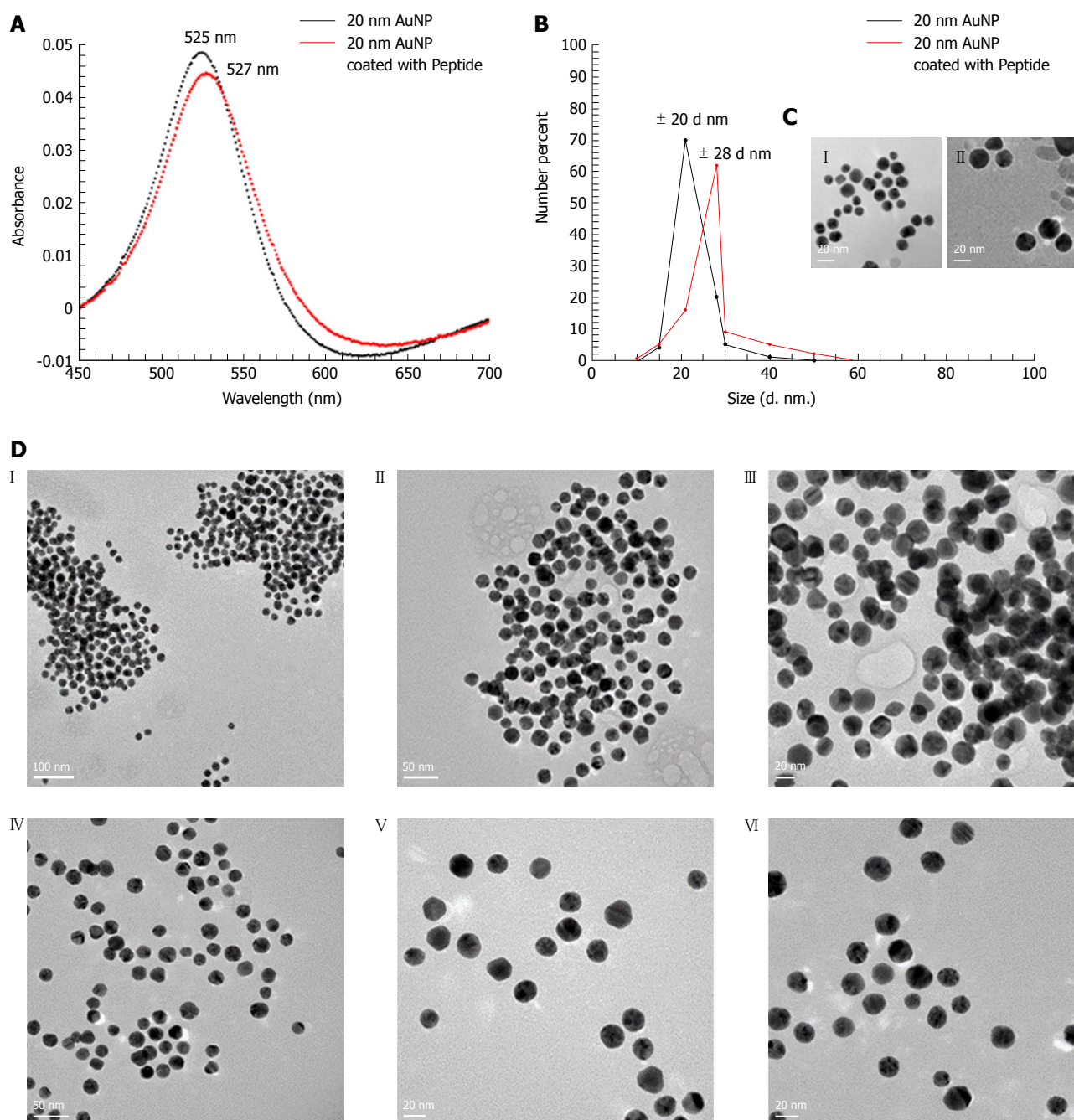


Figure 2 Characterization of peptide coated AuNPs. A: Characterization of AuNP coated with peptide using a UV-Vis spectrophotometer indicating a spectral red shift in wavelength from 525 nm (for 20 nm AuNP only) to 527 nm (for 20 nm AuNP coated with peptide); B: Characterization of AuNP coated with peptide using DLS that showed an increase in the hydrodynamic size of the uncoated vs coated particles from 20 nm to 28 nm respectively; C: High resolution TEM images of (1) uncoated AuNPs, (2) AuNPs coated with peptide showing a "halo" layer surrounding the surface of the nanoparticles indicating coating of the gold with the peptide had occurred. In contrast, the "halo" effect was not observed on the surface of the un-coated AuNPs; D: High resolution TEM images following the incubation with AGA (12 μ g/mL) (1, 2, 3) AuNPs coated with peptide showing aggregation confirming coating of peptide on AuNP (4, 5, 6) Uncoated AuNPs remained dispersed. DLS: Dynamic light scattering; TEM: Transmission electron microscopy.

hydrodynamic diameter of NeutrAvidin coated AuNPs is presented in Supplementary Figure 1.

To directly observe the coating of peptide onto the surface of the AuNPs, high-resolution TEM imaging was used. Our results showed the presence of a thin layer of material (< 1 nm) surrounding the nanoparticles [Figure 2C (II)], which was not observed on the surface of the uncoated nanoparticles [Figure 2C (I)] that indicated peptide coating. As the layer was very thin, peptide

coated and uncoated AuNPs were incubated with AGA (12 μ g/mL), wherein the peptide coated AuNPs aggregated [Figure 2D (I, II, III)] while uncoated AuNPs remained dispersed [Figure 2D (IV, V, VI)].

Incubation of peptide-coated AuNPs with AGA

Peptide coated AuNPs were incubated with serial dilutions of rabbit anti-gliadin IgG polyclonal antibody, after 45 min incubation we observed a significant reduction in color

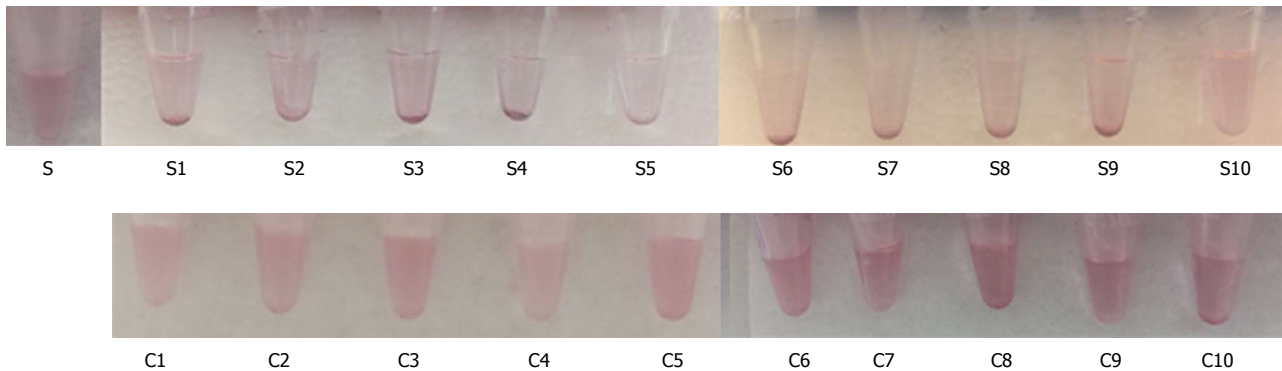
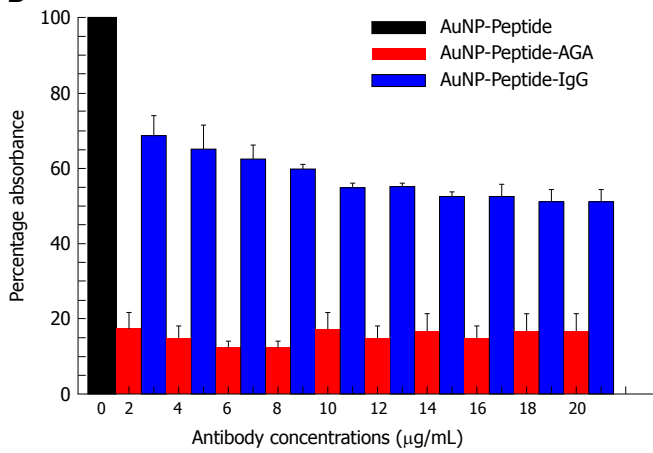
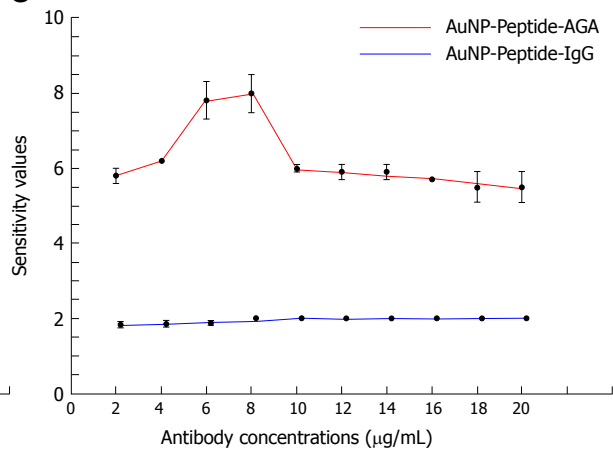
A**B****C**

Figure 3 Testing peptide-coated AuNPs with anti-gliadin. A: Reduction in color from red to translucent and absorbance was observed in AuNP coated with peptide (S) and incubated with AGA at various dilutions (S1) 2 μg/mL, (S2) 4 μg/mL, (S3) 6 μg/mL, (S4) 8 μg/mL, (S5) 10 μg/mL, (S6) 12 μg/mL, (S7) 14 μg/mL, (S8) 16 μg/mL, (S9) 18 μg/mL and (S10) 20 μg/mL. No significant reduction in color or shift in peak wavelength was observed in peptide coated AuNP incubated with control rabbit IgG at dilutions (C1) 2 μg/mL, (C2) 4 μg/mL, (C3) 6 μg/mL, (C4) 8 μg/mL, (C5) 10 μg/mL, (C6) 12 μg/mL, (C7) 14 μg/mL, (C8) 16 μg/mL, (C9) 18 μg/mL and (C10) 20 μg/mL; B: Representation of specificity based on UV-Vis absorbance spectra for the antibody interactions at equal concentrations of AGA and control antibody; C: Colorimetric response curve plotted on AuNP coated with peptide following the addition of AGA at different dilutions. AGA: Anti-gliadin.

as well as a shift in absorbance from 527 nm to 580 nm (Figure 3A and B, Supplementary Figure 2).

To confirm the specificity of the interactions, we tested normal IgG antibody with the peptide coated AuNPs as a control, where we observed no significant reduction in color or shift in the wavelength or aggregation of AuNPs. (Figure 3A and B, Supplementary Figure 3). At all the tested concentrations, the absorbance was significantly lower using AGA as compared to normal IgG ($P < 0.005$, Figure 3B, Supplementary Table 1).

To confirm the sensitivity of the AGA toward peptide coated AuNPs, we calculated a colorimetric response between our assay (Figure 3C). The colorimetric response reaches a maximum value at a concentration of 8 μg/mL of AGA meaning the highest sensitivity occurred at this concentration. This interaction of the peptide coated AuNPs with AGA resembles the precipitin reaction of antibody-antigen immune complexes. The near constant colorimetric response curve obtained for the control antibody as compared to the response curve obtained for AGA demonstrates the distinct sensitivity of the assay.

Testing anti-gliadin in spiked serum

A variety of proteins, peptides as well as nucleic acids are constituents of human serum, making it a complex fluid. To reduce background binding, we used 1 μL of 20% BSA as a blocking agent, to lower the non-specific interaction with the peptide coated AuNPs. Spiked human serum containing 2-20 μg/mL AGA was incubated with the peptide coated AuNPs. The results showed an increase in aggregation and precipitation, which was easily detectable by eye, with a specificity up to a value of 2 μg/mL of AGA (Figure 4A). We also observed a reduction in the color of the solution from red to translucent. This change was supported by the increase in the colorimetric response reaching a maximum sensitivity at 8 μg/mL of AGA. The curve then begins to drop off at 10 μg/mL of AGA, however, it remains well above the control IgG level (Figure 4B). In comparison, when normal rabbit IgG was added to the human serum, no precipitate formation or change in color was observed. Normal serum itself did not show any precipitate formation or change in absorbance with a constant response curve at all IgG concentrations.

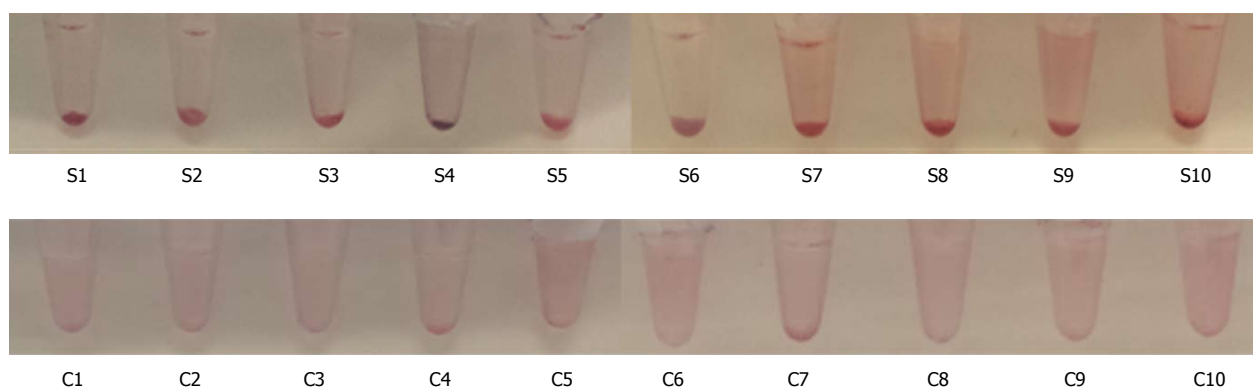
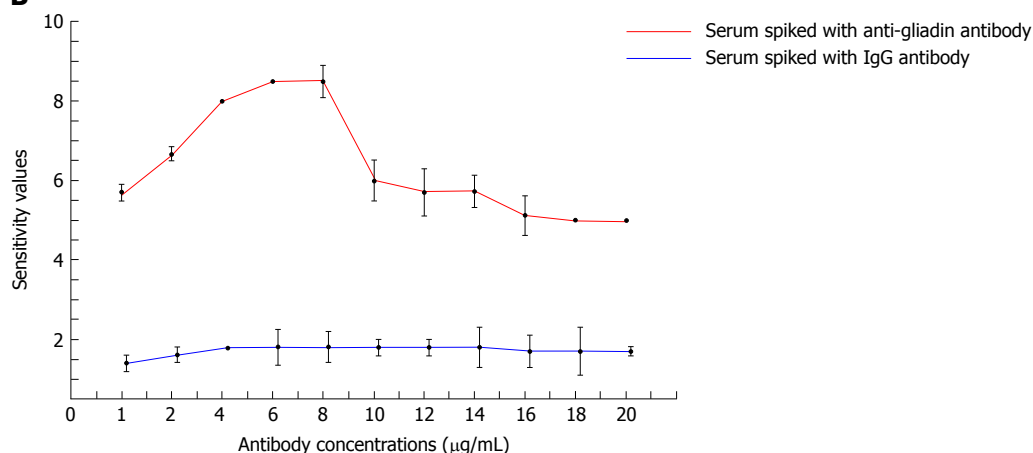
A**B**

Figure 4 Detection of anti-gliadin in spiked human serum using peptide-coated AuNPs. A: Reduction in color from red to translucent as well as precipitate formation was observed in AuNP coated with peptide in the presence of AGA and serum at different concentrations (S1-S10). No reduction in color from red to translucent or precipitate formation was observed in AuNP coated with peptide in the presence of control IgG and serum (C1-C10); B: Colorimetric response curve plotted in AuNP coated with peptide in 1:20 diluted serum following the addition of AGA at different dilutions. AGA: Anti-gliadin.

Testing clinical samples

The results for the 30 non-haemolytic, clinical samples were recorded after the visual examination of precipitate formation and determination of shift or change in absorbance values using a UV-vis spectrophotometer. Based on the results observed by eye, the samples have been divided into three categories: clear precipitation, aggregation and colloidal suspension.

The assay sensitivity was determined based on the colorimetric response obtained for each serum sample and is calculated as colorimetric response = $I_{\text{max at 580 nm}}/I_{\text{at 527 nm}}$. Using this method, the calculated colorimetric response for normal serum (serum without AGA) is 1 and this acts as the cut-off value. Therefore, for the clinical samples, based on the spectral absorbance data, a value of ≤ 1 is indicated as negative for CD and a value above 1 is indicated as CD positive. Based on the observation and calculation of the colorimetric response curve, we summarized the outcomes in Tables 1 and 2 and Figure 5 along with the results reported using other serological methods, biopsy and histology.

DISCUSSION

The hexapeptide sequence QXQPFP (X being P, Q and

L) within gliadin was previously identified as the dominant epitope for IgA and IgG antibodies against deamidated gliadin peptides (a-DGP)^[26]. This sequence overlaps with residues 57-62 of native α -gliadin and has been shown to occur with high specificity in sera from CD individuals^[27,28]. The 17-mer peptide sequence (QLQFPQPQLPYPQPQC) used as the antigen in our study is a small, 2 kDa molecular weight hexapeptide containing sequence.

In order to use peptide to coat AuNPs and to develop an assay for AGA, we needed to overcome the potential problem of aggregation of the coated nanoparticles prior to adding the AGA in the test. This was achieved by using a long chain PEG linker containing Maleimide at the Ω -end and Biotin group at the α -end. Following the reaction of maleimide group with the thiol (-SH) side chain of the cysteine amino acid in the peptide sequence, the biotinylated and PEGylated peptide was added to the NeutrAvidin coated AuNPs leading to the formation of peptide coated AuNPs. The coating of peptide onto the AuNPs surface was examined by UV-vis measurements that was based on the observation of a change in the absorbance peak for the nanoparticle or a red-shift^[29]. The UV-vis absorbance spectra showed that upon coating of peptide onto the AuNPs, there was a shift in

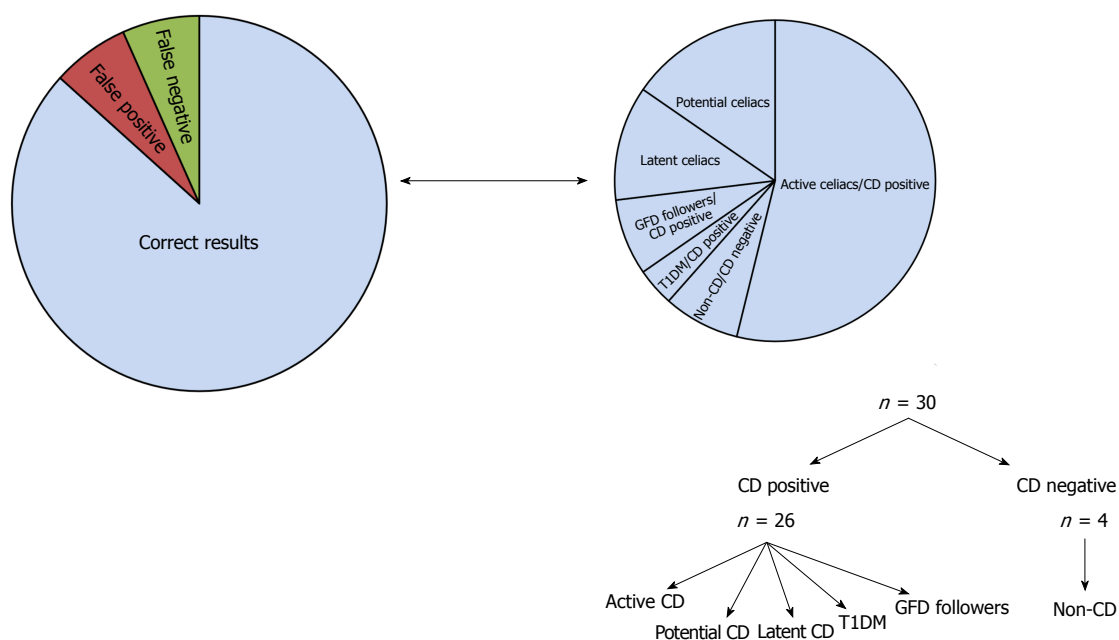


Figure 5 Representation of the distribution of clinical samples using AuNP-peptide-anti-gliadin test.

absorbance maximum from 525 nm to 527 nm (red-shift) (Figure 2A). Also, we did not observe any measurable decrease of absorbance at peak wavelength or increase of absorbance at long wavelengths (600-700 nm). These results indicate that no strong AuNP-to-AuNP interactions took place after being coated with peptide and were stable in a dispersed colloidal state with minimal aggregation. In addition, a small peak at 210 nm was also observed following the binding of peptide to AuNPs, as observed in previous studies on peptide coating^[30].

We further confirmed the absence of aggregation using DLS, that showed an increase in hydrodynamic diameter from 20 nm to 28 nm following coating with peptide (Figure 2B). The increase in hydrodynamic diameter is larger than that expected for a 2 kDa peptide sequence and can be attributed to the larger molecular weight (68 kDa) NeutrAvidin that coated the AuNPs (Supplementary information S1) through the biotin-maleimide PEG linker. Since the hydrodynamic radius in solution compares directly to the molar mass of the protein^[31], in this case, being the peptide sequence as well as NeutrAvidin, an increase in hydrodynamic radius to 28 nm can be correlated. High resolution TEM images of AuNPs coated with peptide showed a "halo" layer surrounding the surface of the nanoparticles indicating that coating of the gold with the peptide had occurred and this helped to confirm the peptide coating to AuNPs. The peptide coats the AuNPs as a monolayer with a sharp border with constant thickness on the gold nanoparticle surface^[32].

To assess the capability of peptide-coated AuNPs to detect AGA, serial dilutions of rabbit anti-gliadin IgG polyclonal antibody in a range that normally exists in human serum, were tested^[33]. A significant reduction in color as well as a shift in absorbance from 527 nm to 580 nm with a decrease in the absorbance peak (Figure

3), indicated that in the presence of the AGA there was an increase in the intermolecular association of the peptide coated AuNPs. These inter-particle interactions caused aggregation, leading to precipitation and a drop in absorbance. These results obtained for the peptide coated AuNPs-AGA interaction are consistent with previous work, on the addition of specific analytes, such as metal ions, to citrate stabilised gold nanoparticles^[34,35]. Spiked human serum containing 2-20 µg/mL AGA was then incubated with the peptide coated AuNPs. An increased aggregation and precipitation, which was easily detectable by eye in the presence of the AGA was observed (Figure 4). No color change or precipitation was observed in the serum spiked with normal IgG rabbit.

Peptide-coated AuNPs were next tested in a selected set of human serum samples obtained from patients with CD or controls without CD. The main aim was to clearly distinguish the CD affected from the non-CD affected. To achieve that, serum was diluted with PBS, concentrated, purified and then allowed to react with AuNPs coated with peptide. This ensured that the range of the AGA in the sera fell in the peak sensitivity range (2-20 µg/mL).

Out of the thirty samples analysed, fourteen samples that were diagnosed with active CD with high antibody titres as shown by serology and intestinal damage as per biopsy were identified as CD positive using AuNP-Peptide-AGA assay as well. These samples showed the formation of a precipitate and had a clear shift as well as drop in UV-vis absorbance values as well as a high colorimetric response value (refer Table 1). The remaining samples were then classified into various sub-classes based on the analysis using the AuNP-Peptide-AGA assay as described below (refer Tables 1 and 2, Figure 5).

The AuNP-Peptide-AGA assay could correctly identify the patient suffering from another autoimmune disease,

Type 1 diabetes (T1DM), as positive for CD and this result matched with the previously conducted biopsy and serology profile of the patient. In comparison, an existing commercially available point-of-care test, SimtomaX® blood drop (Augurix diagnostics) that uses a combination of three different peptides as the DGP antigens was found to be less specific in diagnosing CD in children suffering from T1DM^[36].

The elevated risks of patients with T1DM to develop celiac disease arises because of multiple environmental and immunological factors and common genetic background^[37]. The prevalence of celiac disease in T1DM is reported high with a mean prevalence rate of 8%^[38] making regular monitoring of patients, particularly children with T1DM a necessity. AuNP-Peptide-AGA diagnostic assay shows improved specificity over the existing point-of-care test based on DGP. This test result shows immense potential of the assay in pre-selecting CD sufferers particularly those belonging to high-risk pediatric populations and, therefore, needs to be further explored in large clinical studies.

The cohort of tested samples included two cases where the patients had previously been diagnosed with CD and therefore followed a gluten free diet (GFD). While one person had been on a GFD for more than 8 wk (volunteer number n.11), the other person had been on a GFD for less than 2 wk (volunteer number n.12). While the conventional serology test identified these two patients as negative, the peptide-based assay obtained a positive for CD that is similar to the diagnosis based on mucosal biopsy.

A clear precipitate using the AuNP-Peptide-AGA assay was obtained for three samples (volunteer numbers n.24, n.25, n.26, Table 2) with patchy/irregular mucosal lesions, classified as a broad sub-type of potential or latent celiac. The UV-vis absorbance data supported the visual examination. These three samples were classified as positive for CD as these may be latent celiac sufferers that initially, display mild mucosal atrophy, that then develops to typical atrophy of small intestine mucosa along with a presentation of positive CD serology^[39].

Aggregation of nanoparticles along with a drop in UV-vis absorbance values was demonstrated by four clinical samples (volunteer numbers n.27, n.28, n.29, n.30, Table 2). These samples had positive or low positive serology along with mucosal inflammation. The AuNP-Peptide-AGA assay showed results similar to those found using the existing serological assays. These four cases have been identified as "potential" CD positives, a subtype of CD that displays a normal villous architecture but also shows clinical symptoms, such as increased $\gamma\delta$ + intraepithelial lymphocytes along with the presence of gliadin specific antibodies, that are mostly at low titres ($< 1:40$)^[40]. Potential CD cases are often difficult to diagnose by histology which has a lowered predictive value in recognizing such cases. Correct diagnosis for potential CD cases therefore necessitates an evaluation of both serological markers as well as pathological symptoms.

The cohort included four samples identified as nega-

tive for CD based on biopsy and existing serology tests (volunteer numbers n.2, n.13, n.20 and n.21, Table 1). Out of the four samples, two samples were correctly identified as CD negative by AuNP-Peptide-AGA assay while the other two samples showed the formation of aggregates and were identified as positive (volunteer numbers n.2 and n.20). As intestinal biopsy has been used as the gold standard for CD confirmation, these two samples have been referred to as a false positive.

Overall, upon comparing the results for the 30 clinical samples, while 26 samples were interpreted similar to the analysis using the existing serology and histology, 2 false positive results and 2 false negative results were obtained using the AuNP-Peptide-AGA assay giving the AuNP-Peptide-AGA assay an overall accuracy of 86.6%.

Celiac disease is induced by the protein gliadin, present in wheat and some other cereals causing damage to the small intestine. In the present study, we demonstrated that a peptide sequence derived from gliadin in conjunction with AuNPs can be used as an efficient tool to detect a biomarker for CD from serum. This was achieved by developing a methodology to coat the small antigenic peptide sequence on the surface of AuNPs without causing aggregation. A color change and absorbance peak shift caused by the aggregation of AuNPs was observed following the addition of AGA to peptide coated AuNPs at levels associated with CD. We confirmed that the developed assay can detect AGA not only in quantitatively spiked samples but also in a small-scale study on real non-hemolytic CD patient's samples.

The present study shows that this novel peptide functionalised AuNP based assay is useful for pre-selecting CD diseases particularly in high-risk pediatric populations that can be then confirmed by mucosal biopsy. The developed assay has high accuracy levels and is relatively cheaper to develop, the assay format has potential to be adapted as point-of-care test that would be useful in an exclusion diagnostic strategy as positive result would strengthen the possibility of CD that can be confirmed using intestinal biopsy.

ARTICLE HIGHLIGHTS

Research background

Celiac disease is a chronic immune mediated disorder of the small intestine caused by consuming the protein gluten present in wheat and some other cereals. Following the activation of the innate immune system, a number of cytokines as well as antibodies are released in celiac patients that can be used as specific biomarkers to develop diagnostic tests. Over the years, a number of diagnostic tests have been developed, however, in spite of the good initial results in terms of sensitivity and specificity, when these tests are used on a large scale they have lowered predictive values. In the present study, a novel assay using peptide functionalised gold nanoparticles was developed that can be useful in an exclusion based diagnostic strategy.

Research motivation

The number of celiac disease sufferers are rapidly increasing throughout the world, and there is an increased need for newer detection methods that are easy to use, accurate as well as cheaper to enable early identification of the disease. The present study addresses this issue through the development of a novel assay combining the unique properties of gold nanoparticles with the

specificity of the antibodies. The developed assay shows great potential to be developed as a point-of-care test that would be beneficial for large scale screening of celiac disease.

Research objectives

In order to develop a celiac diagnostic assay based on the properties of the gold nanoparticles combined with the specificity of the antibodies from serum the following aims have been addressed in this work: (1) To develop method for the binding and adsorption of peptide derived from gliadin, the main antigenic protein causing celiac disease on the surface of gold nanoparticles; (2) to detect and measure the concentrations of antibodies to be used as biomarkers in serum; (3) to test and validate the developed test on real patient serum samples.

Research methods

The peptide coated gold nanoparticles were characterized using UV-vis spectra, dynamic light scattering and transmission electron microscopy. The UV-vis absorbance readings of peptide coated AuNPs following interactions with AGA and IgG from rabbit serum (control antibody) were used to calculate the percentage absorbance values. The students t-test was used to compare the sets of quantitative data that were collected independently of one another to calculate the p value and determine statistical significance. The assay sensitivity was determined based on the colorimetric response values.

The clinical accuracy of the peptide coated AuNPs was determined using a selected, varied set of thirty human serum samples obtained from patients with celiac disease or controls without celiac disease. The results for the thirty clinical samples were recorded after the visual examination of precipitate formation and the determination of a shift or change in absorbance values using a UV-vis spectrophotometer. The assay sensitivity was determined based on the colorimetric response values obtained for each serum sample.

Research results

The peptide sequence was successfully coated to the AuNP and characterization methods indicated that a stable colloidal suspension of the peptide coated AuNPs was achieved that was sustained by the high affinity biotin-avidin interactions.

The addition of anti-gliadin antibody to peptide coated AuNPs as well as in spiked serum at a threshold level resulted in lowering as well as a shift of absorbance peaks that indicated the aggregation of AuNPs. On the other hand, in the presence of a non-specific, normal IgG antibody there was no interaction between the peptide coated AuNPs, with no reduction in color or shift in wavelength or aggregation of AuNPs.

The clinical accuracy of the peptide coated AuNPs was tested using 30 clinical samples, where 26 samples were shown to have the same analysis as that obtained with existing serology and histology, however, 2 false positive results and 2 false negative results were also obtained using the AuNP-peptide-AGA assay giving the AuNP-peptide-AGA assay an overall accuracy of 86.6%.

Research conclusions

In this study, we demonstrate the potential of peptide functionalised gold nanoparticles as a colorimetric sensor for screening celiac disease. The AuNP-peptide assay seems promising for development as a point-of-care test, this is because it is based on the formation of a precipitate as well as a reduction in color for a positive sample in the presence of a celiac disease specific autoantibody, thereby, eliminating the need for secondary antibody. This greatly reduces the cost of development for the assay and would be a step in the direction of one-step detection for celiac disease based on single antibody detection.

Research perspectives

The AuNP-Peptide based approach shows great potential and would be particularly useful in aiding large-scale screening of the general population, particularly in the pre-selection of young Celiac disease (CD) sufferers which can be then confirmed by mucosal biopsy. A positive result would strengthen the possibility of CD while a negative test would help avoid unnecessary intestinal biopsy thereby reducing the economic burden on healthcare resources resulting in cost savings.

ACKNOWLEDGMENTS

The authors thank Dr. Jason Tye-Din, MBBS, PhD, FRACP, Immunology Division, The Walter and Eliza Hall Institute of Medical Research, Parkville, Victoria, Australia, for providing clinical samples as well for his critical review and feedback on the manuscript.

REFERENCES

- 1 Lee JS, Han MS, Mirkin CA. Colorimetric detection of mercuric ion (Hg²⁺) in aqueous media using DNA-functionalized gold nanoparticles. *Angew Chem Int Ed Engl* 2007; **46**: 4093-4096 [PMID: 17461429 DOI: 10.1002/anie.200700269]
- 2 Hung YL, Hsiung TM, Chen YY, Huang YF, Huang CC. 2010, Colorimetric Detection of Heavy Metal Ions Using Label-Free Gold Nanoparticles and Alkanethiols. *J Phys Chem C* 2010; **114**: 16329-16334 [DOI: 10.1021/jp1061573]
- 3 Chen GH, Chen WY, Yen YC, Wang CW, Chang HT, Chen CF. Detection of mercury(II) ions using colorimetric gold nanoparticles on paper-based analytical devices. *Anal Chem* 2014; **86**: 6843-6849 [PMID: 24932699 DOI: 10.1021/ac5008688]
- 4 Chen W, Cao F, Zheng W, Tian Y, Xianyu Y, Xu P, Zhang W, Wang Z, Deng K, Jiang X. Detection of the nanomolar level of total Cr(III) and (VI) by functionalized gold nanoparticles and a smartphone with the assistance of theoretical calculation models. *Nanoscale* 2015; **7**: 2042-2049 [PMID: 25553787 DOI: 10.1039/c4nr06726f]
- 5 Elghamian R, Storhoff JJ, Mucic RC, Letsinger RL, Mirkin CA. Selective colorimetric detection of polynucleotides based on the distance-dependent optical properties of gold nanoparticles. *Science* 1997; **277**: 1078-1081 [PMID: 9262471 DOI: 10.1126/science.277.5329.1078]
- 6 Wang Q, Liu R, Yang X, Wang K, Zhu J, He L, Li Q. Surface plasmon resonance biosensor for enzyme-free amplified microRNA detection based on gold nanoparticles and DNA sandwich. *Sens Actuators B Chem* 2016; **223**: 613-620 [DOI: 10.1016/j.snb.2015.09.152]
- 7 Tsai DH, DelRio FW, Keene AM, Tyner KM, MacCuspie RI, Cho TJ, Zachariah MR, Hackley VA. Adsorption and conformation of serum albumin protein on gold nanoparticles investigated using dimensional measurements and in situ spectroscopic methods. *Langmuir* 2011; **27**: 2464-2477 [PMID: 21341776 DOI: 10.1021/la104124d]
- 8 Wang J, Wu L, Ren J, Qu X. Visualizing human telomerase activity with primer-modified Au nanoparticles. *Small* 2012; **8**: 259-264 [PMID: 22083963 DOI: 10.1002/smll.201101938]
- 9 Gao H, Xiong Y, Zhang S, Yang Z, Cao S, Jiang X. RGD and interleukin-13 peptide functionalized nanoparticles for enhanced glioblastoma cells and neovasculature dual targeting delivery and elevated tumor penetration. *Mol Pharm* 2014; **11**: 1042-1052 [PMID: 24521297 DOI: 10.1021/mp400751g]
- 10 Lee GY, Qian WP, Wang L, Wang YA, Staley CA, Satpathy M, Nie S, Mao H, Yang L. Theranostic nanoparticles with controlled release of gemcitabine for targeted therapy and MRI of pancreatic cancer. *ACS Nano* 2013; **7**: 2078-2089 [PMID: 23402593 DOI: 10.1021/nn3043463]
- 11 Gupta S, Andresen H, Ghadiali JE, Stevens MM. Kinase-actuated immunoaggregation of Peptide-conjugated gold nanoparticles. *Small* 2010; **6**: 1509-1513 [PMID: 20578112 DOI: 10.1002/smll.201000099]
- 12 Gupta S, Andresen H, Stevens MM. Single-step kinase inhibitor screening using a peptide-modified gold nanoparticle platform. *Chem Commun (Camb)* 2011; **47**: 2249-2251 [PMID: 21246106 DOI: 10.1039/c0cc04903d]
- 13 Ludvigsson JF, Leffler DA, Bai JC, Biagi F, Fasano A, Green PH, Hadjivassiliou M, Kaukinen K, Kelly CP, Leonard JN, Lundin KE, Murray JA, Sanders DS, Walker MM, Zingone F, Ciacci C. The Oslo definitions for coeliac disease and related terms. *Gut* 2013; **62**: 43-52 [PMID: 22345659 DOI: 10.1136/gutjnl-2011-301346]
- 14 Marsh MN, Vincenzo V, Srivastava A. Histology of gluten related

- disorders. *Gastroenterol Hepatol Bed Bench* 2015; **8**: 171-177
- 15 **Rostami K**, Marsh MN, Johnson MW, Mohaghegh H, Heal C, Holmes G, Ensari A, Aldulaimi D, Bancel B, Bassotti G, Bateman A, Becheanu G, Bozzola A, Carroccio A, Catassi C, Ciacci C, Ciobanu A, Danciu M, Derakhshan MH, Elli L, Ferrero S, Fiorentino M, Fiorino M, Ganji A, Ghaffarzadehgan K, Going JJ, Ishaq S, Mandolesi A, Mathews S, Maxim R, Mulder CJ, Neefjes-Borst A, Robert M, Russo I, Rostami-Nejad M, Sidoni A, Sotoudeh M, Villanacci V, Volta U, Zali MR, Srivastava A. ROC-king onwards: intraepithelial lymphocyte counts, distribution & role in coeliac disease mucosal interpretation. *Gut* 2017; **66**: 2080-2086 [PMID: 28893865 DOI: 10.1136/gutjnl-2017-314297]
 - 16 **Dahlbom I**, Nyberg BI, Berntson L, Hansson T. Simultaneous detection of IgA and IgG antibodies against tissue transglutaminase: The preferred pre-biopsy test in childhood celiac disease. *Scand J Clin Lab Invest* 2016; **76**: 208-216 [PMID: 26924622 DOI: 10.3109/00365513.2015.1137348]
 - 17 **Benkebil F**, Combescure C, Anghel SI, Besson Duvanel C, Schäppi MG. Diagnostic accuracy of a new point-of-care screening assay for celiac disease. *World J Gastroenterol* 2013; **19**: 5111-5117 [PMID: 23964145 DOI: 10.3748/wjg.v19.i31.5111]
 - 18 **Wieser H**. Relation between gliadin structure and coeliac toxicity. *Acta Paediatr Suppl* 1996; **412**: 3-9 [PMID: 8783747 DOI: 10.1111/j.1651-2227.1996.tb14239.x]
 - 19 **Piper JL**, Gray GM, Khosla C. High selectivity of human tissue transglutaminase for immunoactive gliadin peptides: implications for celiac sprue. *Biochemistry* 2002; **41**: 386-393 [PMID: 11772038 DOI: 10.1021/bi011715x]
 - 20 **Lundin KE**, Scott H, Hansen T, Paulsen G, Halstensen TS, Fausa O, Thorsby E, Sollid LM. Gliadin-specific, HLA-DQ(alpha 1*0501,beta 1*0201) restricted T cells isolated from the small intestinal mucosa of celiac disease patients. *J Exp Med* 1993; **178**: 187-196 [PMID: 8315377 DOI: 10.1084/jem.178.1.187]
 - 21 **Sollid LM**, Jabri B. Triggers and drivers of autoimmunity: lessons from coeliac disease. *Nat Rev Immunol* 2013; **13**: 294-302 [PMID: 23493116 DOI: 10.1038/nri3407]
 - 22 **du Pré MF**, Sollid LM. T-cell and B-cell immunity in celiac disease. *Best Pract Res Clin Gastroenterol* 2015; **29**: 413-423 [PMID: 26060106 DOI: 10.1016/j.bpg.2015.04.001]
 - 23 **Dieterich W**, Laag E, Schöpfer H, Volta U, Ferguson A, Gillett H, Riecken EO, Schuppan D. Autoantibodies to tissue transglutaminase as predictors of celiac disease. *Gastroenterology* 1998; **115**: 1317-1321 [PMID: 9834256 DOI: 10.1016/S0016-5085(98)70007-1]
 - 24 **Amarri S**, Alvisi P, De Giorgio R, Gelli MC, Cicola R, Tovoli F, Sassatelli R, Caio G, Volta U. Antibodies to deamidated gliadin peptides: an accurate predictor of coeliac disease in infancy. *J Clin Immunol* 2013; **33**: 1027-1030 [PMID: 23558824 DOI: 10.1007/s10875-013-9888-z]
 - 25 **Anderson RP**, Degano P, Godkin AJ, Jewell DP, Hill AV. In vivo antigen challenge in celiac disease identifies a single transglutaminase-modified peptide as the dominant A-gliadin T-cell epitope. *Nat Med* 2000; **6**: 337-342 [PMID: 10700238 DOI: 10.1038/73200]
 - 26 **Osman AA**, Günzel T, Dietl A, Uhlig HH, Amin M, Fleckenstein B, Richter T, Mothes T. B cell epitopes of gliadin. *Clin Exp Immunol* 2000; **121**: 248-254 [PMID: 10931138 DOI: 10.1046/j.1365-2249.2000.01312.x]
 - 27 **Piaggio MV**, Demonte AM, Sihufe G, Garcilazo S, Esper MC, Waggner M, Aleanzi M. Serological diagnosis of celiac disease: anti-gliadin peptide antibodies and anti-tissue transglutaminase. *Medicina* 1999; **59**: 693-697
 - 28 **Aleanzi M**, Demonte AM, Esper C, Garcilazo S, Waggner M. Celiac disease: antibody recognition against native and selectively deamidated gliadin peptides. *Clin Chem* 2001; **47**: 2023-2028 [PMID: 11673371]
 - 29 **Link S**, El-Sayed MA. Size and Temperature Dependence of the Plasmon Absorption of Colloidal Gold Nanoparticles. *J Phys Chem B* 1999; **103**: 4212-4217 [DOI: 10.1021/jp984796o]
 - 30 **Slocik JM**, Govorov AO, Naik RR. Plasmonic circular dichroism of Peptide-functionalized gold nanoparticles. *Nano Lett* 2011; **11**: 701-705 [PMID: 21207969 DOI: 10.1021/nl1038242]
 - 31 **Jans H**, Liu X, Austin L, Maes G, Huo Q. Dynamic light scattering as a powerful tool for gold nanoparticle bioconjugation and biomolecular binding studies. *Anal Chem* 2009; **81**: 9425-9432 [PMID: 19803497 DOI: 10.1021/ac901822w]
 - 32 **Jürgens L**, Nichtl A, Werner U. Electron density imaging of protein films on gold-particle surfaces with transmission electron microscopy. *Cytometry* 1999; **37**: 87-92 [PMID: 10486520 DOI: 10.1002/(SICI)1097-0320(19991001)37:2<87::AID-CYTO1>3.0.CO;2-1]
 - 33 **O'Farrelly C**, Kelly J, Hekkens W, Bradley B, Thompson A, Feighery C, Weir DG. Alpha gliadin antibody levels: a serological test for coeliac disease. *Br Med J (Clin Res Ed)* 1983; **286**: 2007-2010 [PMID: 6409205 DOI: 10.1136/bmj.286.6383.2007]
 - 34 **Wang Z**, Lee JH, Lu Y. Label-free colorimetric detection of lead ions with a nanomolar detection limit and tunable dynamic range by using gold nanoparticles and DNAzyme. *Adv Mater* 2008; **20**: 3263-3267 [DOI: 10.1002/adma.200703181]
 - 35 **Guo Y**, Wang Z, Qu W, Shao H, Jiang X. Colorimetric detection of mercury, lead and copper ions simultaneously using protein-functionalized gold nanoparticles. *Biosens Bioelectron* 2011; **26**: 4064-4069 [PMID: 21543219 DOI: 10.1016/j.bios.2011.03.033]
 - 36 **Bienvenu F**, Besson Duvanel C, Seignovet C, Rouzaire P, Lachaux A, Bienvenu J. Evaluation of a point-of-care test based on deamidated gliadin peptides for celiac disease screening in a large pediatric population. *Eur J Gastroenterol Hepatol* 2012; **24**: 1418-1423 [PMID: 23032795 DOI: 10.1097/MEG.0b013e3283582d95]
 - 37 **Volta U**, Tovoli F, Caio G. Clinical and immunological features of celiac disease in patients with Type 1 diabetes mellitus. *Expert Rev Gastroenterol Hepatol* 2011; **5**: 479-487 [PMID: 21780895 DOI: 10.1586/egh.11.38]
 - 38 **Ventura A**, Magazù G, Gerarduzzi T, Greco L. Coeliac disease and the risk of autoimmune disorders. *Gut* 2002; **51**: 897; author reply 897-897; author reply 898 [PMID: 12427802 DOI: 10.1136/gut.51.6.897]
 - 39 **Kaukinen K**, Mäki M, Partanen J, Sievänen H, Collin P. Celiac disease without villous atrophy: revision of criteria called for. *Dig Dis Sci* 2001; **46**: 879-887 [PMID: 11330428 DOI: 10.1023/A:1010729207320]
 - 40 **Volta U**, Villanacci V. Celiac disease: diagnostic criteria in progress. *Cell Mol Immunol* 2011; **8**: 96-102 [PMID: 21278763 DOI: 10.1038/cmi.2010.64]

P- Reviewer: Ciaccio EJ, Prasad KK, Rostami K, Rostami-Nejad M

S- Editor: Wang XJ **L- Editor:** A **E- Editor:** Yin SY



Case Control Study

Analyzing predictors of graft survival in patients undergoing liver transplantation with donors aged 70 years and over

Oscar Caso-Maestro, Carlos Jiménez-Romero, Iago Justo-Alonso, Jorge Calvo-Pulido, David Lora-Pablos, Alberto Marcacuzco-Quinto, Félix Cambra-Molero, Alvaro García-Sesma, Marina Pérez-Flecha, Carlos Muñoz-Arce, Carmelo Loinaz-Seguro, Alejandro Manrique-Municio

Oscar Caso-Maestro, Carlos Jiménez-Romero, Iago Justo-Alonso, Jorge Calvo-Pulido, Alberto Marcacuzco-Quinto, Félix Cambra-Molero, Alvaro García-Sesma, Marina Pérez-Flecha, Carlos Muñoz-Arce, Carmelo Loinaz-Seguro, Alejandro Manrique-Municio, Unit of HBP Surgery and Abdominal Organs Transplantation, Department of General Surgery, "12 de octubre" University Hospital, Madrid 28041, Spain

David Lora-Pablos, Clinical Research Department, Consortium for Biomedical Research in Epidemiology and Public Health (CIBERESP), "12 de octubre" University Hospital, Madrid 28041, Spain

ORCID number: Oscar Caso-Maestro (0000-0002-8953-269X); Carlos Jiménez-Romero (0000-0002-1965-0666); Iago Justo-Alonso (0000-0002-0553-5835); Jorge Calvo-Pulido (0000-0002-4377-7501); David Lora-Pablos (0000-0002-3317-5689); Alberto Marcacuzco-Quinto (0000-0001-6266-8792); Félix Cambra-Molero (0000-0001-5799-0170); Alvaro García-Sesma (0000-0002-4377-7501); Marina Pérez-Flecha (0000-0002-4714-4859); Carlos Muñoz-Arce (0000-0002-6841-1688); Carmelo Loinaz-Seguro (0000-0002-1873-0568); Alejandro Manrique-Municio (0000-0003-4758-9927).

Author contributions: Caso-Maestro O designed research, analyzed data and wrote the paper; Jiménez-Romero C designed the research and analyzed data; Justo-Alonso I participated collected and analyzed data; Calvo-Pulido J, Marcacuzco-Quinto A, Cambra-Molero F, García-Sesma A, Pérez-Flecha M, Muñoz-Arce C and Loinaz-Seguro C collected data; Lora-Pablos D performed the research and contributed new reagents or analytic tools; Manrique-Municio A participated collected and analyzed data.

Institutional review board statement: This study was approved by the institutional review board of "12 de octubre" University Hospital.

Informed consent statement: Patients were not required to give the informed consent to the study because the analysis used the anonymous data that were collected after each patient agreed to treatment.

Conflict-of-interest statement: The authors have declared no conflicts of interest.

Data sharing statement: No additional data is available.

STROBE statement: The authors have read the STROBE checklist and have checked the manuscript accordingly.

Open-Access: This article is an open-access article which was selected by an in-house editor and fully peer-reviewed by external reviewers. It is distributed in accordance with the Creative Commons Attribution Non Commercial (CC BY-NC 4.0) license, which permits others to distribute, remix, adapt, build upon this work non-commercially, and license their derivative works on different terms, provided the original work is properly cited and the use is non-commercial. See: <http://creativecommons.org/licenses/by-nc/4.0/>

Manuscript source: Unsolicited manuscript

Corresponding author to: Oscar Caso-Maestro, MD, PhD, Associate Professor, Staff Physician, Surgeon, Unit of HBP Surgery and Abdominal Organs Transplantation, Department of General Surgery, "12 de octubre" University Hospital, Av. Córdoba s/n, Madrid 28041, Spain. oscar.casomaes@salud.madrid.org
Telephone: +34-91-3908294

Received: October 5, 2018

Peer-review started: October 5, 2018

First decision: November 7, 2018

Revised: November 24, 2018

Accepted: November 30, 2018

Article in press: November 30, 2018

Published online: December 21, 2018

Abstract

AIM

To increase the number of available grafts.

METHODS

This is a single-center comparative analysis performed between April 1986 and May 2016. Two hundred and twelve liver transplantation (LT) were performed with donors ≥ 70 years old (study group). Then, we selected the first cases that were performed with donors < 70 years old immediately after the ones that were performed with donors ≥ 70 years old (control group).

RESULTS

Graft and patient survivals were similar between both groups without increasing the risk of complications, especially primary non-function, vascular complications and biliary complications. We identified 5 risk factors as independent predictors of graft survival: recipient hepatitis C virus (HCV)-positivity [hazard ratio (HR) = 2.35; 95% confidence interval (CI): 1.55-3.56; $P = 0.00$]; recipient age (HR = 1.04; 95%CI: 1.02-1.06; $P = 0.00$); donor age X model for end-stage liver disease (D-MELD) (HR = 1.00; 95%CI: 1.00-1.00; $P = 0.00$); donor value of serum glutamic-pyruvic transaminase (HR = 1.00; 95%CI: 1.00-1.00; $P = 0.00$); and donor value of serum sodium (HR = 0.96; 95%CI: 0.94-0.99; $P = 0.00$). After combining D-MELD and recipient age we obtained a new scoring system that we called DR-MELD (donor age X recipient age X MELD). Graft survival significantly decreased in patients with a DR-MELD score ≥ 75000 , especially in HCV patients (77% *vs* 63% at 5 years in HCV-negative patients, $P = 0.00$; and 61% *vs* 25% at 5 years in HCV-positive patients; $P = 0.00$).

CONCLUSION

A DR-MELD ≥ 75000 must be avoided in order to obtain the best results in LT with donors ≥ 70 years old.

Key words: Liver transplantation; Aged donors; Old donors; Marginal donors; Donor age

© The Author(s) 2018. Published by Baishideng Publishing Group Inc. All rights reserved.

Core tip: The use of aged grafts is one of the main strategies to increase the number of available grafts. After analyzing the results of liver transplantation performed with donors ≥ 70 years old, we identified as independent predictors of graft survival: donor age X model for end-stage liver disease (D-MELD), recipient age and hepatitis C virus (HCV) infection. After combining D-MELD and recipient age we obtained a new scoring system that we called DR-MELD (donor age X recipient age X MELD), which seems to be a good measure to predict graft survival when using grafts ≥ 70 years old, regardless of the HCV infection.

Caso-Maestro O, Jiménez-Romero C, Justo-Alonso I, Calvo-Pulido J, Lora-Pablos D, Marcacuzco-Quinto A, Cambra-Molero F, García-Sesma A, Pérez-Flecha M, Muñoz-Arce C, Loinaz-Seguro C, Manrique-Municio A. Analyzing predictors of graft survival in patients undergoing liver transplantation with donors

aged 70 years and over. *World J Gastroenterol* 2018; 24(47): 5391-5402

URL: <https://www.wjgnet.com/1007-9327/full/v24/i47/5391.htm>

DOI: <https://dx.doi.org/10.3748/wjg.v24.i47.5391>

INTRODUCTION

The increase of indications for liver transplantation (LT) and the shortage of liver donors has been one of the main problems for performing LTs in the past years^[1-8].

The use of aged donors is one of the main strategies to increase the number of available grafts. Spain is the country with the highest donation rate per million population (pmp) worldwide^[9]. Several studies comparing Spain and the United States showed that in Spain between 1999 and 2009 there was an increase in the donation rate by the population ≥ 70 years old from 3.8 donors pmp to 8.8 donors pmp (132% increase), while in the United States this rate only increased from 1 donor pmp to 1.3 donor pmp^[10,11]. Spain represents one of the countries with the most experience using aged liver grafts.

There have been multiple studies analyzing the impact of donor age on LT results since Emre *et al.*^[12] published in 1996 the first long series of LTs with donors ≥ 70 years old. Initially the results were disappointing, but as the number of LTs performed with such grafts increased, the results progressively improved until becoming comparable to those obtained with younger grafts^[12-22].

The aim of the present study is to identify predictors of graft survival with the use of donors ≥ 70 years old, and formulate a score able to predict graft survival in an attempt to develop a tool for daily donor-recipient matching.

MATERIALS AND METHODS

Data source and study population

This is a single-center comparative, longitudinal and retrospective analysis of all LTs performed at the "12 de Octubre" University Hospital of Madrid between April 1986 and May 2016. During this period 1848 LTs were performed in 1659 patients. Of these, 232 (12.6%) were performed with grafts from donors ≥ 70 years old. Recipients < 18 years old, retransplantation, acute liver failure, human immunodeficiency virus (HIV) positivity, combined transplants, split grafts, *in-vivo* donation, non-heart-beating donation, LTs due to metastatic liver disease and LTs with incomplete medical records were excluded from the analysis. Thus, 212 cases (study group) were included in the study (Figure 1). To minimize the impact of the era when the LT was performed, we selected as controls the first cases that were performed with a graft < 70 years old immediately after the ones that were performed with a graft > 70

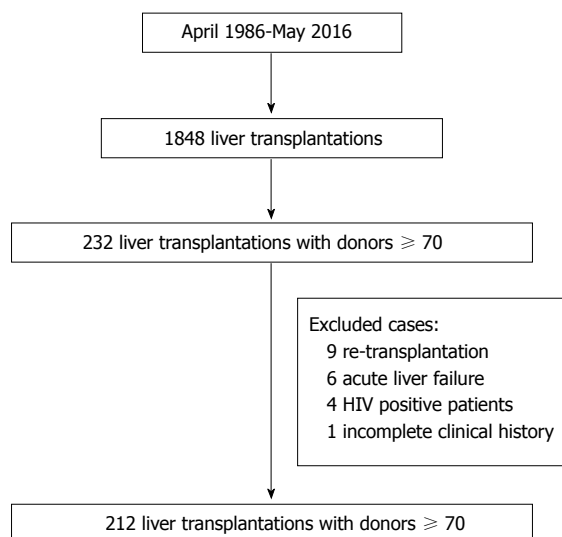


Figure 1 Flowchart of the selection of the cases included in the present study. HIV: Human immunodeficiency virus.

years old; thus, the control group also consisted of 212 cases.

The first LT with a graft from a donor > 70 years old was performed on January 17, 1994. The use of donors ≥ 70 years old increased progressively over the years, and now stands at around 30% of all LTs performed annually in our department (Figure 2).

Donor and recipient evaluation

All donors were evaluated according to our institution's policy and according to the Spanish National Transplant Organization's [Organización Nacional de Trasplantes (ONT)] guidelines.

Uncontrolled active sepsis, parenteral drug addiction, untreated primary or secondary hepatobiliary disease, severe traumatic injury, untreated tumor disease (except small cutaneous carcinomas, cervical carcinoma in situ, central nervous system tumors except glioblastoma and medulloblastoma, and renal cell carcinomas < 4 cm) and severe intoxication were considered contraindications for donation.

All donors were procured with dual perfusion (aortic and portal) and all LTs were performed with cava vein preservation. End-to-end choledochal anastomosis was routinely performed. In cases of size disparity, a T-tube was used and in cases of biliary disease a cholangiojejunostomy was made.

Donor, recipient and perioperative characteristics, and post-LT complications were analyzed. Patient and graft survival were also recorded.

All grafts ≥ 70 years old were biopsied during procurement to assess the presence of steatosis. All biopsies were reviewed at the pathology department of our institution.

The presence of severe arteriosclerosis with no possibility of arterial reconstruction was considered a contraindication for the use of these grafts.

All LT recipients were evaluated before transplant in our department. The indication for LT was established according to our own policy and according to the ONT guidelines. The follow-up of each patient after the transplant was carried out based on the different protocols existing in our department.

The degree of hepatic insufficiency was evaluated with the Child-Pugh classification until 2003, and after that with the model for end-stage liver disease (MELD) score^[23]. Refractory encephalopathy or ascites, hepatopulmonary syndrome, portopulmonary hypertension, refractory pruritus, recurrent cholangitis in patients with cholestatic liver disease, hereditary hemorrhagic teleangiectasia, polycystic disease, multiple hemangiomatosis and hepatocellular carcinoma (HCC) were considered exceptions to MELD.

Immunosuppressive regimen

In all cases, an initial immunosuppressive (IMS) regimen based on the administration of a calcineurin inhibitor (tacrolimus or cyclosporine) and steroids was used. Other drugs (azathioprine, mycophenolate or mTOR inhibitors) were added in an individualized way depending on the clinical situation. Steroids were usually discontinued between 3 and 12 mo after LT in the cyclosporine regimen, and after 3 mo in the tacrolimus regimen.

Definitions

Primary non-function (PNF) was defined as early failure of liver function manifested by signs of acute liver failure: severe hypoglycemia, persistent coagulopathy, encephalopathy III-IV, acute renal failure, severe metabolic acidosis, hemodynamic instability and abnormal hepatic enzyme levels.

Acute rejection episodes were classified based on the Banff grades^[24]. The initial treatment was based on the degree of rejection. Grade 1 rejections were treated by increasing the dose of IMS drugs, and grade 2 and 3 rejections were treated with 1 g of methylprednisolone intravenously for 3 d and steroid recycling. Corticosteroid-refractory rejections were treated with monoclonal antibodies: ATG and OKT3 in the initial period, and with thymoglobulin and basiliximab thereafter.

Hepatitis C virus (HCV) recurrence in the graft was confirmed by histology based on the presence of periportal and lobular inflammation and the presence of fibrosis^[25]. In our department, we do not have a biopsy follow-up protocol for HCV-patients undergoing LT, and therefore biopsies were only performed in the presence of elevated hepatic enzymes in the absence of abnormal vascular, biliary and IMS levels.

Vascular complications were defined as all post-transplant abnormalities in the hepatic artery, portal vein or cava vein requiring therapeutic procedures such as radiological or surgical procedures.

Biliary complications were defined as all post-

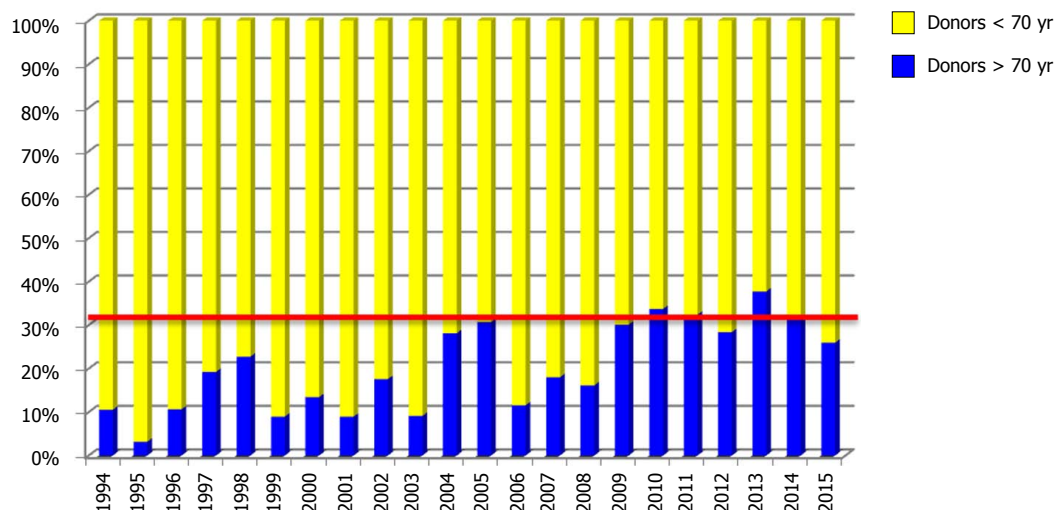


Figure 2 Rate of transplants performed in our department from 1996 to 2015 with donors ≥ 70 years old.

transplant abnormalities in the biliary tree requiring radiological, endoscopic or surgical procedures.

In order to carry out the graft survival analysis, we took into account the number of months from the LT day to the day on which one of the following events occurred: (1) end of study (August 31, 2016), (2) death, (3) loss of follow-up, or (4) re-transplantation. When the patient died, the graft was considered as non-functioning graft.

Statistical analysis

Statistical analysis was done using the SPSS software package, version 20.0.0 (SPSS Inc., Chicago, IL, United States). Quantitative variables were expressed as mean \pm standard deviation with a normal distribution of the variable, and as median and interquartile range when the variable did not have a normal distribution. Qualitative variables were expressed as absolute frequencies (n) and relative frequencies (%). To compare qualitative variables, the chi-square test and Fisher's exact test were used. To compare quantitative variables with qualitative variables, Student's t -test was used. Non-parametric tests were employed when appropriate. Graft survival was studied using the Kaplan-Meier method and comparisons between the different curves obtained were performed using the log-rank test. Regarding the multivariate analysis, we considered those variables in which statistically significant differences were found during the comparative analysis and those that we considered clinically relevant. The multivariate Cox proportional hazard model was applied to analyze the prognostic value for the risk of graft loss in all LTs performed with donors ≥ 70 years old. A stepwise backward conditional procedure was used. Finally, based on the results obtained, we studied graft survival according to the risk factors identified during the multivariate analysis. A P -value < 0.05 was considered statistically significant in all studies performed.

RESULTS

Donor characteristics

The donor characteristics are shown in Table 1. Aged donors were predominantly female whereas younger donors were predominantly male ($P = 0.00$). Obesity (27% vs 16%; $P = 0.00$), hypertension (58% vs 26%; $P = 0.00$) and diabetes (20% vs 7%; $P = 0.00$) were more common among aged donors. Although we found more cases of cerebrovascular deaths in the study group (81% vs 51%; $P = 0.06$), this difference was not statistically significant. Cardiac arrest was significantly lower in donors ≥ 70 years old (7% vs 25%; $P = 0.00$). Median serum sodium level was high in both groups, but significantly lower in the study group. Median serum glutamic-pyruvic transaminase (GPT) and glutamic-oxaloacetic transaminase (GOT) levels were normal in both groups but, like sodium levels, they were significantly lower in aged donors. Biopsy findings were similar in both groups, with more than half of all cases without steatosis in each group.

Recipient characteristics

Table 2 lists recipient characteristics of the 2 groups. Mean recipient age was higher in recipients of older grafts. HCV-positivity was more common among patients undergoing LT with younger donors (34% vs 49%; $P = 0.00$). Median product of donor age and preoperative MELD (D-MELD) value was higher in the recipients of the study group (1051 vs 629; $P = 0.00$), but all laboratory parameters analyzed were similar in both groups.

Perioperative characteristics

Table 3 shows perioperative characteristics in the 2 groups. Mean cold ischemia time (CIT) was longer in the study group (445 min vs 386 min; $P = 0.00$). This is because most aged donors were from hospitals outside

Table 1 Donor characteristics *n* (%)

	Donors < 70 years old (<i>n</i> = 212)	Donors ≥ 70 years old (<i>n</i> = 212)	<i>P</i> value
Age (yr)	47 (26)	76 (7)	0.00
Gender (male/female)	139/73 (65.6/34.3)	87/125 (41.0/59.0)	0.00
BMI ≥ 30 (kg/m ²)	33 (15.6)	57 (27.3)	0.00
Cause of death			
Trauma	72 (34.0)	32 (15.1)	
Cerebrovascular	108 (50.9)	172 (81.1)	0.06
Other	32 (15.1)	8 (3.8)	
History of hypertension	55 (25.9)	122 (57.5)	0.00
History of diabetes	14 (6.6)	43 (20.3)	0.00
ICU stay (h)	48 (24-96)	211 (24-48)	0.00
Cardiac arrest	53 (25.0)	14 (6.6)	0.00
Hemodynamic instability	68 (32.1)	60 (28.3)	0.39
Vasopressor use	173 (81.6)	159 (75.0)	0.09
Glucose (mg/dL)	145 (63)	156 (69)	0.00
Creatinine (mg/dL)	0.9 (0.5)	0.8 (0.3)	0.24
Sodium (mEq/L)	148 (12)	145 (11)	0.00
GOT (IU/L)	39 (55)	28 (19)	0.00
GPT (IU/L)	27 (53)	20 (17)	0.00
Biopsy findings			
Normal	125 (57.8)	107 (49.8)	
Microsteatosis	26 (12.6)	41 (19.5)	
Mild macrosteatosis (< 30%)	54 (26.1)	56 (26.7)	0.12
Moderate macrosteatosis (30%-60%)	7 (3.5)	7 (3.5)	
Severe macrosteatosis (≥ 60%)	0 (0.0)	1 (0.5)	

BMI: Body mass index; ICU: Intensive care unit; GOT: Glutamic-oxaloacetic transaminase; GPT: Glutamic-pyruvic transaminase.

Table 2 Recipient characteristics *n* (%)

	Donors < 70 years old (<i>n</i> = 212)	Donors ≥ 70 years old (<i>n</i> = 212)	<i>P</i> value
Age (yr)	54 (14)	59 (13)	0.00
Gender (male/female)	161/51 (75.9/24.1)	167/45 (78.8/21.2)	0.48
Cirrhosis			
Alcoholic	61 (28.8)	95 (44.8)	
HBV	13 (6.1)	24 (11.3)	0.00
HCV	105 (49.5)	72 (34.0)	
Other	33 (15.6)	21 (9.9)	
HCC	82 (38.7)	84 (39.3)	0.89
Child-Pugh			
A	47 (22.1)	46 (21.7)	
B	75 (35.4)	89 (42)	0.22
C	90 (42.5)	77 (36.3)	
MELD	15 (8)	13 (5)	0.20
MELD-Na	16 (11)	14 (9)	0.12
D-MELD	629 (475)	1051 (842)	0.00
Glucose (mg/dL)	107 (44)	105 (48)	0.70
Creatinine (mg/dL)	0.9 (0.4)	0.9 (0.3)	0.07
Total bilirubin (mg/dL)	2.7 (3.4)	1.9 (2.4)	0.10
GOT (IU/L)	54 (67)	58 (58)	0.77
GPT (IU/L)	40 (49)	37 (43)	0.60
Albumin (mg/dL)	3.3 (0.9)	3.4 (1.0)	0.77
Prothrombin activity (%)	62 ± 20 (11.8-120)	65 ± 18 (5-119)	0.07
Platelets (<i>n</i>)	77900 (54925)	82500 (60250)	0.16
UNOS			
ICU	0	3 (1.4)	0.77
Hospital	17 (8)	12 (5.7)	
Home	195 (92)	197 (92.9)	

HBV: Hepatitis B virus; HCV: Hepatitis C virus; HCC: Hepatocellular carcinoma; MELD: Model for end-stage liver disease; D-MELD: The product of donor age and preoperative MELD; GOT: Glutamic-oxaloacetic transaminase; GPT: Glutamic-pyruvic transaminase; UNOS: United network for organ sharing; ICU: Intensive care unit.

of Madrid, and in some cases, it took up to 3 h for the grafts to reach our hospital. Transfusion requirements

were similar in both groups and no differences were observed in the immunosuppressive treatment.

Table 3 Perioperative characteristics and post-liver transplantation complications *n* (%)

	Donors < 70 years old (<i>n</i> = 212)	Donors ≥ 70 years old (<i>n</i> = 212)	<i>P</i> value
CIT (min)	386 ± 168 (100-1038)	445 ± 158 (60-975)	0.00
WIT (min)	64 ± 17 (40-200)	61 ± 13 (30-130)	0.04
RBC (U)	6 (3-10)	5 (3-10)	0.98
FFP (U)	12 ± 9 (0-60)	13 ± 9 (0-58)	0.40
Platelets (U)	3 ± 3 (0-37)	3 ± 3 (0-16)	0.53
Basal immunosuppressant drugs			
Cyclosporine plus steroids	33 (15.6)	30 (14.3)	0.71
Tacrolimus plus steroids	179 (84.4)	180 (85.7)	
ICU stay (d)	4 (2-5)	4 (2-6)	0.58
Hospital stay (d)	18 ± 17 (0-105)	16 ± 12 (0-83)	0.34
Primary non-function	6 (2.8)	7 (3.3)	0.24
Acute rejection	61 (28.8)	53 (25.1)	0.39
Infectious complications	56 (26.4)	41 (19.3)	0.08
Medical complications	90 (42.5)	93 (43.9)	0.76
Surgical complications	38 (17.9)	34 (16)	0.60
Vascular complications	11 (5.2)	14 (6.6)	0.80
Biliary complications	24 (11.3)	11 (5.2)	0.41
Reoperation	27 (12.7)	20 (9.4)	0.28
<i>De novo</i> tumors	24 (11.3)	22 (10.4)	0.57
HCV recurrence	73 (61.9)	42 (57.5)	0.55
Days	141 (58-535)	148 (51-316)	0.90
Hepatitis F3 or F4	18 (24.7)	21 (50)	0.00
Fibrosing cholestatic hepatitis	7 (9.6)	7 (16.7)	0.26
Re-transplantation	11 (5.2)	12 (5.7)	0.83

CIT: Cold ischemia time; WIT: Warm ischemia time; RBC: Red blood cells; FFP: Fresh frozen plasma; ICU: Intensive care unit.

Complications after LT

In Table 3 we can also observe the differences between the 2 groups regarding the development of different complications. Hospital stay in both intensive care unit (ICU) and conventional hospitalization unit were similar in both groups. No differences were found in relation to PNF, and acute rejection rate was similar in both groups (25% vs 29%; *P* = 0.39). Infectious complications were lower in the study group, but differences were not statistically significant. The rate of vascular complications was similar in both groups (6.6% vs 5.2%; *P* = 0.80). Although biliary complications were lower in the group of LTs performed with aged donors, differences were not statistically significant (5.2% vs 11.3%; *P* = 0.41). Finally, HCV recurrence was similar in both groups, but severe HCV recurrence (F3-F4 hepatitis) was higher in the study group (50% vs 25%; *P* = 0.00).

Survival analysis

After a mean follow-up of 67 ± 59 (range: 0-271) mo in the control group and a mean follow-up of 67 ± 61 (range: 0-269) mo in the study group, there were 67 (31.6%) deaths in the control group and 80 (37.7%) deaths in the study group. These differences were not statistically significant.

We also did not observe significant differences between the causes of death in each group, and the main causes in both groups were infections and medical complications.

Patient survival at 1, 3 and 5-years was 86.3%, 79.8% and 72.8%, respectively, in the control group and 83.8%, 78.1% and 69%, respectively, in the

study group. Differences between the groups were not significant.

Graft survival at 1, 3 and 5-years was 85.3%, 78.4% and 70.2%, respectively, in the control group and 80.5%, 73.6% and 64.5%, respectively, in the study group. Again, differences between the groups were not significant.

Multivariate analysis

A Cox-regression analysis to investigate risk factors for graft loss in LTs performed with donors ≥ 70 years old was performed including all variables where we found differences during the comparative analysis and the ones that we considered clinically relevant. Table 4 shows the results. We identified 5 risk factors as independent predictors of graft survival: recipient HCV-positivity [hazard ratio (HR) = 2.35; 95% confidence interval (CI): 1.55-3.56; *P* = 0.00]; recipient age (HR = 1.04; 95%CI: 1.02-1.06; *P* = 0.00); D-MELD (HR = 1.00; 95%CI: 1.00-1.00; *P* = 0.00); donor value of serum GPT (HR = 1.00; 95%CI: 1.00-1.00; *P* = 0.00); and donor value of serum sodium (HR = 0.96; 95%CI: 0.94-0.99; *P* = 0.00).

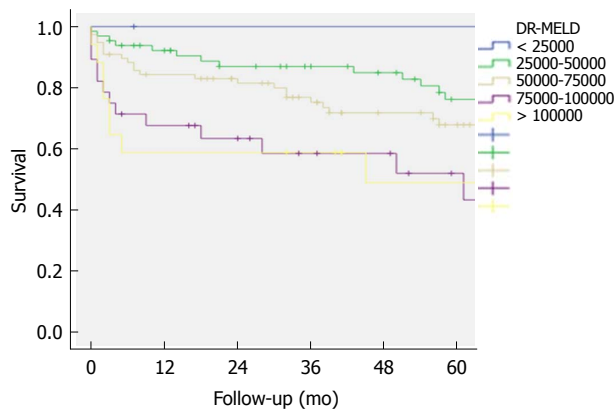
Graft survival according to risk factors

After combining D-MELD and recipient age we obtained a new scoring system that we called DR-MELD (product of donor age, recipient age and preoperative MELD). Median (interquartile range) DR-MELD in the study group was 58309 (27861). We stratified the recipients into 5 groups (DR-MELD < 25000; DR-MELD 25000-49999; DR-MELD 50000-74999; DR-

Table 4 Multivariate Cox-regression analysis for the risk of graft loss

	Univariate analysis		Multivariate analysis	
	HR (95%CI)	P value	HR (95%CI)	P value
Donor age	1.23 (0.90-1.68)	0.19	1.15 (0.73-1.81)	0.52
Female donor	1.08 (0.78-1.49)	0.63		
Donor BMI				
25-29	1.56 (1.05-2.31)	0.08		
≥ 30	1.53 (0.95-2.47)	0.07		
Cause of death				
Cerebrovascular	1.091 (0.75-1.58)	0.65		
Others	0.68 (0.34-1.36)	0.28		
Donor history of hypertension	1.53 (1.10-2.12)	0.00	1.43 (0.97-2.12)	0.07
Donor history of diabetes	0.99 (0.62-1.58)	0.97		
Donor ICU stay	1.00 (0.99-1.00)	0.37		
Donor cardiac arrest	0.94 (0.59-1.52)	0.82		
Donor last serum sodium level	0.97 (0.96-0.99)	0.01	0.96 (0.94-0.99)	0.00
Donor last serum GOT	1.00 (1.00-1.00)	0.13		
Donor last serum GPT	1.00 (1.00-1.00)	0.02	1.00 (1.00-1.00)	0.00
Biopsy findings				
Normal	1.00 (0.64-1.59)	0.96		
Microsteatosis	1.22 (0.82-1.82)	0.31		
Mild macrosteatosis (< 30%)	1.89 (0.93-3.82)	0.07		
Moderate macrosteatosis (30%-60%)	0.93 (0.57-1.53)	0.78		
Recipient age	1.03 (1.01-1.05)	0.00	1.04 (1.02-1.06)	0.00
HCV ⁺ recipient	1.82 (1.32-2.50)	0.00	2.35 (1.55-3.56)	0.00
HCC presence	1.24 (0.90-1.71)	0.18		
MELD	1.03 (1.00-1.06)	0.05		
D-MELD	1.00 (1.00-1.00)	0.00	1.00 (1.00-1.00)	0.00
Prothrombin activity	0.99 (0.98-1.00)	0.28		
CIT	0.99 (0.99-1.00)	0.13		
WIT	1.01 (0.99-1.02)	0.38		

HR: Hazard ratio; CI: Confidence interval; BMI: Body mass index; ICU: Intensive care unit; GOT: Glutamic-oxaloacetic transaminase; GPT: Glutamic-pyruvic transaminase; HCV: Hepatitis C virus; HCC: Hepatocellular carcinoma; MELD: Model for end-stage liver disease; D-MELD: The product of donor age and preoperative MELD; CIT: Cold ischemia time; WIT: Warm ischemia time.



DR-MELD score	< 25000	25000-49999	50000-74999	75000-99999	≥ 100000
1 yr	100%	92%	84%	68%	59%
3 yr	100%	87%	75%	59%	59%
5 yr	100%	76%	68%	52%	49%

Figure 3 Graft survival according to donor age X recipient age X model for end-stage liver disease score in patients undergoing liver transplantation with grafts ≥ 70 years old. Chi-square = 12.358, degrees of freedom = 1, $P = 0.00$. DR-MELD: Donor age X recipient age X model for end-stage liver disease.

MELD 75000-99999; and DR-MELD ≥ 100000), and we analyzed the graft survival according to this new

score. Figure 3 shows the results. Overall, we obtained a graft survival of more than 70% at 5 years in patients with a DR-MELD score ≤ 75000, and of less than 50% in patients with a DR-MELD score ≥ 75000. Finally, we calculated graft survival according to DR-MELD and HCV infection status, and we observed that graft survival significantly decreased in patients with a DR-MELD score ≥ 75000, especially in HCV-positive patients (77% vs 63% at 5 years in HCV-negative patients, $P = 0.00$; and 61% vs 25% at 5 years in HCV-positive patients; $P = 0.00$) (Figures 4 and 5).

DISCUSSION

Use of elderly donors is an effective mean to expand the donor pool with results similar to those described with the use of younger donors, as demonstrated in multiple studies over the past years^[12-22,26].

In Europe, the use of these donors has become common. One single-center study reports that almost 40% of all LTs were performed with donors ≥ 70 years old^[26]. However, in the United States, the use of these grafts is lower than in Europe, as shown in a recent study, where the rate of LTs performed with donors ≥ 70 years old in the United States was only 4.3% between January 2002 and September 2014^[27].

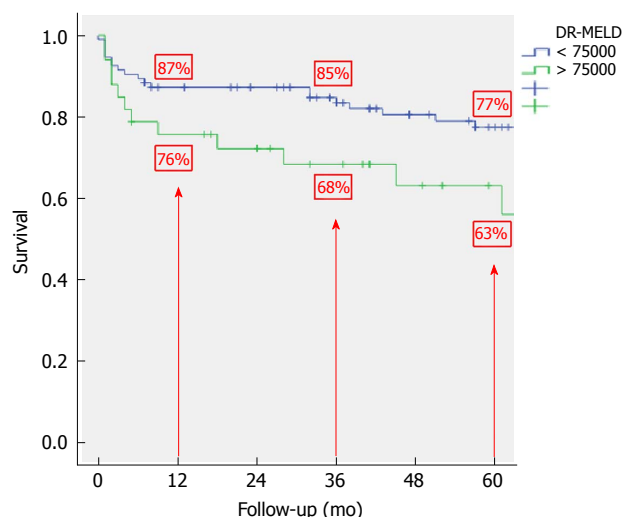


Figure 4 Graft survival in hepatitis C-negative patients according to donor age X recipient age X model for end-stage liver disease score after liver transplantation with grafts ≥ 70 years old. Chi-square = 4.222, degrees of freedom = 1, $P = 0.00$. DR-MELD: Donor age X recipient age X model for end-stage liver disease.

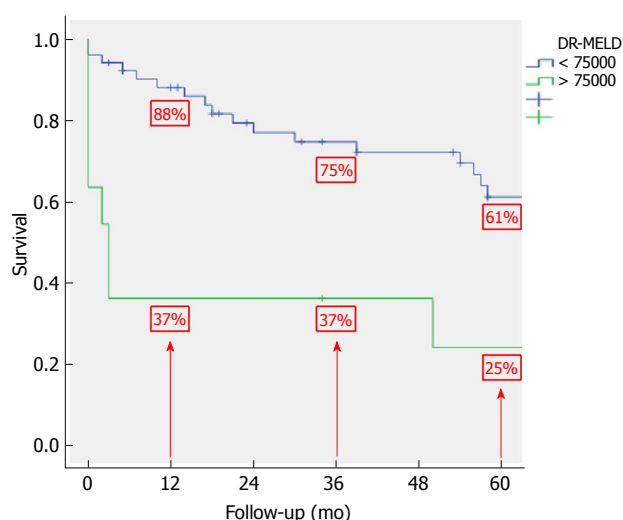


Figure 5 Graft survival in hepatitis C-positive patients according to donor age X recipient age X model for end-stage liver disease score after liver transplantation with grafts ≥ 70 years old. Chi-square = 12.615, degrees of freedom = 1, $P = 0.00$. DR-MELD: Donor age X recipient age X model for end-stage liver disease.

According to the literature, and also as observed in the present study, elderly donors have a number of common characteristics^[12-22,26]. Females predominate over males. The rates of hypertension and diabetes are also higher among these donors. The main cause of donor death is the cerebrovascular accident, followed by trauma (81% vs 15%). Finally, there is a tendency to minimize other donor risk factors for a worse evolution^[28]. Thus, older donors have shorter ICU stays with fewer episodes of hemodynamic instability or cardiac arrest, and laboratory parameters such as serum sodium and transaminases are usually significantly lower.

In the literature, different factors have been described as predictors of graft survival, and most of them have been reported in several studies^[8,13,26,29-33]. A summary of predictors of graft survival with the use of donors ≥ 70 years old that were identified by multivariate analysis (Cox regression), is shown in Table 5. In our study, we identified 5 independent predictors of graft survival: donor serum sodium and serum GPT, recipient age, HCV and D-MELD.

Sodium and GPT are laboratory parameters that in many studies have been identified as risk factors for a poor outcome, regardless of the age of the donor^[28]. However, in studies performed with donors ≥ 70 years old they never were found to be predictors of graft survival^[8,13,26,30-33]. In addition, although differences between these parameters were statistically significant in our study, we think that they are not clinically relevant since they were within the normal range in both groups.

HCV is a long-known survival predictor in LTs performed with aged donors. HCV recurrence is earlier and more aggressive when aged donors are used^[34-38]. In most of the studies performed with donors older than 70 years, we also observed that HCV was an independent predictor of graft survival^[13,26,30-32]. In recent years, younger grafts usually have been implanted in HCV-positive patients, while older livers were used to transplant patients with HCC and without HCV infection^[30]. Currently, with the arrival of direct-acting antivirals (DAA), the results of LT with aged donors in HCV patients have changed and donor age will not influence anymore LT results in HCV recipients.

It has been demonstrated that D-MELD is able to predict the results of LTs with donors older than 70 years, especially in HCV patients^[31,39]. Initially, Halldorson *et al.*^[40] proposed a D-MELD score of 1600 as a cut-off point to identify cases with significantly worse outcomes. In our study, these results were not confirmed when they were applied to recipients of grafts ≥ 70 years old, since we obtained a 5-year graft survival of 68.4% and 62.1% for D-MELD scores < 1600 and ≥ 1600 , respectively ($P > 0.05$). We also did not obtain significant differences when we used different cut-off points proposed by other authors^[31,39], or by applying still different ones. Although D-MELD was an independent predictor of graft survival in our study, we think that it should be used in combination with other parameters to improve its prediction power.

The age of the recipient is another parameter that in many studies has been linked with the result. In multiple series of LT with donors ≥ 70 years old, recipient age was an independent predictor of graft survival^[30,33]. Some authors proposed that these grafts should be limited to young recipients without other associated risk factors to obtain better results^[30,41,42]. However, in recent studies^[13,26,31] the mean age of the recipients was even higher in the group of transplants performed with elderly donors than in the group of

Table 5 Studies comparing liver transplantation with donors ≥ 70 years old vs liver transplantation with younger donors that provide multivariate analysis identifying predictors of graft survival

Author	Country	n	Donor age	Donor diabetes	Donor GPT	Donor Na	Recipient age	Recipient BMI	UNOS	HCV positive	MELD	D-MELD	BAR	CIT	Period	Renal replacement
Segev, 2007	United States	1043					X	X	X	X				X		
Cescon, 2008	Italy	152	X				X	X	X	X						
Jimenez Romero, 2013	Spain	50						X			X					
Cepeda Franco, 2016	Spain	423								X						
Bertuzzo, 2017	Italy	278								X			X		X	X
Montenovo, 2017	United States	1749	X				X		X							
Ghinolfi, 2017	Italy	515	X			X				X				X		
Present study, 2018	Spain	212				X	X			X	X					

GPT: Glutamic-pyruvic transaminase; Na: Serum sodium; BMI: Body mass index; UNOS: United network for organ sharing status; HCV: Hepatitis C virus; MELD: Model for end-stage liver disease; D-MELD: The product of donor age and preoperative MELD; BAR: Balance of risk score; CIT: Cold ischemia time.

transplants performed with younger donors.

In our study, other variables such as CIT, donor body mass index (BMI) and graft steatosis did not show a predictive value of graft survival (Table 4). However, we observed in the univariate analysis that the hazard ratio increased as the donor BMI and the steatosis percentage increased. Based on this observation and on an analysis of the results obtained by other authors^[30,43], we consider that the presence of steatosis $\geq 30\%$ should be a contraindication for the use of these grafts. A graft biopsy should be mandatory to assess the presence of steatosis and it should always be done during the evaluation of an aged donor. More detailed studies are probably necessary to determine what percentage of steatosis should be the maximum recommended when using elderly grafts. Finally, CIT is a risk factor that has been related with a worse graft survival, and multiple studies recommend that it must be less than 8 hours when a graft ≥ 70 years old is used^[8,26,30]. In our study, CIT was not an independent predictor of graft survival. This is probably because the mean CIT in the study group was 445 min, less than the 8 h recommended by most groups. We think, like other authors, that CIT should be as short as possible when aged grafts are going to be used, although a longer CIT should not be an absolute contraindication to use such grafts, and that this parameter must be analyzed case by case.

After analyzing the results of the multivariate analysis, we formulated a score using the D-MELD in combination with the age of the recipient (DR-MELD), and we analyzed its ability to predict graft survival in the study group according to the presence or absence of the HCV. We did not use serum donor GPT and sodium because, as we have previously seen, they were not clinically relevant. Overall, 5-year graft survival with donors ≥ 70 years old with a DR-MELD score < 75000 was 72%, while with a DR-MELD score ≥ 75000 it decreased to 53% ($P = 0.00$). Furthermore, with a DR-MELD score ≥ 75000 , 5-year graft survival decreased significantly in HCV-negative patients (77% vs 63%, $P = 0.00$), but it decreased more significantly in HCV-positive patients (61% vs 25%, $P = 0.00$). Currently, with the effectiveness of the DAA, we can use an aged donor in a HCV-positive recipient with the same results than in a HCV-negative recipient. Given these results, DR-MELD seems to be a good measure to predict graft survival when using grafts ≥ 70 years old.

The present study is a single-center and longitudinal study, which ensures the homogeneity of the sample, the surgical technique and the follow-up. Furthermore, the fact that it is a single-center study and not based on a registry database has allowed the analysis of multiple variables of both donors and recipients. On the other hand, the study is retrospective and there is an important time difference between the first cases and the last ones; this may have a significant influence on the results, as other authors have noted^[32]. Further studies are required to validate our results and compare them with other scores described in the literature, to define which of them is the most accurate.

In conclusion, the use of donors ≥ 70 years old is a safe strategy to expand the donor pool, and in the coming years they will probably become the main source of donation in western countries. Graft and patient survivals are similar to those obtained with the use of younger grafts without increasing the risk of complications, especially PNF, vascular complications and biliary complications. A DR-MELD ≥ 75000 must be avoided in order to obtain the best results. More studies are required to validate these findings.

ARTICLE HIGHLIGHTS

Research background

The increased life expectancy of the general population makes that donor age should also increase to ensure the number of available donors. Concerns regarding the use of aged organs are the perception of greater susceptibility to ischemic damage resulting in higher risk of initial poor function or primary non-function. There are limited published data evaluating results of liver transplantation (LT) with these donors and only a few of them try to identify predictors of graft survival.

Research motivation

Some authors have suggested that if we identify which variables are able to predict survival, careful donor to recipient matching could avoid some complications after LT with aged donors and improve patient and graft survival.

Research objectives

The main objective of our study is to evaluate LT outcomes with donors ≥ 70 years old using a large single-center cohort, identify predictors of graft survival and compare our results with previously published.

Research methods

We analyzed all LT performed at our department between April 1986 and May 2016 with donors ≥ 70 years old, then we compared the outcomes with those obtained using younger donors in the same period and finally a multivariate Cox proportional hazard model was applied to analyze the prognostic value for the risk of graft loss in all LT performed with aged donors.

Research results

The use of donors ≥ 70 years old is a safe strategy to expand the donor pool. Graft and patient survivals are similar to those obtained with the use of younger grafts without increasing the risk of complications, especially primary non-function, vascular complications and biliary complications. We identified 5 independent predictors of graft survival: donor serum sodium and serum glutamic-pyruvic transaminase, recipient age, hepatitis C virus (HCV) and donor age X model for end-stage liver disease (D-MELD). Finally, we formulated a score using the D-MELD in combination with the age of the recipient (we called it DR-MELD), and we analyzed its ability to predict graft survival in the study group according to the presence or absence of the HCV. A DR-MELD < 75000 was a good measure to predict graft survival when using grafts ≥ 70 years old regardless the presence of HCV.

Research conclusions

The use of aged donors in LT is not associated with higher primary non-function or other complications if we perform a careful donor selection. The current study emphasizes on the importance of identifying predictors of graft survival before donor to recipient matching. With the arrival of direct-acting antivirals, the results of LT with aged donors in HCV patients have changed and donor age will not influence anymore LT results in HCV recipients. Donor age, recipient age, MELD, cold ischemia time and the presence of steatosis seems to be the best predictors of graft survival after analyze the outcomes of several studies.

Research perspectives

The use of aged donors is a safe alternative to expand the donor pool in LT with

brain death donors. Additional studies are needed to investigate if the donor age could also be increased with marginal donors such as non-heart beating, split or living donors.

ACKNOWLEDGMENTS

The authors want to thank all members of the HBP surgery and Abdominal Organs Transplantation Unit for their contributions to this valuable resource.

REFERENCES

- 1 **Memoria Trasplante Hepático.** Accessed October 4, 2018 Available from: URL: <http://www.ont.es/infesp/Memorias/Memoria%20Hepático%202016.pdf>
- 2 **Strasberg SM,** Howard TK, Molmenti EP, Hertl M. Selecting the donor liver: risk factors for poor function after orthotopic liver transplantation. *Hepatology* 1994; **20**: 829-838 [PMID: 7927223 DOI: 10.1002/hep.1840200410]
- 3 **Adam R,** Sanchez C, Astarcioglu I, Bismuth H. Deleterious effect of extended cold ischemia time on the posttransplant outcome of aged livers. *Transplant Proc* 1995; **27**: 1181-1183 [PMID: 7878841]
- 4 **Ureña MA,** Ruiz-Delgado FC, González EM, Seguro CL, Romero CJ, García IG, González-Pinto I, Gómez Sanz R. Assessing risk of the use of livers with macro and microsteatosis in a liver transplant program. *Transplant Proc* 1998; **30**: 3288-3291 [PMID: 9838454]
- 5 **López-Navidad A,** Caballero F. Extended criteria for organ acceptance. Strategies for achieving organ safety and for increasing organ pool. *Clin Transplant* 2003; **17**: 308-324 [PMID: 12868987]
- 6 **Busuttil RW,** Tanaka K. The utility of marginal donors in liver transplantation. *Liver Transpl* 2003; **9**: 651-663 [PMID: 12827549 DOI: 10.1053/jlts.2003.50105]
- 7 **Cuende N,** Grande L, Sanjuán F, Cuervas-Mons V. Liver transplant with organs from elderly donors: Spanish experience with more than 300 liver donors over 70 years of age. *Transplantation* 2002; **73**: 1360 [PMID: 11981439 DOI: 10.1097/00007890-200204270-00033]
- 8 **Jiménez-Romero C,** Clemares-Lama M, Manrique-Municio A, García-Sesma A, Calvo-Pulido J, Moreno-González E. Long-term results using old liver grafts for transplantation: sexagenarian versus liver donors older than 70 years. *World J Surg* 2013; **37**: 2211-2221 [PMID: 23703639 DOI: 10.1007/s00268-013-2085-7]
- 9 **Matesanz R,** Domínguez-Gil B, Coll E, Mahillo B, Marazuela R. How Spain Reached 40 Deceased Organ Donors per Million Population. *Am J Transplant* 2017; **17**: 1447-1454 [PMID: 28066980 DOI: 10.1111/ajt.14104]
- 10 **Halldorson J,** Roberts JP. Decadal analysis of deceased organ donation in Spain and the United States linking an increased donation rate and the utilization of older donors. *Liver Transpl* 2013; **19**: 981-986 [PMID: 23780795 DOI: 10.1002/lt.23684]
- 11 **Chang GJ,** Mahanty HD, Ascher NL, Roberts JP. Expanding the donor pool: can the Spanish model work in the United States? *Am J Transplant* 2003; **3**: 1259-1263 [PMID: 14510699 DOI: 10.1046/j.1600-6143.2003.00255.x]
- 12 **Emre S,** Schwartz ME, Altaca G, Sethi P, Fiel MI, Guy SR, Kelly DM, Sebastian A, Fisher A, Eickmeyer D, Sheiner PA, Miller CM. Safe use of hepatic allografts from donors older than 70 years. *Transplantation* 1996; **62**: 62-65 [PMID: 8693547]
- 13 **Cescon M,** Mazziotti A, Grazi GL, Ravaioli M, Pierangeli F, Ercolani G, Cavallari A. Evaluation of the use of graft livers procured from old donors (70 to 87 years) for hepatic transplantation. *Transplant Proc* 2001; **33**: 934-935 [PMID: 11267135]
- 14 **Gastaca M,** Valdivieso A, Pijoan J, Errazti G, Hernandez M, Gonzalez J, Fernandez J, Matarranz A, Montejo M, Ventoso A, Martinez G, Fernandez M, de Urbina JO. Donors older than 70 years in liver transplantation. *Transplant Proc* 2005; **37**: 3851-3854 [PMID: 16386560 DOI: 10.1016/j.transproceed.2005.10.040]
- 15 **Kim DY,** Cauduro SP, Bohorquez HE, Ishitani MB, Nyberg SL, Rosen CB. Routine use of livers from deceased donors older than

- 70: is it justified? *Transpl Int* 2005; **18**: 73-77 [PMID: 15612987 DOI: 10.1111/j.1432-2277.2004.00017.x]
- 16 **Nardo B**, Masetti M, Urbani L, Caraceni P, Montalti R, Filipponi F, Mosca F, Martinelli G, Bernardi M, Daniele Pinna A, Cavallari A. Liver transplantation from donors aged 80 years and over: pushing the limit. *Am J Transplant* 2004; **4**: 1139-1147 [PMID: 15196073 DOI: 10.1111/j.1600-6143.2004.00472.x]
 - 17 **Fouzas I**, Sgourakis G, Nowak KM, Lang H, Cicinnati VR, Molmenti EP, Saner FH, Nadalin S, Papanikolaou V, Broelsch CE, Paul A, Sotiropoulos GC. Liver transplantation with grafts from septuagenarians. *Transplant Proc* 2008; **40**: 3198-3200 [PMID: 19010233 DOI: 10.1016/j.transproceed.2008.08.061]
 - 18 **Cescon M**, Grazi GL, Cucchetti A, Ravaioli M, Ercolani G, Vivarelli M, D'Errico A, Del Gaudio M, Pinna AD. Improving the outcome of liver transplantation with very old donors with updated selection and management criteria. *Liver Transpl* 2008; **14**: 672-679 [PMID: 18433035 DOI: 10.1002/lt.21433]
 - 19 **Faber W**, Seehofer D, Puhl G, Guckelberger O, Bertram C, Neuhaus P, Bahra M. Donor age does not influence 12-month outcome after orthotopic liver transplantation. *Transplant Proc* 2011; **43**: 3789-3795 [PMID: 22172848 DOI: 10.1016/j.transproceed.2011.10.048]
 - 20 **Sampedro B**, Cabezas J, Fábrega E, Casafont F, Pons-Romero F. Liver transplantation with donors older than 75 years. *Transplant Proc* 2011; **43**: 679-682 [PMID: 21486572 DOI: 10.1016/j.transproceed.2011.01.084]
 - 21 **Cascales Campos P**, Ramírez P, Gonzalez R, Domingo J, Martínez Frutos I, Sánchez Bueno F, Robles R, Miras M, Pons JA, Parrilla P. Results of liver transplantation from donors over 75 years: case control study. *Transplant Proc* 2011; **43**: 683-686 [PMID: 21486573 DOI: 10.1016/j.transproceed.2011.01.087]
 - 22 **Darius T**, Monbaliu D, Jochmans I, Meurisse N, Desschans B, Coosemans W, Komuta M, Roskams T, Cassiman D, van der Merwe S, Van Steenberghe W, Verslype C, Laleman W, Aerts R, Nevens F, Pirenne J. Septuagenarian and octogenarian donors provide excellent liver grafts for transplantation. *Transplant Proc* 2012; **44**: 2861-2867 [PMID: 23146543 DOI: 10.1016/j.transproceed.2012.09.076]
 - 23 **Wiesner R**, Edwards E, Freeman R, Harper A, Kim R, Kamath P, Kremers W, Lake J, Howard T, Merion RM, Wolfe RA, Krom R; United Network for Organ Sharing Liver Disease Severity Score Committee. Model for end-stage liver disease (MELD) and allocation of donor livers. *Gastroenterology* 2003; **124**: 91-96 [PMID: 12512033 DOI: 10.1053/gast.2003.50016]
 - 24 Banff schema for grading liver allograft rejection: an international consensus document. *Hepatology* 1997; **25**: 658-663 [PMID: 9049215 DOI: 10.1002/hep.510250328]
 - 25 **Sreekumar R**, Gonzalez-Koch A, Maor-Kendler Y, Batts K, Moreno-Luna L, Poterucha J, Burgart L, Wiesner R, Kremers W, Rosen C, Charlton MR. Early identification of recipients with progressive histologic recurrence of hepatitis C after liver transplantation. *Hepatology* 2000; **32**: 1125-1130 [PMID: 11050065 DOI: 10.1053/jhep.2000.19340]
 - 26 **Ghinolfi D**, Lai Q, Pezzati D, De Simone P, Rreka E, Filipponi F. Use of Elderly Donors in Liver Transplantation: A Paired-match Analysis at a Single Center. *Ann Surg* 2018; **268**: 325-331 [PMID: 28549011 DOI: 10.1097/SLA.0000000000002305]
 - 27 **Halazun KJ**, Rana AA, Fortune B, Quillin RC 3rd, Verna EC, Samstein B, Guarrera JV, Kato T, Griesemer AD, Fox A, Brown RS Jr, Emond JC. No country for old livers? Examining and optimizing the utilization of elderly liver grafts. *Am J Transplant* 2018; **18**: 669-678 [PMID: 28960723 DOI: 10.1111/ajt.14518]
 - 28 **Bruzzone P**, Giannarelli D, Adam R; European Liver and Intestine Transplant Association; European Liver Transplant Registry. A preliminary European Liver and Intestine Transplant Association-European Liver Transplant Registry study on informed recipient consent and extended criteria liver donation. *Transplant Proc* 2013; **45**: 2613-2615 [PMID: 24034004 DOI: 10.1016/j.transproceed.2013.07.024]
 - 29 **Ghinolfi D**, De Simone P, Lai Q, Pezzati D, Coletti L, Balzano E, Arenga G, Carrai P, Grande G, Pollina L, Campani D, Biancifiore G, Filipponi F. Risk analysis of ischemic-type biliary lesions after liver transplant using octogenarian donors. *Liver Transpl* 2016; **22**: 588-598 [PMID: 26784011 DOI: 10.1002/lt.24401]
 - 30 **Segev DL**, Maley WR, Simpkins CE, Locke JE, Nguyen GC, Montgomery RA, Thuluvath PJ. Minimizing risk associated with elderly liver donors by matching to preferred recipients. *Hepatology* 2007; **46**: 1907-1918 [PMID: 17918247 DOI: 10.1002/hep.21888]
 - 31 **Cepeda-Franco C**, Bernal-Bellido C, Barrera-Pulido L, Álamo-Martínez JM, Ruiz-Matas JH, Suárez-Artacho G, Marín-Gómez LM, Tinoco-González J, Díaz-Aunión C, Padillo-Ruiz FJ, Gómez-Bravo MÁ. Survival Outcomes in Liver Transplantation With Elderly Donors: Analysis of Andalusian Transplant Register. *Transplant Proc* 2016; **48**: 2983-2986 [PMID: 27932125 DOI: 10.1016/j.transproceed.2016.09.026]
 - 32 **Bertuzzo VR**, Cescon M, Odaldi F, Di Laudo M, Cucchetti A, Ravaioli M, Del Gaudio M, Ercolani G, D'Errico A, Pinna AD. Actual Risk of Using Very Aged Donors for Unselected Liver Transplant Candidates: A European Single-center Experience in the MELD Era. *Ann Surg* 2017; **265**: 388-396 [PMID: 28059967 DOI: 10.1097/SLA.0000000000001681]
 - 33 **Montenovo MI**, Hansen RN, Dick AAS, Reyes J. Donor Age Still Matters in Liver Transplant: Results From the United Network for Organ Sharing-Scientific Registry of Transplant Recipients Database. *Exp Clin Transplant* 2017; **15**: 536-541 [PMID: 27759559 DOI: 10.6002/ect.2016.0011]
 - 34 **Berenguer M**, López-Labrador FX, Wright TL. Hepatitis C and liver transplantation. *J Hepatol* 2001; **35**: 666-678 [PMID: 11690716 DOI: 10.1016/B978-0-7216-0118-2.50015-X]
 - 35 **Boin IF**, Ataide EC, Leonardi MI, Stucchi R, Sevã-Pereira T, Pereira IW, Cardoso AR, Caruy CA, Luzo A, Leonardi LS. Elderly donors for HCV(+) versus non-HCV recipients: patient survival following liver transplantation. *Transplant Proc* 2008; **40**: 792-796 [PMID: 18455019 DOI: 10.1016/j.transproceed.2008.02.069]
 - 36 **Lake JR**, Shorr JS, Steffen BJ, Chu AH, Gordon RD, Wiesner RH. Differential effects of donor age in liver transplant recipients infected with hepatitis B, hepatitis C and without viral hepatitis. *Am J Transplant* 2005; **5**: 549-557 [PMID: 15707410 DOI: 10.1111/j.1600-6143.2005.00741.x]
 - 37 **Mutimer DJ**, Gunson B, Chen J, Berenguer J, Neuhaus P, Castaing D, Garcia-Valdecasas JC, Salizzoni M, Moreno GE, Mirza D. Impact of donor age and year of transplantation on graft and patient survival following liver transplantation for hepatitis C virus. *Transplantation* 2006; **81**: 7-14 [PMID: 16421468 DOI: 10.1097/01.tp.0000188619.30677.84]
 - 38 **García-Reyne A**, Lumbreras C, Fernández I, Colina F, Abradelo M, Magan P, San-Juan R, Manrique A, López-Medrano F, Fuertes A, Lizasoain M, Moreno E, Aguado JM. Influence of antiviral therapy in the long-term outcome of recurrent hepatitis C virus infection following liver transplantation. *Transpl Infect Dis* 2013; **15**: 405-415 [PMID: 23725370 DOI: 10.1111/tid.12097]
 - 39 **Avolio AW**, Cillo U, Salizzoni M, De Carlis L, Colledan M, Gerunda GE, Mazzaferro V, Tisone G, Romagnoli R, Caccamo L, Rossi M, Vitale A, Cucchetti A, Lupo L, Gruttadauria S, Nicolotti N, Burra P, Gasbarrini A, Agnes S; Donor-to-Recipient Italian Liver Transplant (D2R-ILTx) Study Group. Balancing donor and recipient risk factors in liver transplantation: the value of D-MELD with particular reference to HCV recipients. *Am J Transplant* 2011; **11**: 2724-2736 [PMID: 21920017 DOI: 10.1111/j.1600-6143.2011.03732.x]
 - 40 **Halldorson JB**, Bakthavatsalam R, Fix O, Reyes JD, Perkins JD. D-MELD, a simple predictor of post liver transplant mortality for optimization of donor/recipient matching. *Am J Transplant* 2009; **9**: 318-326 [PMID: 19120079 DOI: 10.1111/j.1600-6143.2008.02491.x]
 - 41 **Chedid MF**, Rosen CB, Nyberg SL, Heimbach JK. Excellent long-term patient and graft survival are possible with appropriate use of livers from deceased septuagenarian and octogenarian donors. *HPB (Oxford)* 2014; **16**: 852-858 [PMID: 24467292 DOI: 10.1111/hpb.12221]
 - 42 **Selzner M**, Kashfi A, Selzner N, McCluskey S, Greig PD, Cattral MS, Levy GA, Lilly L, Renner EL, Therapondos G, Adcock

Caso-Maestro O *et al.* LT with aged donors

LE, Grant DR, McGilvray ID. Recipient age affects long-term outcome and hepatitis C recurrence in old donor livers following transplantation. *Liver Transpl* 2009; **15**: 1288-1295 [PMID: 19790152 DOI: 10.1002/lt.21828]

43 **Jiménez-Romero C**, Caso Maestro O, Cambra Molero F, Justo

Alonso I, Alegre Torrado C, Manrique Municio A, Calvo Pulido J, Loinaz Seguro C, Moreno González E. Using old liver grafts for liver transplantation: where are the limits? *World J Gastroenterol* 2014; **20**: 10691-10702 [PMID: 25152573 DOI: 10.3748/wjg.v20.i31.10691]

P- Reviewer: Mikulic D, Nah YW **S- Editor:** Ma RY **L- Editor:** A
E- Editor: Huang Y



Retrospective Cohort Study

Five years of fecal microbiota transplantation - an update of the Israeli experience

Sharon A Greenberg, Ilan Youngster, Nathaniel A Cohen, Dan M Livovsky, Jacob Strahilevitz, Eran Israeli, Ehud Melzer, Kalman Paz, Naomi Fliss-Isakov, Nitsan Maharshak

Sharon A Greenberg, Nathaniel A Cohen, Naomi Fliss-Isakov, Nitsan Maharshak, Department of Gastroenterology and Liver Diseases, Tel Aviv Sourasky Medical Center, affiliated with the Sackler Faculty of Medicine, Tel Aviv University, Tel Aviv 6423906, Israel

Nitsan Maharshak, Bacteriotherapy Clinic, Tel Aviv Sourasky Medical Center, affiliated with the Sackler Faculty of Medicine, Tel Aviv University, Tel Aviv 6423906, Israel

Ilan Youngster, Assaf Harofe Medical Center, Zerifin 70300, Israel

Dan M Livovsky, Kalman Paz, Digestive Diseases Institute, Shaare Zedek Medical Center, Jerusalem 91031, Israel

Jacob Strahilevitz, Department of Clinical Microbiology and Infectious Diseases, Hadassah-Hebrew University, Jerusalem 91120, Israel

Eran Israeli, Department of Gastroenterology and Liver Diseases, Hadassah-Hebrew University, Jerusalem 91120, Israel

Ehud Melzer, Gastrointestinal and Liver Diseases Institute, Kaplan Medical Center, Rehovot 76100, Israel

ORCID number: Sharon A Greenberg (0000-0001-7346-1746); Ilan Youngster (0000-0001-5233-1213); Nathaniel A Cohen (0000-0002-3997-4174); Dan M Livovsky (0000-0002-8212-9638); Jacob Strahilevitz (0000-0002-9192-7164); Eran Israeli (0000-0001-8679-4363); Ehud Melzer (0000-0002-3021-6684); Kalman Paz (0000-0001-5357-1593); Naomi Fliss-Isakov (0000-0003-4849-0291); Nitsan Maharshak (0000-0002-9324-0024).

Author contributions: All authors helped to perform the research; Greenberg SA contributed to collecting data, data analysis and writing the manuscript; Youngster I, Livovsky DM, Melzer E and Paz K contributed to performing procedures and data collection; Cohen NA contributed to data collection and writing the manuscript; Strahilevitz J contributed to data collection; Israeli E contributed to performing procedures; Fliss-

Isakov N contributed to data analysis; Maharshak N contributed to drafting conception and design, performing procedures, writing the manuscript and data collection.

Institutional review board statement: This study was approved by the institutional review board of Tel Aviv Sourasky Medical Center.

Informed consent statement: Informed consent was obtained from the patients.

Conflict-of-interest statement: The authors have declared no conflicts of interest.

Data sharing statement: No additional data are available.

STROBE statement: The authors have checked the manuscript according to STROBE checklist.

Open-Access: This article is an open-access article which was selected by an in-house editor and fully peer-reviewed by external reviewers. It is distributed in accordance with the Creative Commons Attribution Non Commercial (CC BY-NC 4.0) license, which permits others to distribute, remix, adapt, build upon this work non-commercially, and license their derivative works on different terms, provided the original work is properly cited and the use is non-commercial. See: <http://creativecommons.org/licenses/by-nc/4.0/>

Manuscript source: Unsolicited manuscript

Corresponding author to: Nitsan Maharshak, MD, Chief Doctor, Director, Doctor, Senior Lecturer, Department of Gastroenterology and Liver Diseases, Tel Aviv Sourasky Medical Center, 6 Weizmann St., Tel Aviv 6423906, Israel. nitsanm@tlvmc.gov.il
Telephone: +972-3-6947305
Fax: +972-3-6974184

Received: August 10, 2018

Peer-review started: August 10, 2018

First decision: October 24, 2018

Revised: November 26, 2018

Accepted: December 6, 2018

Article in press: December 6, 2018

Published online: December 21, 2018

Abstract

AIM

To evaluate and describe the efficacy of fecal microbiota transplantation (FMT) for *Clostridium difficile* infection (CDI) in a national Israeli cohort.

METHODS

All patients who received FMT for recurrent (recurrence within 8 wk of the previous treatment) or refractory CDI from 2013 through 2017 in all the five medical centers in Israel currently performing FMT were included. Stool donors were screened according to the Israeli Ministry of Health guidelines. Clinical and laboratory data of patients were collected from patients' medical files, and they included indications for FMT, risk factors for CDI and disease severity. Primary outcome was FMT success (at least 2 mo free of CDI-related diarrhea post-FMT). Secondary outcomes included initial response to FMT (cessation of diarrhea within 7 d) and recurrence at 6 mo.

RESULTS

There were 111 FMTs for CDI, with a median age of 70 years [interquartile range (IQR): 53-82], and 42% (47) males. Fifty patients (45%) were treated *via* the lower gastrointestinal (LGI, represented only by colonoscopy) route, 37 (33%) *via* capsules, and 24 (22%) *via* the upper gastrointestinal (UGI) route. The overall success rate was 87.4% (97 patients), with no significant difference between routes of administration ($P = 0.338$). In the univariate analysis, FMT success correlated with milder disease ($P = 0.01$), ambulatory setting ($P < 0.05$) and lower Charlson comorbidity score ($P < 0.05$). In the multivariate analysis, only severe CDI [odds ratio (OR) = 0.14, $P < 0.05$] and inpatient FMT (OR = 0.19, $P < 0.05$) were each independently inversely related to FMT success. There were 35 (32%) patients younger than 60 years of age, and 14 (40%) of them had a background of inflammatory bowel disease.

CONCLUSION

FMT is a safe and effective treatment for CDI, with capsules emerging as a successful and well-tolerated route. Severe CDI is less likely to respond to FMT.

Key words: *Clostridium difficile* infection; Capsules; Israel; Fecal microbiota transplantation

© The Author(s) 2018. Published by Baishideng Publishing Group Inc. All rights reserved.

Core tip: Fecal microbiota transplantation (FMT) emerged as a promising treatment for *Clostridium difficile* infection (CDI). Our aim was to summarize

the national Israeli experience in FMT. One-hundred and eleven patients with CDI underwent FMT, 37 (35%) of which *via* oral capsules and 50 (45%) *via* colonoscopy. The overall success rate was 87.4%, with no difference between administration routes. Success was independently related to mild disease and an ambulatory setting. One-third of the patients were younger than 60 years. 14 of which (40%) also suffered from inflammatory bowel disease. FMT is an effective treatment for recurrent CDI. FMT *via* capsules was shown to be a successful alternative to endoscopy.

Greenberg SA, Youngster I, Cohen NA, Livovsky DM, Strahilevitz J, Israeli E, Melzer E, Paz K, Fliss-Isakov N, Maharshak N. Five years of fecal microbiota transplantation - an update of the Israeli experience. *World J Gastroenterol* 2018; 24(47): 5403-5414

URL: <https://www.wjgnet.com/1007-9327/full/v24/i47/5403.htm>

DOI: <https://dx.doi.org/10.3748/wjg.v24.i47.5403>

INTRODUCTION

Background

The incidence of *Clostridium difficile* infection (CDI) is rising in parallel to the increased use of broad-spectrum antibiotics, with more than 500000 cases and 29000 related deaths annually in the United States alone^[1]. The resistance to current treatment with metronidazole and vancomycin is also increasing, with recurrence rates of up to 20% after the first episode and 40%-65% after the second^[2-4]. Fecal microbiota transplantation (FMT) has cure rates ranging between 85%-95%, and it has emerged as being a safe and promising treatment option that is widely accepted for recurrences and refractory or severe cases of CDI^[5-10]. FMT is considered the most effective treatment for recurrent CDI^[11,12] in both young and elderly patient populations^[13]. FMT is also a promising potential treatment for conditions other than CDI, such as inflammatory bowel diseases (IBD), irritable bowel syndrome, neuropsychiatric conditions, obesity, insulin resistance, and autoimmune diseases^[14,15].

Current techniques for FMT administration vary considerably between institutions and can be performed *via* a nasogastric/nasojejunal tube, gastroscopy, oral capsules, enema, sigmoidoscopy or colonoscopy^[6,15-18]. The procedure is considered safe and is mostly free of severe adverse events, although peri-procedural transient gastrointestinal (GI) symptoms may develop in some patients. The mortality cited in previous studies was attributed to the patients' pre-morbid conditions, and generally occurred in elderly and critically ill patients^[5,15-17,19].

Objective

We had earlier described the initial Israeli experience of 22 patients that were treated with FMT for CDI and

experienced an overall cure rate above 89%^[20]. However, during the past 5 years, the procedure has been performed in additional Israeli centers that processed feces from a wide range of donors in a significantly larger number of patients with different disease conditions, and using all acceptable transplantation routes. Therefore, our aim was to examine whether FMT continued to demonstrate efficacy despite this wider range of donors and patients, to investigate FMT-dependent variables, and to examine the efficacy of individual FMT routes.

MATERIALS AND METHODS

Study design and settings

This multi-center retrospective study included all the patients who were treated with FMT for CDI in Israel between January 2013 and October 2017. The participating medical centers were the Tel Aviv Medical Center (TLVMC), Tel Aviv; Shaare Zedek Medical Center (SZMC) and Hadassah Medical Center (HMC), Jerusalem; Assaf Harofe Medical Center (AHMC), Zerifin; and Kaplan Medical Center (KMC), Rehovot. All the patients or their legal surrogates provided written informed consent. The study was approved by the ethics committees of each medical center. Patients were followed routinely at 48 h, 7 d, 2 mo, and 6 mo after the procedure for the assessment of side effects and treatment outcome.

Following the Society for Healthcare Epidemiology of America (SHEA) and the Infectious Diseases Society of America (IDSA) practice guidelines^[21], CDI was defined as diarrhea (≥ 3 unformed stools per day) and a stool test that was positive for *Clostridium difficile* antigen and its toxins by either an ELISA (immunocheck™) or by PCR if the glutamate dehydrogenase antigen was positive and the toxin assessment was negative^[22]. Recurrence was defined as another episode occurring within the 8 wk following the previous treatment. Refractory CDI was defined as disease that did not respond to medical therapy. Severe disease was defined by leukocytosis ≥ 15000 cells/ μ L and/or a serum creatinine level ≥ 1.5 times the premorbid level^[21]. Initial response to FMT was defined as fewer than 3 liquid stools per day within the 7 d following FMT, and cure was defined as at least 2 mo free of CDI-related diarrhea post-FMT.

Donor stool preparation

The donor stool was delivered to the institution within a few hours of evacuation in a clean closed plastic container. It was immediately diluted with sterile saline (NaCl 0.9%) and blended into a homogenous liquid. The liquid was then filtered to remove particulate matter. Stool donations were processed and kept frozen at -80°C until use at TLVMC or AHMC, while a fresh donor stool was delivered to SZMC or HMC on the day of FMT for processing and transplantation. KMC used both frozen and fresh donor stools. The preparation of

capsules was the same as that described in our previous reports^[6,23].

Participants

All patients aged 10 to 92 years who were treated with FMT for refractory, recurrent, or severe CDI in all five centers were included. Donor selection, FMT procedure and patient follow-up were the same as those described in our earlier report^[20], and they were carried out according to practice guidelines^[24]. Capsule FMT was administered following practice guidelines as reported elsewhere^[6,7].

Variables

The primary outcome was FMT success (at least 2 mo free of CDI-related diarrhea post-FMT). Secondary outcomes included initial response to FMT (see above) and recurrence at 6 mo. The key variables were age, Charlson comorbidity score, and the risk factors for CDI in the 3 mo preceding the infection (hospitalization, exposure to antibiotics, IBD and chemotherapy).

Data sources

Clinical data were obtained from medical records, and they included epidemiologic information, risk factors for CDI, the Charlson comorbidity score^[25], and follow-up information up to 6 months post-FMT. Patients were excluded if FMT was indicated for an etiology other than CDI or if follow-up was incomplete.

Statistical analysis

All continuous variables were displayed as mean [standard deviation (SD)] or median [interquartile range (IQR)], while categorical variables were displayed as number (percent) of patients within each group. Continuous variables were analyzed by the Student *t* test for normally distributed variables and by the Mann-Whitney *U* test and the Kruskal-Wallis test for non-normally distributed variables. We used the χ^2 test to assess associations among categorical variables. Statistical significance is expressed as $P \leq 0.05$ or $P \leq 0.01$. Multivariate logistic regression analysis was used to test the association between patient and FMT characteristics and successful FMT while controlling for potential confounders. The SPSS 22.0 statistical package was used to perform all statistical analyses (SPSS Inc., Chicago, IL, United States).

RESULTS

Participants

A total of 113 CDI patients were treated with FMT in five Israeli medical centers. Two patients were excluded due to insufficient follow-up. The median age of the 111 participating patients was 70 years (IQR: 53-82), 47 (42%) of them were males, and the median 1-year Charlson comorbidity score for the cohort was 6 (IQR:

Table 1 Study population characteristics according to fecal microbiota implantation route

	Overall		Upper GI ¹		Lower GI		Capsules		P value
	n (valid)	% (IQR)	n	% (IQR)	n	% (IQR)	n	% (IQR)	
Patients	111	100	24	22 ²	50	45	37	33	
Male gender	47 (111)	42	16	67 ³	19	38	12	32	
Age, median (IQR)	70 (111)	(53-82)	68	(51-86)	78	(61-83)	68	(45-75)	0.114
Charlson comorbidity score, median	6 (81)	3-7	5.5	(3-7.25)	6	(1.75-7.5)	5	(2-7)	0.734
CDI risk factors									
Prior hospitalization	80 (111)	72	18	75 ³	26	52	36	97	< 0.01
Prior antibiotics use	66 (108)	59	15	63 ³	15	30	36	97	0.012
PPI usage	37 (110)	33	8	33 ³	14	28	15	41	0.470
Chemotherapy	19 (111)	17	4	17 ³	3	6	12	32	0.005
IBD	20 (111)	18	5	21 ³	7	14	8	22	0.606
Previous CDI episode, median	2 (107)	(2-3)	2	(1-3)	2	(1-3)	3	(2-4)	0.275
Prior therapy									
Metronidazole	89 (110)	80	17	71 ³	41	82	31	84	0.365
Vancomycin	109 (110)	98	24	100 ³	48	96	37	100	0.534
Combination	31 (110)	28	10	42 ³	15	30	6	16	0.099
Severe CDI	20 (111)	18	8	33.3 ³	10	20	2	5.40	0.019
Indication									
Refractory	29 (111)	26	6	25 ³	19	38	4	11	0.017
Recurrent	82 (111)	74	18	75 ³	31	62	33	89	
Outpatient	78 (111)	70	12	50 ³	36	72	30	81	0.032

¹Upper GI: Gastroscopy, nasogastric tube or through percutaneous endoscopic gastrostomy; ²Percentages refer to the total number of subjects in the cohort;

³Percentages refer to the number of subjects in the specific group. CDI: *Clostridium difficile* infection; IBD: Inflammatory bowel diseases; PPI: Proton pump inhibitor; GI: Gastrointestinal; FMT: Fecal microbiota implantation; IQR: Interquartile range; Prior hospitalization: Hospitalization in the 3 mo prior to the FMT; Prior antibiotics: Antibiotics use in the 3 mo prior to the FMT.

3-7 points; expected one-year survival of 79% ± 9%).

Descriptive data

The risk factors for CDI in the 3 mo preceding the infection included hospitalization (80 patients, 72%), exposure to antibiotics (65 patients, 59%), IBD (20 patients, 18%) and chemotherapy (19 patients, 17%). The patients' demographics, epidemiological data, and risk factors for CDI are summarized in Table 1.

Seventy-eight (70%) of the FMT procedures were performed in an ambulatory setting. FMT was performed through the lower GI route (LGI; only by colonoscopy) in 50 patients (45%), followed by capsules in 37 patients (33%), and through the upper GI route (UGI; gastroscopy, nasogastric tube or through their percutaneous endoscopic gastrostomy) in 24 patients (22%). The median age of the patients in the LGI group was 78 years (IQR: 61-83), which was significantly older than the median age of 68 years for the capsules group (IQR: 45-75) ($P < 0.05$). Twenty (18%) patients had severe CDI infection: they included 8 of the 24 patients (33.3%) who received FMT *via* the UGI route compared with 10 of the 50 patients [20% who received FMT *via* the LGI route ($P = 0.21$) and 5.4% (2/37) who received FMT *via* capsules ($P = 0.004$)].

Outcome data and main results

Successful FMT is more likely in ambulatory patients with milder CDI: A total of 97 (87.4%) patients achieved clinical remission (79% UGI, 88%

LGI, and 92% capsules, $P = 0.338$). Ninety-nine patients were followed-up 6 mo after FMT initiation (11 patients died, and one had not reached this endpoint by study closure). Sixteen of them (16.2%) had a recurrence of CDI: 3 in the UGI group (15.8% of the UGI group), 5 in the LGI group (11.4%), and 8 (22.2%) in the capsule group ($P = 0.141$) (Figure 1 and Table 2). Four patients required multiple FMT infusions due to recurrence: 3 underwent a second FMT infusion (of which 2 were *via* colonoscopy and 1 was *via* capsules) and one patient had 3 FMTs (all *via* colonoscopy). Only 2 had a successful FMT (1 *via* capsules and 1 *via* colonoscopy).

We further divided the cohort based on FMT success and achievement/non-achievement of clinical remission (Table 3). The 97 patients who experienced clinical remission were more likely to have undergone an ambulatory FMT (92.3% compared with 73.8% hospitalized patients, $P < 0.05$), were less likely to have a severe form of disease (14% compared with 44% of the treatment failure group, $P = 0.01$), and had a lower Charlson comorbidity score (average 4.82 ± 3.2 compared with 6.6 ± 2.3 , mean difference 1.78, 95%CI: 0.02-3.55, $P < 0.05$). In addition, patients who had a successful FMT tended to be younger (mean age 63.2 ± 22.4 years compared with 73.7 ± 12.1 years; 95%CI: -1.61 to 22.6, $P = 0.09$). Finally, more patients in the FMT failure group died during the study period (37.5% vs 6.2% for the treatment success groups, $P < 0.001$) (Figure 2 and Table 3). Frozen stool was used in

Table 2 Fecal microbiota implantation outcome and patients' follow-up

	Overall		Upper GI		Lower GI		Capsules		P value
	n (valid)	%/IQR	n	%/IQR	n	%/IQR	n	%/IQR	
Patients	111 (111)		24	22 ²	50	45	37	33	
Response within 7 d	94 (111)	84.7 ²	17	71 ³	42	84	34	92	0.198
Days to response, median	2 (111)	1-2	2	1-3	1	0-2	2	2-3	0.069
No. of patients in follow-up at 6 mo ⁵	99 (99)	89.2 ²	19	79 ³	44	88	36	97	
Recurrence at 6 mo	16 (99)	16.2 ²	3	15.8 ³	5	11.40	8	22.20	0.141
Total death	11 (111)	9.9 ²	5	21 ³	6	12	0	0	0.023
Death - unrelated	6 (11)	5.4 ²	4	80 ³	2	33	0	0	
Death - CDI-related	3 (11)	2.7 ²	1	20 ³	4	66	0	0	
No. of adverse events	19 (107)	17.1 ²	1	4 ³	14	28	4	11	0.006
Success ⁴	97 (111)	87.4 ²	19	79 ³	44	88	34	92	0.338

¹Upper GI: Gastroscopy, nasogastric tube or through percutaneous endoscopic gastrostomy; ²Percentages refer to the total number of subjects in the cohort;

³Percentages refer to the number of subjects in the specific group; ⁴Success: diarrhea-free two months post-fecal microbiota implantation; ⁵Eleven patients died before this endpoint, and one had not yet reached it at study closure. Patients who died before this endpoint from a reason other than *Clostridium difficile* infection (CDI) and were diarrhea-free were regarded as success, while patients who died before this endpoint from their CDI were considered as failures. CDI: *Clostridium difficile* infection; IQR: Interquartile range; GI: Gastrointestinal.

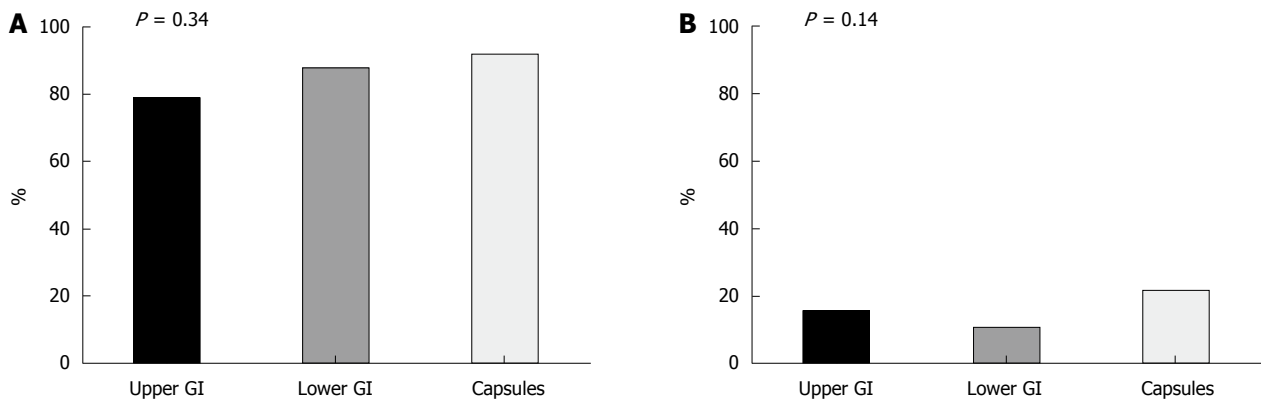


Figure 1 Comparison of success and recurrence rates of *Clostridium difficile* infection fecal microbiota transplantation treatment according route of administration. Fecal microbiota transplantation (FMT) was performed in recurrent *Clostridium difficile* infection (CDI) patients through upper gastrointestinal (GI) ($n = 24$), lower GI ($n = 50$) or capsules ($n = 37$). Success rates at 2 mo (A) and recurrence rates (B) at 6 mo post-FMT were similar between the groups. GI: Gastrointestinal.

91 of all the patients in the cohort, with slightly higher success rates than those obtained by fresh stool (89% vs 80%, $P = 0.272$).

The multivariate analysis revealed severe disease and inpatient status as being independently inversely related to FMT success, with odd ratios (ORs) of 0.14 ($P < 0.05$) and 0.19 ($P < 0.05$), respectively (Table 4). The Charlson score did not affect FMT success or failure.

Other analysis

IBD is prevalent among young FMT patients: We next divided the cohort into one group of those below 60 years of age (mean 37.2 ± 14.7 years) and another group above 60 years of age (mean 77.1 ± 8.9 years, mean difference 39.8, 95%CI: 35.3-44.3, $P < 0.001$) (Table 5). The success rates were slightly higher in the former group, but this difference did not reach a level of significance. Forty percent (14/35) of the patients younger than 60 years of age had IBD compared to only 7.9% (6/76) of the older group ($P < 0.001$). FMT was

performed significantly earlier after diagnosis among the older patients compared to the younger ones (within 102 ± 112 d compared to 198 ± 279 d, respectively, $P = 0.024$). The elderly were less likely to be treated as outpatients (63% vs 86%, $P < 0.05$) and less likely to receive corticosteroids (10.5% vs 26%, $P < 0.05$). No patient in the younger group died during the follow-up period (Table 5).

Adverse effects: Peri-procedural side effects were recorded in 19 patients. They were mild and self-limiting in 17 of them, and included abdominal discomfort, constipation, nausea/vomiting, flatulence and decreased appetite. Most of these effects occurred in patients who underwent colonoscopy [14 (28%) compared with 4 (11%) for capsules, and 1 (4%) for UGI routes, $P < 0.01$]. There were 2 cases of post-endoscopy aspirations, one involving a patient with severe CDI who had an aspiration after FMT via colonoscopy and died from sepsis 12 d post-FMT, and the other involving a

Table 3 Fecal microbiota implantation success and failure

	Valid	No.	Success		Failure		P value
			Number	%	Number	%	
Patients	111	111	97	87.4 ²	14	12.6	
Male gender	111	47	40	41.2 ³	7	50.0	0.535
Ambulatory	111	78	72	92.3 ²	6	7.7	0.016
Hospitalized	111	33	25	75.8 ²	8	24.2	
CDI risk factors							
Prior hospitalization	111	80	68	70.1 ³	12	85.7	0.224
Antibiotics use	108	89	77	81.1 ³	12	92.3	0.318
PPI usage	110	37	32	33.3 ³	5	35.7	0.86
Chemotherapy	111	19	17	17.5 ³	2	14.3	0.764
IBD	111	20	18	18.6 ³	2	14.3	0.698
Steroid usage	111	17	13	13.4 ³	4	28.6	0.141
Fever	76	21	19	27.9 ³	2	25.0	0.86
Severe disease	111	20	14	14.4 ³	6	42.9	0.01
Death	111	11	6	6.2 ³	5	37.5	0.001
Adverse events	107	19	15	16.0 ³	4	30.8	0.19
Route: Lower GI FMT	111	50	45	88.0 ²	5	12.0	0.338
Upper GI FMT ¹	111	24	19	79.2 ²	5	20.8	
Capsules FMT	111	37	34	91.9 ²	3	8.1	
Frozen stool	111	91	81	89.0 ²	10	11.0	0.272
Fresh stool	111	20	16	80.0 ²	4	20.0	
0-1 Previous CDI	107	24	23	24.2 ³	1	8.3	0.214
2+ previous CDI	107	83	72	74.2 ³	11	78.6	
Indication							0.824
Refractory	111	29	25	86.2 ²	4	13.8	
Recurrent	111	82	72	87.8 ²	10	12.2	
Prior therapy							
Metronidazole	110	89	80	83.3 ³	9	64.3	0.09
Vancomycin	110	109	95	99.0 ³	14	100.0	0.701
Combination	109	31	27	28.1 ³	4	30.8	0.843
	Valid		Mean	SD	Mean	SD	Sigma
Age (yr)	111		63.2	22.4	73.7	12.1	0.089
Charlson comorbidity score	81		4.82	3.18	6.6	2.32	0.048
Previous CDI episodes (<i>n</i>)	107		2.47	1.7	2.38	0.9	0.864
Time from 1 st CDI (d)	89		140.4	200.8	108.56	120.3	0.643
Creatinine (mg/dL)	76		1.37	1.2	2.19	2.6	0.098
Albumin (mg/L)	54		3.32	0.8	2.76	0.5	0.053
WBC (10 ³ /dL)	76		13.6	18.7	15.6	10.4	0.756

¹Upper GI: Gastroscopy, nasogastric tube or through percutaneous endoscopic gastrostomy; ²Percentages referral is the total number of subjects in the cohort; ³Percentages referral is the number of subjects in the specific group. CDI: *Clostridium difficile* infection; IBD: Inflammatory bowel diseases; PPI: Proton pump inhibitor; GI: Gastrointestinal; FMT: Fecal microbiota implantation; IQR: Interquartile range; WBC: White blood cells; Prior hospitalization: Hospitalization during the 3 mo prior to the FMT; Prior hospitalization: Antibiotics use in the 3 mo prior to the FMT.

Table 4 Multivariate analysis of the association between patient characteristics and a successful fecal microbiota implantation procedure

Patient characteristics	OR (95%CI)	P value
Hospitalized patient	0.19 (0.04-0.86)	0.032
Severe disease	0.14 (0.02-0.76)	0.023
Charlson score categories	0.82 (0.38-1.76)	0.622

Adjusted to previous hospitalization, metronidazole treatment prior to fecal microbiota implantation (FMT), previous *Clostridium difficile* infection (CDI), recurrent CDI, inflammatory bowel diseases, route of administration, stool preparation method (fresh/frozen) and FMT dosage.

severely ill patient who was hospitalized in the intensive care unit (ICU) due to fulminant CDI, with distended colon and increased intra-abdominal pressure.

Mortality: The characteristics of the 11 patients in our

cohort who did not survive are compared to the rest of the cohort in Table 6. They were much older (84.0 ± 5.8 years compared with 62.4 ± 21.6 years, mean difference 21.6 years, 95%CI: 8.6-34.7, $P < 0.001$), had higher Charlson comorbidity index scores (8.0 ± 2.4 compared with 4.57 ± 2.98 , mean difference 3.42, 95%CI: 1.54-5.31, $P = 0.001$), and had fewer episodes of CDI (average of 1.45 ± 1.4 compared with 2.57 ± 1.6 , mean difference 1.1, 95%CI: 0.1-2.1, $P < 0.05$). None of the deceased had undergone FMT via capsules, and only one was performed on an ambulatory basis. All 11 deceased patients were hospitalized at least once within the 3 months prior to undergoing the FMT procedure. The CDI of 6 of the deceased patients had improved significantly, and they died from causes unrelated to either CDI or to the FMT procedure itself. The other 5 showed no clinical response to FMT and they died shortly after undergoing it, with continuing deterioration

Table 5 Comparison of patients' characteristics by age

	Valid	No.	Below 60 yr		Above 60 yr		P value
			Number	%	Number	%	
Patients	111	111	35	31.5 ²	76	68.5	
Male gender	111	47	15	42.9 ³	32	42.1	0.941
Ambulatory	111	78	30	85.7 ³	48	63.2	0.011
CDI risk factors							
Prior hospitalization	111	80	22	62.9 ³	58	76.3	0.142
Antibiotics use	108	89	28	80.0 ³	61	83.6	0.649
PPI usage	110	37	9	25.7 ³	28	37.3	0.230
Chemotherapy	111	19	7	20.0 ³	12	15.8	0.584
IBD	111	20	14	40.0 ³	6	7.9	0.000
Steroid usage	111	17	9	25.7 ³	8	10.5	0.039
Fever	76	21	7	35.0 ³	14	25.0	0.391
Severe	111	20	3	8.6 ³	17	22.4	0.079
Route							
Lower GI	111	50	12	34.3 ³	38	50.0	0.254
Upper GI ¹	111	24	8	22.9 ³	16	21.1	
Capsules	111	37	15	42.9 ³	22	28.9	
0-1 Previous CDI	107	24	8	22.9 ³	16	22.2	0.941
2+ previous CDI	107	83	27	77.1 ³	56	77.8	
Indication							
Refractory	111	29	8	22.9 ³	21	27.6	
Recurrent	111	82	27	77.1 ³	55	72.4	
Prior therapy							
Metronidazole	110	98	29	82.9 ³	69	80.0	0.722
Vancomycin	109	109	35	100.0 ³	74	98.7	0.493
Combination	109	31	12	34.3 ³	19	25.7	0.352
Outcomes							
Success	111	97	33	94.3 ³	64	84.2	0.137
Recurrence by 6 m	99	16	7	20 ³	9	14.1	0.443
Death	111	11	0	0 ³	11	100.0	0.018
Adverse events	107	19	5	14.3 ³	14	19.4	0.512
			Mean	SD	Mean	SD	Sigma
Age (yr)	111		37.26	14.72	77.07	8.9	0.000
Charlson comorbidity score	81		1.29	1.95	6.35	2.3	0.000
Previous CDI episodes (n)	107		2.63	1.9	2.38	1.51	0.455
Time from 1 st CDI (d)	89		198.75	279.04	102.68	112.19	0.024
Creatinine (mg/dL)	76		0.91	0.51	1.67	1.63	0.051
Albumin (mg/L)	54		3.51	0.99	3.17	0.69	0.153
WBC (10 ³ /dL)	76		11.33	90.36	14.78	19.86	0.468

¹Upper GI: Gastroscopy, nasogastric tube or through percutaneous endoscopic gastrostomy; ²Percentages refer to the total number of subjects in the cohort; ³Percentages refer to the number of subjects in the specific group. CDI: *Clostridium difficile* infection; IBD: Inflammatory bowel diseases; PPI: Proton pump inhibitor; GI: Gastrointestinal; FMT: Fecal microbiota implantation; IQR: Inter quartile range; WBC: White blood cells; Prior hospitalization: Hospitalization in the 3 mo prior to the FMT; Prior hospitalization: Antibiotics use in the 3 mo prior to the FMT.

of their general clinical condition.

DISCUSSION

Key results and interpretation

In this multi-center cohort study, we described the real-world experience of FMT procedures for CDI in a heterogeneous national Israeli population during the 5 years since the procedure was approved. We examined the distribution of the various techniques, routes and success rates in 111 FMT procedures.

There was an 85% response to treatment within the first 7 d post-FMT, and the success rates rose to 88% at 2 mo. These rates are compatible with reports and reviews of others^[5,7-9,12,15-19]. Comparison of the 3 usual methods of FMT administration, UGI, LGI and capsules, revealed a higher success rates for the

capsules and LGI routes over the UGI route although not to a level of statistical significance. Nevertheless, capsules-treated patients had the highest recurrence rates (22% at 6 mo), again not reaching a level of statistical significance. These results can be interpreted in several ways. First, there were higher rates of severe CDI within the UGI group compared with the 2 other groups (Figure 1 and Table 1). Second, previous reports showed lower success rates for the UGI route compared with LGI: one systematic review of 325 cases of FMT for CDI suggested a lower success rate for upper gut administration (76%) compared with colonoscopy (89%) and enema (95%) administration^[17], while Kassam *et al.*^[19] reported a trend for higher resolution rates through the LGI route compared with the UGI route. Cure from CDI was associated with a milder disease and undergoing treatment in an outpatient

Table 6 Mortality

	Valid	No.	Alive		Dead		P value
			Number	%	Number	%	
Patients			100	90.1 ²	11	9.9	
Male gender	111	47	38	38.0 ³	9	81.8	0.005
Ambulatory	104	75	74	77.9 ³	1	10.0	0.000
CDI risk factors							
Prior hospitalization	111	80	69	69.0 ³	11	100.0	0.030
Antibiotics use	108	89	81	82.7 ³	8	80.0	0.834
PPI usage	110	37	31	31.3 ³	6	54.5	0.122
Chemotherapy	111	19	19	19.0 ³	0	0.0	0.112
IBD	111	20	20	20.0 ³	0	0.0	0.101
Steroid usage	111	17	16	16.0 ³	1	9.1	0.546
Fever	76	21	15	23.1 ³	6	54.5	0.031
Severe	110	20	13	13.0 ³	7	63.6	0.000
Adverse events	107	19	15	15.5 ³	4	40.0	0.053
Route							
Lower GI	111	50	44	44.0 ³	6	54.5	0.023
Upper GI ¹		24	19	19.0 ³	5	45.5	
Capsules		37	37	37.0 ³	0	0.0	
0-1 previous CDI	107	24	19	19.8 ³	5	45.5	0.053
2+ previous CDI		83	77		6		
Indication	111						0.306
Refractory		23	19	19.0 ³	4	36.4	
Recurrent		82	76	76.0 ³	6	54.5	
Prior therapy							
Metronidazole	110	89	80	80.8 ³	9	81.8	0.936
Vancomycin	110	109	98	99.0 ³	11	100.0	0.738
Combination	109	31	25	25.5 ³	6	54.5	0.043
Outcomes							
Adverse events	107	19	15	15.5 ³	4	40.0	0.053
Response to FMT	111	94	88	88.0 ³	6	54.5	0.003
			Mean	SD	Mean	SD	Sigma
Age (yr)	111		62.37	21.656	84	5.797	0.000
Charlson comorbidity score	81		4.57	2.98	8	2.4	0.001
Previous CDI episodes (n)	107		2.57	1.633	1.45	1.368	0.025
Time from 1 st CDI (d)	89		138.47	197.991	110.75	63.036	0.493
Creatinine (mg/dL)	76		1.44	1.507	1.74	1.193	0.482
Albumin (mg/L)	54		3.34	0.782	2.4	0.408	0.010
WBC (10 ³ /dL)	76		13.65	18.87	15.64	78.62	0.564

¹Upper GI: Gastroscopy, nasogastric tube or through percutaneous endoscopic gastrostomy; ²Percentages refer to the total number of subjects in the cohort;

³Percentages refer to the number of subjects in the specific group. CDI: *Clostridium difficile* infection; IBD: Inflammatory bowel diseases; PPI: Proton pump inhibitor; GI: Gastrointestinal; FMT: Fecal microbiota implantation; IQR: Inter quartile range; WBC: White blood cells; Prior hospitalization: Hospitalization within the 3 mo prior to the FMT; Prior hospitalization: Antibiotics use in the 3 mo prior to the FMT.

setup. Other factors, such as age, Charlson score, albumin levels, and creatinine levels were not significantly different between the groups, since the study was probably underpowered to detect significant differences in these variables. Multiple infusions were seldom and relatively unsuccessful in our cohort (4 patients, 50% success rate), but the numbers are too low to arrive at any conclusions and the results cannot be compared with those of recent meta analyses which showed increased success rates with multiple FMTs^[26,27].

Multivariate analysis revealed that severe CDI (OR = 0.14, $P < 0.05$) and inpatient FMT (OR = 0.19, $P < 0.05$) were each independently inversely related to FMT success, while patients' background illnesses as reflected by the Charlson comorbidity score were not associated with either success or failure of FMT. Similar results were reported by Ianiro *et al.*^[28] in their single-center cohort study that showing that severe CDI

and inadequate bowel preparation were independent predictors of FMT failure, and by Fischer *et al.*^[29] in their multi-center study, in which predictors for FMT failure included severe or severe-complicated CDI, inpatient status during FMT and previous CDI-related hospitalization. Taken together, this data implies that the severe form of CDI is less likely to be successfully treated with FMT, and that future studies are warranted in order to find the optimal treatment. Other factors, including the patients' comorbidities as determined by the Charlson comorbidity score, did not seem to affect the FMT outcome.

To maintain continuity with a previous report^[13], we compared the outcomes of the patients below and above 60 years of age and found that almost one-third (35/111) of the patients who underwent FMT for treatment of CDI in Israel were below 60 years of age (mean age 37.2 years). These patients had much

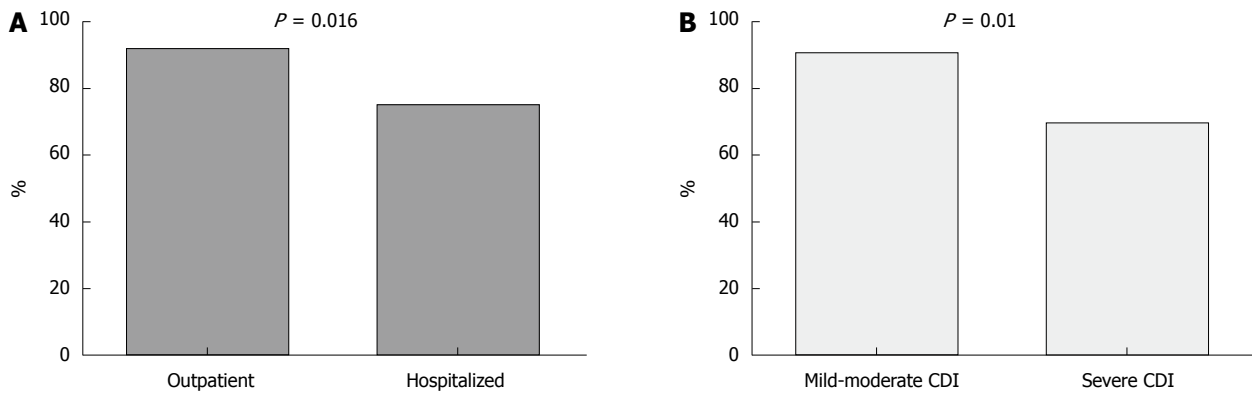


Figure 2 Comparison of fecal microbiota transplantation success rates among hospitalized and ambulatory patients. Seventy-eight patients who underwent ambulatory fecal microbiota transplantation had a success rate of 92.3% compared with 75.8% for hospitalized patients, $P = 0.016$ (A). Success rates were much lower among patients with severe *Clostridium difficile* infection compared with mild-moderate disease (B). CDI: *Clostridium difficile* infection.

lower Charlson comorbidity scores, underwent FMT on an ambulatory basis, and tended to have lower rates of severe CDI. Interestingly, there were no differences between the groups regarding hospitalizations in the 3 mo prior to the FMT. In a population-based study from Olmsted county, Minnesota, United States, community-acquired CDI accounted for 41% of CDI cases and was characterized by a younger population with less severe disease, which is in line with our findings^[30]. We observed a significantly higher percentage (40%) of IBD patients among this group compared to the older group (8%). Interestingly, the waiting period between the first CDI episode to undergoing FMT was longer among the younger patients compared to the older ones, possibly due to a delay in diagnosis or to a lower compliance rate to undergo the procedure, as well as a lower index of suspicion among physicians caring for younger patients with diarrhea compared to older ones leading to a delay in diagnosis. The higher rates of IBD among younger patients might also contribute to the delay in diagnosis, since diarrhea can be attributed to illnesses, such as IBD and other GI disorders other than CDI. Indeed, time to FMT from first CDI in IBD patients tended to be longer compared to non-IBD patients (207.2 and 116.9 d, respectively, $P = 0.066$). Interestingly, the IBD patients in our study experienced higher success rates than reported in the literature (90% compared to 74.4% reported by Khoruts *et al.*^[31]), although the group of IBD patients group in our study is much smaller ($n = 20$) compared with theirs ($n = 272$), and that might explain the difference in results.

Finally, severe CDI may be a fatal disease, especially in elderly and frail populations. The patients in our study group who died were much older, had significantly higher Charlson comorbidity scores, and much higher rates of severe CDI than the survivors. The CDI-associated diarrhea had improved significantly in 6 of them, while the condition of the others continued to deteriorate despite broad-spectrum antibiotic coverage treatment and ICU support, including mechanical

ventilation and vasopressors. None of the deaths were attributed to the FMT procedure in any of them, which correlates with previous reports^[13,19]. Although an approximately 10% mortality rate is quite high for FMT, it represents the natural history of weakened senior patients with multiple comorbidities in a large cohort rather than the FMT itself, as reported earlier^[19,32]. Similar numbers can be found in other long follow-up studies, such as the one by Brandt *et al.*^[12] which reported the demise of 7 of the 77 patients in their long-term study (mean follow-up 17 mo).

Most of the adverse events were mild and self-resolving, and they included abdominal discomfort, nausea, flatulence and constipation, which can be attributed to the procedure itself (*i.e.*, most of these complications occurred in the LGI group). In addition, they are generally self-limiting and rather common post-colonoscopy events, occurring after up to 33% of colonoscopies^[33]. Severe complications were recorded for 2 patients (< 2% of the cohort) who were severely ill in an ICU setting and each suffered post-endoscopy aspirations.

The strength of this study is its ability to capture real-life data from the 5 medical centers throughout Israel that perform FMT through various routes and use different donors with negligible differences in preparing donors' fecal filtrate. These are important for creating balanced data regarding the efficacy and safety of FMT.

Limitations

There were several limitations in the present study. Firstly, it is retrospective in design, warranting a prospective double blind randomized placebo-controlled study. Secondly, some of the data were collected *a posteriori* and information on laboratory findings, class of antibiotic used prior to CDI and Charlson scores of some of the patients (especially the ambulatory ones) were not available. Other limitations were the power of the study and the fact that the study population consisted only of Israeli patients.

Generalizability

The results of this study correlate with previous works regarding overall success rates^[5,7,8,12,15-19], different routes of FMT administration^[17,19] and predictors of failure^[28,29] (see above), and reflect a multi-center data of heterogeneous population from several districts in Israel and from different stool donors, making its results generalizable worldwide.

The corresponding author can provide complete data upon request.

In conclusion, FMT is a safe and effective treatment for CDI, which has been occurring in growing numbers in both older and younger populations. While both LGI and capsule administration of FMT seem to be more efficient than the UGI endoscopic route, FMT *via* capsules has emerged as a successful and well-tolerated alternative. Severe CDI and inpatient status were related to FMT failure. Prospective and well-powered studies are needed to conclusively determine the best route of administration, regarding patient safety, ease of administration, side effects and costs.

ARTICLE HIGHLIGHTS

Research background

The incidence of *Clostridium difficile* infection (CDI) is rising, and the increase is associated with significant morbidity and mortality rates. Fecal microbiota transplantation (FMT) is a promising and safe treatment. FMT has been performed in 5 medical centers in Israel since 2013, but its efficacy and safety had not yet been assessed.

Research motivation

To summarize all the FMT procedures performed in Israel for CDI between 2013-2017 and provide a detailed report on its current status, success rates, safety, and modes of administration.

Research objectives

The main objectives were to assess FMT success and failure rates as well as predictors of success with respect to mode of administration.

Research methods

This multi-center retrospective study included all the patients who were treated with FMT for CDI in Israel between January 2013 and October 2017. Clinical data were obtained from medical records, and they included epidemiologic information, risk factors for CDI, Charlson co-morbidity scores, and follow-up information up to 6 mo post-FMT. The Student *t* test was used for normally distributed variables and the Mann-Whitney *U* test was applied for non-normally distributed variables. We also used the χ^2 test to assess associations among categorical variables. Multivariate logistic regression analysis tested the association between patient and FMT characteristics and successful FMT, controlling for potential confounders.

Research results

A total of 111 CDI patients were included. The median age of the 111 participating patients was 70 years [interquartile range (IQR): 53-82], 47 (42%) of the patients were males, and the median 1-year Charlson comorbidity score for the entire cohort was 6 (IQR: 3-7 points; expected one-year survival of 79% \pm 9%). Seventy-eight (70%) of the FMT procedures were performed in an ambulatory setting. FMT was performed through the lower gastrointestinal route (LGI) in 50 patients (45%), followed by capsules in 37 patients (33%), and through the upper GI route (UGI) in 24 patients (22%). A total of 97 (87.4%) patients achieved clinical remission (79% UGI, 88% LGI, and 92%

capsules, $P = 0.338$). Multiple FMT infusions were rare and unsuccessful. The multi-variance analysis revealed that severe disease and inpatient status were independently inversely related to FMT success, with an OR of 0.14 and 0.19, respectively. Patients younger than 60 years ($n = 35$, 32%) had higher percentages of background inflammatory bowel disease (IBD; 14/35, 40%) compared patients older than 60 years (6/76, 8%, $P < 0.01$), and waited much longer to undergo the FMT procedure (time between diagnosis of CDI to FMT of 102 d for the older group and 198 d for the younger group, $P < 0.05$). Eleven patients who died during the study period (no death was attributed to the FMT procedure) were much older (84 years compared with 62 years, $P < 0.01$), and had higher Charlson comorbidity index scores (8 compared with 4.5, $P < 0.01$).

Research conclusions

This is the first comprehensive description of the FMT experience in Israel since the procedure was introduced in 2013. This study shows FMT success rates which are similar to other reports worldwide, and provides the information about the efficacy and safety of the procedure, with respect to different administration routes. Predictors of FMT failure were CDI-related (severe disease and inpatient status) but not patient-related (as reflected by the Charlson comorbidity score). Concomitant IBD did not affect clinical outcomes. FMT through capsules was an efficient mode of FMT administration, and emerged as being a safe and well-tolerated alternative to endoscopy.

Research perspectives

FMT is a safe and effective treatment for CDI. The association between severe CDI with higher FMT failure rates raises the need for the future investigation of other approaches. FMT through capsules seems to be at least as good as FMT by means of endoscopies and its potential as a primary route should be investigated.

ACKNOWLEDGMENTS

The authors thank Esther Eshkol for editorial assistance.

REFERENCES

- 1 Lessa FC, Mu Y, Bamberg WM, Beldavs ZG, Dumyati GK, Dunn JR, Farley MM, Holzbauer SM, Meek JJ, Phipps EC, Wilson LE, Winston LG, Cohen JA, Limbago BM, Fridkin SK, Gerding DN, McDonald LC. Burden of *Clostridium difficile* infection in the United States. *N Engl J Med* 2015; **372**: 825-834 [PMID: 25714160 DOI: 10.1056/NEJMoa1408913]
- 2 Kelly CP, LaMont JT. *Clostridium difficile*--more difficult than ever. *N Engl J Med* 2008; **359**: 1932-1940 [PMID: 18971494 DOI: 10.1056/NEJMra0707500]
- 3 Petrella LA, Sambol SP, Cheknis A, Nagaro K, Kean Y, Sears PS, Babakhani F, Johnson S, Gerding DN. Decreased cure and increased recurrence rates for *Clostridium difficile* infection caused by the epidemic *C. difficile* BI strain. *Clin Infect Dis* 2012; **55**: 351-357 [PMID: 22523271 DOI: 10.1093/cid/cis430]
- 4 Burke KE, Lamont JT. *Clostridium difficile* infection: a worldwide disease. *Gut Liver* 2014; **8**: 1-6 [PMID: 24516694 DOI: 10.5009/gnl.2014.8.1.1]
- 5 Cammarota G, Ianiro G, Gasbarrini A. Fecal microbiota transplantation for the treatment of *Clostridium difficile* infection: a systematic review. *J Clin Gastroenterol* 2014; **48**: 693-702 [PMID: 24440934 DOI: 10.1097/MCG.0000000000000046]
- 6 Youngster I, Mahabamunuge J, Systrom HK, Sauk J, Khalili H, Levin J, Kaplan JL, Hohmann EL. Oral, frozen fecal microbiota transplant (FMT) capsules for recurrent *Clostridium difficile* infection. *BMC Med* 2016; **14**: 134 [PMID: 27609178 DOI: 10.1186/s12916-016-0680-9]
- 7 Bakken JS, Borody T, Brandt LJ, Brill JV, Demarco DC, Franzos MA, Kelly C, Khoruts A, Louie T, Martinelli LP, Moore TA, Russell G, Surawicz C; Fecal Microbiota Transplantation Workgroup. Treating *Clostridium difficile* infection with fecal microbiota transplantation. *Clin Gastroenterol Hepatol* 2011; **9**:

- 1044-1049 [PMID: 21871249 DOI: 10.1016/j.cgh.2011.08.014]
- 8 **Cammarota G**, Ianiro G, Tilg H, Rajilić-Stojanović M, Kump P, Satokari R, Sokol H, Arkkila P, Pintus C, Hart A, Segal J, Aloï M, Masucci L, Molinaro A, Scaldaferri F, Gasbarrini G, Lopez-Sanroman A, Link A, de Groot P, de Vos WM, Högenauer C, Malfertheiner P, Mattila E, Milosavljević T, Nieuwdorp M, Sanguinetti M, Simren M, Gasbarrini A; European FMT Working Group. European consensus conference on faecal microbiota transplantation in clinical practice. *Gut* 2017; **66**: 569-580 [PMID: 28087657 DOI: 10.1136/gutjnl-2016-313017]
- 9 **Surawicz CM**, Brandt LJ, Binion DG, Ananthakrishnan AN, Curry SR, Gilligan PH, McFarland LV, Mellow M, Zuckerbraun BS. Guidelines for diagnosis, treatment, and prevention of *Clostridium difficile* infections. *Am J Gastroenterol* 2013; **108**: 478-98; quiz 499 [PMID: 23439232 DOI: 10.1038/ajg.2013.4]
- 10 **Mullish BH**, Quraishi MN, Segal JP, McCune VL, Baxter M, Marsden GL, Moore DJ, Colville A, Bhala N, Iqbal TH, Settle C, Kontkowski G, Hart AL, Hawkey PM, Goldenberg SD, Williams HRT. The use of faecal microbiota transplant as treatment for recurrent or refractory *Clostridium difficile* infection and other potential indications: joint British Society of Gastroenterology (BSG) and Healthcare Infection Society (HIS) guidelines. *Gut* 2018; **67**: 1920-1941 [PMID: 30154172 DOI: 10.1136/gutjnl-2018-316818]
- 11 **Mattila E**, Uusitalo-Seppälä R, Wuorela M, Lehtola L, Nurmi H, Ristikankare M, Moilanen V, Salminen K, Seppälä M, Mattila PS, Anttila VJ, Arkkila P. Fecal transplantation, through colonoscopy, is effective therapy for recurrent *Clostridium difficile* infection. *Gastroenterology* 2012; **142**: 490-496 [PMID: 22155369 DOI: 10.1053/j.gastro.2011.11.037]
- 12 **Brandt LJ**, Aroniadis OC, Mellow M, Kanatzar A, Kelly C, Park T, Stollman N, Rohlke F, Surawicz C. Long-term follow-up of colonoscopic fecal microbiota transplant for recurrent *Clostridium difficile* infection. *Am J Gastroenterol* 2012; **107**: 1079-1087 [PMID: 22450732 DOI: 10.1038/ajg.2012.60]
- 13 **Friedman-Korn T**, Livovsky DM, Maharshak N, Aviv Cohen N, Paz K, Bar-Gil Shitrit A, Goldin E, Koslowsky B. Fecal Transplantation for Treatment of *Clostridium Difficile* Infection in Elderly and Debilitated Patients. *Dig Dis Sci* 2018; **63**: 198-203 [PMID: 29134299 DOI: 10.1007/s10620-017-4833-2]
- 14 **Cohen NA**, Maharshak N. Novel Indications for Fecal Microbial Transplantation: Update and Review of the Literature. *Dig Dis Sci* 2017; **62**: 1131-1145 [PMID: 28315032 DOI: 10.1007/s10620-017-4535-9]
- 15 **Brandt LJ**, Aroniadis OC. An overview of fecal microbiota transplantation: techniques, indications, and outcomes. *Gastrointest Endosc* 2013; **78**: 240-249 [PMID: 23642791 DOI: 10.1016/j.gie.2013.03.1329]
- 16 **Borody TJ**, Paramsothy S, Agrawal G. Fecal microbiota transplantation: indications, methods, evidence, and future directions. *Curr Gastroenterol Rep* 2013; **15**: 337 [PMID: 23852569 DOI: 10.1007/s11894-013-0337-1]
- 17 **Gough E**, Shaikh H, Manges AR. Systematic review of intestinal microbiota transplantation (fecal bacteriotherapy) for recurrent *Clostridium difficile* infection. *Clin Infect Dis* 2011; **53**: 994-1002 [PMID: 22002980 DOI: 10.1093/cid/cir632]
- 18 **König J**, Siebenhaar A, Högenauer C, Arkkila P, Nieuwdorp M, Norén T, Ponsioen CY, Rosien U, Rossen NG, Satokari R, Stallmach A, de Vos W, Keller J, Brummer RJ. Consensus report: faecal microbiota transfer - clinical applications and procedures. *Aliment Pharmacol Ther* 2017; **45**: 222-239 [PMID: 27891639 DOI: 10.1111/apt.13868]
- 19 **Kassam Z**, Lee CH, Yuan Y, Hunt RH. Fecal microbiota transplantation for *Clostridium difficile* infection: systematic review and meta-analysis. *Am J Gastroenterol* 2013; **108**: 500-508 [PMID: 23511459 DOI: 10.1038/ajg.2013.59]
- 20 **Cohen NA**, Livovsky DM, Yaakovovitch S, Ben Yehoyada M, Ben Ami R, Adler A, Guzman-Gur H, Goldin E, Santo ME, Halpern Z, Paz K, Maharshak N. A Retrospective Comparison of Fecal Microbial Transplantation Methods for Recurrent *Clostridium Difficile* Infection. *Isr Med Assoc J* 2016; **18**: 594-599 [PMID: 28471618]
- 21 **Cohen SH**, Gerding DN, Johnson S, Kelly CP, Loo VG, McDonald LC, Pepin J, Wilcox MH; Society for Healthcare Epidemiology of America; Infectious Diseases Society of America. Clinical practice guidelines for *Clostridium difficile* infection in adults: 2010 update by the society for healthcare epidemiology of America (SHEA) and the infectious diseases society of America (IDSA). *Infect Control Hosp Epidemiol* 2010; **31**: 431-455 [PMID: 20307191 DOI: 10.1086/651706]
- 22 **Ota KV**, McGowan KL. *Clostridium difficile* testing algorithms using glutamate dehydrogenase antigen and *C. difficile* toxin enzyme immunoassays with *C. difficile* nucleic acid amplification testing increase diagnostic yield in a tertiary pediatric population. *J Clin Microbiol* 2012; **50**: 1185-1188 [PMID: 22259201 DOI: 10.1128/JCM.05620-11]
- 23 **Youngster I**, Russell GH, Pindar C, Ziv-Baran T, Sauk J, Hohmann EL. Oral, capsulized, frozen fecal microbiota transplantation for relapsing *Clostridium difficile* infection. *JAMA* 2014; **312**: 1772-1778 [PMID: 25322359 DOI: 10.1001/jama.2014.13875]
- 24 **Woodworth MH**, Neish EM, Miller NS, Dhere T, Burd EM, Carpentieri C, Sitchenko KL, Kraft CS. Laboratory Testing of Donors and Stool Samples for Fecal Microbiota Transplantation for Recurrent *Clostridium difficile* Infection. *J Clin Microbiol* 2017; **55**: 1002-1010 [PMID: 28077694 DOI: 10.1128/JCM.02327-16]
- 25 **Charlson M**, Szatrowski TP, Peterson J, Gold J. Validation of a combined comorbidity index. *J Clin Epidemiol* 1994; **47**: 1245-1251 [PMID: 7722560 DOI: 10.1016/0895-4356(94)90129-5]
- 26 **Quraishi MN**, Widlak M, Bhala N, Moore D, Price M, Sharma N, Iqbal TH. Systematic review with meta-analysis: the efficacy of faecal microbiota transplantation for the treatment of recurrent and refractory *Clostridium difficile* infection. *Aliment Pharmacol Ther* 2017; **46**: 479-493 [PMID: 28707337 DOI: 10.1111/apt.14201]
- 27 **Ianiro G**, Maida M, Burisch J, Simonelli C, Hold G, Ventimiglia M, Gasbarrini A, Cammarota G. Efficacy of different faecal microbiota transplantation protocols for *Clostridium difficile* infection: A systematic review and meta-analysis. *United European Gastroenterol J* 2018; **6**: 1232-1244 [PMID: 30288286 DOI: 10.1177/2050640618780762]
- 28 **Ianiro G**, Valerio L, Masucci L, Pecere S, Bibbò S, Quaranta G, Posteraro B, Currò D, Sanguinetti M, Gasbarrini A, Cammarota G. Predictors of failure after single faecal microbiota transplantation in patients with recurrent *Clostridium difficile* infection: results from a 3-year, single-centre cohort study. *Clin Microbiol Infect* 2017; **23**: 337.e1-337.e3 [PMID: 28057560 DOI: 10.1016/j.cmi.2016.12.025]
- 29 **Fischer M**, Kao D, Mehta SR, Martin T, Dimitry J, Keshteli AH, Cook GK, Phelps E, Sipe BW, Xu H, Kelly CR. Predictors of Early Failure After Fecal Microbiota Transplantation for the Therapy of *Clostridium Difficile* Infection: A Multicenter Study. *Am J Gastroenterol* 2016; **111**: 1024-1031 [PMID: 27185076 DOI: 10.1038/ajg.2016.180]
- 30 **Khanna S**, Pardi DS, Aronson SL, Kammer PP, Orenstein R, St Sauver JL, Harmsen WS, Zinsmeister AR. The epidemiology of community-acquired *Clostridium difficile* infection: a population-based study. *Am J Gastroenterol* 2012; **107**: 89-95 [PMID: 22108454 DOI: 10.1038/ajg.2011.398]
- 31 **Khoruts A**, Rank KM, Newman KM, Viskocil K, Vaughn BP, Hamilton MJ, Sadowsky MJ. Inflammatory Bowel Disease Affects the Outcome of Fecal Microbiota Transplantation for Recurrent *Clostridium difficile* Infection. *Clin Gastroenterol Hepatol* 2016; **14**: 1433-1438 [PMID: 26905904 DOI: 10.1016/j.cgh.2016.02.018]
- 32 **Furuya-Kanamori L**, Doi SA, Paterson DL, Helms SK, Yakob L, McKenzie SJ, Garborg K, Emanuelsson F, Stollman N, Kronman MP, Clark J, Huber CA, Riley TV, Clements AC. Upper Versus Lower Gastrointestinal Delivery for Transplantation of Fecal Microbiota in Recurrent or Refractory *Clostridium difficile*

Infection: A Collaborative Analysis of Individual Patient Data From 14 Studies. *J Clin Gastroenterol* 2017; **51**: 145-150 [PMID: 26974758 DOI: 10.1097/MCG.0000000000000511]

- 33 **Ko CW**, Dominitz JA. Complications of colonoscopy: magnitude and management. *Gastrointest Endosc Clin N Am* 2010; **20**: 659-671 [PMID: 20889070 DOI: 10.1016/j.giec.2010.07.005]

P- Reviewer: Ianiro G, Konig J, Tahan V **S- Editor:** Ma RY
L- Editor: A **E- Editor:** Huang Y





Published by **Baishideng Publishing Group Inc**
7901 Stoneridge Drive, Suite 501, Pleasanton, CA 94588, USA
Telephone: +1-925-223-8242
Fax: +1-925-223-8243
E-mail: bpgoffice@wjgnet.com
Help Desk: <https://www.f6publishing.com/helpdesk>
<https://www.wjgnet.com>



ISSN 1007-9327

